

Vascular and Metabolic Actions of Insulin and AMPK Activation in Muscle

by

Eloise Bradley BSc. (Biochemistry)

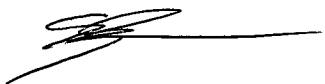
**Submitted in fulfilment of the requirements for the degree of Master of Medical
Science**

**Menzies Research Institute
University of Tasmania**

December 2009

STATEMENT

This work in this thesis has been taken exclusively for the use of a Master of Medical Science in the area of biochemistry and has not been used for any other higher degree or graduate diploma in any university. All written and experimental work is my own, except which has been referenced accordingly. Dr. Etto Eringa and colleagues carried out the *in vitro* experimental work contained in methods sections 2.2 and 5.2.2 in results section 5.3.1.

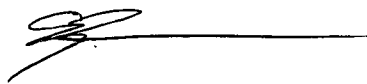


15. 12. 2009

Eloise Bradley

AUTHORITY OF ACCESS

This thesis may be available for loan and limited copying in accordance with the Copyright Act 1968.



15. 12. 2009.

Eloise Bradley

ABSTRACT

It has been well established that both insulin and muscle contraction increase total blood flow to skeletal muscle. A number of studies have also demonstrated that insulin and muscle contraction increase muscle microvascular perfusion *in vivo* in both humans and animals. The haemodynamic responses to insulin have been thought to promote delivery of glucose and hormones to the myocyte to enhance glucose disposal. In models of insulin resistance, insulin mediated increases in blood flow (total and microvascular) and glucose uptake are impaired. In contrast contraction stimulated increases in blood flow and glucose uptake are generally not impaired in insulin resistant rodents and humans. Although increases in total blood flow, microvascular perfusion and glucose uptake in skeletal muscle can be stimulated by either insulin or muscle contraction these processes use different signalling pathways. The main focus of this thesis was to explore mechanisms involved in insulin- and contraction-stimulated haemodynamics in skeletal muscle and their impact on insulin-mediated glucose uptake.

The *in vivo* techniques employed in this thesis include hyperinsulinemic euglycaemic clamps performed in anaesthetised rats, arterial blood flow measurements by Transonic® flow probes, microvascular perfusion measurements by either metabolism of exogenously infused 1-methylxanthine (1-MX) or contrast enhanced ultrasound (CEU). Test agents were administered either systemically or locally into one hindlimb via the epigastric artery. Isolated resistance arteries were used in one study to compliment the *in vivo* studies.

The hypothesis that a PI3K dependant signalling pathway, leading to activation of eNOS and the production of NO, is involved in the hemodynamic actions of insulin in muscle was examined. Wortmannin, a PI3K inhibitor, was infused systemically during an insulin clamp *in vivo*. Wortmannin administration resulted in inhibition of the haemodynamic effects of insulin including total flow and microvascular perfusion as well as

glucose uptake. The relationship between insulin mediated NOS activation and microvascular perfusion was also studied. A NOS inhibitor, L-NAME, was infused locally in one leg and attenuated insulin action in skeletal muscle by inhibiting microvascular perfusion and blunting glucose uptake.

AMPK is a potential mediator of metabolic changes in muscle during contraction and can be artificially activated by the compound AICAR. Acute activation of AMPK *in vivo* by low dose AICAR resulted in increased microvascular blood volume without effects on blood pressure, femoral blood flow or hindleg glucose uptake. In addition, in isolated resistance arteries, AICAR induced vasodilatation, which was abolished by the NO synthase inhibitor L-NA or the AMPK inhibitor compound C. Activation of AMPK by AICAR also sensitised smooth muscle cells to sodium nitroprusside (SNP) mediated vasodilatation and induced vasodilatation of resistance arteries. AMPK activation by AICAR resulted in marked enhancement of insulin-mediated microvascular perfusion and glucose uptake.

Collectively the findings in this thesis highlight the important role of microvascular perfusion for facilitating skeletal muscle glucose metabolism and explore some of the mechanisms which are involved. Insulin mediated microvascular perfusion occurs via a PI3K dependant pathway and is strongly associated with NOS activation. Activation of AMPK increases microvascular perfusion which is also associated with NOS activation. The combination of AMPK activation and insulin resulted in marked enhancement of insulin-mediated microvascular perfusion and glucose uptake. Improvement of microvascular perfusion through targeting AMPK activation may provide a potential therapeutic avenue for enhancing glucose metabolism.

ACKNOWLEDGEMENTS

I especially extend my sincere thanks to my supervisor Associate Professor Steve Rattigan. This thesis would not have been possible without his input and supervision.

I also wish to thank Professor Michael Clark and Dr. Stephen Richards for their help and support during this study.

Importantly, I acknowledge and thank Dr. Etto Eringa and colleagues for the *in vitro* studies included in chapter 5. Their contribution and ongoing collaboration is greatly appreciated.

In addition I would like to thank my colleagues at the muscle research group past and present for their friendship and support; Dr. Lucy Clerk, Dr. Nathan Parry, Maree Smith, Dr. Cate Wheatley, Dr. Zhang Lei, Georgie Vollus, Sara Jackson, Dr. Hema Mahajan, Dr. Cathryn Kolka and Dr. Renee Dwyer. In particular I would like to thank Dr. Michelle Wallis for help with animal surgery and Geoff Appleby for technical assistance. I would also like to thank the members of the central animal house, particularly Murray and Marcus for care of the animals.

I would like to thank Steve Rattigan and Prof Clark for enabling my visit to Dr. Gene Barrett's group at the University of Virginia, Charlottesville, USA. I would like to thank Dr. Lucy Clerk for her help and for sharing her expertise in the technique of contrast enhanced ultrasound during this visit. I would also like to thank Dr. Lucy Clerk and Dr. Michelle Wallis for their hospitality during my stay.

I would especially like to thank Alan Williams for his continued support and encouragement throughout this study.

Sections of this work were supported by the grants from the National Health and Medical Research Council, Australian Research Council and the National Heart Foundation of Australia.

LIST OF ABBREVIATIONS

AICAR	5-aminoimidazole-4-carboxamide-1- β -D-ribofuranoside
ACC	Acetyl-CoA carboxylase
ADP	Adenosine diphosphate
AMP	Adenosine monophosphate
AMPK	AMP- activated protein kinase
AMPKK	AMP- activated protein kinase kinase
ANOVA	Analysis of variance
ATP	Adenosine triphosphate
BAECs	Bovine aortic endothelial cells
BH ₄	Tetrahydrobiopterin
BP	Blood pressure
bpm	Beats per minute
BSA	Bovine serum albumin
CaMKK	Calcium calmodulin-dependant kinase kinase
CEU	Contrast enhanced ultrasound
cGMP	cyclic guanosine monophosphate
EDL	Extensor Digitorum Longus
ELISA	Enzyme linked immuno-sorbent assay
ESMIRO	Endothelium specific mutant insulin receptor over expression
eNOS	Endothelial nitric oxide synthase
FFAs	Free fatty acid
nNOS	neuronal nitric oxide synthase
EPI	epitrochlearis
ERK	extracellular signal-regulated kinase
FBF	Femoral blood flow
FVR	Femoral vascular resistance
GIR	Glucose infusion rate

GU	Glucose uptake
GLUT4	Insulin-responsive glucose transporter
HFF	High fat fed
HGO	Hepatic glucose output
HLGU	Hindleg glucose uptake
HR	Heart rate
HPLC	High performance liquid chromatography
HUVEC	Human umbilical vein endothelial cells
IGF-1	Insulin-like growth factor
IMCR	Insulin mediated microvascular perfusion
IMGU	Insulin mediated glucose uptake
iNOS	Inducible nitric oxide synthase
IR	Insulin receptor
IRS	Insulin receptor substrate
LKB1	Peutz-Jeghers syndrome kinase LKB1
L-NAME	N ^ω -Nitro-L-arginine-methyl ester hydrochloride
L-NMMA	N ^G -monomethyl-L-arginine
L-NA	N ^ω -Nitro-L-arginine
MAP	Mean arterial pressure
MAPK	Mitogen activated protein kinase
MB	Microbubble
MFR	Microvascular flow rate
MV	Microvascular volume
MVEC	Microvascular endothelial cells
1-MU	1-methyl urate
1-MX	1-methyl xanthine
NE	Norepinephrine
NHGO	Net hepatic glucose out-put
NIDDM	Non-insulin dependant diabetes mellitus (type 2 diabetes)
nNOS	Neuronal nitric oxide synthase
NO	Nitric oxide
NOS	Nitric oxide synthase
PI3K	Phosphoinositide 3-kinase

PKC	Protein kinase C
Plan	Plantaris
Ra	Rate of glucose appearance
Rd	Rate of glucose disappearance
RG	Red gastrocnemius
R'g	Glucose uptake
R.U.	Resistance units
SEM	Standard error of the mean
SNS	Sympathetic nervous system
Sol	Soleus
TNF-	Tumour necrosis factor
VENIRKO	Vascular endothelial cell insulin receptor knock-out
VR	Vascular resistance
VSMC	Vascular smooth muscle cell
WG	White gastrocnemius
WT	Wild type
XO	Xanthine oxidase
ZMP	5-aminoimidazole-4-carboxamide ribotide
[³ H] 2-DG	2-Deoxy-D-[2,6- ³ H] glucose
[¹⁴ C] 2-DG	2-Deoxy-D-[1- ¹⁴ C] glucose
[³ H] glucose	D-[3- ³ H] glucose

PREFACE

Some of the data presented in this thesis has been published or presented at scientific meetings as listed below.

LIST OF PUBLICATIONS DIRECTLY ARISING FROM THIS THESIS

Rattigan S., **Bradley E. A.**, Richards S.M. and Clark M.G., *Muscle metabolism and control of capillary blood flow: insulin and exercise*. Essays Biochem, 2006. **42**: p. 133-44.

Bradley E. A., Clark M.G. and Rattigan S., *Acute effects of wortmannin on insulin's hemodynamic and metabolic actions in vivo*. Am. J. Physiol. Endocrinol. Metab., 2007. **292** (3): p. E779-87.

Bradley E. A., Eringa E. C., Stehouwer C. D. A., Korstjens I., van Nieuw Amerongen G. P., Verloop R. E., Musters R., Sipkema P., Clark M. G. and Rattigan S., *Activation of AMPK by AICAR in the muscle microcirculation acutely increases NO activity and microvascular perfusion*. Arteriosclerosis, Thrombosis, and Vascular Biology. 2009. (Manuscript under review).

Bradley E. A., Clark M. G. and Rattigan S., *Acute In Vivo Effects of AICAR Administration upon Microvascular Perfusion and Insulin-mediated Glucose Metabolism in the Rat*. 2009. (Manuscript in preparation).

OTHER PUBLICATIONS

Vollus G., **Bradley E. A.**, Roberts M.K., Newman J. M. B., Richards S. M., Rattigan S., Barrett E. J. and Clark M.G., *Graded occlusion of perfused rat*

muscle vasculature decreases insulin action. Clin Sci (Lond), 2007. **112**(8): p. 457-66.

Bradley E. A., Willson K., Choi-Lundberg D., Clark M. G. and Rattigan S.
Effects of central administration of insulin or L-NMMA on rat skeletal muscle microvascular perfusion. Am. J. Physiol. Endocrinol. Metab. 2009.
(Submitted for publication)

ORAL PRESENTATIONS AT SCIENTIFIC MEETINGS

Frontiers in Vascular Medicine, 2nd International Conference. Melbourne, VIC, Australia. October 2007. **Bradley E. A.**, Eringa E. C., Stehouwer C. D. A, Korstjens I., van Nieuw Amerongen G. P., Verloop R. E., Musters R. and Sipkema P., Clark M. G. and Rattigan S., *AICAR administration vasodilates isolated resistance arteries by enhancing NO sensitivity of smooth muscle in vitro and stimulates capillary recruitment in muscle in vivo.* (Presented by Stephen Rattigan)

AMPK in sickness and Health: From Molecules to Man. Snekkersten, Denmark. 2008. Rattigan S., **Bradley E. A.**, Eringa E. C. *AMPK and muscle microvascular blood flow.* Menzies Research Institute, University of Tasmania, Hobart, Australia and Institute for Cardiovascular Research, VU University Medical Center, Amsterdam, The Netherlands. (Presented by Stephen Rattigan)

POSTERS AT SCIENTIFIC MEETINGS

American Diabetes Association 62nd Scientific Sessions. San Francisco, USA. June 2002. Wheatley, C. M., **Bradley E. A.**, Wallis M.G., Rattigan S., Richards S. M., Barret E. J. and Clark M. G., *Contraction-mediated capillary recruitment is not impaired in muscle of insulin resistant obese Zucker rats*. Diabetes, Vol. 51, Suppl. 2: A564: 2333-PO. (Presented by M.G. Clark)

American Diabetes Association 63rd Scientific Sessions. New Orleans, Louisiana, USA. June 2003. **Bradley E. A.**, Zhang L., Newman J. M., Richards S. M., Clark M. G. and Rattigan S., *Acute, Divergent Effects of AICAR on Insulin Action in vivo*. Diabetes. Vol. 52, Suppl. 1: A344, 490-PO. (Presented by E. A. Bradley)

American Diabetes Association 63rd Scientific Sessions. New Orleans, Louisiana, USA. June 2003. Rattigan S., **Bradley E. A.**, and Clark M. G., *Effects of wortmannin on insulin-mediated action in vivo*. Diabetes, Vol. 52, Suppl. 1: A543. (Presented by S. Rattigan)

Muscle Research Group, University of Tasmania, "Diabetes and Exercise: Impact of Muscle Blood Flow". Freycinet, Tasmania, Australia. August 2004. **Bradley E. A.**, Rattigan S. and Clark M. G. *Effects of Wortmannin on Insulin-Mediated Action in Vivo*. (Presented by E. A. Bradley)

American Diabetes Association 64th Scientific Sessions. Orlando, Florida, USA. June 2004. Wheatley, C.M., Barrett, E.J., **Bradley, E.A.**, Richards, S.M., Clark, M.G. and Rattigan, S., *Muscle capillary recruitment and glucose uptake of genetically obese rats responds to contractions but not insulin*. Diabetes, Vol. 53, Suppl. 2: A371. (Presented by Clark, M.G)

American Diabetes Association (ADA) 66th Scientific Sessions. Washington, DC, USA. June 2006. **Bradley E. A.**, Clark M. G. and Rattigan S. *Acute*

AICAR Infusion Stimulates Capillary Recruitment in Rat Skeletal Muscle.
Diabetes, Vol. 55, Suppl. 1. A336, 1444-PO. (Presented by S. Rattigan)

American Diabetes Association (ADA) 67th Scientific Sessions. Chicago, IL, USA. June 2007. **Bradley E. A.**, Ross R. M., Clark M. G., McConell G. K. and Rattigan S., *Local L-NAME Administration Blocks Insulin-mediated but not Contraction-mediated Capillary Recruitment in Rat Hindleg Muscles.* Diabetes, Vol. 56, Suppl. 1. A397, 1558-PO. (Presented by S. Rattigan)

European Association for the Study of Diabetes (EASD) 44th Annual Meeting. Rome, Italy, September 2008. Genders A. J., **Bradley E. A.**, Richards S. M., Clark M.G. and Rattigan S., *Zaprinast Acutely Augments Insulin-mediated Capillary Recruitment and Glucose Disposal in Rats In Vivo.* (Presented by A. J. Genders)

European Association for the Study of Diabetes (EASD) 44th Annual Meeting. Rome, Italy, September 2008. Clark M. G., **Bradley E. A.**, Willson K., Choi-Lundberg D., Richards S. M. and Rattigan S. *Insulin-mediated capillary recruitment in muscle is sensitive to intra-cerebroventricular NOS inhibitor.* (Presented by M. G. Clark)

Australian Diabetes Society and Australian Diabetes Educators Association, Annual Scientific Meeting. Adelaide Convention Centre, South Australia, Australia. August 2009. Genders, A. J., **Bradley E. A.**, Keske, M. A., Rattigan, S. and Richards S. M. *cGMP Phosphodiesterase Inhibition Improves the Vascular and Metabolic Actions of Insulin in Skeletal Muscle.* (Presented by S. M. Richards)

TABLE OF CONTENTS

ACKNOWLEDGEMENTS..... IV

STATEMENT I

AUTHORITY OF ACCESS I

LIST OF ABBREVIATIONS..... V

PREFACE VIII

LIST OF PUBLICATIONS DIRECTLY ARISING FROM THIS

THESIS viii

OTHER PUBLICATIONS..... viii

ORAL PRESENTATIONS AT SCIENTIFIC MEETINGSix

POSTERS AT SCIENTIFIC MEETINGS x

ABSTRACT II

CHAPTER 1 1

Introduction 1

1.1 Insulin2

1.2 Effects of Insulin on Total Flow in Skeletal Muscle3

1.3 Insulin Stimulated Microvascular Perfusion in Skeletal Muscle 4

1.3.1 Anatomy of Skeletal Muscle Microvasculature5

1.3.1.1 The Endothelial Barrier7

1.3.2 Evidence for Macrovascular and Microvascular flow Routes in Muscle 7

1.3.3 Techniques for Measuring Microvascular Blood Flow.....9

1.4 Physiological Relevance of Blood Flow on Glucose Uptake10

1.5 Mechanisms for the Vascular Actions of Insulin.....11

1.6 Role of Nitric Oxide during Insulin12

1.7 Mechanisms for Insulin-mediated Increases in Microvascular

Perfusion15

1.8 Insulin Signalling Pathways16

1.8.1 Mitogen-activated Protein Kinase Cascade.....17

1.8.2 Wortmannin.....18

1.9	Insulin Resistance	19
1.9.1	Impaired Total Flow Response in Insulin Resistance	21
1.9.2	Impaired Microvascular Flow in Insulin Resistance	21
1.10	Exercise and Insulin Sensitivity	22
1.10.1	Exercise Increases Glucose Uptake.....	22
1.10.2	Exercise Increases Insulin Sensitivity	23
1.11	AMP-Activated Protein Kinase.....	24
1.11.1	Structure of AMPK	25
1.11.1.1	AMPK Subunits	26
1.11.2	Regulation of AMPK.....	27
1.11.3	Activators of AMPK	27
1.11.3.1	Exercise	28
1.11.3.2	AICAR.....	28
1.11.3.3	Antidiabetic Drugs	30
1.11.3.4	Other AMPK Activators.....	31
1.12	Role of AMPK in the Vasculature	32
1.13	AICAR Stimulated Glucose Uptake	33
1.13.1	Limitations of AICAR.....	35
1.14	The Present Study: Summary and Aims	37
CHAPTER 2	39	
Materials and Methods	39	
2.1	<i>In Vivo</i> Experiments	40
2.1.1	Animal Care	40
2.1.2	Surgical Procedures	40
2.1.2.1	Contrast Enhanced Ultrasound (CEU)	41
2.1.2.2	The Epigastric Artery Technique	43
2.1.3	<i>In Vivo</i> Experimental Procedures	45
2.1.3.1	Blood Sampling.....	45
2.1.3.1.1	Glucose and Lactate Assay.....	45
2.1.3.1.2	Plasma Insulin Assay (ELISA).....	45
2.1.4	Euglycaemic Hyperinsulinemic Clamp Technique	46
2.1.4.1	Glucose Homeostasis	47
2.1.5	Glucose Tracers	48
2.1.5.1	Whole Body Rate of Glucose Disposal	48
2.1.5.2	Muscle Specific Glucose Uptake (R'g).....	49
2.1.6	Experimental Protocols	51
2.1.6.1	Wortmannin Protocol	51
2.1.6.2	Local L-NAME Protocol.....	51
2.1.6.3	AICAR Protocols	52
2.1.7	Infusate Preparation.....	52
2.1.7.1	Insulin.....	52
2.1.7.2	Glucose.....	52
2.1.7.3	1-MX and Allopurinol.....	52

2.1.7.4	Microbubbles.....	53
2.1.8	Techniques for Measuring Microvascular Perfusion	53
2.1.8.1	1-MX Metabolism Measurements.....	53
2.1.8.2	Contrast Enhanced Ultrasound (CEU)	55
2.1.9	Muscle ZMP and AICAR Assay	61
2.1.10	Western Blots	62
2.2	<i>In Vitro</i> Experiments	63
2.2.1	Animal Care	63
2.2.2	Preparation and Set-up for the Isolated Vessels.....	63
2.2.3	Isolated Endothelial Cells.....	65
2.3	Data Analysis	65
2.4	Statistical Analysis.....	65
CHAPTER 3		66
Acute Effects of Wortmannin on Haemodynamic and Metabolic Actions of Insulin <i>In Vivo</i>		66
3.1	INTRODUCTION.....	67
3.1.1	Aim of the Study	69
3.2	RESEARCH AND DESIGN METHODS	69
3.2.1	Animals	69
3.2.2	<i>In Vivo</i> Experiments	69
3.2.3	Experimental Protocols	70
3.2.3.1	Microvascular Perfusion.....	71
3.2.3.2	Muscle Specific Glucose Uptake (R'g).....	72
3.2.3.3	Whole Body Rate of Glucose Disposal	72
3.2.3.4	Blood Sampling.....	72
3.2.4	Plasma Insulin Assay.....	73
3.2.5	Western Blots for P-Akt	73
3.2.6	Data Analysis	73
3.2.7	Statistical Analysis	73
3.3	RESULTS.....	75
3.3.1	Plasma Insulin and Glucose.....	75
3.3.2	Glucose Metabolism.....	77
3.3.3	Haemodynamic Effects	81
3.3.4	1-MX Metabolism: Microvascular Perfusion.....	85
3.3.5	Western Blots for P-Akt and Akt _{total}	87
3.4	DISCUSSION.....	89
CHAPTER 4		94
Effects of Nitric Oxide Synthase Inhibition on the Actions of Insulin in Muscle.....		94

4.1	INTRODUCTION	95
4.1.1	Aim of the Study	96
4.2	RESEARCH AND DESIGN METHODS	97
4.2.1	Animals	97
4.2.2	Surgical Preparation	97
4.2.3	Preliminary Experiments	97
4.2.4	Experimental Protocols	98
4.2.4.1	Microvascular Perfusion.....	100
4.2.4.2	Technique for 2-Deoxy Glucose Measurement.....	100
4.2.4.2.1	Blood Sampling.....	100
4.2.5	Data Analysis	101
4.2.6	Statistical Analysis	101
4.3	RESULTS.....	102
4.3.1	Glucose Metabolism.....	102
4.3.2	Haemodynamic Effects	105
4.3.3	Microvascular Perfusion.....	110
4.4	DISCUSSION.....	112
CHAPTER 5	116
Acute Effects of AMPK Activation by AICAR on Muscle Microvascular		
Perfusion <i>In Vivo</i> & Isolated Muscle Resistance Arteries <i>In Vitro</i> 116		
5.1	INTRODUCTION	117
5.1.1	Aim of the Study	118
5.2	RESEARCH AND DESIGN METHODS	118
5.2.1	Animals	118
5.2.2	<i>In vitro</i> Experiments.....	118
5.2.2.1	Preparation of Isolated Resistance Arteries.....	118
5.2.2.2	Preparation of Isolated Endothelial Cells.....	119
5.2.2.3	Enzyme Activation and Phosphorylation	119
5.2.3	<i>In vivo</i> Experiments.....	120
5.2.3.1	Experimental Protocols	120
5.2.3.2	Plasma AICAR Assay	123
5.2.3.3	Skeletal Muscle AICAR and ZMP Assay	123
5.2.3.4	Microvascular Perfusion <i>In Vivo</i>	123
5.2.3.4.1	Microbubbles.....	123
5.2.4	Data Analysis	124
5.2.5	Statistics for <i>In Vitro</i> Studies.....	124
5.2.6	Statistics for <i>In Vivo</i> Studies	124
5.3	RESULTS.....	125
5.3.1	<i>In Vitro</i> Effects of AICAR	125
5.3.1.1	Effects of AICAR on Isolated Resistance Arteries	125
5.3.1.2	Effects of AICAR on Endothelial Cells	126
5.3.2	<i>In Vivo</i> Effects of AICAR	130

5.3.2.1	Plasma and Muscle AICAR and Muscle ZMP Content	130
5.3.2.2	Glucose Metabolism	131
5.3.2.3	Haemodynamic Changes	132
5.3.2.4	Microvascular Perfusion.....	134
5.4	DISCUSSION.....	138
CHAPTER 6	142
Acute Effects of AICAR on Haemodynamic and Metabolic Actions of		
Insulin <i>In Vivo</i>		142
6.1	INTRODUCTION	143
6.1.1	Aim of the Study	144
6.2	RESEARCH AND DESIGN METHODS	144
6.2.1	Animals	144
6.2.2	<i>In Vivo</i> Experiments	144
6.2.2.1	Experimental Protocols	145
6.2.2.1.1	Euglycaemic Hyperinsulinemic Clamp.....	146
6.2.2.2	Plasma Insulin Assay.....	149
6.2.2.3	Plasma AICAR Assay	149
6.2.2.4	Skeletal Muscle AICAR and ZMP Assay	149
6.2.2.5	Microvascular Perfusion Measurement <i>In Vivo</i>	150
6.2.2.5.1	Microbubbles.....	150
6.2.3	Data Analysis	151
6.2.4	Statistical Analysis	151
6.3	RESULTS.....	152
6.3.1	Plasma Insulin and AICAR Content	152
6.3.2	Muscle AICAR and ZMP Content	153
6.3.3	Glucose Metabolism	154
6.3.4	Lactate Metabolism	159
6.3.5	Haemodynamic Measurements	160
6.3.6	Microvascular Perfusion.....	163
6.3.7	Additional Experiments: Glycogen Depleted.....	166
6.3.7.1	Glucose Metabolism.....	166
6.4	DISCUSSION.....	168
CHAPTER 7	172
General Discussion		
7.1	Major Findings	173
7.2	Insulin Mediated Microvascular Perfusion and its Effects on	
Glucose Uptake.....		174
7.3	Involvement of NO in Insulin Action.....	177

7.4	Microvascular Perfusion: Dependant on PI3K	177
7.5	Local NOS Inhibition: Blocks Insulin Action	178
7.6	AMPK Activation Stimulates Microvascular Perfusion by Association with NO.....	178
7.7	Other Future Directions	179
7.8	Conclusions	181
	REFERENCES	182

CHAPTER 1

Introduction

The ability of insulin to maintain glucose homeostasis in healthy individuals is well known, following a meal insulin acts to stimulate glucose disposal and inhibit hepatic glucose production [1]. More recently it has been demonstrated that insulin increases microvascular flow by increasing the number of perfused capillaries in skeletal muscle vascular beds [2]. The physiological effect of insulin to increase blood flow to peripheral tissues may promote cellular glucose uptake by increasing hormone and nutrient access to muscle. In insulin resistance, the precursor to type 2 diabetes, the increases in capillary blood flow and glucose uptake become unresponsive to stimulation via insulin [2]. Physical activity which has been shown to be protective against the development of insulin resistance also stimulates capillary recruitment. A greater understanding of the vascular mechanisms used by insulin and muscle contraction will provide targets for future drug therapies for type 2 diabetes.

1.1 Insulin

Insulin is a peptide hormone, produced in the pancreas by the β cells of the islets of Langerhans. Insulin acts as a regulator during periods of glucose surplus, by promoting peripheral glucose uptake and hepatic glucose storage following a meal. Following ingestion of a carbohydrate containing meal, a rise in plasma glucose concentration initiates insulin release into the bloodstream which stimulates glucose transport in insulin responsive tissues (skeletal muscle and adipose tissue) by causing GLUT4 translocation to the plasma membrane. Skeletal muscle accounts for up to 75% of insulin-dependant glucose disposal, whereas adipose tissue accounts for a small portion [3]. In the liver, insulin acts to suppress glucose production by inhibiting gluconeogenesis and glycogenolysis and stimulates glycogen storage. The additional longer term cellular effects of insulin include growth promotion, protein synthesis and gene regulation.

1.2 Effects of Insulin on Total Flow in Skeletal Muscle

In addition to insulin's direct metabolic effects on glucose homeostasis, interest in insulin's vasodilatory activity in skeletal muscle has increased in recent years. It has been proposed that the vasodilatory actions of insulin to increase blood flow to skeletal muscle improve delivery of glucose and nutrients as well as its own access [2]. In 1990, Baron and colleagues first reported the concept that insulin may function to increase blood flow and improve substrate delivery to skeletal muscle. Baron's group demonstrated that high physiological concentrations of insulin, in lean human subjects, increased total flow to skeletal muscle [4] during hyperinsulinemic euglycaemic clamps. In support of these findings, increased total blood flow due to insulin was also observed following intravenous glucose, oral glucose and a carbohydrate meal [5]. In addition Baron *et al.* demonstrated that insulin sensitivity was decreased in obese humans, measured by both lower glucose extraction and lower total blood flow to insulin sensitive tissues, compared to lean subjects [4]. Subsequent experiments have confirmed that insulin mediated increases in total flow and decreases in vascular resistance are impaired in obese and type 2 diabetic subjects compared with lean controls [6-9].

Insulin-mediated increases in total blood flow have been demonstrated by others in humans [6, 7] as well as in animals [8] however there was considerable variation in the extent of this vascular response to insulin. In contrast, other studies observed no changes in flow with insulin [9-13]. Studies by Sjostrand *et al.* [14] on type 2 diabetic subjects suggested that decreased insulin-mediated glucose uptake is caused by insulin resistance at the cellular level rather than impaired access of insulin and glucose to the myocyte. The physiological relevance of decreased total blood flow was challenged by investigators who have found that blood flow had a minor influence on insulin stimulated glucose uptake [15], skeletal muscle interstitial glucose [16] and insulin levels [17]. Some researchers have shown the direct effect of local hyperinsulinemia in humans had no effect [13, 18, 19] or only

slight vasodilation [20, 21] in large vessels. Cardillo *et al.* [22] demonstrated that in humans systemic but not local hyperinsulinemia induced large vessel vasodilation in the forearm. The total flow effects observed during systemic infusion suggests that centrally mediated sympathetic changes may play a role. In contrast, Hermann *et al.* [23] demonstrated that four hours of local hyperinsulinemia caused a sustained increase in vasodilation in resistance vessels of healthy humans. The type of administration may have been important as vasodilation was greater with systemic rather than local infusion. Methodological differences including insulin dose and technique of flow measurement as well as individual heterogeneity in vascular response to insulin may account for some of the differences noted.

The effect of insulin on total flow was most pronounced when circulating concentrations of insulin during systemic hyperinsulinemia are supra-physiological or when insulin was administered over extended time periods [24]. Thus, some have questioned the physiological relevance of these observations since high levels of insulin are not normally sustained following a meal.

1.3 Insulin Stimulated Microvascular Perfusion in Skeletal Muscle

Earlier studies on the vascular actions of insulin had focused on the effect of insulin to increase total blood flow to skeletal muscle however more recent studies have highlighted the importance of insulin upon the microcirculation to increase capillary surface area for enhanced delivery of insulin and glucose to the myocytes. It was demonstrated that insulin has direct vasodilatory action on peripheral vessels, mainly in skeletal muscle vascular beds to increase microvascular flow to ensure adequate supply of glucose and nutrients [2, 24-26]. A study from Vincent *et al.* [27] indicated that insulin mediated vasodilation occurred rapidly in muscle microvasculature and was then followed by relaxation of larger vessels leading to increased total flow in muscle.

1.3.1 Anatomy of Skeletal Muscle Microvasculature

The microvasculature is widely taken to include vessels less than 150 μ m in diameter and includes arterioles, capillaries and venules. The anatomical arrangement of muscle microvasculature has been mapped using muscles such as the cremaster, hamster retractor, tenuissimus or the spinotrapezius since the anatomical properties of these muscles allows relatively easy access for visualization. Many similarities exist between the microvasculature of these muscle types however consideration must be given to the specialized nature of these muscles compared with load bearing skeletal muscle. Sweeney *et al.* [28] classified the arrangement of arterioles in the hamster cremaster as follows; blood flows to a skeletal muscle from a feed artery, which is external to the muscle. Within the muscle the first branch of the arteries are classified as a first order arteriole. Subsequent branches are numbered in increasing order, with transverse arterioles being third order and fifth-order arterioles lead to the capillaries [29]. Flow to muscles is controlled by the first to third-order arterioles and flow to individual capillary networks is controlled by third to fifth-order arterioles [30]. A study by Borgstrom [31] schematically illustrates (Figure 1, pg. 6) the vasculature in the rabbit tenuissimus muscle, the transverse arteriole supplies capillaries, muscle tissue and adjacent connective tissue. During the basal state, muscle is minimally perfused [29, 32, 33] and undergoes vasomotion [34], a rhythmic fluctuation of microvascular blood flow, which is thought to be a protective mechanism against hypoxia.

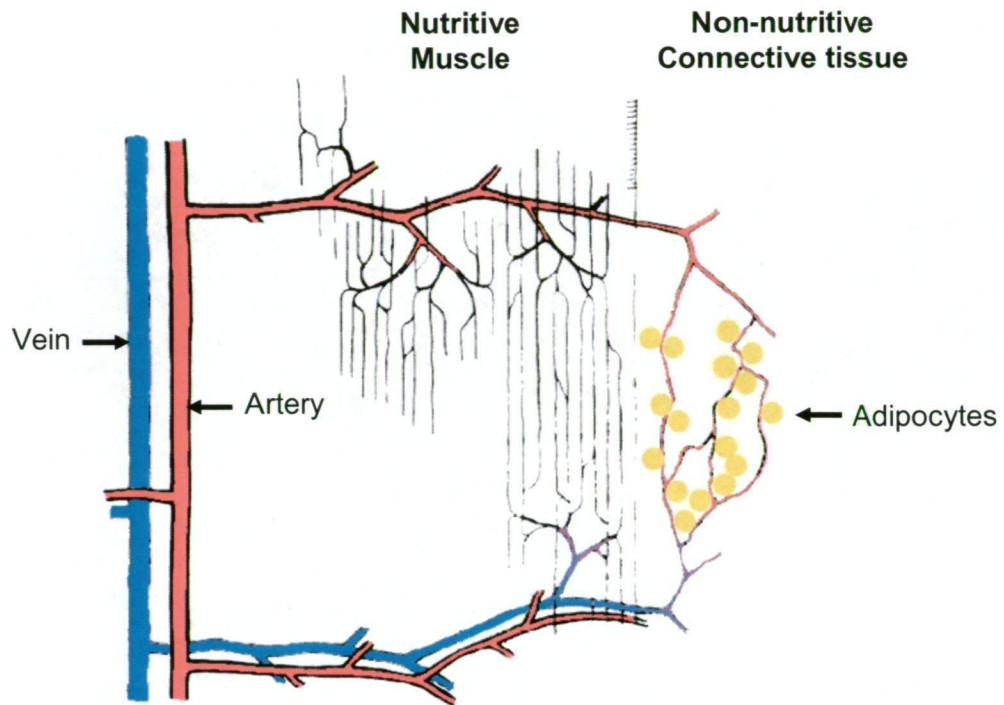


Figure 1: Blood flow in the rabbit tenuissimus muscle (adapted from Borgstrom *et al.*, 1988 [31] to show connective tissue adipocytes)

The principal function of the microcirculation is to optimize nutrient and oxygen supply to tissues in response to various physical stimuli. At the microvascular level insulin mediated vasodilation begins when insulin acts at the terminal arterioles thus increasing the number of perfused capillaries. As noted by Vincent *et al.* this action occurs within a few minutes [27]. This is followed by relaxation of larger resistance vessels which increase the total blood flow [35]. Dilation of terminal arterioles can result in maximal recruitment of downstream capillaries without initially altering the total blood flow [36]. This may occur due to the redistribution of blood flow between two vascular routes within the muscle, termed nutritive and non-nutritive (described further in section 1.3.2).

1.3.1.1 The Endothelial Barrier

The endothelium is a single layer of cells that lines the lumen of all blood vessels including; conduit vessels, resistance vessels, pre-capillary arterioles and capillaries. The endothelial layer is in direct contact with the circulating blood and vessel wall and plays an important role in maintaining vascular function. The vessel wall endothelium adjusts vascular tone and permeability by secreting vasoactive substances such as NO, endothelin, prostacyclin and endothelium-derived hyperpolarising factors. It has been demonstrated that endothelial cells have insulin receptors and that insulin stimulates phosphorylation and activation of Akt which can phosphorylate and activate eNOS to induce NO production and vasorelaxation [37, 38].

Endothelial dysfunction has been linked to the initiation and development of atherosclerotic vascular diseases [39, 40] and is associated with an imbalance between vasodilator and vasoconstrictor activity due to reduced NO activity. Insulin is reported to increase blood flow and microvascular perfusion via production of NO [41] (see section 1.6) thus endothelial dysfunction may contribute to impaired vascular actions of insulin in insulin resistance.

1.3.2 Evidence for Macrovascular and Microvascular flow Routes in Muscle

Evidence for different flow routes in muscle came from experiments using the pump-perfused rat hindlimb. These early studies indicated the existence of separate total blood flow and microvascular blood flow routes in skeletal muscle. These two flow routes have been termed nutritive and non-nutritive, a concept which has been extensively researched in our laboratory (reviewed in [2]). The nutritive route is thus named as it is thought to consist of long tortuous capillaries which are in direct contact with muscle cells. The non-nutritive flow route is thought to consist of shorter and possibly larger capillaries of lower resistance which supply the muscle connective tissue (septa and tendon) [42] as well as associated adipocytes [43] (Figure 1). It has

been proposed that the non-nutritive route can act as a flow reserve which can rapidly redistribute flow to the nutritive route during periods of high metabolic demand such as exercise [44] and insulin. It is thought that the balance between these two flow routes is controlled by vasomodulators and neural input [45].

The agents which control metabolism in constant-flow pump perfused skeletal muscle by vasoconstriction have been classified as either type A or type B vasoconstrictors [46]. Type A vasoconstrictors include low-dose norepinephrine (NE), angiotensin II, vasopressin and low frequency sympathetic nerve stimulation (SNS). Type A vasoconstrictors are thought to constrict non-nutritive feed arterioles and thus re-direct flow to the nutritive route increasing oxygen consumption. Type B vasoconstrictors including serotonin, high-dose NE and high frequency SNS activation result in reduced oxygen consumption and metabolism by decreasing perfusion to the nutritive route [46]. During type B vasoconstriction the sites for constriction are likely to be large vessels which can sustain constriction by anaerobic metabolism. The changes in flow distribution from type A and B vasoconstrictors have been suggested from the patterns of red blood cell washout and visualisation using vascular casts [47].

The pump perfused hindlimb studies enabled important initial observations for the presence of two flow routes in skeletal muscle. These early findings may explain previous observations of the ability of many systemic vasodilators to markedly increase limb blood flow without affecting insulin-mediated glucose uptake [15, 48]. Studies on microvascular flow routes in intact animals were lacking and so what followed was the development of specific techniques for measuring changes in microvascular perfusion *in vivo*.

1.3.3 Techniques for Measuring Microvascular Blood Flow

Direct evidence for insulin-mediated microvascular flow *in vivo* first appeared in 1997 when Rattigan, Clark and colleagues developed the 1-methylxanthine (1-MX) method in rats [49]. This technique is based on the metabolism of infused 1-MX which is an exogenous substrate for xanthine oxidase (XO). Xanthine oxidase exists in many tissues, however immunohistochemical evidence had shown that in rodent muscle XO is concentrated in the capillary endothelium with much less in the endothelium of large arteries, vascular smooth muscle and skeletal muscle [50, 51]. The substrate 1-MX was selected because it does not alter haemodynamics, is converted to a single product 1-methylurate (1-MU), is not further metabolized, the metabolism of 1-MX is solely due to XO and both 1-MX and 1-MU are easily detectable using HPLC [52]. The extent of the metabolism of infused 1-MX reflects the availability of capillary surface area and provides a measurement of microvascular perfusion.

The newly developed 1-MX method was initially validated in the pump-perfused rat hindlimb by altering the flow distribution using specific vasoconstrictors to enable predominantly nutritive or non-nutritive flow patterns [53, 54]. It was demonstrated that the change in 1-MX metabolism correlated positively with various nutritive or non nutritive states. For example in the constant flow perfused hindlimb, it was demonstrated using a vasoconstrictor serotonin which reduces nutritive flow, that there was reduced conversion of 1-MX to 1-MU [52]. Additionally, under conditions which were positive for microvascular perfusion such as muscle contraction, there was an increased conversion of 1-MX to 1-MU in the constant flow pump perfused hindlimb [54].

After initial testing in the perfused hindlimb, the 1-MX method was subsequently applied to the anaesthetized rat *in vivo*. It was demonstrated that physiological doses ($3\text{mU}\cdot\text{min}^{-1}\cdot\text{kg}^{-1}$) and high doses ($10\text{mU}\cdot\text{min}^{-1}\cdot\text{kg}^{-1}$) of insulin increased 1-MX metabolism by approximately 80% [49] and it was observed that this increase was associated with increases in muscle glucose

uptake. Epinephrine administration *in vivo* increased total blood flow to the same extent as high dose insulin but did not alter microvascular perfusion [49]. This observation indicated that microvascular perfusion does not depend on total flow *in vivo* [55].

A second more recent method employed to measure microvascular perfusion is contrast enhanced ultrasound (CEU) imaging. An advantage of the CEU imaging technique over 1-MX is that it can be used in humans as well as animals, is less invasive and allows continuous real-time assessment of microvascular perfusion under various stimuli [56-58]. The technique is based on that described by Wei *et al.* [59] for the myocardium. The method involves systemic infusion of gas filled albumin or phospholipid microbubbles as a contrast agent which is detected by the ultrasound probe positioned over the area of interest (methodological details in section 2.1.8.2). The acoustic signal generated from the microbubbles when exposed to ultrasound produces tissue opacification which is proportional to the number of microbubbles within the imaged area. In animals, physiological doses of insulin lead to increases in microvascular volume [58, 60]. Comparisons of measures of microvascular perfusion using CEU and 1-MX methods in animals treated with insulin and contraction have demonstrated excellent correlation [60-62].

1.4 Physiological Relevance of Blood Flow on Glucose Uptake

As previously discussed, initial studies in the pump perfused rat hindlimb gave recognition to the presence of a non-nutritive route in muscle which may explain the ability of many systemic vasodilators to markedly increase limb blood flow without affecting insulin-mediated glucose uptake or ameliorating insulin resistance. The development of 1-MX and CEU techniques allowed further insights into the relationship between total blood flow, microvascular perfusion and glucose uptake. It was demonstrated by Vincent *et al.* [27] using the CEU technique, that insulin-stimulated increases in microvascular flow occur within minutes, prior to increases in total flow. In

that same study a tight and positive correlation between microvascular perfusion and glucose uptake in the same muscle bed indicated that microvascular perfusion contributes to insulin-mediated increases in glucose uptake *in vivo*. Zhang *et al.*, using CEU and 1-MX techniques also demonstrated that microvascular perfusion precedes increases in total blood flow [63]. In that study; microvascular perfusion was fully stimulated by physiological doses of insulin below the threshold for stimulation of glucose uptake or total blood flow. From these studies it became apparent that precapillary arterioles that regulate microvascular perfusion are more sensitive to insulin than resistance arterioles that regulate total blood flow. Together these observations may provide an explanation for reports which questioned the relevance of total blood flow where insulin mediated glucose uptake had been observed in the absence of increases in total blood flow [64, 65].

1.5 Mechanisms for the Vascular Actions of Insulin

There are a number of possible mechanisms by which insulin can cause vasodilation. In order to better understand these mechanisms it is useful to examine the action of insulin on cultured cells and isolated vessels. The results of *in vitro* studies must be viewed with caution since the conditions, which often use supraphysiological concentrations of insulin, do not necessarily reflect conditions *in vivo*. Insulin at high concentrations may interact with the insulin-like growth factor (IGF-1) receptor rather than the insulin receptor [66].

Insulin may mediate vasodilation directly by acting on the vascular smooth muscle cell (VSMC) or indirectly via metabolic stimulation within the myocytes. Studies by Chen and Messina *et al.* [67] and Schroeder *et al.* [68] suggest that insulin acts directly on blood vessels to induce dilation. Schroeder *et al.* [68] examined 1st order arterioles isolated from red and white gastrocnemius muscle. In that study it was demonstrated that physiological insulin (60 and 600pM) increased vessel diameter. Removal of the

endothelium or incubation with the nitric oxide synthase inhibitor N^G-nitro-L-arginine (L-NNA) abolished these effects.

Metabolic activation, similar to exercise, is where blood flow to muscle increases to facilitate supply of oxygen and nutrients to the working muscle via release of metabolic vasodilators such as adenosine, potassium, NO or lactate [69]. It has been suggested that lactate may induce skeletal muscle arteriolar dilation which is dependant on VSMC cGMP [70]. McKay and Hester [71] demonstrated that insulin mediated dilation of second and fourth-order arterioles was blocked by an adenosine receptor agonist, suggesting a role for adenosine in response to insulin.

While insulin may act directly on endothelial cells, it has been demonstrated that human VSMC express NOS [38] which is activated by insulin to increase cGMP. Increases in cGMP in human VSMCs following incubation with insulin (240-960pM) have been reported by Trovati *et al.* [72, 73]. Treatment with the NOS inhibitor N^G-monomethyl-L-arginine (L-NMMA) or the guanylate cyclase inhibitor methylene blue blocked this effect, indicating that insulin stimulates NOS in VSMCs.

In addition, insulin is known to activate the Na⁺/K⁺ ATPase in VSMC resulting in hyperpolarisation of the cell, blocking of voltage-dependant calcium channels and relaxation [74]. Insulin also decreases intracellular calcium by stimulating calcium efflux and inhibiting calcium influx by receptor-operated calcium channels leading to VSMC relaxation.

1.6 Role of Nitric Oxide during Insulin

Nitric oxide (NO) is a key signalling molecule that causes vascular relaxation. In endothelial cells, endothelial NO synthase (eNOS) catalyzes the conversion of the substrate L-arginine to the products NO and L-citrulline [75, 76]. The reaction requires co-factors such as Ca²⁺/calmodulin, flavin adenine, dinucleotide, flavin mononucleotide and tetrahydrobiopterin (BH₄) [77, 78].

The nNOS isoform, reported to be present in vascular smooth muscle [79], has an uncertain role in vascular function.

Vascular NO has a variety of functions and one of those is to dilate blood vessels and maintain vascular homeostasis. Vascular smooth muscle relaxation occurs when NO or NO donors diffuse to neighbouring VSMC and activate soluble guanylate cyclase which catalyses the production of guanosine 3':5'-cyclic monophosphate (cGMP) [80, 81]. Cyclic GMP is known to be involved in vasodilation by reducing intracellular Ca^{2+} in VSMC [82]. A number of compounds infused *in vivo* have demonstrated local vasodilation via endothelial NO, including acetylcholine, methacholine and bradykinin [83].

There is significant evidence available from *in vitro* studies which demonstrate that insulin's vasodilatory action in muscle is NO-dependant. Studies using cultured human umbilical vein endothelial cells (HUVEC) demonstrate that insulin stimulates the production of NO [37]. This process was shown to involve phosphoinositide 3-kinase (PI3K) and Akt [37, 38, 84]. Insulin has been shown to directly activate a signalling cascade leading to eNOS phosphorylation on cultured endothelial cells via IRS-1, PI3K and Akt [85]. Insulin induced (60-600pM) dilation of first-order arterioles was abolished with endothelial cell removal or L-NNA treatment [68], suggesting the involvement of endothelial cell derived NO.

Evidence from *in vivo* studies indicates that insulin's vasodilatory action in muscle is NO-dependant in support of *in vitro* findings. Steinberg *et al.* [41] demonstrated that local L-NMMA ($16\text{mg}\cdot\text{min}^{-1}$) following a 3 hour euglycaemic hyperinsulinemic clamp ($120\text{mU}\cdot\text{m}^{-2}\cdot\text{min}^{-1}$) in humans inhibited insulin-mediated vasodilation and blunted insulin-mediated leg glucose uptake by 25%. Baron *et al.* [86] reported that acute systemic administration of high doses of L-NMMA (30 and 15 $\text{mg}\cdot\text{kg}^{-1}$) in healthy male rats resulted in development of insulin resistance. Roy *et al.* [87] demonstrated in rats that systemic L-NAME ($30\text{mg}\cdot\text{min}^{-1}\cdot\text{kg}^{-1}$) during an insulin clamp ($64\text{mU}\cdot\text{min}^{-1}\cdot\text{kg}^{-1}$) significantly blunted muscle 2-DG uptake in soleus, red and white

gastrocnemius and tibialis muscles. Vincent *et al.* [88] reported that acute systemic infusion of L-NAME ($50\mu\text{g}\cdot\text{min}^{-1}\cdot\text{kg}^{-1}$) in rats completely inhibited insulin-mediated microvascular perfusion and blunted insulin-mediated glucose uptake (insulin clamp $10\text{mU}\cdot\text{min}^{-1}\cdot\text{kg}^{-1}$). Together with *in vitro* studies [68], this evidence indicates that insulin has a direct interaction with insulin receptors on the vascular endothelium for increased production of NO [37], which suggests an NO dependant mechanism by which insulin controls total blood flow and microvascular perfusion. Scherrer *et al.* [89] demonstrated that NOS inhibition by L-NMMA ($1\text{-}8\mu\text{mol}\cdot\text{min}^{-1}$) infused locally during a 2 hour hyperinsulinemic euglycaemic clamp ($6\text{pmol}\cdot\text{min}^{-1}\cdot\text{kg}^{-1}$) in humans blocked insulin mediated increases in total blood flow however glucose uptake was unchanged.

A study by Shankar *et al.* [90] examined the effects of acute central intracerebroventricular (ICV) administration of L-NMMA which resulted hyperglycaemia, hypertension and reduced glucose disposal rates by 22% during an insulin clamp ($12\text{mU}\cdot\text{min}^{-1}\cdot\text{kg}^{-1}$). Similarly, Bradley *et al.* [91] demonstrated that systemic insulin-mediated ($10\text{mU}\cdot\text{min}^{-1}\cdot\text{kg}^{-1}$) increases in limb blood flow, muscle microvascular perfusion and glucose uptake were significantly blocked by central L-NMMA ($500\mu\text{g}$ ICV). Together these data suggest that a central pathway that is NO-dependant may regulate peripheral insulin action. Thus central NO-dependant pathways may be involved in the pathogenesis of insulin resistance.

The aforementioned studies demonstrate that the haemodynamic actions of insulin are NO-dependant. One of the aims of the present thesis is to determine whether local infusion of the NOS inhibitor L-NAME during systemic insulin affects insulin's haemodynamic and metabolic actions in muscle.

1.7 Mechanisms for Insulin-mediated Increases in Microvascular Perfusion

The mechanism of insulin-mediated microvascular perfusion has not been fully resolved. Microvascular perfusion is likely to be mediated by third to fifth order arterioles whereas total flow is likely to be mediated by first to third order arterioles. It is now accepted that insulin has a direct vasodilator action on larger peripheral arterioles *in vitro* but it is not known whether a similar mechanism occurs in small arterioles.

Insulin signalling leading from the receptor to the activation of eNOS has been demonstrated using vascular endothelial cells. Small arterioles of the rat cremaster muscle respond to subcutaneously injected insulin (835pM insulin in serum) viewed by intravital microscopy [92]. Insulin receptors are present on endothelial, vascular smooth muscle and skeletal muscle cells so it is feasible that insulin has a direct effect on these cell types resulting in the formation of a vasodilator. It is likely that the vasodilator acts locally, diffusing from the site of formation to the VSMC of the terminal arterioles.

Current data from Vincent *et al.* [27] and Zhang *et al.* [63] suggest that insulin mediated microvascular perfusion occurs before increases in total flow. Clark *et al.* [2] suggests that flow is redistributed from the non-nutritive vessels to nutritive capillaries. A direct dilatory action of insulin on muscle micro-vessel endothelial cells is supported by evidence from euglycaemic hyperinsulinemic clamp studies where it was demonstrated that the NOS inhibitor, L-NAME, blunted microvascular perfusion [88]. In addition, methacholine, a NO producer, increases insulin-mediated microvascular perfusion and glucose uptake [93].

1.8 Insulin Signalling Pathways

The cellular effects of insulin begin when it binds to the cell surface insulin receptor (IR) [94, 95] and initiates activation signal transduction pathways that regulate diverse cellular functions [96]. There are two major signalling branches; the phosphoinositide 3-kinase (PI3K) branch of the cascade and mitogen activated protein kinase (MAPK) dependant pathway. The PI3K branch is involved in glucose metabolism and stimulation of NO production in the vascular endothelium. The MAPK branch mediates the non-metabolic mitogenic and growth effect of insulin and controls secretion of endothelin 1 (ET-1) in the vascular endothelium.

The insulin receptor (IR) is a large heterotetrameric glycoprotein containing two α -subunits (M_r 140kDa) and two β -subunits (M_r 95kDa) linked by disulfide bonds [97]. Insulin binding to the α -subunit leads to a conformational change [98] resulting in auto-phosphorylation of tyrosine residues of the transmembrane β -subunit which initiates intracellular signalling [99]. The first down stream targets of the β -subunit are the insulin receptor substrate (IRS) [100, 101] and Shc that serve as docking proteins for downstream signalling molecules [102]. Once phosphorylated the IRS proteins are able to bind to Shc homology (SH2) domain binding for effectors such as the PI3K complex [103] and Grb-2 leading to MAPK phosphorylation.

The actions of insulin that have been shown to depend on PI3K activity include stimulatory effects on glucose transport, glycogen synthesis, protein synthesis and inhibitory effects on lipolysis [104]. PI3K is a tightly associated heterodimeric enzyme consisting of a M_r 85,000 regulatory subunit and a M_r 110,000 catalytic subunit [105-108]. PI3K is activated by the binding of tyrosyl phosphorylated IRS-1 through the SH2 domain of the p85 subunit of PI3K [109]. Figure 2 illustrates a simplified representation of the insulin signalling, involving the PI3K cascade, leading to glucose uptake. PI3K catalyses the phosphorylation of the lipid product phosphatidylinositol 4,5-bisphosphate (PIP-2) on the D3 position of inositol [105] to PI 3,4,5-

triphosphate (PIP-3)[110]. PIP-3 binds and activates the signalling protein pleckstrin homology domain in 3-phosphoinositide-dependant protein kinase-1 (PDK-1). PDK-1 activates downstream effectors such as Akt and protein kinase C (PKC) [111-113]. The glucose transporter GLUT4 is then stimulated to migrate from the intracellular compartment to the plasma membrane [1, 114, 115] resulting in glucose transport into the cell. Akt has been implicated as a key signalling protein for several of the actions of insulin, including activation of glycogen synthesis, protein synthesis and GLUT4 translocation [111, 116, 117].

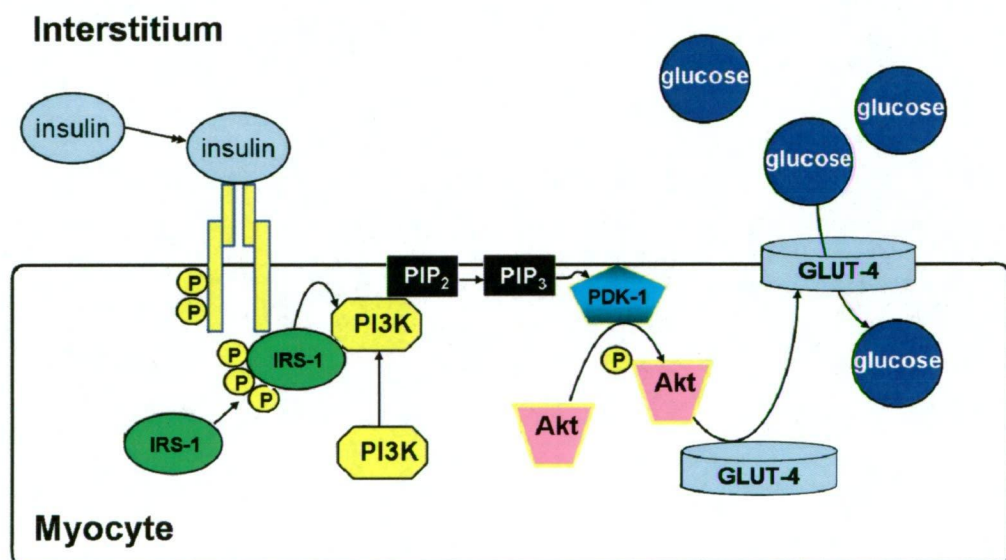


Figure 2: A simplified schematic diagram of the insulin signalling cascade in skeletal muscle leading to glucose uptake.

1.8.1 Mitogen-activated Protein Kinase Cascade

The MAPK-dependant branch of insulin-signalling pathway generally regulates biological actions such as growth, mitogenesis and differentiation. MAPK responds to extracellular stimuli and have been found to play a role in variety of cellular processes including inflammation, cell growth and

differentiation, cell cycle and cell death [118-121]. There are four subgroups within the MAPK family which include extracellular signal-regulated kinases (ERK), c-jun N-terminal or stress-activated protein kinases (JNK/SAPK), ERK5 or big MAP kinase 1 (BMK1) and the p38 group of protein kinases [120, 122, 123]. The p38 MAPK mitogen-activated protein kinases (p38 MAPKs) are activated by ischemia, exercise, muscle contraction, oxidative stress, heat shock and inflammation [124]. Studies using mouse skeletal muscle and L6 myotubes have indicated that p38 MAPK pathway may be involved in regulation of glucose transport [125]. Skeletal muscle contraction, which has been demonstrated to increase GLUT4- mediated glucose transport, has been shown to activate p38 MAPK [126]. Ischemia pre-conditioning in rat hearts increases glucose transport which been shown to is mediated by p38 MAPK [127]. Metabolic stress conditions such as contraction and hypoxia increase glucose uptake and AMPK activity in skeletal muscle which is also associated with p38 MAPK activation [128]. AICAR, an AMPK activator, increases phosphorylation and activity of both p38 and MAPK α and p38 MAPK β in EDL muscle [129]. It has been demonstrated by Xi *et al.* [130] in clone 9 cells, that p38 MAPK is a downstream component of AMPK signalling pathway in AICAR-stimulated glucose transport. This finding suggests that there are interactions between AMPK and the MAPK signalling pathway in the regulation of glucose transport.

1.8.2 Wortmannin

Studies of the role of PI3K have been facilitated by the availability of relatively specific inhibitors such as wortmannin and LY294002. Wortmannin is toxic to fungi and was originally isolated from the soil bacteria culture broth of *Penicillium wortmannii* [131]. The low molecular weight (MW = 428.4) cell permeable compound which has a sterol-like structure is shown in Figure 3 [132, 133] and is soluble in methanol and DMSO. Wortmannin has been extensively applied to cell cultures and is one of the major tools used to elucidate the biological functions of PI3K activation at a cellular level [134]. Studies using wortmannin have deduced that PI3K is essential for the

stimulation of glucose transport in adipocytes [105, 135] and skeletal muscle [136].

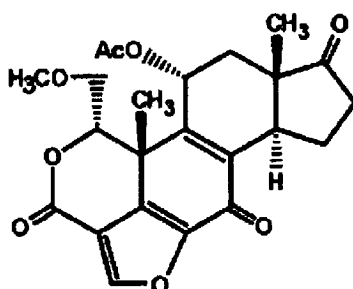


Figure 3: The chemical structure of wortmannin [134].

Activation of PI3K appears to be necessary for insulin-induced stimulation of glucose transport [127] and is involved in insulin-mediated signalling mechanisms leading to Akt activation and subsequent NO production. One of the aims of the present thesis is to determine whether administration of wortmannin during an insulin clamp blocks the haemodynamic and metabolic processes involved in insulin action.

1.9 Insulin Resistance

Insulin resistance is typically defined as a decreased responsiveness to the metabolic actions of insulin to promote glucose disposal [137-139]. Impaired insulin action in diabetes is coupled with elevated blood glucose concentration due to decreased muscle glucose uptake and reduced ability of insulin to suppress hepatic glucose output. This is compensated for by increased secretion of insulin by the pancreas resulting in hyperinsulinemia. Type 2 diabetes results when the pancreas can no longer maintain insulin hyper-secretion which results in chronic hyperglycaemia [137, 140]. The

incidence of type 2 diabetes is rapidly increasing in developed and developing countries and it is now considered an epidemic [139, 141-144].

At the cellular level many proteins are involved in insulin signalling and disruption of any of these proteins can lead to impaired insulin action. *In vivo* studies in humans have demonstrated multiple defects in muscle cells in insulin resistant subjects, including disturbances of the insulin receptor signal [145], glucose transporter proteins [146] and glycogen synthase activity [147]. Mutations in genes responsible for insulin signalling leading to insulin resistance occur in a small number of human subjects however in most cases the disease is an acquired condition which is strongly associated with a sedentary life style and obesity [139]. It has also been demonstrated that muscle obtained from the obese Zucker rat, a commonly used animal model for insulin resistance which carries a recessive mutation in the gene for the leptin receptor, is insulin resistant when isolated and incubated [148]. In addition, studies have shown decreased PI3K activity in insulin resistant humans [149].

Insulin resistance is a metabolic disorder however vascular effects may contribute to the pathogenesis of the disease. Later stage complications of type 2 diabetes include microvascular abnormalities resulting in damage to the retina, nephrons of the kidney and the blood supply and cells of the peripheral nervous system. Macrovascular complications include altered blood flow in the cardiovascular system which may contribute to heart attack and stroke [150]. Pathological changes in skeletal muscle include diminished capillarisation which may reduce the capacity for exchange of glucose and insulin to muscle cells, contributing to insulin resistance.

There are a number of studies using human and animal models of insulin resistance which have demonstrated impaired vascular function which may contribute to insulin resistance. The vascular actions of insulin to stimulate production of nitric oxide from the endothelial cell lead to vasodilation and increased blood flow and microvascular perfusion which enhances glucose uptake in skeletal muscle [151]. Since microvascular

perfusion contributes to glucose uptake in normal individuals the question remains whether blood flow is altered in states of insulin resistance, contributing to diminished insulin-mediated glucose uptake. Resistance to these vascular actions of insulin, characterized by reduced nitric oxide dependant vascular activity, is a consistent feature in obesity and diabetes [152]. A number of studies have also demonstrated that the vasodilatory action of insulin is blunted in peripheral tissues such as skeletal muscle in insulin resistant subjects [153-155].

1.9.1 Impaired Total Flow Response in Insulin Resistance

Baron and colleagues [156] first reported on the decreased ability of insulin to stimulate total blood flow in insulin resistant humans. In this study dose response curves were shifted to the right in the obese and type 2 diabetic subjects compared with lean controls. In insulin resistant subjects, basal limb blood flow is generally not impaired [4, 26, 157-162], although it has been demonstrated that insulin's ability to increase total flow and glucose uptake is impaired in states of insulin resistance [156]. Conversely a number of studies have found no impairment of insulin stimulated blood flow in type 2 diabetes as previously discussed in section 1.2 and reviewed in Clark *et. al.* [163].

1.9.2 Impaired Microvascular Flow in Insulin Resistance

Several studies have demonstrated that during states of insulin resistance, microvascular perfusion measured using the 1-MX method, is impaired thus restricting the availability of glucose and insulin available to muscle cells. It has been shown, that insulin mediated microvascular perfusion is abolished in the insulin resistant Zucker rat [164] which is coupled with impaired glucose uptake in hind limb muscle during supraphysiological insulin. Studies involving obese human subjects have demonstrated, using contrast enhanced ultrasound, that systemic physiological insulin failed to increase forearm microvascular perfusion, glucose uptake or brachial artery flow compared with lean controls [165].

A number of interventions can induce acute insulin resistance. Firstly infusion of the vasoconstrictor α -methylserotonin has been shown to decrease microvascular flow and glucose uptake in perfused rat hindlimb studies [47]. *In vivo*, α -methylserotonin abolished the ability of insulin to increase total flow and microvascular perfusion was blunted [55]. In incubated muscles it was demonstrated that α -methylserotonin had no effect on glucose uptake, compared with the perfused hindlimb studies, suggesting a role of the vascular system in insulin resistance [166]. Secondly, it was demonstrated by Youd *et al.* [167] that insulin resistance can be induced by acute administration of TNF- α , a cytokine which is elevated in various states of insulin resistance and obesity. TNF- α infusion during an insulin clamp decreased glucose infusion rate (GIR) and muscle glucose uptake as well as decreasing total blood flow and microvascular perfusion. In aortic endothelial cells TNF- α inhibits IRS-1, PI3K and phosphorylation of eNOS [85], suggesting TNF- α can inhibit the haemodynamic actions of insulin directly. Thirdly, Clerk *et al.* [168] demonstrated that microvascular perfusion and glucose disposal is impaired in rats following acute elevation of free fatty acid (FFA) by administration of Intralipid[®] heparin. In that study it was noted that insulin-mediated microvascular perfusion and increased limb blood flow was completely blocked, which was coupled with a 50% reduction in glucose uptake. Taken together, these studies demonstrate that impaired microvascular recruitment is associated with a decline in skeletal muscle insulin-mediated glucose disposal and that muscle metabolism is dependant on the extent of microvascular perfusion.

1.10 Exercise and Insulin Sensitivity

1.10.1 Exercise Increases Glucose Uptake

Exercise or muscle contraction stimulates glucose uptake into skeletal muscle in the absence of insulin [169, 170]. The contracting muscle has increased demand for energy during exercise and requires an adequate supply

of oxygen and glucose. Muscle contraction stimulates the translocation of GLUT4 to the plasma membrane and glucose uptake is promoted [171, 172]. There is evidence that exercise and insulin use different signalling pathways for glucose uptake since the two stimuli act synergistically [172-175]. Exercise-mediated glucose uptake, unlike insulin-mediated glucose uptake which involves PI3K signalling, is not inhibited by wortmannin [176]. Part of the signal that generates an increase in exercise mediated glucose uptake may be the activation of the enzyme AMP-activated protein kinase (AMPK) [177] (section 1.11).

1.10.2 Exercise Increases Insulin Sensitivity

Evidence from several studies demonstrates that physical activity is beneficial for the prevention of insulin resistance [178-180] through increasing insulin sensitivity [181, 182]. The signalling mechanisms involved in exercise mediated glucose uptake may provide important targets for drug therapies for insulin resistance [183].

Acute exercise induces GLUT4 translocation in skeletal muscle of normal and insulin resistant subjects [184]. A number of researchers have shown that a single bout of light exercise by human subjects improves whole body insulin sensitivity measured during a hyperinsulinemic euglycaemic clamp [185-188]. This beneficial effect of the single bout of exercise can be observed for up to 16 hours [189, 190]. The improved insulin sensitivity after exercise is mainly observed in muscles recruited during exercise [191] [192].

Exercise training, which is a repetition of several exercise bouts, has been shown to increase insulin sensitivity and maximal insulin responsiveness [193, 194] [195, 196] in healthy and insulin resistant individuals. In insulin resistant type 2 diabetic subjects one-legged physical training has been shown to increase insulin action in skeletal muscle compared with control subjects [197]. During a hyperinsulinemic euglycaemic clamp in individuals which

had undergone six weeks of exercise training resulted in a 30% increase in glucose uptake compared with no prior exercise training [198].

During exercise, perfusion of the muscle is dramatically increased. It has been demonstrated that muscle contraction increases total flow to muscle [199] and microvascular perfusion [200]. It is possible that haemodynamic factors contribute to improved insulin sensitivity following exercise [201] since the delivery and surface area available for insulin is markedly enhanced. It has been demonstrated that exercise training increases capillary density in skeletal muscle in humans [202, 203] and in rats [204] which may contribute to enhanced glucose uptake. Rattigan *et al.* [205] demonstrated in rats that 14 days of voluntary exercise training increased insulin-mediated whole body glucose infusion rate (by 24%) and hind leg glucose uptake (by 93%) as well as improvements in microvascular perfusion compared with sedentary controls [205].

1.11 AMP-Activated Protein Kinase

An enzyme now known as AMP-activated protein kinase (AMPK) was first reported in two independent articles published in 1973. These studies demonstrated that the enzyme inactivated 2 key metabolic enzymes involved in lipid synthesis; acetyl-CoA carboxylase (ACC) (involved in FA synthesis) and 3-hydroxy-3-methylglutaryl-CoA (HMG-CoA) reductase (involved in isoprenoid/cholesterol synthesis). The report from Carlson and Kim [206] described regulation of ACC by reversible phosphorylation, using rat hepatocytes. Beg *et al.* [207] described modulation of HMG-CoA reductase using protein fractions of rat liver. The ability of the kinase to phosphorylate the ACC kinase (1980) [208] and the HMG-CoA reductase kinase (1985) [209] were dependant on the presence of AMP. It was reported by David Carling and Grahame Hardie *et al.* [210] in 1987, that inactivation of ACC and HMG-CoA was performed by the same protein kinase. The enzyme was

subsequently named AMP-activated protein kinase (AMPK) by the same group the following year [211].

Further investigations and cloning of AMPK revealed that the kinase is related to a family of metabolic stress-sensing protein kinases of the yeast SNF-1 protein kinase sub-family which is found in fungi, plants and nematodes [212-217]. The kinase is highly conserved through evolution and is present in mammalian tissues.

Recent research has established that AMPK is an energy sensing enzyme which is regulated in mammalian tissue by physiological stimuli such as nutrients and changes in ATP consumption [218]. AMPK has been proposed to function as a 'metabolic master switch' which co-ordinates cellular energy metabolism by regulating catabolic pathways that produce ATP and anabolic pathways that consume ATP [219] (see section 1.11.2).

1.11.1 Structure of AMPK

AMPK is a serine/threonine protein kinase consisting of a catalytic α -subunit (63 kDa) and regulatory β - (38 kDa) and γ -subunits (35 kDa) [217, 220-222] which associate to form a heterotrimer [223, 224]. The β - and γ -subunits are important for maintaining the stability of the heterotrimer complex [225]. All three subunits are encoded by distinct genes ($\alpha 1$, $\alpha 2$, $\beta 1$, $\beta 2$, $\gamma 1$, $\gamma 2$, $\gamma 3$) which gives rise to at least 12 different heterotrimic combinations of the isoform which have alternative transcription sites [226]. The genes encoding the α -, β - and γ -subunits are highly conserved in all eukaryote species [220]. Co-expression of all three subunits is required for kinase activity [225, 227, 228]. The expression pattern for the isoforms appears to vary among tissues [229] suggesting that there are different physiological roles depending on the complex formation.

1.11.1.1 AMPK Subunits

The α subunit contains the serine/threonine protein kinase catalytic domain including a phosphorylation residue at Thr¹⁷². Phosphorylation of this site is essential for enzyme activity [221]. Expression of AMPK complexes containing $\alpha 2$ (the first catalytic subunit to be cloned [230]) are predominantly found in skeletal and heart muscle [231], whereas adipocytes express the $\alpha 1$ isoform [232]. Approximately equal proportions of $\alpha 1$ and $\alpha 2$ are found in liver [233]. AMPK $\alpha 1$ and $\alpha 2$ isoforms are expressed in arterial smooth muscle cells in different proportions between different arteries [234]. In endothelial cells $\alpha 1$ and $\alpha 2$ isoforms are expressed [235] with a higher proportion of $\alpha 1$ expression [236].

The β subunit is thought to act as a scaffolding protein for binding of the α and γ subunits [223]. It has been proposed that binding of the β and γ subunits stabilizes the subunit [217, 222, 237]. Both α - and β -subunits are phosphorylated by AMPK kinases(s) and by auto-phosphorylation. It has also been suggested that the β -subunit is involved in phosphorylating glycogen synthase [238] and that high glycogen in muscle may regulate AMPK [239-241]. The $\beta 1$ -subunit is widely expressed, whereas the $\beta 2$ -subunit is predominantly expressed in skeletal [242] and heart muscle [229].

The γ isoform contains 4 cystathionine- β -synthase (CBS) domains [221]. The function of the CBS domain is not known but it has been suggested that the γ subunit binds to the adenosine portion of AMP [228]. The $\gamma 1$ subunit is widely expressed and is the predominant isoform contributing to kinase activity in skeletal muscle [228]. The $\gamma 1$ - and $\gamma 2$ -subunits are widely expressed [228, 231, 243] and the $\gamma 3$ -subunit has been shown to display a high degree of specificity for skeletal muscle [228] and in particular white skeletal muscle [244].

1.11.2 Regulation of AMPK

AMPK acts as a metabolic sensor to the energy status of a cell [230] and plays a critical role in many metabolic processes, including glucose uptake and fatty acid oxidation in muscle, fatty acid synthesis and gluconeogenesis in the liver [245]. Once activated, AMPK phosphorylates several downstream substrates to switch off ATP-consuming pathways (e.g. fatty acid synthesis and cholesterol synthesis) and to switch on ATP-generating pathways (e.g. fatty acid oxidation and glycolysis) [217, 220, 230].

AMPK can be activated allosterically by increases in the AMP to ATP ratio or by covalent modification by AMP dependant AMPK kinase (AMPKK) which phosphorylates the α -subunit on Thr¹⁷² [246]. Woods *et al.* [247] and Carlson *et al.* [248] demonstrated that AMP binds to AMPK which enables the complex to be more susceptible to phosphorylation by AMPKK. Protein kinases which may phosphorylate AMPK include LKB1 [248] and the Ca²⁺/calmodulin-dependant protein kinase kinase (CaMKK) [249]. It has recently been reported that LKB1 is sufficient to activate AMPK *in vitro* and is genetically required for AMPK activation by energy stress in a number of mammalian cell lines [248]. Studies using cell extracts have demonstrated that LKB1 acts by directly phosphorylating AMPK rather than promoting auto phosphorylation of AMPK [247].

1.11.3 Activators of AMPK

The activity of AMPK increases in response to stressors such as muscle exercise, nutrient starvation, hypoxia and oxidant stress [230]. AMPK can also be activated by pharmacological agents such as AICAR and some anti-diabetic drugs such as metformin and thiozolidinediones as well as hormones that act through G_q receptors [250], leptin [251], adiponectin [252, 253], α - and β -adrenoreceptor agonists [232, 254].

1.11.3.1 Exercise

Muscle contraction is associated with an increase in energy turnover in the muscle cell as it depletes ATP and generates AMP resulting in AMPK activation (reviewed in [255]). The first report of AMPK involvement in exercise signalling was by Winder and Hardie in 1996 [256] who demonstrated that AMPK activity increases in rats by 2 to 3 fold within 5 minutes of commencing treadmill running exercise. A number of subsequent studies have demonstrated that AMPK is activated during muscle contraction. For example; the activity of AMPK increases in sciatic nerve-stimulated rat muscle *ex vivo* [257, 258] and by motor nerve stimulation *in vivo* and perfused rat hindlimb *in situ* [177, 259-261]. *In vivo* studies have revealed that AMPK is activated in rat muscle during treadmill running [260, 262]. In humans, exercise significantly increases AMPK activity during cycling exercise at 70% of VO₂ max [263] and 75% of VO₂ max [264].

In general, in rodent muscle both $\alpha 1$ and $\alpha 2$ associated AMPK complexes are activated during contraction/exercise. In human muscle, AMPK $\alpha 2$ is activated during moderate and high intensity exercise whereas the $\alpha 1$ isoform is only activated during high intensity exercise such as sprint cycling [264, 265].

There are beneficial effects of regular physical activity for prevention of pathological conditions such as obesity and diabetes. It has been demonstrated that individuals with type 2 diabetes subjected to exercise activate AMPK $\alpha 2$ to a similar extent as controls [266]. This finding indicates that individuals with diabetes have normally functioning AMPK, which has implications for targeting AMPK for drug development.

1.11.3.2 AICAR

AMPK can be activated artificially by the compound 5-aminoimidazole-4-carboxamide-1- β -D-ribofuranoside (AICAR) [267-272] which has featured as a major tool for research on AMPK. AICAR, an

analogue of adenosine, can be transported across the plasma membrane. After AICAR enters the cell, it is phosphorylated by adenosine kinase [273] to its monophosphorylated form called 5-aminoimidazole-4-carboxamide-1- β -D-ribofuranotide (ZMP) [270] (Figure 4). ZMP (Z-base compound) is a normal intermediate in the pathway of synthesis of purine nucleotides and may be metabolised to form inosine monophosphate (IMP), AMP, ZDP or ZTP [267, 270, 273]. The monophosphate ZMP mimics the effect of AMP which activates AMPK both by direct allosteric activation [274] and via promoting increased phosphorylation by AMPKK [255, 267, 268].

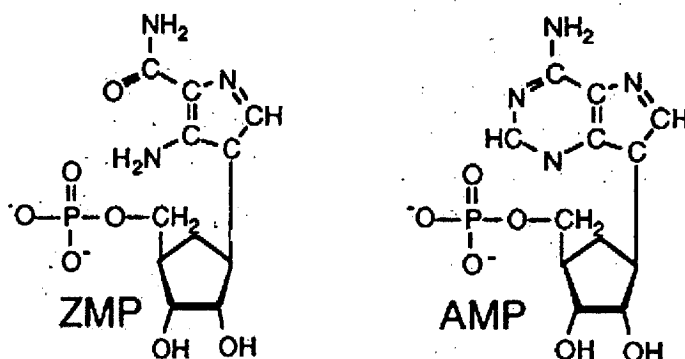


Figure 4: ZMP and AMP. The chemical structure of AICAR monophosphate (ZMP) and adenosine monophosphate (AMP).

Early reports of AICAR to be a specific pharmacological activator of AMPK were made by Sullivan *et. al.* [271] in 1994 and Corton *et. al.* [267] in 1995, which proved to be a major development in AMPK research. It was demonstrated that AICAR markedly activated cellular AMPK in a time and dose dependant manner in rat adipocytes [271]. Similarly, it was demonstrated that incubation of rat hepatocytes with AICAR activates AMPK due to phosphorylation and inactivation of a known target for AMPK (3-hydroxy-3-methylglutaryl-CoA reductase) [267]. The overall effect was that ZMP mimicked the effect of AMP on allosteric activation of AMPK [267]. In these

experiments, using rat hepatocytes, it was also noted that AICAR was a specific method for activating AMPK since the cellular contents of ATP, ADP or AMP were not altered which avoided non-specific side effects.

1.11.3.3 Antidiabetic Drugs

Oral medication as a treatment of diabetes began with the use of *Gallega officinalis* (goat's-rue or French lilac) in medieval Europe [275, 276]. Guanidine, the active component of Galega, was used to synthesise anti-diabetic compounds which lead to the production of two main biguanides; metformin and phenformin in the 1950s [277, 278]. Biguanides and Thiazolidinedions (TZDs) are two currently prescribed drug treatments for type 2 diabetes.

Metformin is currently the most prescribed oral antidiabetic agent. Metformin suppresses hepatic glucose production [279], increases skeletal muscle glucose disposal and reduces circulating free fatty acids [276, 280]. Unlike other prescribed antidiabetic agents metformin is not associated with weight gain. The mechanism of action of metformin has not been fully determined however Zhou *et al.* demonstrated that metformin activates AMPK in isolated rat hepatocytes [278]. In isolated rat muscle metformin activates AMPK together with stimulation of glucose uptake [278]. In type 2 diabetic humans, after 4 weeks of metformin treatment, a significant increase in AMPK $\alpha 2$ activity and glucose disposal was observed [281].

Thiazolidinedions are a class of drugs to which pioglitazone and rosiglitazone belong. Fryer *et al.* demonstrated that rosiglitazone is able to activate AMPK in muscle cell cultures, which was associated with an increase in the ratio of AMP:ATP [282]. In addition pioglitazone has been shown to activate AMPK [283, 284].

1.11.3.4 Other AMPK Activators

It has been demonstrated by a number of studies that hypoxia stimulates glucose uptake and AMPK activity in skeletal muscle [285]. The increase in hypoxia stimulated glucose uptake has been shown to be additive to insulin but not muscle contraction. In muscle which is dominant negative for AMPK, AICAR and hypoxia mediated glucose uptake is blocked [286]. In heart muscle, hypoxia [287] or ischemia [288] have been shown to activate AMPK. During ischemic reperfusion in the heart it was demonstrated that glucose transport was increased [289], which was independent of PI3K [127].

Leptin and adiponectin are adipokine hormones secreted by adipocytes. AMPK can be activated by leptin in skeletal muscle [290] and adiponectin in skeletal muscle and liver [291, 292].

The traditional activators of AMPK have included exercise or muscle contraction, anti-diabetic drugs such as metformin, TZDs and AICAR. More recently other AMPK activators such as polyphenols, estrogen, lipoic acid and rimonabant have emerged potential targets for diabetes treatments.

Polyphenols, such as resveratrol (a major polyphenol in red wine), apigenin and S17834 increase phosphorylation of AMPK and the downstream target, acetyl-CoA carboxylase (ACC) and they increase the activity of AMPK with 200 times the potency of metformin in HepG2 hepatocytes [293]. Epigallocatechin-3-gallate (EGCG) a polyphenol found in green tea, has been shown to be an effective treatment of type 2 diabetes in rodents [294], possibly through its reported ability to activate AMPK [295-297]. Additionally, EGCG treatment of spontaneously hypertensive rats (SHR) improved insulin sensitivity and dose dependently increased vasodilation of isolated mesenteric beds (MVB) by increasing NO production [298], suggesting a role of the vasculature for improving the action of insulin.

Studies by Watt *et al.* [299] have shown that ciliary neurotrophic factor (CNTF) which signals through the CNTF α -IL-6R-gp130 β receptor

complex, acts to increase fatty-acid oxidation and reduce insulin resistance by activating AMPK in isolated mouse skeletal muscle. There is also some evidence to suggest that estrogen plays a role in AMPK activation since ovaectomised mice exhibited promoted visceral fat accumulation by inhibiting AMPK activation and stimulating lipogenesis [300].

More recently, Cool *et al.* [301] identified A-769662 as the first small molecule direct pharmacological activator of AMPK. *In vivo* administration of the compound to *ob/ob* mice lowered plasma glucose by 40% and reduced body weight gain and plasma and liver triglycerides [301]. Studies in mouse embryonic fibroblasts or hepatocytes determined that A-769662 is a direct and specific activator of AMPK which is independent of upstream kinases [302]. In addition, it has been demonstrated that the compound activates AMPK both allosterically and by inhibiting dephosphorylation of AMPK on Thr¹⁷² via an AMP independent mechanism [303]. More recently evidence has suggested that this action is dependant on the β sub-unit carbohydrate-binding molecule and the γ sub-unit [304], which is a novel function of AMPK.

The traditional Chinese medicine berberine activates AMPK and improves insulin sensitivity [305]. Recently a berberine derivative, dihydroberberine (dhBBR) has been demonstrated to improve *in vivo* efficacy by counteracting increased adiposity, tissue triglyceride accumulation and insulin resistance in HFF rodents [306].

1.12 Role of AMPK in the Vasculature

It has been reported that AMPK phosphorylates and activates the endothelial NO synthase (eNOS). Chen *et al.* [307], using ischemic rat hearts, demonstrated that AMPK phosphorylates eNOS at Ser¹¹⁷⁷. Morrow *et al.* [308], using human aorta endothelial cells, have also demonstrated that AMPK causes increased phosphorylation of eNOS at Ser¹¹⁷⁷ and increased NO production. Studies using cultured endothelial cells have demonstrated that AMPK phosphorylates and activates eNOS [309]. AMPK is also

activated by hypoxia in HUVEC cells and it was demonstrated that adenoviral expression of a dominant negative AMPK mutant in those cells blocked increased eNOS phosphorylation at Ser¹¹⁷⁷ [310]. It has also been demonstrated that fenofibrate activates AMPK and increases eNOS phosphorylation and NO production in HUVEC cells [311]. Taken together these findings indicate that AMPK, through increased NO production, could have a positive effect to increase blood flow to tissues possibly through increasing microvascular blood flow [312]. It has been demonstrated that AICAR activates AMPK (section 1.11.3.2), therefore one of the aims of the present thesis it to determine whether AICAR increases vasodilation through AMPK activation and enhances microvascular perfusion *in vivo*.

1.13 AICAR Stimulated Glucose Uptake

Numerous studies have demonstrated that AICAR increases glucose transport in rat skeletal muscle [313], perfused muscle [269] and isolated muscles [177]. In 1997, Merrill *et al.* [269], using perfused rat hindlimb was the first to describe AMPK involvement in glucose uptake when it was demonstrated that AICAR simultaneously enhanced fatty acid oxidation and increased insulin stimulated glucose uptake. It was then demonstrated by Hayashi *et al.* [177] in 1998 and Bergeron *et al.* [313] in 1999 that AICAR can increase glucose uptake in isolated rat muscle in the absence of insulin.

Studies performed *in vitro* have determined that AICAR is effective in causing enhanced uptake of glucose into isolated perfused muscle [177, 269]. Similarly, *in vivo* studies have demonstrated that AICAR causes enhanced muscle glucose uptake [313]. The increases in glucose uptake correspond with increased glucose transporter 4 (GLUT4) fusion with the plasma membrane [314] and activation of AMPK [286]. These AICAR induced increases in glucose transport resemble the acute effects of muscle contraction.

It has been demonstrated that the over expression of a dominant-negative AMPK in H-2K^b skeletal muscle cells blocked the stimulation of

glucose uptake by AICAR and osmotic stress, but did not alter insulin mediated glucose uptake [315]. Sakoda *et al.* [316] demonstrated that over expression of a dominant-negative AMPK in rat soleus muscle blocked AICAR mediated glucose uptake. In addition, AICAR mediated glucose uptake in mice over expressing a kinase inactive AMPK mutant in skeletal muscle was completely blocked [286], however contraction-stimulated glucose uptake was only partially blocked, suggesting that AMPK is not the only mechanism involved in contraction. It appears that AMPK activation is essential for AICAR-induced glucose uptake in skeletal muscle. In contrast, Sakoda *et al.* demonstrated that over expression of a dominant-negative AMPK in 3T3-L1 adipocytes had no effect on AICAR induced 2-DG uptake, suggesting that AICAR mediated glucose uptake in these cells is AMPK-independent [316].

Similar to exercise, AICAR mediated increases in muscle glucose uptake are not inhibited by the PI3K inhibitor wortmannin [177, 313]. These studies demonstrated that AICAR and insulin have additive effects on glucose uptake in contrast to AICAR and contraction which do not have additive effects on glucose uptake.

AICAR increases glucose uptake in the insulin resistant rat model. For example, Bergeron *et al.* [317] have examined the acute effects of AICAR in the obese insulin resistant rat *in vivo*. A constant AICAR infusion ($10\text{mg}\cdot\text{kg}^{-1}\cdot\text{min}^{-1}$) to Zucker obese and lean rats increased glucose transport in red gastrocnemius muscle. In addition, insulin clamps ($4\text{mU}\cdot\text{min}^{-1}\cdot\text{kg}^{-1}$) combined with AICAR increased glucose transport activity in gastrocnemius muscle of lean but not obese rats [317]. In another study using insulin-resistant high fat fed rats *in vivo*, Iglesias *et al.* [318] examined the effect of subcutaneous injection of AICAR ($250\text{mg}\cdot\text{kg}^{-1}$) one day prior to commencing a hyperinsulinemic insulin clamp. In this study [318] AICAR was found to enhance glucose infusion rate during the clamp and improve insulin stimulated glucose uptake in white quadriceps.

The first reported study in human subjects was by Cuthbertson *et al.* in 2007 [319], which demonstrated that AICAR infusion ($10\text{mg}\cdot\text{kg}^{-1}$ for 3 hours) acutely stimulates skeletal muscle 2-deoxyglucose uptake in healthy men, which occurred in the absence of AMPK $\alpha 1$ or $\alpha 2$ activity. Similarly a study by Boon *et al.* [320] in 2008, revealed that AICAR infusion ($0.75\text{ mg}\cdot\text{min}^{-1}\cdot\text{kg}^{-1}$) in humans increased blood glucose disposal without increasing phosphorylation of AMPK. The absence of AMPK activation in human subjects highlights the difference between humans and rodents subjects in terms of AMPK activation due to AICAR.

Several studies have reported that when administered *in vivo*, AICAR induced glucose uptake shows a preference for white, glycolytic skeletal muscle. As mentioned previously, Iglesias *et al.* demonstrated that AICAR enhanced insulin stimulated glucose uptake in white quadriceps but not red quadriceps [318]. A study by Winder *et al.* [321] also demonstrated that after sub-cutaneous injections of AICAR in rats, AMPK activity increased in the white region of the quadriceps but not in the deep red region of the quadriceps muscles. Similar to AICAR mediated glucose uptake, contraction mediated glucose uptake differs between muscles with different fiber-type compositions [322].

In isolated rat soleus muscle, Ai *et al.* [323] demonstrated that AICAR increased 2-deoxyglucose transport and total AMPK activity approximately two fold in epitrochlearis (EPI), less in flexor digitorum brevis and not at all in the soleus muscle. In the perfused hind-limb, muscle 2-deoxyglucose uptake increased with AICAR, especially in the white gastrocnemius which corresponded with a larger stable activation of the $\alpha 2$ AMPK subunit compared to the soleus muscle [239].

1.13.1 Limitations of AICAR

A number of investigators have noted that caution should be taken when interpreting the results from experiments using AICAR.

Pharmacological activators of AMPK, such as AICAR, could act through non-AMPK mediated mechanisms [267, 324-326]. For example, AICAR does not have strict specificity to AMPK, activating all enzymes directly activated by AMP [325], such as glycogen phosphorylase [327, 328] and glycogen synthase [239]. In rat muscle and L6 myotubes, AICAR activates the extracellular signal-regulated kinase (ERK) / atypical protein kinase C (aPKC) pathway, resulting in increased glucose uptake [329]. A study in cultured hepatocytes has also demonstrated inhibition of fructose-1,6-bisphosphatase [330] and 6-phosphofructo-2-kinase (PFK-2) by AICAR, raising the possibility of non-AMPK mediated effects.

AICAR may also act via adenosine receptors [331] or adenosine transporters [324]. This raises the possibility that AICAR may compete with released adenosine for re-uptake into the cells, therefore increasing adenosine accumulation and exert effects via adenosine receptors [332]. Han *et al.* [333] provided evidence that extracellular adenosine plays a role in mediating increased glucose uptake into skeletal muscle. The effect of adenosine on contraction or insulin stimulated glucose uptake is controversial. A study by Merrill *et al.* [269] has demonstrated that skeletal muscle perfused with AICAR show no change in ATP, ADP or AMP. In isolated epitrochlearis muscles 10 μ M 8-(p-sulphophenyl)-theophylline, an adenosine receptor agonist, did not block AICAR stimulated 2-deoxyglucose uptake [313].

AICAR can also have systemic effects when administered *in vivo* [334]. Daily subcutaneous injections of high dose AICAR (1mg.g⁻¹ body weight) for 4 weeks in rats results in liver hypertrophy [335]. In a similar study, acute subcutaneous AICAR injection (1mg.g⁻¹ body weight) resulted in increased lactate production [336]. Due to these side effects it is unlikely that AICAR will be a drug of choice for pharmacological treatment of diabetes.

1.14 The Present Study: Summary and Aims

The work presented in this thesis was designed to investigate mechanisms involved in microvascular perfusion and glucose metabolism in skeletal muscle. Insulin and muscle contraction modulate haemodynamic actions in muscle; increase blood flow, microvascular perfusion and stimulate glucose uptake [49, 337]. In models of insulin resistance the action of insulin to increase blood distribution within the muscle is impaired [338] and this may contribute, in part, to the state of insulin resistance. The mechanisms involved in muscle contraction induced glucose uptake and vasodilation are generally not impaired in insulin resistance and thus provide an attractive therapeutic target for type 2 diabetes.

Acute Effects of Wortmannin on Haemodynamic and Metabolic Actions of Insulin In Vivo.

The mechanisms of insulin leading to glucose uptake are dependant on PI3K, which can lead to downstream phosphorylation and activation of eNOS resulting in vascular relaxation [38, 84]. Wortmannin is an effective inhibitor of PI3K and it's downstream effects [132]. Wortmannin was infused *in vivo* during a hyperinsulinemic euglycaemic clamp to determine if the microvascular effects of insulin are dependant on PI3K.

Effects of Nitric Oxide Synthase Inhibition on the Actions of Insulin in Skeletal Muscle.

The actions of insulin to increase total blood flow and microvascular perfusion have been linked to the activation of eNOS and the production of the potent vasodilator NO. Local NOS inhibition during a hyperinsulinemic euglycaemic clamp by L-NAME was utilised to determine if the action of

insulin to increase glucose uptake in muscle *in vivo* is dependant on insulin mediated microvascular perfusion.

Acute Effects of AMPK Activation by AICAR on Muscle Microvascular Perfusion In Vivo and Isolated Muscle Resistance Arteries In Vitro.

Skeletal muscle contraction leads to AMPK activation, increased blood flow and microvascular perfusion. AMPK has been shown to enhance endothelium-dependant vasodilation [235] and increase eNOS phosphorylation at Ser¹¹⁷⁷ [308]. The AMPK activator AICAR was used to investigate the role of AMPK activation in microvascular perfusion *in vivo* in the rat and *in vitro* using muscle resistance arteries and isolated endothelial cells.

Acute Effects of AICAR on Haemodynamic and Metabolic Actions of Insulin In Vivo.

Skeletal muscle contraction can lead to glucose uptake, which is not inhibited by Wortmannin and is therefore independent of insulin. Muscle contraction and direct activation of AMPK by AICAR have been shown to enhance insulin-mediated muscle glucose uptake and ameliorate insulin resistance [339]. Infusion of AICAR during the hyperinsulinemic euglycaemic clamp was used to determine if increased microvascular perfusion, due to AMPK activation, contributes to enhancement of insulin-mediated glucose uptake.

The overall aim of this study was to directly explore the mechanisms in muscle microvasculature leading to microvascular perfusion and glucose uptake. Mechanisms involved in microvascular perfusion may contribute to new targets for the treatment of insulin resistance.

CHAPTER 2

Materials and Methods

2.1 *In Vivo* Experiments

2.1.1 Animal Care

The Animal Ethics Committee (University of Tasmania, Hobart, Tasmania, Australia) in accordance with the National Health and Medical Research Council of Australia (NHMRC) guidelines on animal experimentation approved all experimental protocols and procedures.

Male Hooded Wistar rats, obtained from the University Animal House (Hobart, Tasmania, Australia), were housed at a constant temperature of $21 \pm 1^{\circ}\text{C}$ with a 12:12 hour light:dark cycle (lights on at 0600 hours). All rats were allowed access to a commercial rat chow (Pivot, Launceston, Australia) together with water *ad libitum*. The rat chow contained 21.4% protein, 4.6% lipid, 68% carbohydrate and 6% crude fiber with added vitamins and minerals. Food and water was freely available (unless otherwise stated in individual chapters ie: fasted) until the animals were administered anaesthetic.

2.1.2 Surgical Procedures

The rats were anesthetized using a bolus intra-peritoneal (IP) injection of pentobarbital sodium ($50 \text{ mg}\cdot\text{kg}^{-1}$ body weight). The surgical procedure began with a tracheotomy to avoid respiratory problems during anesthesia. Polyethylene cannulas (PE-60, Intramedic®) were then surgically implanted into the carotid artery for arterial sampling and measurement of blood pressure (pressure transducer Transpac IV, Abbott Critical Systems) and into both jugular veins for continuous infusion of anesthetic and other intravenous infusions.

For rats undergoing venous blood sampling and femoral blood flow monitoring, small incisions (1.5cm) were made in the right and left sides of the skin overlaying the femoral vein and artery of both legs. A section of the femoral artery (1cm) on the right side was separated from the saphenous nerve and the femoral vein. A small animal flow probe (Transonic Systems, VB series 0.5 mm)

was positioned around the artery just distal to the rectus abdominus muscle of the right leg. The cavity in the leg surrounding the probe was filled with conductive gel (Medical Equipment Services, Melbourne, Australia) to provide acoustic coupling to the probe. The probe was connected to the flow meter (Model T206 small animal blood flow meter, Transonic Systems). This was connected with a computer which acquired the data (at a sampling frequency of 100Hz) for femoral blood flow, heart rate and blood pressure using WINDAQ data acquisition software (DATAQ Instruments). The femoral vein of the left leg was exposed and used for venous sampling, using an insulin syringe fitted with a 29G needle (Becton Dickinson).

The surgical procedure was conducted over approximately 30 minutes. Rats were then maintained under anesthesia for the duration of the experiment using a continual infusion of pentobarbital sodium ($0.6\text{mg}\cdot\text{min}^{-1}\cdot\text{kg}^{-1}$) via the left jugular cannula. The body temperature was maintained at 37°C using a water-jacketed platform and a heating lamp positioned above the rat with the ambient room temperature controlled at 20°C . At the completion of the experiment the rat was euthanased by a bolus injection of pentobarbital sodium via the carotid artery cannulation before tissues were excised and stored for later analysis.

2.1.2.1 Contrast Enhanced Ultrasound (CEU)

Rats receiving microbubbles (Chapter 5 and 6) had the left leg shaved, keeping the skin intact. Ultrasound transmission gel (Aqua Sonic 100) was applied to the surface of the leg for acoustic coupling to the ultrasound probe. A linear-array transducer (L7-4) interfaced with an ultrasound system (HDI-500; Philips Ultrasound, Santa Ana, CA, USA) was positioned over the left hindlimb of the rat to image the proximal adductor muscle group and the transducer was secured with a clamp for the duration of the experiment. A schematic diagram of the position of the ultrasound probe for experiments using the CEU technique is shown in Figure 5. Details of the technique are described in section 2.1.8.2.

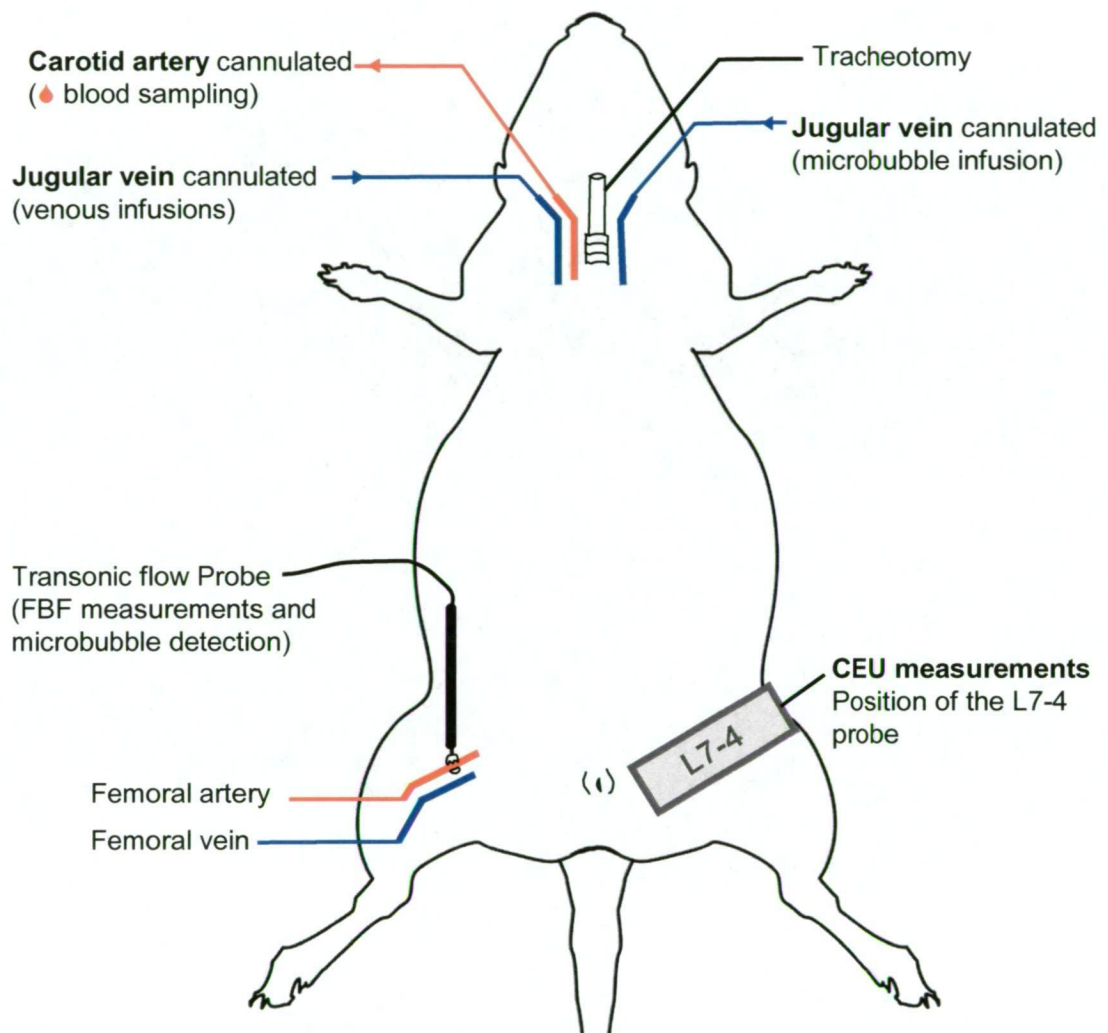


Figure 5: A schematic diagram of the *in vivo* set up for experiments using the CEU technique.

2.1.2.2 The Epigastric Artery Technique

Cannulation of the epigastric artery is a technique first developed by Hema Mahajan in our laboratory in 2004, for the infusion of test substances locally into one leg (see Chapter 4). The epigastric artery is a branch of the femoral artery, in the middle part of the thigh. A schematic diagram of the *in vivo* set-up for experiments employing the epigastric technique is shown in Figure 6. The epigastric artery of the test leg was tied off and had a polyethylene cannula (PE-20, Intramedic® tubing attached to a blunt 29G syringe needle) surgically implanted at the junction immediately at the femoral artery. Retrograde infusion of the epigastric artery resulted in delivery of substances to the leg via the femoral artery.

A transonic flow probe was placed around the femoral artery of both legs to measure the femoral blood flow simultaneously; the contra-lateral leg served as a control. At the end of the experiment, after taking the arterial sample (100µL plasma) from the carotid cannula, the venous samples (100µL plasma) were taken from the femoral veins of control and test legs in rapid succession and used for subsequent analysis.

Cannulation of the epigastric artery is a technique which was developed for administration of vasoactive substances such as L-NAME which, when administered systemically, have a profound effect on the blood pressure thus activating counter-regulatory reflex mechanisms. Infusion via the epigastric artery avoids unwanted systemic effects of the test substance. The cannula was used to infuse the test substance L-NAME (Chapter 4). An advantage of this technique is that the opposite leg can be used as control. Substances must be readily metabolized in the test leg to use this technique. Since L-NAME is vasoactive, any effect on blood pressure and heart rate were taken as an indication that the substance had appeared in systemic circulation. An effect on femoral blood flow in the test leg was taken as a definitive indicator of the substance being infused. The infusion of the test substance was regularly adjusted according to the measure of femoral blood flow in the test leg so that a constant and optimal dose could be maintained in the test leg.

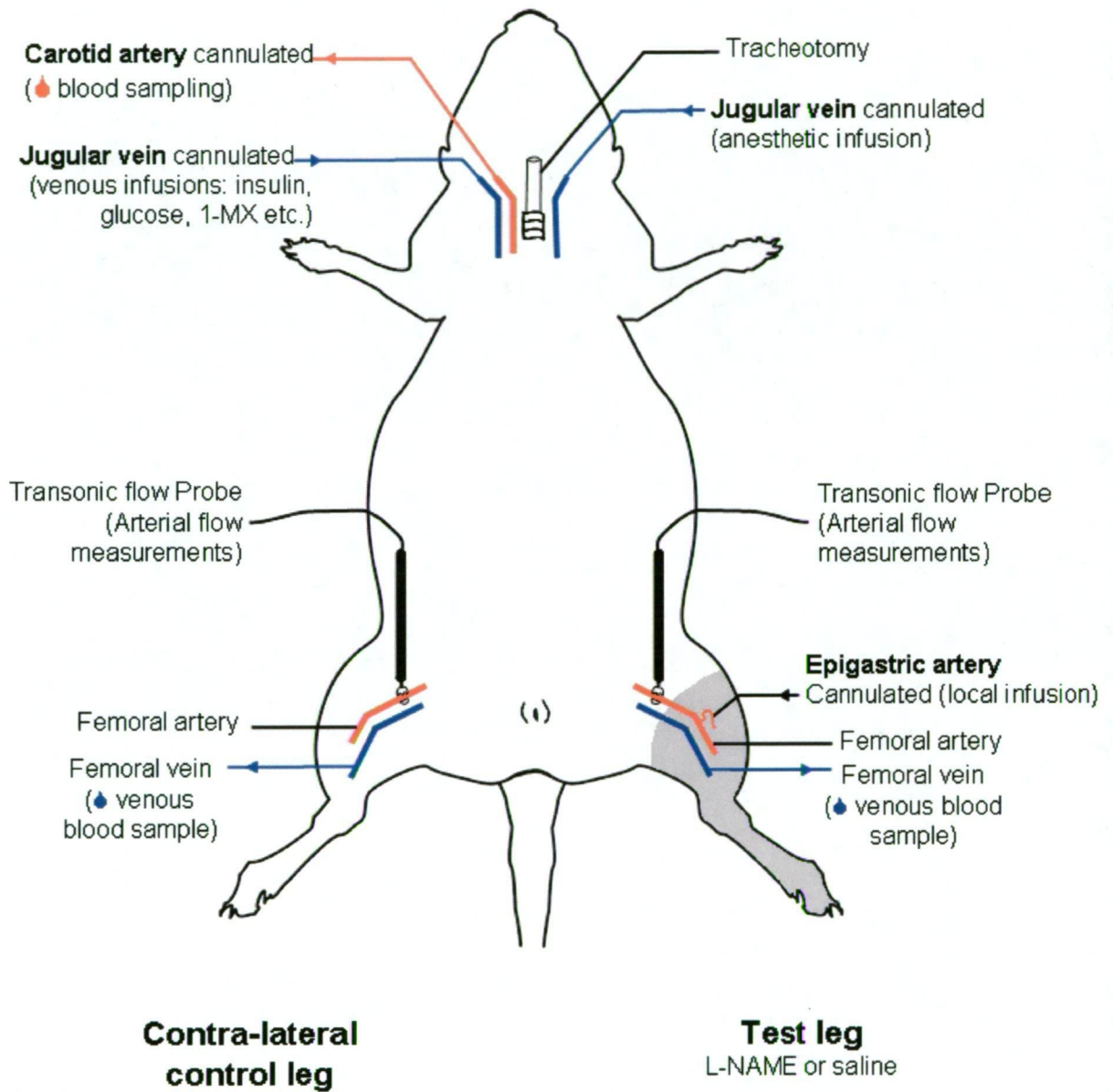


Figure 6: A schematic diagram of the *in vivo* set up for experiments using the epigastric technique for local infusion of test agents in the rat.

2.1.3 *In Vivo* Experimental Procedures

Once the surgical procedures were completed a 30 to 60 minute equilibration period was allowed so that the leg blood flow and pressure could become constant and stable before commencement of the experimental protocol. Detailed experimental protocols are given in each of the experimental chapters.

2.1.3.1 Blood Sampling

An arterial blood sample (approximately 25 μ L) was taken 2 minutes prior to the commencement and at regular intervals throughout the experiment in order to monitor blood glucose and lactate concentrations. At the conclusion of the experiment arterial blood and venous blood (300-500 μ L) samples were collected after other measurements of blood flow had been completed. The total blood volume withdrawn from the animals before the final arterial and venous blood samples did not exceed 1.5mL and was compensated by the volume of fluid infused.

2.1.3.1.1 Glucose and Lactate Assay

Blood and plasma glucose and lactate was determined with a glucose analyser (Yellow Springs Instruments, Model 2300 Stat Plus, USA) at regular intervals throughout the experiments. A sample volume of 25 μ L of whole blood or blood plasma was required for each glucose and lactate determination. The blood glucose assay was performed immediately after collection of the arterial sample. Plasma glucose was determined immediately after spinning down whole blood and separating the plasma into a fresh vial.

2.1.3.1.2 Plasma Insulin Assay (ELISA)

Plasma insulin concentration was determined from arterial plasma samples (kept frozen at -20°C) using a commercial rat insulin enzyme

immunoassay kit (ELISA, Mercodia AB, Sweden). The detection range of the assay was between $0.15\text{--}5.5\mu\text{g.L}^{-1}$ and if necessary samples were diluted to fall into this range. A correction factor calculation was performed on samples containing exogenously infused human insulin, which had 120% or 167% cross-reactivity (depending on the kit batch) within the assay compared with rat insulin. Plasma insulin was determined immediately before the commencement of the experiment and at the conclusion of the experimental protocols.

2.1.4 Euglycaemic Hyperinsulinemic Clamp Technique

The euglycaemic hyperinsulinemic clamp is a method used for quantifying whole body insulin sensitivity *in vivo* and was first established by R. DeFronzo in humans in 1979 [340]. Soon after the clamp technique was adapted for use in the laboratory rat [341-343] and has since been widely used. The clamp consists of a continuous intravenous infusion of exogenous insulin to achieve elevated insulin levels which stimulates glucose removal from the plasma into the insulin responsive tissues such as skeletal muscle. This action is compensated by simultaneous infusion of exogenous glucose which is adjusted to maintain blood glucose at a stable basal value (euglycaemia) and represents the net effect of insulin on glucose metabolism. After repeated adjustments of the glucose infusion rate (GIR), a steady state is achieved where the glucose infusion remains constant and reflects the animals insulin sensitivity [341]. In the presence of insulin, in an insulin responsive individual, the liver responds by suppressing glucose output and stimulating glucose uptake. In states of insulin resistance or pharmacological interventions the hepatic glucose output may not be completely suppressed and the glucose secreted by the liver may contribute to glucose taken up by tissues in response to insulin. Insulin sensitivity or resistance is estimated by comparison to a normal control group. The clamp technique can be combined with several other techniques as required in order to measure various aspects of metabolism due to insulin [344]. The clamp can be combined with administration of glucose isotope tracers to estimate the glucose dynamics for whole body rates of appearance and disappearance of glucose and in individual muscles (section 2.1.5). During assessment of whole body rates of appearance (R_a) and disappearance of glucose

(Rd), it should be ensured that the animal is fasted which eliminates contributions by absorption of glucose.

The clamp was performed on anaesthetised rats as follows; a basal arterial blood sample was taken (200 μ L) and analyzed for glucose concentration (section 2.1.3.1.1) and the remaining blood plasma was stored at -20°C for subsequent plasma insulin assay (section 2.1.3.1.2). The clamp commenced at the onset of a pre-determined fixed level of continuous insulin infusion (3, 10 or 20mU.min⁻¹.kg⁻¹) resulting in an elevated steady state concentration. Blood samples (50 μ L) were taken at regular intervals from the arterial cannula to monitor blood glucose. The initial basal blood glucose concentration (euglycaemia) of each rat was kept constant by a variable infusion of glucose (30% w/v solution). The glucose infusion rate (GIR) was adjusted to maintain the basal glucose level until a steady state was achieved for glucose delivery. The value obtained for the GIR gave a measure of the insulin sensitivity of the rat. In the control experiments a saline infusion was given which matched the volumes of insulin and glucose administered.

2.1.4.1 Glucose Homeostasis

The GIR gives a measure of insulin sensitivity and reflects the animals' need for glucose in the presence of exogenous insulin. The formula for the GIR calculated for rat weight is given as follows:

$$\text{GIR} = (\text{Si} \times 0.3) / \text{Wt.}$$

Where Si is the setting on the infusion pump (μ L.min⁻¹) at time i; 0.3 is based on the use of a 30% glucose solution and Wt. is the rat weight in kg. The units for GIR are expressed as mg.min⁻¹.kg⁻¹.

The exogenously infused glucose as well as glucose secreted from the liver contributes to the glucose taken up by the insulin sensitive tissues. Once GIR has obtained a steady state, which usually takes approximately 75 minutes,

the clamp technique can be combined with the administration of radio-labelled glucose tracers to measure the glucose homeostasis specifically in the liver and muscles [345, 346]. The use of radio-labelled glucose tracers for estimates of whole body rate of glucose disposal and muscle specific glucose uptake is explained in more detail in section 2.1.5.1 and section 2.1.5.2 respectively.

2.1.5 Glucose Tracers

Analysis of the metabolic fate of infused glucose tracers at conclusion of the clamp has allowed assessment to be made of insulin action at both the whole body and individual tissue level. Three different radio-labelled glucose tracers were used throughout this thesis and are listed in Table 1. Where two tracers have been used in the same animal a combination of ^3H and ^{14}C radiolabels was selected and activity was determined using a dual label counting protocol on a liquid scintillation counter (Perkin Elmer Inc., Tri-Carb 2800TR, IL, USA).

Table 1: Radio-labelled glucose tracers.

COMPOUND	ABBREVIATION	DETERMINATION
2-Deoxy-D-[2,6- ^3H] glucose	[^3H] 2-DG	muscle glucose uptake
2-Deoxy-D-[1- ^{14}C] glucose	[^{14}C] 2-DG	muscle glucose uptake
D-[3- ^3H] glucose	[^3H] glucose	whole body rate of glucose disposal

2.1.5.1 Whole Body Rate of Glucose Disposal

The whole body rate of glucose disposal can be calculated from the rate of glucose disappearance from plasma (R_d). With it, R_a (rate of glucose appearance) can be calculated according to the formula $R_a = R_d - \text{GIR}$, giving an estimation

of the liver insulin sensitivity [345]. During this procedure the animal should be fasted so that glucose contributions arising from the gut are eliminated.

In experiments measuring glucose turnover, a primed (2 μ Ci bolus in 0.2mL saline), continuous (0.1 μ Ci.min⁻¹) dose of [³H] glucose (specific activity = 16.6 Ci.mmol⁻¹, Amersham Pharmacia Biotech) was infused during the final 60 minutes of the experiment when glucose homeostasis had attained steady state. Arterial plasma samples were taken at 105 and 120 minutes and were de-protenated. A 25 μ L sample of the supernatant was evaporated to dryness using a freeze dryer (iLshin Lab Co. Ltd. Netherlands) to remove ³H₂O and re-suspended in 100 μ L of distilled H₂O. Biodegradable counting scintillate BSC (Amersham, Arlington Heights, IL) was added to each sample and [³H] glucose radioactivity was determined using a liquid scintillation analyser (Perkin Elmer Inc., Tri-Carb 2800TR, IL, USA). The rate of appearance (R_a) and rate of disappearance (R_d) of glucose was calculated using the isotope dilution equation

$$R_a = R_d = F/SA,$$

where F is the rate of tracer infusion and SA is the specific activity of glucose [342]. SA was calculated from the plasma radioactivity divided by the glucose concentration.

2.1.5.2 Muscle Specific Glucose Uptake (R'g)

The muscle specific glucose uptake assay relies on the principle that 2-Deoxy-D-[2,6-³H]glucose (2-DG) is taken up by the cell, via the normal transport process and is phosphorylated to 2-Deoxy-D-[2,6-³H]glucose phosphate. This compound cannot be metabolized any further and accumulates in the tissue. The rate of glucose uptake for muscle tissues can be calculated according to the amount of tracer accumulation of 2-DG phosphate in muscle and the amount of 2-DG disappearance from the plasma [347, 348].

In experiments measuring glucose uptake into individual muscles, a 50 μ Ci bolus (in 0.2mL saline) of 2-Deoxy-D-[2,6- 3 H] glucose (3 H] 2-DG) (specific activity = 44.0 Ci.mmol $^{-1}$, Amersham Life Science, Castle Hill, NSW, Australia) was administered 45 minutes before the end of the experiment via the venous cannula. The tracer bolus was flushed into the animal with a bolus of saline (100 μ L) to ensure complete delivery of the tracer. In experiments where Ra and Rd were determined using the 3 H] glucose tracer, a 40 μ Ci bolus of 2-Deoxy-D-[1- 14 C] glucose (14 C] 2-DG) (specific activity = 56.0 mCi.mmol $^{-1}$, Amersham Life Science, Castle Hill, NSW, Australia) was used in order to individually quantify the tracers. Blood samples were taken at 5, 10, 15, 30 and 45 minutes following the injection (45 minute sampling protocol) and the plasma was separated. The plasma (25 μ L) was added to 3mL of biodegradable counting scintillant-BCA (Amersham, USA) and the rate of clearance of 3 H] 2-DG or 14 C] 2-DG was determined over the 45 minute time course. After the final blood sample the animal was euthanised at the end of the experiment before immediate removal of the muscle samples. Soleus, plantaris, red and white gastrocnemius, extensor digitorum longus (EDL) and tibialis muscles were excised and freeze clamped using liquid nitrogen cooled tongs and stored at -20°C until assayed for 3 H] or (14 C] 2-DG uptake.

Individual frozen muscles from the clamps were ground under liquid nitrogen. Approximately 100mg of ground tissue was homogenized in 1.5mL of distilled water using a Silent Crusher M (Heildorf, Germany). The homogenate was centrifuged at 13,000 rpm at 4°C to eliminate debris. A sample of the supernatant (100 μ L) was placed in a scintillation vial and 3mL of scintillation liquid was added, mixed and counted in a scintillation counter. A 1mL sample of the supernatant was loaded into prepared resin columns containing approximately 1mL of ion exchange resin (AG1-X8, Bio-Rad, USA). Free and phosphorylated 3 H] or 14 C] 2-DG were separated and collected from the column using distilled water and 2M HCl washes. Biodegradable Counting Scintillant-BCA, (Amersham, USA) was added to each radioactive sample and radioactivity determined using a liquid scintillation counter (Perkin Elmer Inc., Tri-Carb 2800TR, IL, USA). From this measurement and knowledge of plasma glucose, the time course of plasma 3 H] 2-DG disappearance, which reflects glucose

uptake into the muscle, was calculated as previously described by others [345, 346, 348]. The measurement for $R'g$ is expressed as $\mu\text{mol}\cdot\text{min}^{-1}\cdot 100\text{g}^{-1}$ or $\mu\text{g}\cdot\text{g}^{-1}\cdot\text{min}^{-1}$)

2.1.6 Experimental Protocols

Experimental groups were generally allocated into either control group (saline), hyperinsulinemic euglycaemic insulin clamp (insulin alone or insulin plus test substance) or test substance alone control group.

2.1.6.1 Wortmannin Protocol

After placement of all cannulae, Transonic flow probe and a 60 minute equilibration, rats were infused for 3 hours with either 0.5% (v/v) dimethylsulfoxide (DMSO) or wortmannin ($1\mu\text{g}\cdot\text{min}^{-1}\cdot\text{kg}^{-1}$, Sigma Chemical Co., St. Louis, MO) in 0.5% DMSO as shown in (Chapter 3, Figure 10, page 71). Wortmannin infusions were initiated by a bolus injection of $2.5\mu\text{g}$ in 0.20mL saline at $t = -60$ minutes. One hour later ($t = 0$ minutes) saline or insulin ($10\text{mU}\cdot\text{min}^{-1}\cdot\text{kg}^{-1}$, Humulin R Eli Lilly, Indianapolis, IN) infusion was commenced (Chapter 3, Figure 10, page: 71).

2.1.6.2 Local L-NAME Protocol

Once the surgery was completed, a 60 minute equilibration period was allowed, rats then entered a protocol where they received either local saline or local L-NAME ($10\mu\text{M}$ final concentration calculated from the femoral blood flow) in the test leg (Details are given in Chapter 4, Figure 18). At 15 minutes after the commencement of the local infusion rats underwent a euglycaemic insulin clamp ($3\text{mU}\cdot\text{kg}^{-1}\cdot\text{min}^{-1}$, Humalin R, Eli Lilly & Co., Indianapolis) or received saline alone.

2.1.6.3 AICAR Protocols

Once the surgery was completed a 60 minute equilibration period was allowed, rats then entered a protocol (Chapter 5, Figure 25, page 122 and Chapter 6, Figure 35, page 147) where they underwent a euglycaemic insulin clamp ($3\text{mU.kg}^{-1}.\text{min}^{-1}$, Humalin R, Eli Lilly & Co., Indianapolis) or received saline alone. Animals receiving AICAR were administered a bolus of 5mg in 0.20mL saline, followed by a continuous intravenous infusion of $3.75\text{mg.kg}^{-1}.\text{min}^{-1}$ for 60 minutes.

2.1.7 Infusate Preparation

2.1.7.1 Insulin

Insulin (Humalin R, Eli Lilly & Co., Indianapolis) was diluted 1:10 with 2% bovine serum albumin (BSA, 'Bovostar', Bovogen Biologicals, VIC, Australia) in order to prevent adhesion of insulin to glass ware and plastic surfaces. The insulin infusate is then prepared in heparinised saline to a desired concentration calculated according to rat weight and infused at a constant rate of $10\mu\text{L.min}^{-1}$ for 1 to 2 hours (see individual chapters).

2.1.7.2 Glucose

Glucose (30% w/v solution, glucose monohydrate, Merck, Darmstadt, Germany) was dissolved in heparinised saline using heating to 50°C and then filtered using a $0.45\mu\text{m}$ syringe filter.

2.1.7.3 1-MX and Allopurinol

The 1-methylxanthine (1-MX, Sigma-Aldrich, Inc., St. Louis, MO, USA) infusion solution was made to a final concentration of 30mM by dissolving in 30mM NaOH heparinised saline solution with heating to 50°C . Allopurinol (

Sigma-Aldrich, Inc., St. Louis, MO, USA) was made to a final concentration of 12.5 mM by dissolved in 20mM NaOH heparinised saline solution.

2.1.7.4 Microbubbles

Commercially available albumin microbubbles (Optison™, Molecular Biosystems Inc., San Diego, CA, USA), composed of an albumin shell and a perfluoropropane gas core, were used as a contrast agent to image the vasculature. Microbubbles were diluted 1:50 in saline gassed with perfluoropropane and infused at $40\mu\text{L}\cdot\text{min}^{-1}$ via a dedicated venous cannula (PE-20 tubing).

2.1.8 Techniques for Measuring Microvascular Perfusion

Two techniques employed for measurement of microvascular perfusion are contained within this thesis which include the 1-MX method and contrast enhanced ultrasound (CEU). The 1-MX method is a biochemical technique which is an end-point determination made at steady state. In contrast, using the CEU technique, it possible to make end point determinations as well as continually measure changes in microvascular perfusion during a time course. A study by Vincent *et al.* [60] has demonstrated that the two techniques are comparable for assessing microvascular perfusion in the rat hindlimb.

The 1-MX method was used for studies involving wortmannin and L-NAME. The CEU technique was utilised in the AICAR studies as it was not possible to use the 1-MX technique with AICAR due to interference with the measurements.

2.1.8.1 1-MX Metabolism Measurements

The technique for the measurement of *in vivo* insulin-mediated haemodynamic changes in skeletal muscle microvascular perfusion, by metabolism of exogenously added 1-methylxanthine (1-MX, Sigma Aldrich Inc., St. Louis, MO, USA) was developed and by Rattigan and Clark *et al.* [49] in

1997. Microvascular perfusion was determined by measuring the metabolism of infused 1-MX, a substrate metabolized by xanthine oxidase (XO) which converts 1-MX to a single product 1-methylurate (1-MU) [49, 349]. Both 1-MX and 1-MU are non-vasoactive [49]. In the hindleg muscle xanthine oxidase is predominately located in the endothelial cells of the capillaries [50, 350]. Thus 1-MX metabolism across the hindleg corresponds to hindleg capillary surface area.

1-MX was infused at a constant rate ($0.4\text{mg}\cdot\text{min}^{-1}\cdot\text{kg}^{-1}$) for 60 minutes prior to the conclusion of the experiment. 1-MX clearance from plasma is very rapid and it was necessary to partially inhibit the xanthine oxidase activity [49] thus lowering the K_M of the enzyme, in order to maintain a constant arterial 1-MX concentration. To do this an injection of a specific xanthine oxidase inhibitor, allopurinol (Sigma-Aldrich Inc. St. Louis, MU, USA) [351] was administered as a bolus dose ($10\mu\text{mol}\cdot\text{kg}^{-1}$) 5 minutes prior to commencing the 1-MX infusion. Allopurinol was rapidly converted to oxypurinol which could be detected until the completion of the experiment [49]. This allowed constant arterial concentrations of 1-MX to be maintained at a steady arterial state of approximately $20\mu\text{M}$ throughout the infusion period while the arterial concentration of allopurinol remained at approximately $8\mu\text{M}$.

At the conclusion of the experiment duplicate arterial (A) and venous (V) samples (300 to $500\mu\text{L}$) were collected in clean eppendorf tubes which had been coated in heparin and dried by evaporation at room temperature then placed on ice. Immediately after collection, the blood plasma was separated by centrifugation for 60 seconds at 13,000 rpm in a biofuge *pico* (Heraeus) at room temperature. A $100\mu\text{L}$ sample of the plasma was added to $20\mu\text{L}$ 2M perchloric acid (PCA, for protein precipitation) followed by vortexing to ensure complete mixing. The PCA treated samples were stored at -20°C until assayed for 1-MX concentration. When required, samples were thawed on ice, centrifuged at 13,000 rpm for 10 minutes and the supernatant used to determine 1-MX, 1-MU and oxypurinol concentrations by reverse-phase HPLC. The 1-MX metabolism in $\text{nmol}\cdot\text{min}^{-1}$ was calculated from the following equation:

$$\text{1-MX metabolism (MXD)} = (\text{Art[1-MX]} - \text{Ven[1-MX]}) \times 0.871 \times \text{FBF}$$

Where; Art[1-MX] and Ven[1-MX] are the plasma 1-MX concentrations ($\mu\text{mol.L}^{-1}$) obtained from arterial and venous blood samples respectively, 0.871 is the factor to convert the 1-MX concentration measured in plasma to that in whole blood and FBF is the femoral blood flow rate (mL.min^{-1}) measured immediately before the blood samples are withdrawn.

For separation and quantification of 1-MX, 1-MU and oxypurinol a Gemini C₁₈ 5 μm reverse phase column ($4.6 \times 150\text{mm}$) was used (Phenomenex, NSW, Australia) under isocratic conditions at 1.0mL.min^{-1} . The buffer contained 0.3M KH₂PO₄, 0.5% methanol, 0.5% acetonitrile and 0.2% tetrahydrofuran at pH 4.0. Detection was conducted with a Varian instrument fitted with a Varian Polychron Model 9065 diode array detector equipped with LC Star Workstation reading simultaneously at wavelengths of 254 (oxypurinol), 268 (1-MX) and 282nm (1-MU). The peaks obtained were identified by retention time and absorbance spectra (measured against 100 μM standards) and then quantified using a commercial software package (Star Chromatography Workstation, version 6.41).

2.1.8.2 Contrast Enhanced Ultrasound (CEU)

Contrast enhanced ultrasound (CEU) was used to measure microvascular blood volume. The Optison™ albumin shell perfluoropropane gas filled microbubbles have a mean diameter of 4 μm and share a similar flow pattern to red blood cells through the vasculature [352]. The CEU probe can be positioned to allow imaging of specific regions within skeletal muscle and is not influenced by contributions from non-muscle tissue (skin, adipose and bone, Figure 7). The acoustic signal which is generated from the microbubbles exposed to ultrasound is proportional to the concentration of microbubbles within the volume of tissue being imaged. Each high energy pulse generated by the ultrasound destroys the microbubbles within the ultrasound beam at that time. The time between each successive pulse is prolonged and the area being sampled becomes progressively filled with microbubbles until all perfused vessels are filled, so that further

increases in the time between each pulse will not affect the microbubble signal in tissue. The rate at which the microbubbles re-appear within the ultrasound beam provides an indication of microvascular flow velocity and the plateau video intensity reached at long pulsing intervals provides a measurement of microvascular volume or a measure of microvascular perfusion. Once the images are collected, the signal from the tissue as well as larger rapid filling vessels was eliminated using a background subtraction (pulsing interval of 0.5 seconds, Figure 9), so that only the microvascular volume is observed. A linear-array transducer interfaced with an ultrasound system (HDI-5000, Philips Ultrasound) was positioned over the left proximal adductor muscle (adductor magnus and semimembranosus, Figure 7). Pulse imaging was performed using a L7-4 MHz probe with a transmission frequency of 3.3MHz and the mechanical index (a measure of acoustic power), set at 0.8. Gain settings were optimized and set at the same values for each experiment. Albumin microbubbles (Optison™, GE Health Care, USA), the contrast-enhancement agent, were diluted 1:50 with perfluoropropanegassed saline and infused via the left jugular vein cannula (PE-20, Intramedic®) at $40\mu\text{L}\cdot\text{min}^{-1}$ for the duration of data acquisition. A microbubble infusion rate of $40\mu\text{L}\cdot\text{min}^{-1}$ was chosen because this rate resulted in video intensity measurements that were well within the linear range of the microbubble concentration and video intensity. Images were acquired during continuous imaging and at pulsing intervals of 0.5, 1, 2, 3, 5, 8, 12 and 15 seconds. The pulsing intervals chosen allowed for incremental microvascular (capillary) replenishment with microbubbles between each pulse until the volume within the beam was completely refilled [353]. Approximately 3 frames were acquired at each PI. Data was analysed using QLAB™ software (Version 2.0, Philips Ultrasound, Bothwell). The ultrasound intensity in decibels (dB) within the region of interest (ROI) was converted to acoustic intensity (AI). Images acquired at 0.5 seconds were considered to be the large rapid flow vessels (velocity $> 0.1\text{cm}\cdot\text{s}^{-1}$, larger than $\sim 100\mu\text{m}$ [354]) and these values were background subtracted from images obtained at subsequent pulsing intervals, which represented the microvascular compartment. The background-subtracted video intensity at each pulsing interval (seconds) was measured from the region

of interest in muscle and pulsing interval versus acoustic-intensity curve was plotted (Figure 8 and typical trace Figure 33).

Acoustic-intensity curves, were constructed using the following equation:

$$y = A (1 - e^{-\beta(t-0.5)})$$

where; y is the acoustic intensity at a given pulsing interval,

A is the plateau AI representing the total vascular volume being perfused at the current state of the muscle bed [355],

β is the rate of AI rise and reflects the velocity of microbubbles [353].

The values of A and β represent the values for the microcirculation and the product of A and β ($A \times \beta$) represent the filling velocity [59, 353].

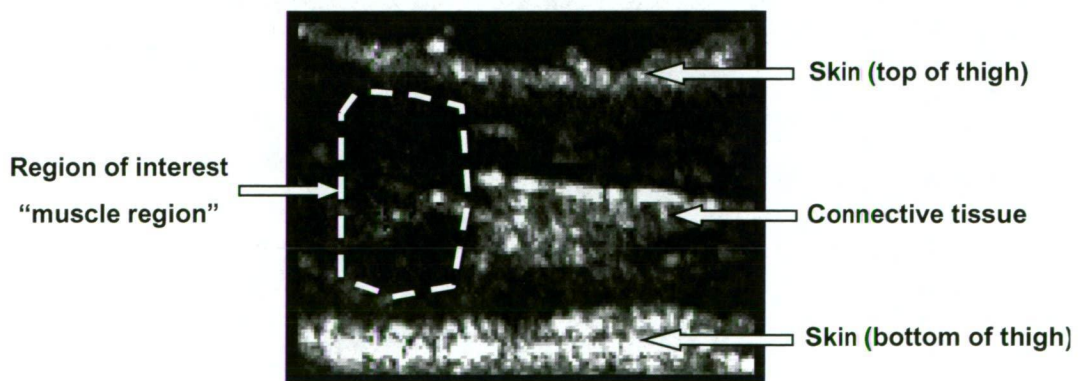


Figure 7: A section of rat thigh muscle showing video intensity (VI) image and region of interest (ROI) used for analysis. Perspective is essentially transverse. Connective tissue (used to help orientate the image) and skin are also shown.

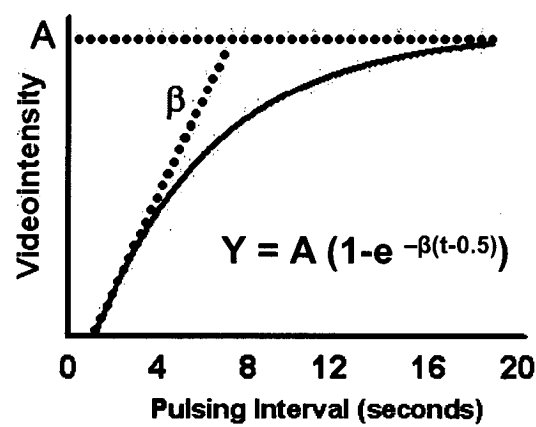


Figure 8: A typical relation between pulsing interval and acoustic signal, measured as video intensity. As the pulsing interval is prolonged, the number of microbubbles within the capillaries increases, resulting in a higher video intensity. Eventually a plateau is reached where an increase in the time between each pulsing interval does not cause a further increase in video intensity due to complete replenishment of the vessels in the beam. The asymptote that intercepts the y-axis is the maximal video intensity signal and a measurement of microvascular volume (microvascular perfusion). The x-intercept of the y-axis

asymptote and the tangent to the upward sloping intensity rise (β), is an indicator of microvascular flow velocity. Reproduced from Vincent [60].

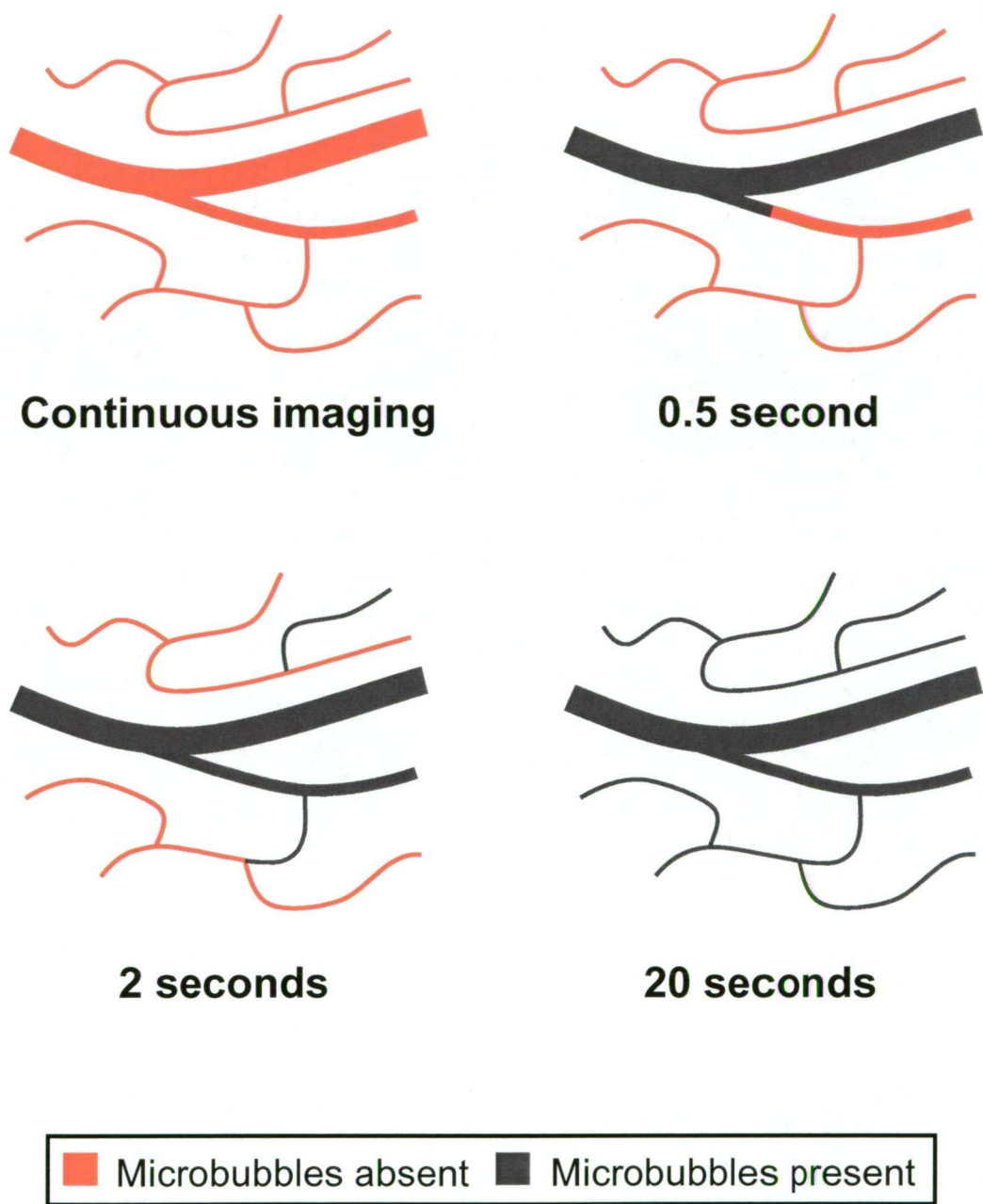


Figure 9: A schematic depiction of the replenishment of microbubbles in capillaries and larger vessels after a pulses of high-energy ultrasound. As time between each ultrasound pulse is prolonged more microbubbles reappear. A pulsing interval of 0.5 seconds allows replenishment of large blood vessels and is used for background subtraction.

2.1.9 Muscle ZMP and AICAR Assay

High performance liquid chromatography (HPLC) was used to determine ZMP and AICAR content in skeletal muscle and AICAR content in plasma, based on methods described by Rattigan *et al.* [52] and Wynants *et al.* [356].

For muscle determination; a sample of pulverized gastrocnemius muscle (100-200mg) was de-proteinised using perchloric acid (PCA, 0.42M) and then centrifuged (IEC centrifuge) at 3,000 rpm at 4°C for 5 minutes. The supernatant (1mL) was transferred to a clean eppendorf tube and neutralized with K₂CO₃ (230µL, 1M). The extract remained on ice for at least 10 minutes to allow precipitation of potassium perchlorate. The salt precipitate was removed by centrifugation at 13,000 rpm in a Biofuge *pico* (Heraeus) for 5 minutes at 4°C and the samples were then stored at -80°C for subsequent AICAR and ZMP analysis using HPLC. For the plasma samples; 100µL of arterial plasma was de-proteinised using 20µL of PCA (2M) and then centrifuged at 13,000 rpm in a Biofuge *pico* (Heraeus) for 5 minutes at room temperature. The supernatant was stored at -20°C for subsequent AICAR analysis by HPLC.

For separation and quantification of AICAR and ZMP a Gemini C₁₈ 5µm reverse phase column (4.6 × 150mm) was used (Phenomenex, NSW, Australia) using a gradient buffer system. Buffer A was composed of 174mM ammonium dihydrogen phosphate (NH₄H₂PO₄) and 1.77mM tetrabutyl-ammonium hydrogen sulfate (TBAHS) (pH 6.0) and ran from 0 to 10 minutes while buffer B contained 174mM NH₄H₂PO₄, 1.77mM TBAHS and 10% acetonitrile (pH 6.0) and ran from 10 to 20 minutes. Detection was conducted with a Varian instrument fitted with a Varian Polychron (Model 9065) diode array detector equipped with LC Star Workstation reading at 254nm. Solutions of known amounts of the pure compounds AICAR (Toronto Research Chemicals, Canada) and ZMP (Sigma-Aldrich Inc., St. Louis, MO, USA) were used as standards. The peaks obtained in the plasma samples were then identified by retention times and absorbance spectra and then quantified using a commercial software package (Star Chromatography Workstation, version 6.41).

2.1.10 Western Blots

Tissue homogenates were subject to sodium dodecyl sulfate-polyacrylamide gel electrophoresis (SDS-PAGE) for the separation of proteins and further identification was determined by immunoblotting.

The tissues for the homogenates were obtained at the end of the experiment. The thoracic aorta, a portion of the liver and the lower leg muscles (gastrocnemius group) were removed and freeze-clamped (muscles and liver *in situ*; aorta as quickly as possible after removal) using liquid nitrogen-cooled tongs and stored at -80°C until assayed. The frozen tissue samples were ground into a fine powder under liquid nitrogen and homogenized in (1/60 w/v) ice cold solubilizing buffer with a Silent Crusher S (Heidolph). The solubilizing buffer was composed of 25mM Tris (pH 7.5), 2.6M potassium fluoride and 250mM EDTA. The insoluble material was removed by centrifugation at 13,000 rpm in a Biofuge *pico* (Heraeus) for 10 minutes at 4°C. The protein concentration of the supernatants was determined using Bio-Rad Protein Assay (Bio-Rad Protein Assay, Bio-Rad Laboratories, Hercules, CA, USA). Aliquots of the resulting supernatant containing 10µg of protein were then heated treated with 70mM Tris buffered (pH 6.8) sodium dodecylsulphate (2% SDS) for 5 minutes in a dry block heater (Ratek) for 5 minutes at 90 to 100°C. Heat treated aliquots were subjected to SDS gel electrophoresis run at 200V for 1 hour at room temperature using a pre-cast 10% Bis-Tris Gel (Invitrogen). The BenchMark™ Pre-Stained Protein Ladder (Invitrogen) was used for molecular weight comparison.

Electrotransfer of proteins from the gel to nitrocellulose membranes was performed at 30V (constant voltage) at 4°C over night. After transfer membranes were blocked with Tris Buffered Saline (TBS), 0.1% Tween-20 with 5% w/v nonfat dry milk for 1hour. The membranes were then incubated with the primary antibody Phospho-Akt (Ser473) diluted at 1:2000 or Akt Antibody (Cell Signalling) diluted at 1:2000 in buffer containing Tris Buffered Saline (TBS), 0.1% Tween-20 with 5% BSA overnight at 4°C. Membranes were then washed and incubated with the secondary horse radish linked antibody (Cell Signaling) diluted at 1:2000 Tris Buffered Saline (TBS), 0.1% Tween-20 with 5% w/v non-

fat dry milk, for 1 hour at room temperature. The membranes were developed using an enhanced chemiluminescence system (ECL, Progen Biosciences). Bound antibodies were detected by exposure to x-ray Hyper film (Amersham Biosciences). The protein band intensities were quantified by optical density using a commercial software package (DScan EX software version 3.1).

2.2 *In Vitro* Experiments

2.2.1 Animal Care

All experimental protocols and procedures were approved by the Animal Ethics Committee of the Vrije University Medical Center, Amsterdam, Netherlands under the guidelines for Institutional Animal Care and Use.

Male Harlan Wistar rats weighing 324 ± 9 g were obtained from the University Animal House (Amsterdam) and were kept at a constant temperature of $21 \pm 0.6^\circ\text{C}$ on a 12:12 hour light:dark cycle (lights on at 0600 hours). All rats were allowed free access to standard laboratory rat chow and water *ad libitum*.

2.2.2 Preparation and Set-up for the Isolated Vessels

Male wistar rats were anaesthetised with pentobarbital sodium (Nembutal; $70\text{mg}\cdot\text{kg}^{-1}$ i.p) and ketamine ($25\text{mg}\cdot\text{kg}^{-1}$ i.m). The right cremaster muscle was exposed by a ventral incision of the scrotal sac and cleared from connective tissue. The muscle was opened by an incision and the testes were removed. The cremaster was excised and pinned in a dissecting dish containing cold MOPS buffer (approximately 5°C). The buffer consisted of 145mM NaCl, 5mM KCl, 2mM CaCl_2 , 1mM MgSO_4 , 1mM NaH_2PO_4 , 5mM dextrose, 2mM pyruvate, 0.02mM EDTA and 3mM 3-(N-morpholino) propanesulfonic acid.

A first-order arteriole (passive inner diameter 150-200 μm) was dissected from the surrounding muscle and a 1-2 mm long segment was transferred to a pressure monograph. A video camera mounted on a microscope was connected to an electronic measurement system to continuously monitor inner arteriolar diameters. The vessel chamber contained two glass cannulas (outer diameter of tip $\sim 100\mu\text{m}$), a circular heating coil and a thermistor. The vessel chamber was filled with MOPS buffer and sealed with a glass cover. The arteriolar segment was cannulated at one end and secured with a 20 μm suture. The vessel preparation was pressurized to 5 mmHg and flushed to remove blood cells. The other end of the vessel was then cannulated and secured with a suture. The second cannula was then connected to a column filled with MOPS buffer. Pressure inside the vessel was set at 65 mmHg, which has been reported to be in the normal range for first-order arterioles in the cremaster muscle of anesthetized rats [357]. The temperature was raised gradually to 34°C, the *in vivo* temperature of a cremaster muscle. Experiments were performed under low flow conditions and vessels were exposed to vasoactive substances by adding them directly to the vessel chamber.

Prior to experiments, vessel segments were super-fused with MOPS buffer for at least 15 minutes. Segments were then equilibrated for at least 15 minutes. Segments were equilibrated for at least 30 minutes after the end of the washout period. Arterioles included in this study had to full-fill three criteria. First, arterioles that showed signs of leakage were excluded from the study. Second, the arterioles had to develop a level of spontaneous tone corresponding to a reduction in diameter of 40-60% of the passive diameter. Finally the arterioles had to dilate for a long period of time (>6 minutes) in response to the endothelium-dependent vasodilator acetylcholine (ACh, 0.1 μM) before and after the experiment as a measure of the endothelial integrity and stability. At the end of each experiment the passive (maximally dilated) diameter was assessed by adding papaverine (0.1 μM). One or more segments were obtained from one animal. If multiple segments from the same rat were used, each segment was included in a different group (e.g.; insulin and control).

All vasoactive substances were applied to the vessel by adding them to the superfusate. The Krebs buffer consisted of 110mM NaCl, 5mM KCl, 2.5mM CaCl₂, 1mM MgSO₄, 24mM NaHCO₃, 1mM KH₂PO₄, 0.02mM EDTA and 10mM dextrose. It was equilibrated with 5% CO₂, 21% O₂ and 74% N₂ at 33°C. This resulted in a pH of 7.4, a pO₂ of 150 mm Hg and a pCO₂ of 35mm Hg at 33°C (measured by a blood gas analyser, ABL-33; Radiometer, Copenhagen).

2.2.3 Isolated Endothelial Cells

Human microvascular endothelial cells (MVEC) were isolated as described previously [358, 359]. Human microvascular endothelial cells were isolated from the human foreskin and cultured in medium 199 supplemented with 20mmol.L⁻¹ HEPES (pH 7.3), L-glutamine and penicillin/streptomycin (BioWhittaker), newborn calf serum (Gibco), a crude preparation of endothelial cell growth factor (prepared from bovine brain) and human serum (obtained from a local blood bank). Human serum albumin was from Sanguin CLB (Amsterdam, the Netherlands).

2.3 Data Analysis

All data is expressed as means \pm SE. Mean femoral blood flow (FBF), mean heart rate (HR) and mean arterial blood pressure (MAP) were calculated from 5 second sub-samples of the data, representing approximately 500 flow and pressure measurements every 15 minutes. Vascular resistance in the hind leg was calculated as mean arterial blood pressure in millimeters of mercury divided by femoral blood flow in milliliters per minute expressed as resistance units (R.U). Glucose uptake in the hindlimb was calculated as $\mu\text{mol}.\text{min}^{-1}$.

2.4 Statistical Analysis

Details are given in individual chapters.

CHAPTER 3

Acute Effects of Wortmannin on Haemodynamic and Metabolic Actions of Insulin *In Vivo*

3.1 INTRODUCTION

Wortmannin first received widespread attention in 1987 as an inhibitor of agonist-induced superoxide anion production (respiratory burst) in neutrophils [360, 361]. This was studied by Baggiolini *et al.* [360] who demonstrated that sub-molar concentrations of wortmannin were able to inhibit the respiratory burst in neutrophils induced by a number of receptor agonists, including *N*-formylmethionylleucylphenylalanine (fMLP), C5a, leukotriene B₄ (LTB₄) or platelet activating factor (PAF). Studies using platelets later revealed the inhibitory effects of wortmannin appeared to be specific to types of G-protein-coupled receptors [362], however cellular processes triggered by phorbol esters were not effected [133]. Studies using adipose cells demonstrated that micro molar amounts of wortmannin inhibited insulin-stimulated glucose utilization *in vitro* without affecting the insulin receptor tyrosine kinase activity [135]. Studies using neutrophils identified the target for wortmannin inhibition in these cells to be at phosphatidylinositol 3,4,5-triphosphate [PtdIns (3,4,5)P₃] formation from phosphatidylinositol 4,5-bisphosphate [PtdIns (4,5)P₂] by the enzyme phosphoinositide 3-kinase (PI3K) [133]. The concentrations of wortmannin required for the inhibition of PI3K in neutrophils were similar to those reported for the inhibition of fMLP-stimulated superoxide production by the same cell. From these observations it was noted that PI3K was the common site of wortmannin action for both the G protein-coupled fMLP receptors and those leading to superoxide formation [361, 363, 364]. Further evidence for the association between wortmannin inhibition and PI3K was observed using adipose cells treated with insulin which showed that wortmannin abolished the enhanced PI3K activity produced by insulin stimulation. Wortmannin blockade of PI3K activity due to insulin was also shown to effect metabolic outcomes resulting from insulin action, including 2-deoxyglucose uptake [135], reduction of β -adrenergic agonist induced lipolysis [135, 365] and cyclic AMP (cAMP) phosphodiesterase activation [365]. In addition, studies using Chinese hamster ovary (CHO) cells transfected with the insulin receptor showed that wortmannin blocked translocation of GLUT4 glucose transporters to the surface of the cell membrane in response to insulin [366].

After the establishment of wortmannin as a potent and selective inhibitor of PI3K [132, 363, 364, 367, 368], it was found that it could act by covalently and irreversibly binding to the catalytic p110 subunit of PI3K [367, 369] as well as alkylate a lysine residue at the ATP-binding site of p110 α [370]. Concentrations of wortmannin which fully inhibit PI3K have little effect on other signalling molecules. At nanomolar concentrations wortmannin has no effect on the functioning of myosin light-chain kinase (MLCK), protein kinases A, C and G [367], or kinases downstream of PI3K in insulin signalling such as components of the calmodulin-dependant, cAMP dependant and cGMP-dependant protein kinases [371]; mitogen-activated protein kinase [135] and p70^{S6K} [372, 373]. In skeletal muscle nanomolar concentrations of wortmannin can inhibit PI3K insulin-mediated glucose uptake [177, 374]. In contrast hypoxia and muscle contraction which both act to increase glucose uptake are not inhibited by wortmannin in rat skeletal muscle [136, 374]. Wortmannin at nanomolar concentrations, on the other hand has been shown to inhibit a number of signalling components including phospholipases such as PIP₂-phospholipase C, phospholipase D and phospholipase A2 [375] and has also been shown to be non-selective within the PI3K family [134]. Although wortmannin selectively inhibits PI3K at very low concentrations, a number of other signalling pathways have the potential for cross-interferences when exposure to wortmannin is for extended periods [134].

Some studies involving the *in vivo* use of wortmannin have reported various toxic side effects in animals [376, 377]. Other *in vivo* studies have used wortmannin to test effects on tumour growth [378-380] and bone re-absorption [381] but have not examined effects on insulin action *in vivo*. It has been reported previously that when insulin is administered *in vivo* insulin-mediated microvascular perfusion is an early [27] and sensitive [63] event in muscle which aids delivery of insulin and nutrients. It has not been established if insulin-mediated microvascular perfusion *in vivo* is wortmannin sensitive, which requires intact associations between the microvasculature and muscle, as opposed to previous *in vitro* studies.

3.1.1 Aim of the Study

The aim of the present study was to apply wortmannin acutely before and during a hyperinsulinemic euglycaemic clamp in rats *in vivo* to assess effects on haemodynamics and metabolic processes.

3.2 RESEARCH AND DESIGN METHODS

3.2.1 Animals

Male hooded Wistar rats weighing 245 ± 3 g were raised in the University of Tasmania Animal House as described in section 2.1.1. These experiments were performed in accordance with the guidelines of the University of Tasmania Ethics Committee.

3.2.2 *In Vivo* Experiments

Hyperinsulinemic euglycaemic clamps were performed in non-fasted anesthetized rats as described in section 2.1.2. Once the surgery was completed, a period of equilibration of approximately 60 minutes was allowed so that leg blood flow and pressure could become stable and constant. Femoral blood flow in one leg was continuously measured from a Transonic[®] flow probe positioned around the femoral artery.

3.2.3 Experimental Protocols

The experimental protocols are shown in Figure 10. Rats were randomly allocated into one of the five experimental groups outlined in Table 2 (n = 8 per group). Rats received infusion 1 from -60 to 120 minutes and infusion 2 from 0 to 120 minutes (see Table 2).

Table 2: Treatment combinations for the five experimental groups (n = 8 per group).

Group	Infusion 1 (-60 to 120 minutes)	Infusion 2 (0 to 120 minutes)	Abbrev.
1	DMSO	saline	DS
2	Wortmannin ($1\mu\text{g}\cdot\text{min}^{-1}\cdot\text{kg}^{-1}$)	saline	WS
3	Wortmannin ($1\mu\text{g}\cdot\text{min}^{-1}\cdot\text{kg}^{-1}$)	insulin ($10\text{mU}\cdot\text{min}^{-1}\cdot\text{kg}^{-1}$)	WI ₁₀
4	DMSO	insulin ($10\text{mU}\cdot\text{min}^{-1}\cdot\text{kg}^{-1}$)	DI ₁₀
5	DMSO	insulin ($20\text{mU}\cdot\text{min}^{-1}\cdot\text{kg}^{-1}$)	DI ₂₀

Rats were infused with 0.5% (v/v) dimethylsulfoxide (DMSO) or wortmannin ($1\mu\text{g}\cdot\text{min}^{-1}\cdot\text{kg}^{-1}$, Sigma Chemical Co., St. Louis, MO, USA) in 0.5% DMSO (Figure 10). Wortmannin, which is insoluble in aqueous solutions, was dissolved in 0.5% DMSO which was the vehicle for wortmannin. Wortmannin infusions were initiated by a bolus injection of $2.5\mu\text{g}$ in 0.20mL saline at $t = -60$ minutes (Figure 10) followed by a constant infusion (jugular vein) for 3 hours at $1\mu\text{g}\cdot\text{min}^{-1}\cdot\text{kg}^{-1}$. One hour later ($t = 0$ minutes) saline or insulin infusions (10 or $20\text{mU}\cdot\text{min}^{-1}\cdot\text{kg}^{-1}$, Humulin R Eli Lilly, Indianapolis, IN, USA) were commenced and continued for 120 minutes (Figure 10). Glucose infusion 30% (w/v) was commenced 2 minutes after the commencement of insulin infusions at a rate to maintain euglycaemic assessed from arterial blood glucose samples. At $t = 55$ minutes a bolus injection of allopurinol (10

$\mu\text{mol.kg}^{-1}$) was administered followed by infusions of 1-MX ($0.4 \text{ mg.min}^{-1}.\text{kg}^{-1}$) and $[3\text{-}^3\text{H}]$ glucose ($0.1 \mu\text{Ci.min}^{-1}$). Infusions are indicated by the bars (Figure 10).

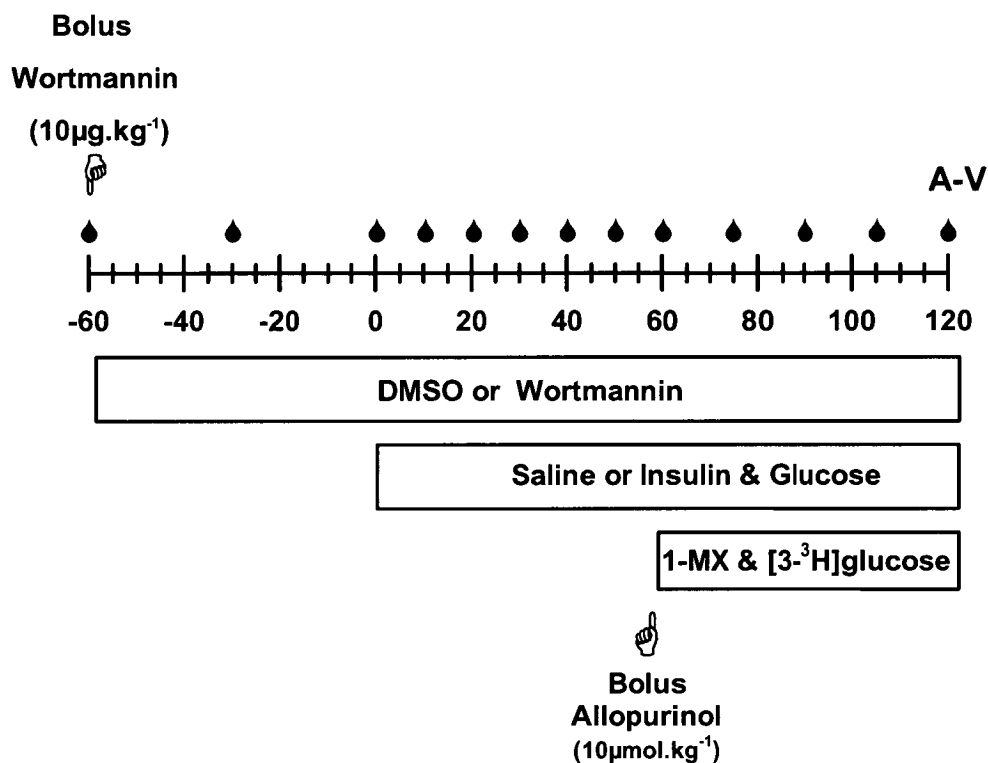


Figure 10: Arterial and venous samples were collected at the times indicated as A-V for HPLC analysis and plasma glucose determination. Arterial blood glucose concentration was determined at times indicated by \blacklozenge . Venous infusion periods are indicated the bars. Bolus infusion periods are indicated by ✎ .

3.2.3.1 Microvascular Perfusion

Microvascular perfusion was determined by measuring the metabolism of infused 1-MX (Section 2.1.8.1). 1-MX was infused intravenously at a constant rate of $0.4 \text{ mg.min}^{-1}.\text{kg}^{-1}$ during the last 60 minutes of each experiment. A bolus injection of allopurinol was given in the carotid artery 5 minutes before the commencement of 1-MX infusion (Figure 10). Allopurinol is converted to oxypurinol, the major inhibitor of the enzyme xanthine oxidase (details in section 2.1.8.1). At the end of the

experiment arterial (A) and femoral vein (V) blood samples were taken. Hind leg glucose uptake and 1-MX metabolism was calculated from the arterio-venous (A-V) difference multiplied by the flow value immediately before the A sample was taken. 1-MX metabolism is an indicator of the perfused microvascular surface area as described in section 2.1.8.1.

3.2.3.2 Muscle Specific Glucose Uptake (R'g)

At 45 minutes prior to the completion of the experiment, a 50 μ Ci bolus of [14 C]2-DG was administered. Plasma samples (25 μ L) were collected at 5, 10, 15, 30 and 45 minutes after the 2-DG injection to determine the time course for plasma radioactive decay. At the conclusion of the experiment, the muscles were removed, freeze clamped in liquid nitrogen and stored at -20°C until 2-DG radioactivity assay as described in section 2.1.5.2.

3.2.3.3 Whole Body Rate of Glucose Disposal

A primed 2 μ Ci continuous (0.1 μ Ci.min $^{-1}$) dose of D-[3- 3 H] glucose was infused during the final 60 minutes of the experiment so that glucose homeostasis could obtain a steady state. Arterial plasma samples were taken at 105 and 120 minutes to determine the plasma [3 H] glucose radioactivity so that the rate of hepatic glucose disappearance (Rd) and rate of hepatic glucose appearance (Ra) could be calculated (details are given in 2.1.5.1).

3.2.3.4 Blood Sampling

Arterial samples were taken at the times indicated (Figure 10) for blood glucose measurements. An arterial blood sample (0.5mL) was taken from the carotid artery at the end of the experiment. This blood sample was used for 1-MX assay and [3- 3 H]-glucose specific activity measurement. A sample of venous blood (0.5mL) was taken from the femoral vein of left leg and was used for subsequent 1-MX assay and HLGU assay. A glucose analyser (Model 2300 Stat plus, Yellow Springs

Instruments, Yellow Springs, OH, USA) was used to determine whole body glucose (by the glucose oxidase method) during the insulin clamp.

3.2.4 Plasma Insulin Assay

Arterial plasma samples were taken before the commencement and at the end of the experimental procedures. Additional experiments were conducted to examine the time course increases of plasma insulin with wortmannin alone treatment. Plasma insulin was determined using the ELISA assay (ELISA, Mercodia AB, Sweden) using rat insulin standards (section 2.1.3.1.2).

3.2.5 Western Blots for P-Akt

Tissue samples for the homogenates were obtained at the end of the experiment. Liver, muscle (taken *in situ*) and aorta (as quickly as possible after euthanising the rat) samples were removed and freeze clamped using liquid nitrogen cooled tongs and then stored at -80°C for subsequent determination of P-Akt and Akt_{total} by Western blot analysis (section 2.1.10)

3.2.6 Data Analysis

All data are expressed as means \pm SE. Data analysis was conducted as described in section 2.3.

3.2.7 Statistical Analysis

Repeated measures two-way analysis of variance was used to test the hypothesis that there were no differences between treatment groups for change in heart rate, change in blood pressure, change in femoral blood flow and change in vascular resistance through out the time course. When a significant difference ($P < 0.05$) was found, pair wise comparisons by the Student-Newman-Keuls *post hoc* test were used to determine at which sampling times the differences were significant. Statistical significance of differences between treatments for arterial glucose (at the

end of the experiment), plasma insulin, GIR (at the end of the experiment), HLGU, Ra, Rd, microvascular perfusion and the ratio of P-Akt/Akt_{total}, arterial 1-MX concentration (data not shown) and oxypurinol concentration (data not shown) were determined by one way ANOVA. The ratio of P-Akt/Akt_{total} were determined by two way ANOVA. When a significant difference ($P < 0.05$) was found, pair wise comparisons by the Student-Newman-Keuls *post hoc* test were used to determine at which sampling times the differences were significant. These tests were performed using SigmaStat™ statistical program (Jandel Software, version 2.03)

3.3 RESULTS

3.3.1 Plasma Insulin and Glucose

Table 3 shows blood glucose (BG) and plasma insulin values measured at the end of the experiment for each of the five protocols: DS, WS, WI₁₀, DI₁₀ and DI₂₀. The BG values were similar for all five protocols (ie., ~5mM). In protocols involving insulin infusion, concentrated glucose (30%) solution was infused in order to maintaining blood glucose at a constant basal value (Figure 12B-C). The plasma insulin values show significant differences between the groups. Insulin infusions of 10 and 20mU.min⁻¹.kg⁻¹ increased the basal value of 410 ± 49 to 1680 ± 430 and 5060 ± 320 pM respectively. Wortmannin treatment alone significantly increased plasma insulin to approximately 5,000 pM (Table 3) and this was not further increased by co-infusion of 10mU.min⁻¹.kg⁻¹ insulin and wortmannin. In summary all groups involving wortmannin treatment as well as 20mU.min⁻¹.kg⁻¹ insulin had a plasma insulin value of approximately 5000 pM at the end of the experiment (Table 3).

The time course for plasma insulin during the wortmannin treatment is shown in Figure 11. Plasma insulin increased significantly after 2 hours of wortmannin infusion and continued to increase to approximately 5,000 pM by the end of the 3 hour infusion period.

Table 3: Blood glucose and plasma insulin values at the end of the experiments.
Details are given in Figure 10.

TREATMENT	DS	DI ₁₀	DI ₂₀	WS	WI ₁₀
Blood Glucose (mmol.L ⁻¹)	5.47 ± 0.23	5.22 ± 0.12	4.81 ± 0.011	5.36 ± 0.31	4.64 ± 0.3
Plasma Insulin (pmol.L ⁻¹)	410 ± 49†#	1680 ± 430*†	5060 ± 230*#	5450 ± 770*#	4090 ± 490*#

Values are means ± SE from groups (n = 8) determined at t = 120 minutes: vehicle (dimethylsulfoxide) + saline (DS), vehicle + insulin 10mU.min⁻¹.kg⁻¹ (DI₁₀), vehicle + insulin 20mU.min⁻¹.kg⁻¹ (DI₂₀), wortmannin + saline (WS) and wortmannin + insulin 10mU.min⁻¹.kg⁻¹ (WI₁₀). * Significantly different (P<0.05) from DS values; # Significantly different from DI₁₀; †significantly different from DI₂₀.

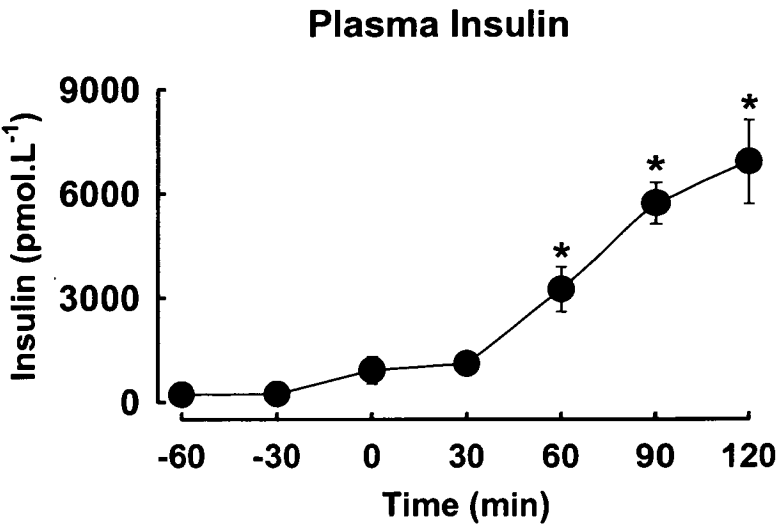


Figure 11: Time course for plasma insulin during wortmannin alone treatment.
Details are given in Figure 10. Values are means ± SE. * Significantly different from

t = -60 minute values (n = 4).

3.3.2 Glucose Metabolism

Figure 12 shows time courses for blood glucose (BG) for each of the five experimental groups and glucose infusion rate (GIR) for experimental groups involving insulin. During the wortmannin + saline treatment, blood glucose started to increase approximately 40 minutes after saline infusion but this increase returned to baseline values by the end of the experiment (Figure 12A). During the insulin clamp conditions, blood glucose was maintained at euglycaemia by infusion of 30% glucose (Figure 12B). Figure 12C shows the time course data for the glucose infusion rate (GIR) required to maintain euglycaemia which is an index of insulin sensitivity. Co-infusion of wortmannin with $10\text{mU}\cdot\text{min}^{-1}\cdot\text{kg}^{-1}$ saw an initial rise followed by a decrease in the GIR in the first 30 minutes which took approximately 1 hour to stabilise. Values for GIR at the end of the experiment are shown in Figure 13A. Both doses of 10 and $20\text{mU}\cdot\text{min}^{-1}\cdot\text{kg}^{-1}$ caused an increase in glucose requirement to maintain euglycaemia, while wortmannin showed a significant inhibition of glucose disposal in the $10\text{mU}\cdot\text{min}^{-1}\cdot\text{kg}^{-1}$ insulin group (Figure 12C).

Hind leg glucose uptake (HLGU, Figure 13B) calculated from the A-V difference (glucose extraction) multiplied by the FBF showed a significant stimulatory effect in the both 10 and $20\text{mU}\cdot\text{min}^{-1}\cdot\text{kg}^{-1}$ insulin groups. Wortmannin alone was also stimulatory but a combination of wortmannin plus $10\text{mU}\cdot\text{min}^{-1}\cdot\text{kg}^{-1}$ insulin was lower than $20\text{mU}\cdot\text{min}^{-1}\cdot\text{kg}^{-1}$ insulin alone (Figure 13B), despite equivalent plasma levels. Values for rate of appearance (Ra) and rate of disappearance (Rd) are shown in Figure 13C-D. Rd is an index of the whole body glucose disappearance rate during insulin stimulation and Ra is calculated as the difference between the GIR and Rd and reflects the liver insulin sensitivity (Details: Chapter 2: section 2.1.5.1, page 48). Ra was significantly inhibited by both doses of insulin. Wortmannin alone significantly increased Ra by approximately 30% compared with saline. When insulin $10\text{mU}\cdot\text{min}^{-1}\cdot\text{kg}^{-1}$ and wortmannin were combined Ra was significantly increased, demonstrating the ability of wortmannin to prevent insulins suppression of Ra. Values for Rd followed a similar pattern to HLGU, with each dose of insulin stimulating glucose uptake by 72 and 144

$\mu\text{mol}\cdot\text{min}^{-1}\cdot\text{kg}^{-1}$ for 10 and 20 $\text{mU}\cdot\text{min}^{-1}\cdot\text{kg}^{-1}$ insulin respectively (Figure 13D). The wortmannin treatment alone significantly increased Rd and wortmannin and 10 $\text{mU}\cdot\text{min}^{-1}\cdot\text{kg}^{-1}$ insulin showed no significant difference from wortmannin alone. The combination of wortmannin and 10 $\text{mU}\cdot\text{min}^{-1}\cdot\text{kg}^{-1}$ insulin was lower than 20 $\text{mU}\cdot\text{min}^{-1}\cdot\text{kg}^{-1}$, even though the plasma insulin levels for these two groups were similar (Table 3).

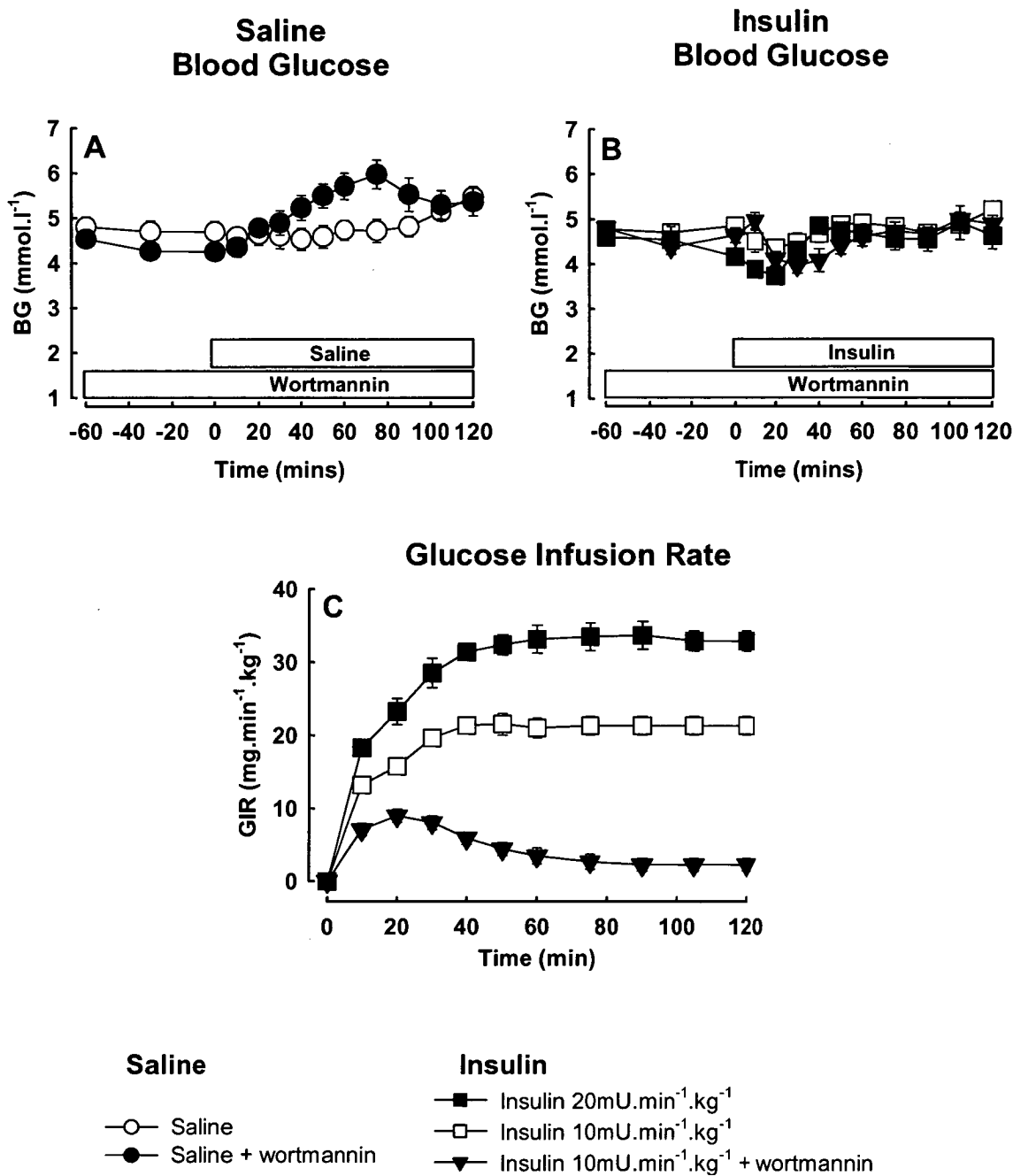


Figure 12: Time course for the effect of wortmannin on blood glucose (BG) in control (saline, **A**) and insulin infusions (**B**) and for whole body glucose infusion rate (GIR, **C**) to maintain euglycaemia in insulin clamps. Details are given in Figure 10. Values are means \pm SE ($n = 8$ per group).

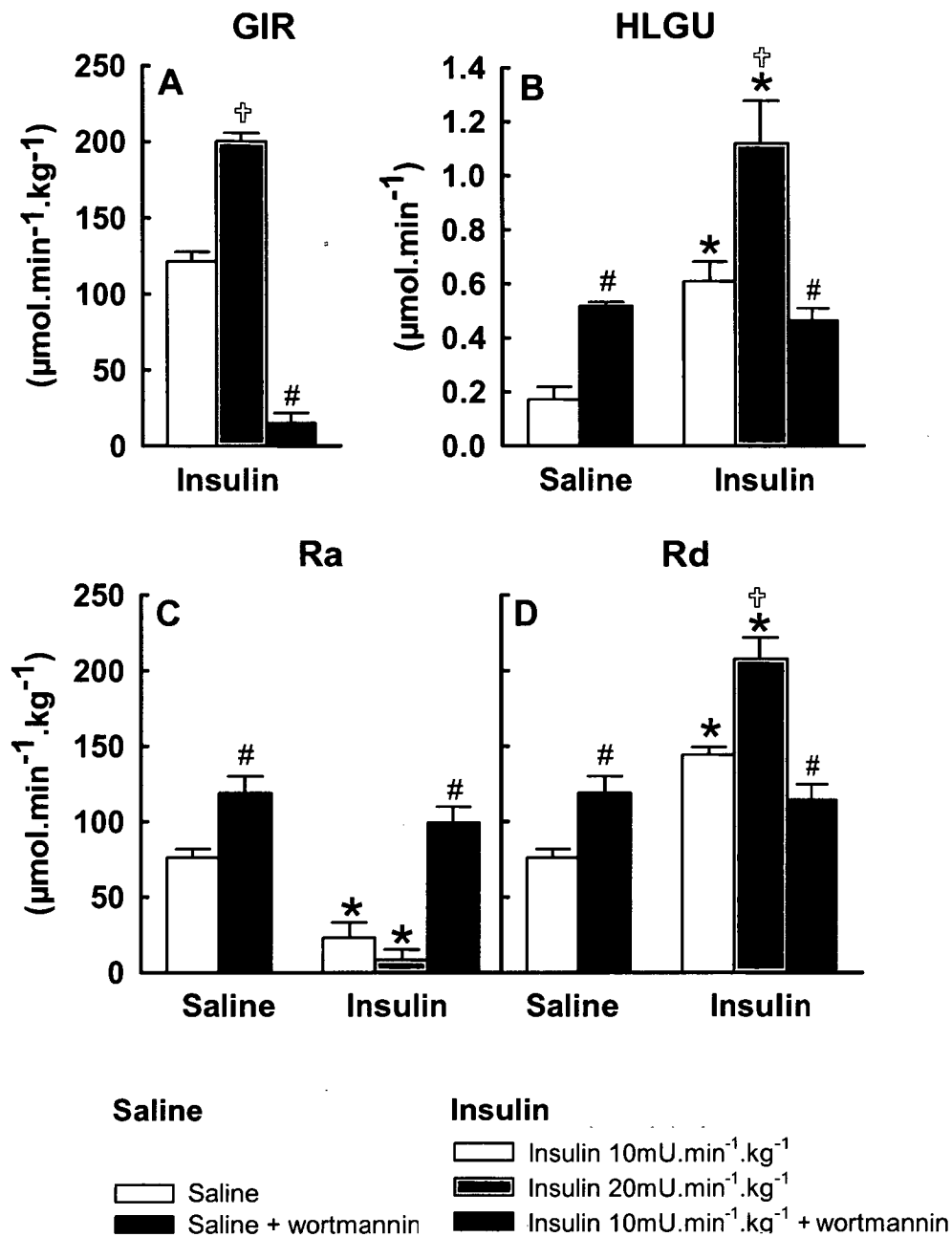


Figure 13: Glucose infusion rate (GIR, **A**), hindleg glucose uptake (HLGU, **B**), glucose appearance (Ra, **C**) and glucose disposal (Rd, **D**). Details are given in Figure 10. Values were determined at the end of the experiment and are means \pm SE. * Insulin treated significantly different ($P < 0.05$) from corresponding saline treated values; # Wortmannin treated significantly different from corresponding vehicle treated values. † 20mU.min⁻¹.kg⁻¹ insulin significantly different from 10mU.min⁻¹.kg⁻¹ treated ($n = 8$ per group).

3.3.3 Haemodynamic Effects

Figure 14 shows the time courses for change in heart rate (Δ HR) and blood pressure (Δ BP) and Figure 15 shows the time courses for change in femoral blood flow (Δ FBF) and vascular resistance (Δ VR) over the preceding 60 minutes before and during saline (control) or 120 minute hyperinsulinemic euglycaemic clamp.

Figure 14A-B shows the Δ HR for all groups. Wortmannin + saline caused a gradual decrease in HR compared with saline which was significant beginning at $t = -15$ minutes and concluding at $t = 60$ minutes then gradually returning to near the basal rate until the conclusion of the experiment (Figure 14A). The HR in the wortmannin + insulin $10\text{mU}\cdot\text{min}^{-1}\cdot\text{kg}^{-1}$ group followed a similar pattern to that of wortmannin alone group. The HR in the wortmannin + insulin group was significantly decreased compared with insulin from $t = 0$ until $t = 60$ minutes, then gradually returned to near the basal rate until the conclusion of the experiment (Figure 14B). There were no significant differences between the HR in the $10\text{mU}\cdot\text{min}^{-1}\cdot\text{kg}^{-1}$ insulin and the $20\text{mU}\cdot\text{min}^{-1}\cdot\text{kg}^{-1}$ insulin groups (Figure 14B).

Figure 14C-D shows Δ BP for all groups. During the wortmannin + saline treatment, there was a significant increase in BP which began at approximately the same time as the decrease in heart rate ($t = -15$ minutes) and remained significantly increased until the end of the experiment (Figure 14C). There was also an increase in BP in the wortmannin + insulin $10\text{mU}\cdot\text{min}^{-1}\cdot\text{kg}^{-1}$ co-infusion group which began at $t = -30$ minutes and followed a similar pattern to the wortmannin + saline group. There were no significant differences between the BP in the $10\text{mU}\cdot\text{min}^{-1}\cdot\text{kg}^{-1}$ insulin and the $20\text{mU}\cdot\text{min}^{-1}\cdot\text{kg}^{-1}$ insulin groups (Figure 14D).

Figure 15A-B and Figure 15C-D show the effects of wortmannin and insulin on Δ FBF and Δ VR for all groups. Both $10\text{mU}\cdot\text{min}^{-1}\cdot\text{kg}^{-1}$ and $20\text{mU}\cdot\text{min}^{-1}\cdot\text{kg}^{-1}$ insulin groups gradually increased FBF, by approximately $0.5\text{ml}\cdot\text{min}^{-1}$ compared with the basal value, over the time course of the experiment after the commencement of insulin infusion (Figure 15B). Groups which included wortmannin (wortmannin + saline and wortmannin + $10\text{mU}\cdot\text{min}^{-1}\cdot\text{kg}^{-1}$ insulin) resulted in a decrease in the FBF below basal. In the wortmannin + saline group there was a trend for the FBF to

decrease below basal at $t = 45$ minutes and this trend continued until the end of the experiment, attaining significance for the last 15 minutes of the experimental period (Figure 15A). During the wortmannin + insulin treatment there was a significant decrease below basal values at $t = 30$ minutes which continued to significantly decrease until the end of the experiment (Figure 15B). In summary, wortmannin + insulin $10\text{mU}\cdot\text{min}^{-1}\cdot\text{kg}^{-1}$ lowered the FBF below that of $20\text{mU}\cdot\text{min}^{-1}\cdot\text{kg}^{-1}$ insulin and so blocked the stimulatory effects that insulin has on FBF, as each group had a similar value for plasma insulin (Table 3).

Figure 15C-D shows the effect of wortmannin on VR. Wortmannin caused a significant increase in vascular resistance in both wortmannin + saline and wortmannin + $10\text{mU}\cdot\text{min}^{-1}\cdot\text{kg}^{-1}$ insulin groups which became significant at $t = 15$ minutes and $t = 30$ minutes respectively and continued to steadily increase until the conclusion of the experiment (Figure 15C-D).

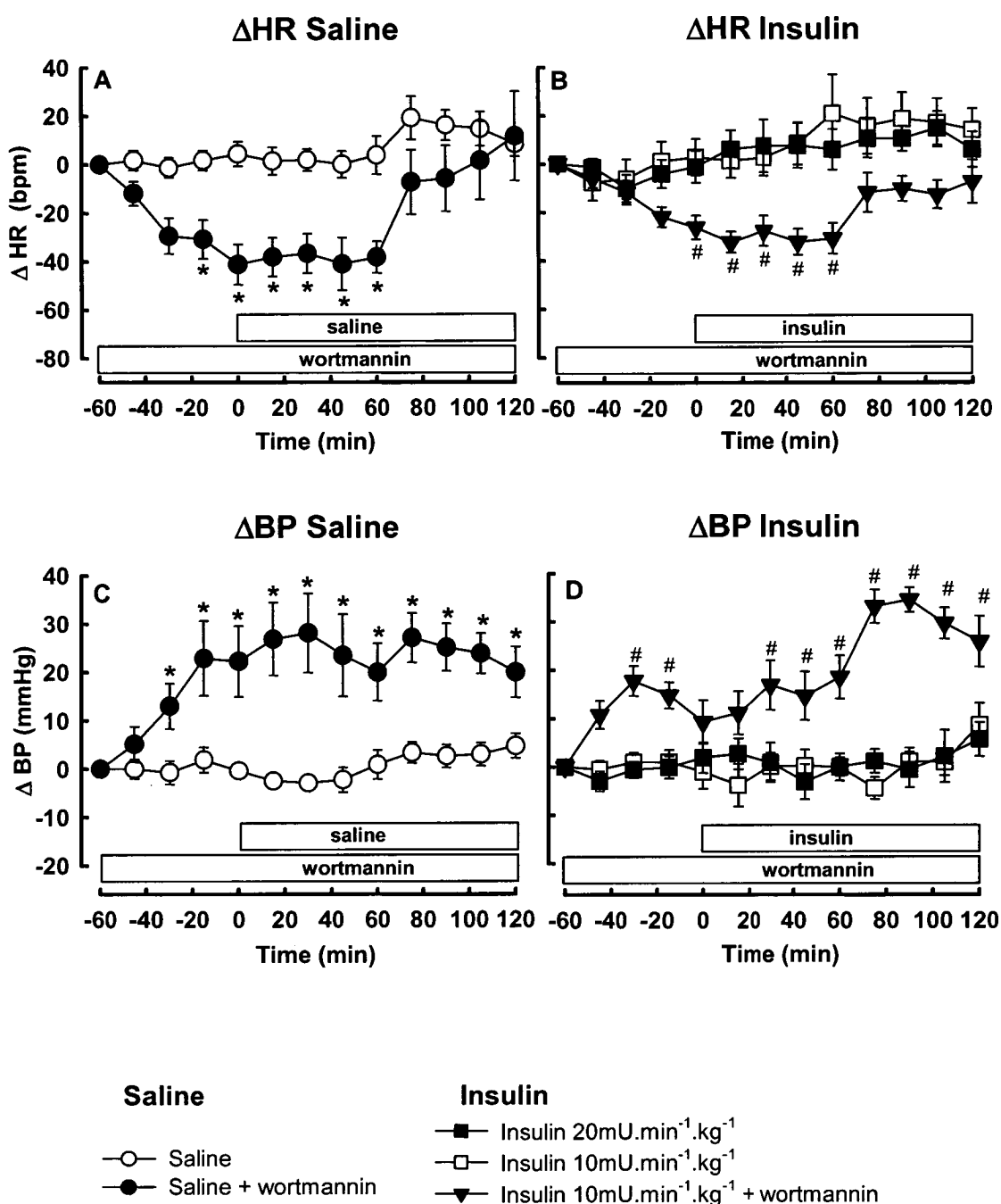


Figure 14: Time course for the effect of wortmannin on changes in heart rate (Δ HR, **A & B**) and blood pressure (Δ BP, **C & D**) in control (saline) and insulin infusions. Details are given in Figure 10. Values are given as means \pm SE. * Indicates a significant difference ($P < 0.05$) between wortmannin + saline treatment and vehicle + saline treatment. # Indicates a significant difference between wortmannin + insulin treatment and both vehicle + insulin treatments ($n = 8$ per group).

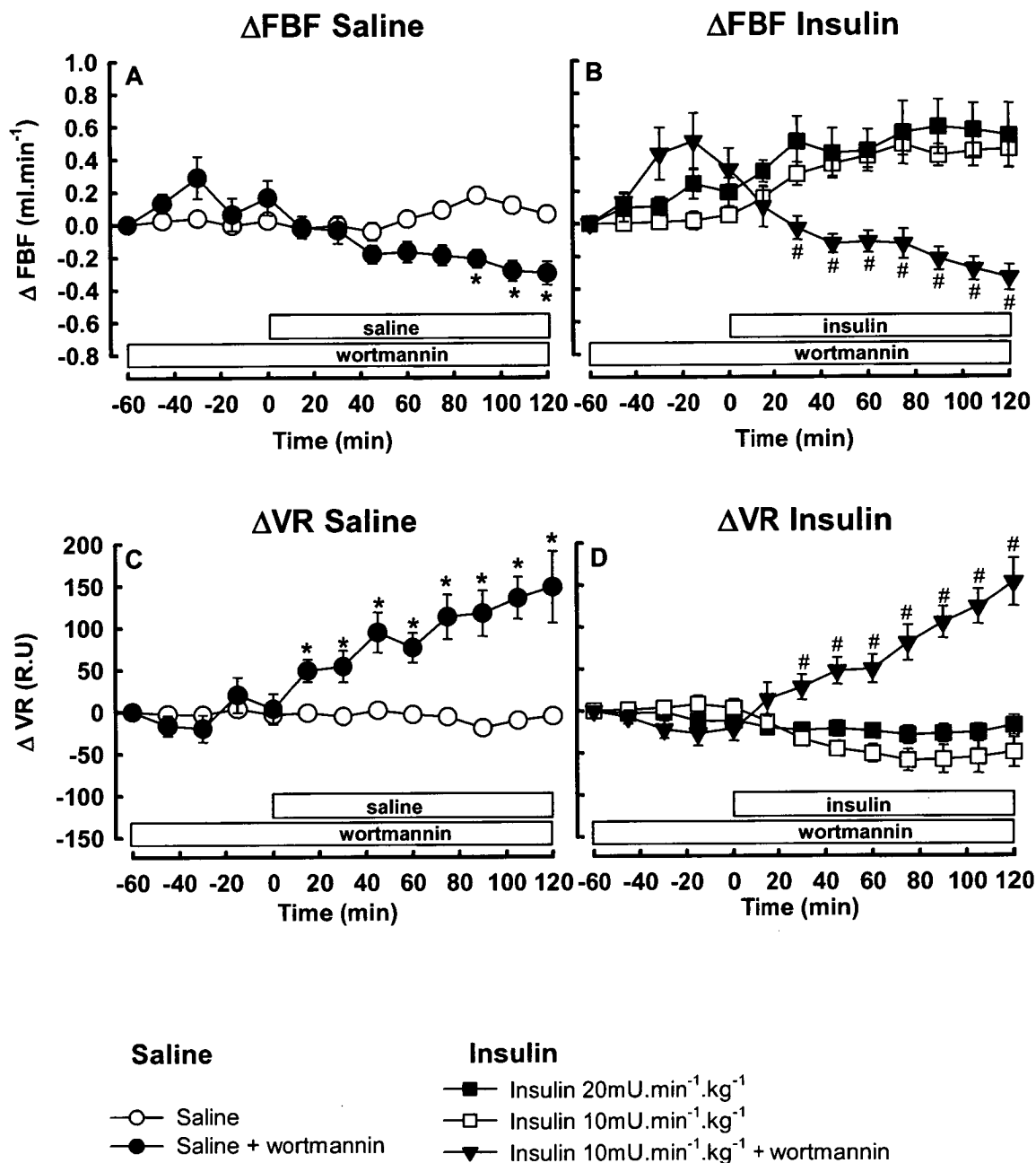


Figure 15: Time course for the effect of wortmannin on changes in femoral blood flow (ΔFBF, **A** & **B**) and vascular resistance (ΔVR, **C** & **D**) in control (saline) and insulin infusions. Details are given in Figure 10. Values are given as means ± SE. * Indicates a significant difference (P<0.05) between wortmannin + saline treatment and vehicle + saline treatment. # Indicates a significant difference between wortmannin + insulin treatment and both vehicle + insulin treatment (n = 8 per group).

3.3.4 1-MX Metabolism: Microvascular Perfusion

Microvascular perfusion, measured by MXD and determined by the A-V differences and FBF at the end of the experiment ($t = 120$ minutes) is shown in Figure 16. There were no significant differences in arterial 1-MX or oxypurinol concentration (data not shown) between all five experimental groups. The mean arterial 1-MX concentration and mean oxypurinol concentration was $22.29 \pm 0.089 \mu\text{mol.L}^{-1}$ and $4.86 \pm 0.15 \mu\text{mol.L}^{-1}$ respectively. Insulin $10\text{mU.min}^{-1}.\text{kg}^{-1}$ significantly increased MXD compared with the saline control. Wortmannin alone was not significantly different from saline. Wortmannin plus $10\text{mU.min}^{-1}.\text{kg}^{-1}$ insulin was also not significantly different from saline indicating that the stimulatory effects insulin had to increase MXD had been completely blocked by wortmannin (Figure 16).

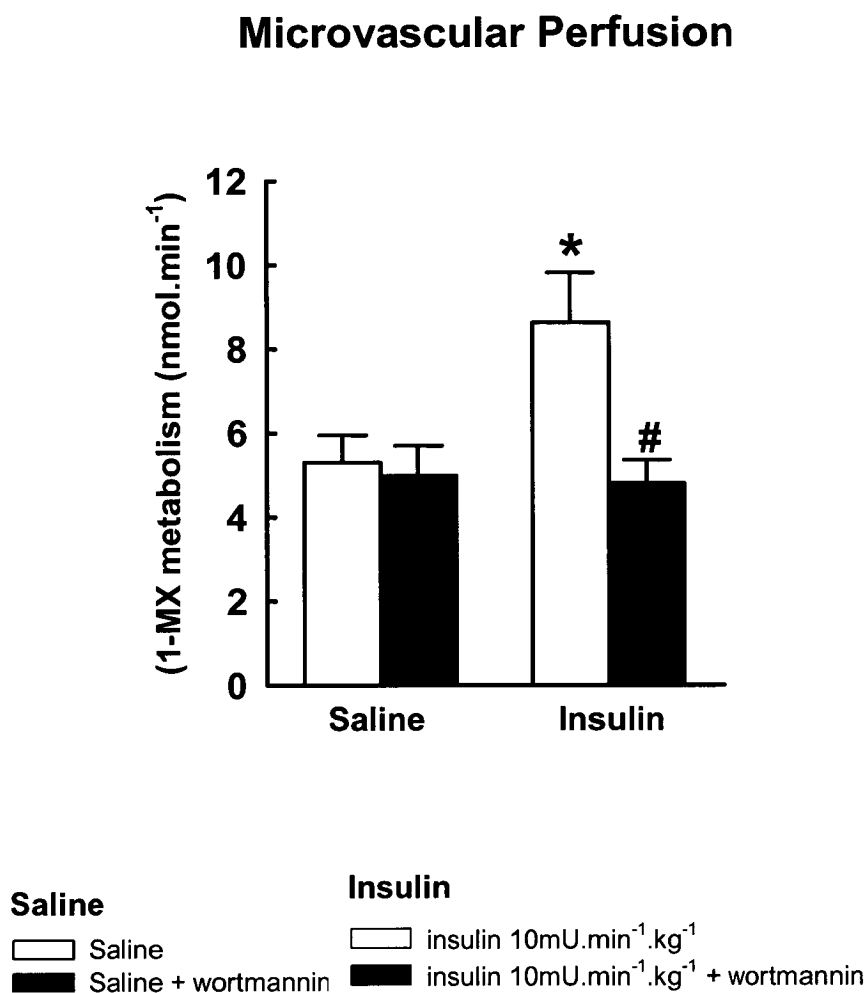


Figure 16: Effect of wortmannin, insulin and a combination of wortmannin + insulin on hindleg muscle microvascular perfusion determined from 1-MX metabolism. Details are given as in Figure 10. Values were determined at the end of the experiments ($t = 120$ minutes) and are means \pm SE. * Insulin treated significantly different ($P < 0.05$) from corresponding saline treated value; # Wortmannin treated significantly different from corresponding vehicle treated value ($n = 8$ per group).

3.3.5 Western Blots for P-Akt and Akt_{total}

Figure 17A-C shows data and representative Western blots for phosphorylated Akt (P-Akt) and total Akt (Akt_{total}) in liver (A), muscle (B) and aorta (C) determined by the Western blot technique. The antibodies were directed to the phospho-Ser⁴⁷³ motif and to Akt. Results are expressed as the ratio P-Akt/Akt_{total}.

During the insulin treatment (20 mU.min⁻¹.kg⁻¹) the relative proportion of P-Akt was significantly increased compared with saline in all tissues. Wortmannin significantly inhibited the insulin mediated increase in P-Akt/Akt_{total} in the liver and aorta but this trend for decrease did not reach significance in the skeletal muscle. There was also an increase in the P-Akt/Akt_{total} in the wortmannin + saline muscle group compared with saline, possibly due to the relatively increased levels of plasma insulin concentrations (Table 3), but this significant increase was not observed in liver and aorta.

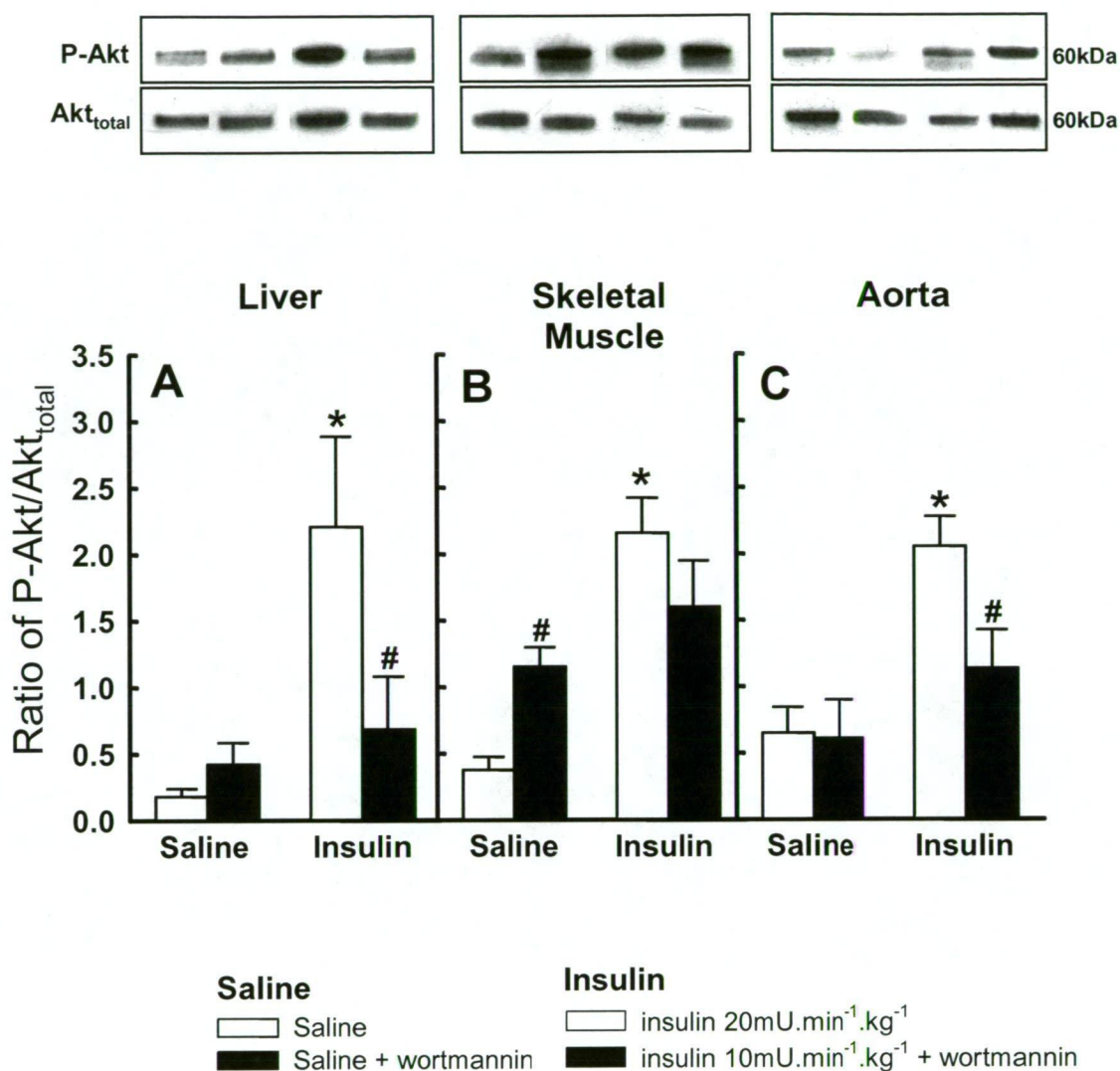


Figure 17: Effect of wortmannin, insulin and a combination of wortmannin + insulin on phosphorylation of Akt in liver (A), skeletal muscle (B) and aorta (C). Details are given in Figure 10 and the materials and methods (section 2.1.10). Ratios of P-Akt to Akt_{total} have been determined by image analysis of gel bands for vehicle treated rats with either saline or 20mU.min⁻¹.kg⁻¹ insulin (open bars) and wortmannin treated rats with either saline or 10mU.min⁻¹.kg⁻¹ insulin (filled bars). * Insulin significantly different ($P < 0.05$) from corresponding saline treated values; # Wortmannin treated significantly different from corresponding vehicle treated values ($n = 4$ per group).

3.4 DISCUSSION

The main findings of the present study are that systemically administered wortmannin *in vivo* inhibited the haemodynamic effects of insulin; including total blood flow and microvascular perfusion as well as glucose uptake. These results suggest that limb blood flow and microvascular perfusion are controlled by an insulin-signalling cascade involving PI3K, the target for wortmannin inhibition, which is coupled with metabolic effects. The study was undertaken because the haemodynamic effects of insulin to increase limb blood flow and microvascular perfusion cannot be studied *in vitro*. This study represents the first report on the use of wortmannin to assess effects on insulin action *in vivo* and particularly to test whether insulin's control of microvascular perfusion in muscle is wortmannin sensitive.

When administered at the low dose used in the current study, there were several unwanted side effects associated with systemic wortmannin infusion *in vivo*. These unwanted side effects included decreases in heart rate and increases in blood pressure, vascular resistance and plasma insulin. An unexpected finding of *in vivo* infusion of wortmannin was the marked increase in plasma insulin by 10 to 20 fold above basal. This increase in plasma insulin occurred independently to any prior increase in blood glucose concentration. An explanation for this response is not clear as previous *in vitro* experiments using isolated β -cells, by others have found that wortmannin can both inhibit [382] and stimulate [383-385] glucose-mediated insulin release. A tissue-specific knockout of the β -cell insulin receptor (β IRKO) displays an insulin secretory defect with a loss of insulin release in response to glucose [386]. Hence in the current study, the increase in insulin suggests that wortmannin may be acting on pancreatic β -cells by an insulin receptor independent pathway. The observed increase in insulin with wortmannin infusion is likely to be due to an increase in insulin secretion but it is also possible that the clearance of insulin is affected by wortmannin treatment. Although not carried out in this study, further studies to resolve these possibilities would involve performing additional experiments using local infusion of wortmannin via the epigastric artery. Local infusion could eliminate other tissue actions. Performing a C-peptide assay would determine if wortmannin is increasing insulin secretion *in vivo*.

The causes for the increase in BP and VR by wortmannin are unknown but may be the result of inhibition of PI3K specific vasodilatory action at the peripheral resistance sites or because of central nervous system actions of wortmannin. The change in VR in the current study appears to parallel changes in plasma insulin levels caused by wortmannin (Figure 11 and Figure 15C-D). Insulin regulates vascular tone by stimulating both vasodilator and vasoconstrictor effects. Insulin has been shown to induce both vasodilation by activation of Akt, which enhances activity of eNOS [387] as well as vasoconstriction through endothelin release from the muscle vasculature [388]. Impairment of insulin mediated vasoreactivity in the muscle vasculature may be due to an imbalance between insulin-mediated nitric oxide and endothelin production. Thus, in the presence of wortmannin, the increased plasma insulin and associated endothelin release may be the cause for the increase in VR and contribute to the raised BP [389].

The rise in plasma insulin produced by wortmannin alone was such that at the end of the experiment the plasma levels were approximately 5,000 pM. Plasma insulin levels produced by infusion of $20\text{mU}\cdot\text{min}^{-1}\cdot\text{kg}^{-1}$ were similar to those produced in the wortmannin and wortmannin + $10\text{mU}\cdot\text{min}^{-1}\cdot\text{kg}^{-1}$ insulin groups. From the comparisons between these three groups, where the concentration of plasma insulin was equivalent, it is clear that the effect of insulin to increase either FBF or microvascular perfusion was completely inhibited by wortmannin. At the higher plasma insulin concentration generated by infusion of $20\text{mU}\cdot\text{min}^{-1}\cdot\text{kg}^{-1}$ insulin, GIR was further increased above that of $10\text{mU}\cdot\text{min}^{-1}\cdot\text{kg}^{-1}$. In the wortmannin + insulin $10\text{mU}\cdot\text{min}^{-1}\cdot\text{kg}^{-1}$ however GIR was completely blocked even at the same high level of plasma insulin ($\sim 5,000\text{pM}$). A similar outcome was evident when the data for Rd and HLGU were examined and $20\text{mU}\cdot\text{min}^{-1}\cdot\text{kg}^{-1}$ insulin was compared.

The effects of wortmannin on metabolic or haemodynamic effects that could be attributed to either liver or the vasculature were generally marked and greater than those associated with muscle. The inhibitory effects of wortmannin on the liver and muscle vasculature included insulin-mediated changes in R_a (liver), liver $P\text{-Akt}/\text{Akt}_{\text{total}}$, FBF (muscle vasculature) and 1-MX metabolism (muscle vasculature). The partial inhibitory effects of wortmannin on muscle included Rd (principally

muscle), HLGU and muscle P-Akt/Akt_{total}. In the aorta, insulin-stimulated increases in P-Akt/Akt_{total}, were significantly blocked by wortmannin. The different responses to wortmannin by liver and aorta compared with the muscle may result from a relatively lower delivery of wortmannin to muscle. In liver, the endothelial barrier is incomplete, and delivery of wortmannin, to the liver plasma membrane insulin receptor signalling cascade would be relatively unrestricted. Thus, the insulin-mediated inhibition of R_d was reversed, with wortmannin treatment. It is also likely that the delivery of wortmannin to vascular endothelial cells of aorta is unrestricted which would explain the significant inhibition of insulin-mediated increases in aorta P-Akt/Akt_{total}, FBF and microvascular perfusion.

The finding that indexes of insulin action in muscle such as R_d , HLGU and muscle P-Akt/Akt_{total} were only partly blocked by wortmannin may in part reflect the constraints imposed by the muscle vasculature on delivery of wortmannin to the interstitium and myocyte insulin receptor signalling cascade. Blockade of insulin-mediated microvascular perfusion would reduce delivery not only of insulin and glucose but also wortmannin. Reduced delivery of insulin and glucose would give rise to a reduced R_d and HLGU. Based on previous studies where insulin-mediated microvascular perfusion has been blocked by a 5-hydroxytryptamine agonist [55], tumour necrosis factor- α (TNF α) [390], free fatty acids [391], or glucosamine [392], this could amount to approximately 50% inhibition of the insulin-mediated increase in muscle glucose uptake, with the expectation of a similar magnitude of inhibition of R_d and muscle P-Akt/Akt_{total}. In addition to this, it appears likely that the relatively water-insoluble wortmannin is unable to fully diffuse to those myocytes that are unaffected by microvascular perfusion (i.e., where insulin delivery is unrestricted). Consequently, a reduced diffusion of wortmannin to these myocytes would limit the extent of inhibition of insulin action and thus, for the combination of wortmannin + insulin HLGU, R_d and muscle P-Akt/Akt_{total} were not fully inhibited compared with liver (Figure 13B&D and Figure 17).

It has been found by a number of workers that insulin-mediated increase in limb blood flow is nitric oxide dependant [41, 89]. Insulin has been shown to induce

vasodilation by activation of Akt which enhances Ser¹¹⁷⁷ phosphorylation and activity of eNOS [84, 387]. It is also possible that microvascular perfusion is controlled at the terminal arterioles where receptor tyrosine kinase on endothelial cells initiates a cascade involving insulin receptor substrate-1, PI3K, Akt and phosphorylation and activation of endothelial nitric oxide synthase. There is evidence from cultured endothelial cells to support such a relationship [84]. There is also evidence which suggests that insulin-mediated microvascular perfusion is a locally mediated response from studies done using the human forearm [57]. Thus the present findings add support to the concept that insulin mediates perfusion of the muscle microvasculature by local control at the terminal arterioles which is susceptible to inhibition by wortmannin at the step involving PI3K.

Finally, it is important to note that this study is built on the assumption that wortmannin at the dose used has specifically inhibited only PI3K of the insulin-signalling cascade. However, non specific effects of wortmannin cannot be entirely ruled out. Low nanomolar concentrations (5-100nM) are considered to be selective for PI3K inhibition [379]. *In vivo*, a single bolus injection of 1mg wortmannin per kilogram body weight was considered by Davol *et al.* [379] to give a similar outcome in reducing implanted tumour cell volumes as noted for 5-100nM wortmannin *in vitro*. The cumulative dose of a constant infusion of 1 μ g.min⁻¹.kg⁻¹ wortmannin used in the present study was only 180 μ g.kg⁻¹ spread over the 180 minutes infusion period and thus likely to be somewhat lower than the peak concentration achieved by Davol *et al.* [379] following a bolus dose of 1mg. In isolated beta-cells, the effect of wortmannin has been reported to occur at concentrations as low as 10nM [385] and at 50 nM gave similar results to 10 μ M LY294002, another PI3K specific inhibitor [385]. In muscle wortmannin inhibits insulin-mediated glucose uptake in either perfused rat hindlimb [393] or isolated incubated epitrochlearis muscles [374] with a half-maximum of ~10nM. Less specific effects such as the inhibition of contraction-induced glucose uptake are either absent (1 μ M; [374]) or require even higher concentrations of wortmannin (eg. 3 and 10 μ M; [393]). A recent study by Wang *et al.* [394] reported that the vascular effects of much larger bolus doses (1,000-7,000 μ g.kg⁻¹) of wortmannin. In that study, wortmannin caused a reduction in BP at the high doses because of inhibition of myosin light-chain phosphorylation. In contrast, in this study with a lower dose of

wortmannin, there was a modest increase in BP and femoral VR. Thus, in the present study where the peak of wortmannin concentrations was likely to have been <100 nM, non-specific effects were likely to be minimal.

In summary, wortmannin infused *in vivo* at concentrations likely to specifically inhibit PI3K had profound effects on insulin release and insulin action. Plasma insulin levels increases markedly, and the haemodynamics effects of insulin of increased limb blood flow and microvascular perfusion were completely inhibited, as was the insulin-mediated inhibition of hepatic glucose output. Delivery of wortmannin to the myocytes may be restricted and insulin-mediated glucose uptake and Rd were only partially inhibited but this may be the result of reduced delivery of insulin and glucose because of the total inhibition of insulin-mediated microvascular perfusion.

CHAPTER 4

Effects of Nitric Oxide Synthase Inhibition on the Actions of Insulin in Muscle

4.1 INTRODUCTION

The insulin mediated increases in total blood flow to skeletal muscle vasculature has been demonstrated by a number of researchers in humans [41, 395] and animals [55, 396]. It has been suggested that insulin stimulates increased perfusion in skeletal muscle to facilitate its own delivery and the delivery of glucose for increased glucose disposal [25]. Insulin mediated increases in skeletal muscle blood flow are blunted in insulin resistant subjects suggesting that reduced muscle perfusion may contribute to the insulin resistance observed in these individuals [338].

Insulin increases nitric oxide (NO) production as part of its action to increase limb blood flow and this has been demonstrated both *in vitro* [397-399] and *in vivo* [41, 89]. NO, a potent dilator, is produced by nitric oxide synthase (NOS) which is located in the vascular endothelium [400] and myocytes [401]. It has also been demonstrated that endothelial cells contain insulin receptors activation of which can lead to eNOS phosphorylation [38], suggesting a direct action of insulin on the endothelium. This is supported by the finding that mice which are eNOS deficient are hypertensive and resistant to insulin-mediated increases in muscle glucose uptake [402, 403].

Studies by Steinberg *et al.* [41] and Scherrer *et al.* [89] have demonstrated that infusion of a nitric oxide synthase inhibitor completely abolishes insulin-induced increases in total blood flow to muscle in humans. Further, Vincent *et al.* [27, 88] and Roy *et al.* [404] showed that infusions of a NOS inhibitor during a hyperinsulinemic euglycaemic clamp decreased insulin mediated glucose uptake in rat skeletal muscle. In the same studies Vincent found that in addition to a significant reduction in glucose uptake there was a corresponding decrease in microvascular perfusion [27, 88]. Taken together these studies suggest a physiological role for insulin on the vasculature.

In studies reporting the involvement of nitric oxide in insulin-mediated glucose uptake in rat skeletal muscle, such as the studies performed by Vincent *et al.* [27,

88], systemic infusions of L-NAME were used. In these studies, infusion of L-NAME raised blood pressure, completely inhibited insulin mediated increases in limb blood flow (at concentrations of insulin which raised blood flow), microvascular perfusion and blunted glucose uptake measured in the hindlimb. NOS inhibitors, when administered systemically, may access central sites which may participate in the effects observed. A study by Shankar *et al.* [90] demonstrated that acute ICV administration of N^ω-mono-methyl-L-arginine (L-NMMA), a competitive inhibitor of nitric oxide synthase (NOS), in Sprague-Dawley rats resulted in the development of peripheral insulin resistance. These effects occurred without any detectable presence of L-NMMA in the peripheral blood. In addition, Bradley *et al.* [91], demonstrated that acute central ICV administration of L-NMMA in rats resulted in impaired whole body glucose uptake, skeletal muscle glucose uptake and microvascular perfusion. The same dose of L-NMMA given systemically had no effect. Conversely, Baron *et al.* [405] demonstrated in human subjects that local infusion of a NOS inhibitor, thus excluding central effects of L-NAME administration, abolished insulin-induced increases in total flow and reduced glucose uptake by approximately 30% in lean humans.

Total limb blood flow is controlled by medium sized arterioles that control vascular resistance. Thus far, the involvement of NO in insulin's vascular action on muscle has been largely assessed by measurement of total limb blood flow [5, 89, 399] with the exception of the study by Vincent *et al.* [88]. The present study was designed to determine whether NOS inhibition affects insulin mediated microvascular perfusion and glucose disposal though local administration of the inhibitor thus isolating the effects to the hind limb and avoiding unwanted systemic effects, such as increased blood pressure and possible interaction with central sites. The effect of local infusion of L-NAME on insulin action in muscle using rodents has not been previously assessed.

4.1.1 Aim of the Study

The aim of the present study is to explore the relationship between microvascular perfusion and activation of NOS and assess whether this pathway is

involved in insulin mediated microvascular perfusion and muscle glucose metabolism by use of local NOS inhibition (intra-arterial infusion into one leg).

4.2 RESEARCH AND DESIGN METHODS

4.2.1 Animals

Male Hooded Wistar rats (weighing 255 ± 2 g) were raised in the University of Tasmania Animal House as described in section 2.1.1. These experiments were performed in accordance with the guidelines of the University of Tasmania Ethics Committee.

4.2.2 Surgical Preparation

In vivo experiments were performed on non-fasted anaesthetised rats as described in section 2.1.2. Epigastric cannulations were performed as described in section 2.1.2.2. A schematic drawing showing the positioning of cannulae and flow probes is given in Chapter 2 (Figure 6, page 44). On completion of the surgery a period of equilibration of approximately 60 minutes was allowed so that leg blood flow and pressure could become stable and constant.

4.2.3 Preliminary Experiments

Preliminary experiments were conducted to determine a dose of N^G -L-nitro-arginine-methyl ester (L-NAME, Sigma Chemicals, St. Louis, MO) that would produce a suppression in femoral blood flow during physiological insulin infusion without effects on mean arterial blood pressure or heart rate. The aim of this protocol was to ensure that the effect of L-NAME occurred prior to insulin-induced vasodilation and microvascular perfusion.

4.2.4 Experimental Protocols

The experimental protocols are shown in Figure 18. Rats were randomly allocated into three experimental groups (n = 6 per group):

1. Systemic saline and local L-NAME ($10\mu\text{mol.l}^{-1}$, in the test leg)
2. Systemic insulin ($3\text{mU.min}^{-1}.\text{kg}^{-1}$) and local saline
3. Systemic insulin ($3\text{mU.min}^{-1}.\text{kg}^{-1}$) and local L-NAME ($10\mu\text{mol.l}^{-1}$, in the test leg)

In each group local infusions of either L-NAME ($10\mu\text{mol.l}^{-1}$) or saline commenced at 0 minutes and concluded at 75 minutes. The systemic infusions of either insulin ($3\text{mU.min}^{-1}.\text{kg}^{-1}$) or saline commenced at 15 minutes and concluded at 75 minutes. L-NAME infusion was commenced locally (epigastric artery) into the test leg 15 minutes prior to the commencement of systemic insulin infusion ($3\text{mU.min}^{-1}.\text{kg}^{-1}$). It was found that the dose of L-NAME used could be infused for 75 minutes without any observable systemic effects. The rate of infusion of L-NAME into the test leg was adjusted according to the femoral blood flow so that the concentration of L-NAME into the test leg remained at $10\mu\text{M}$ at all times. L-NAME is a competitive inhibitor for each of the three common isoforms of NOS.

Protocol

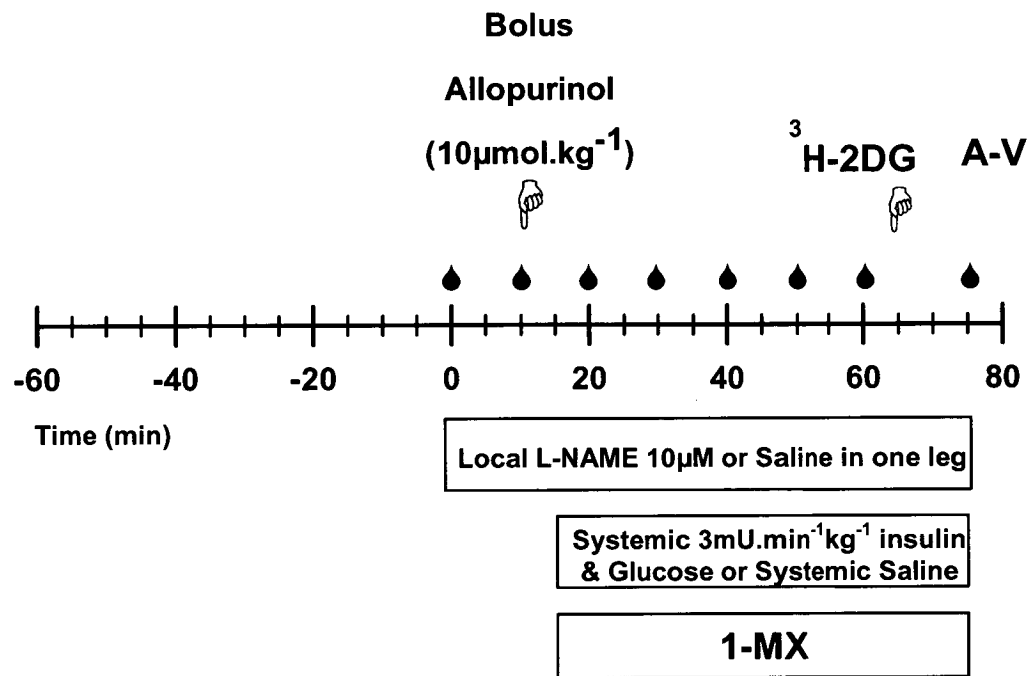


Figure 18: Animals were subject to a 1 hour euglycaemic clamp at $3\text{mU.kg}^{-1}.\text{min}^{-1}$ insulin or saline infusion. The epigastric artery of the test leg was cannulated for local administration of L-NAME into the femoral artery. Arterial blood samples (●) were taken for glucose and lactate analysis. A bolus injection (i.v) of allopurinol ($10\mu\text{mol.kg}^{-1}$) is indicated by ⚡ and preceded 1-MX infusion ($20\text{mg.min}^{-1}.\text{kg}^{-1}$) as indicated by the bar. A [^3H] 2-DG bolus was given at t = 65 minutes as indicated by ⚡. Arterial and venous blood samples were taken (indicated as A-V) for plasma glucose determination. The gastrocnemius group of muscles was freeze clamped at t = 75 minutes for R'g determination.

4.2.4.1 Microvascular Perfusion

Microvascular perfusion was determined by measuring the metabolism of infused 1-MX (Section 2.1.8.1). 1-MX was infused intravenously at a constant rate during the last 60 minutes of each experiment to produce a plasma concentration between 17 and 20 $\mu\text{mol.l}^{-1}$. Plasma (100 μL) from arterial and leg venous blood samples taken at the end of the experiment was mixed with 20 μL of 2M perchloric acid (PCA) and centrifuged for 10 minutes. The supernatant was used to determine 1-MX, 1-MU, allopurinol and oxipurinol concentrations by reverse-phase HPLC as previously described (section 2.1.8.1). Microvascular perfusion, expressed as 1-MX disappearance (MXD) was calculated from arterio-venous plasma 1-MX difference multiplied by femoral blood flow [49].

4.2.4.2 Technique for 2-Deoxy Glucose Measurement

The traditional assay for 2-DG uptake requires a 45 minute sampling period for measurement of the plasma decay curve. In this study the insulin clamps were performed for one hour requiring the 2-DG uptake to be measured over a shorter time period. For the present study a 2-DG protocol was used where the 2-DG glucose uptake was measured over a period of 10 minutes at the end of the experiment. The averaged plasma specific activity of [^3H] 2-DG was obtained by continuous arterial blood withdrawal for 10 minutes at 50 $\mu\text{L.min}^{-1}$ immediately after administering the 2-DG bolus via the jugular vein.. At the conclusion of the experiment the soleus, plantaris, gastrocnemius white and gastrocnemius red group of muscles were clamp frozen together using liquid nitrogen cooled tongs and stored at -20°C for subsequent 2-DG uptake assay as described in section 2.1.5.2.

4.2.4.2.1 Blood Sampling

Arterial samples were taken at the times indicated (Figure 18) for blood glucose measurements. An arterial blood sample (0.5mL) was taken by withdrawing

blood ($50\mu\text{L}\cdot\text{min}^{-1}$) for 10 minutes from $t = 65$ to 75 minutes from the carotid artery using a syringe pump (AL-1000 syringe pump, World Precision Instruments, Sarasota, FL, USA.) at the end of the experiment. This blood sample was used for the 1-MX assay and a [^3H] 2-DG specific activity measurement. The femoral vein of each leg was used for venous sampling, using a 29G insulin syringe (Becton and Dickinson). A sample of venous blood ($300\mu\text{L}$) was taken from the femoral vein of the test and control legs in rapid succession and used for subsequent 1-MX assay. A glucose analyzer (Model 2300 Stat plus, Yellow Springs Instruments, Yellow Springs, OH) was used to determine whole blood glucose (by the glucose oxidase method) during the insulin clamp.

4.2.5 Data Analysis

All data are expressed as means \pm SE. Data analysis was conducted as described in section 2.3.

4.2.6 Statistical Analysis

In order to determine statistical differences between treatment groups during time course experiments, a two-way repeated measures analysis of variance (ANOVA) was used. The two-way ANOVA was used to test the differences among treatment groups for femoral blood flow, blood pressure, heart rate, vascular resistance and glucose infusion rate (GIR) throughout the experimental time course. When a statistical difference ($P < 0.05$) was found between the treatment groups, pair wise comparisons by the Student-Newman-Keuls *post hoc* test was used to determine which time and treatments were significantly different. A paired student's t-test was used in order to determine statistical differences between treatment groups for muscle glucose uptake ($R'g$) and microvascular perfusion at the conclusion of the experiment. When a significant difference ($P < 0.05$) was found pair wise comparisons by the Student-Newman-Keuls *post hoc* test was used to determine which treatments were significantly different. These tests were performed using the statistical program Sigma Stat™ (Jandel Software, version 2.03).

4.3 RESULTS

4.3.1 Glucose Metabolism

Figure 19A shows the time courses for blood glucose (BG) for all three experimental groups. There was no significant difference between the blood glucose values for the three treatment groups. In the groups which received systemic insulin, blood glucose was maintained at or around basal by infusing a 30% glucose solution.

Figure 19B shows the time course for the GIR for the experiments which received systemic insulin infusion. The GIR required to maintain euglycaemia reached a plateau at $t = 60$ minutes and remained unchanged for the final 15 minutes of the experiment. The GIR during the systemic insulin + local L-NAME and the systemic insulin and local saline experiments was not significantly different between the two groups throughout the experimental time course.

Figure 20 shows the 2-deoxy glucose uptake ($R'g$) for the combination of the lower leg muscles. The $R'g$ in the L-NAME test leg within the systemic saline group was not significantly different from the contra-lateral control leg. The $R'g$ in the L-NAME test leg within the systemic insulin group was significantly ($P < 0.05$) decreased by approximately 20% compared with the contra-lateral control leg. The $R'g$ in the local saline test leg within the systemic insulin group was not significantly different from the contra-lateral control leg. The $R'g$ in the control leg in both systemic insulin groups was significantly ($P < 0.001$) increased compared with the control leg in the systemic saline group.

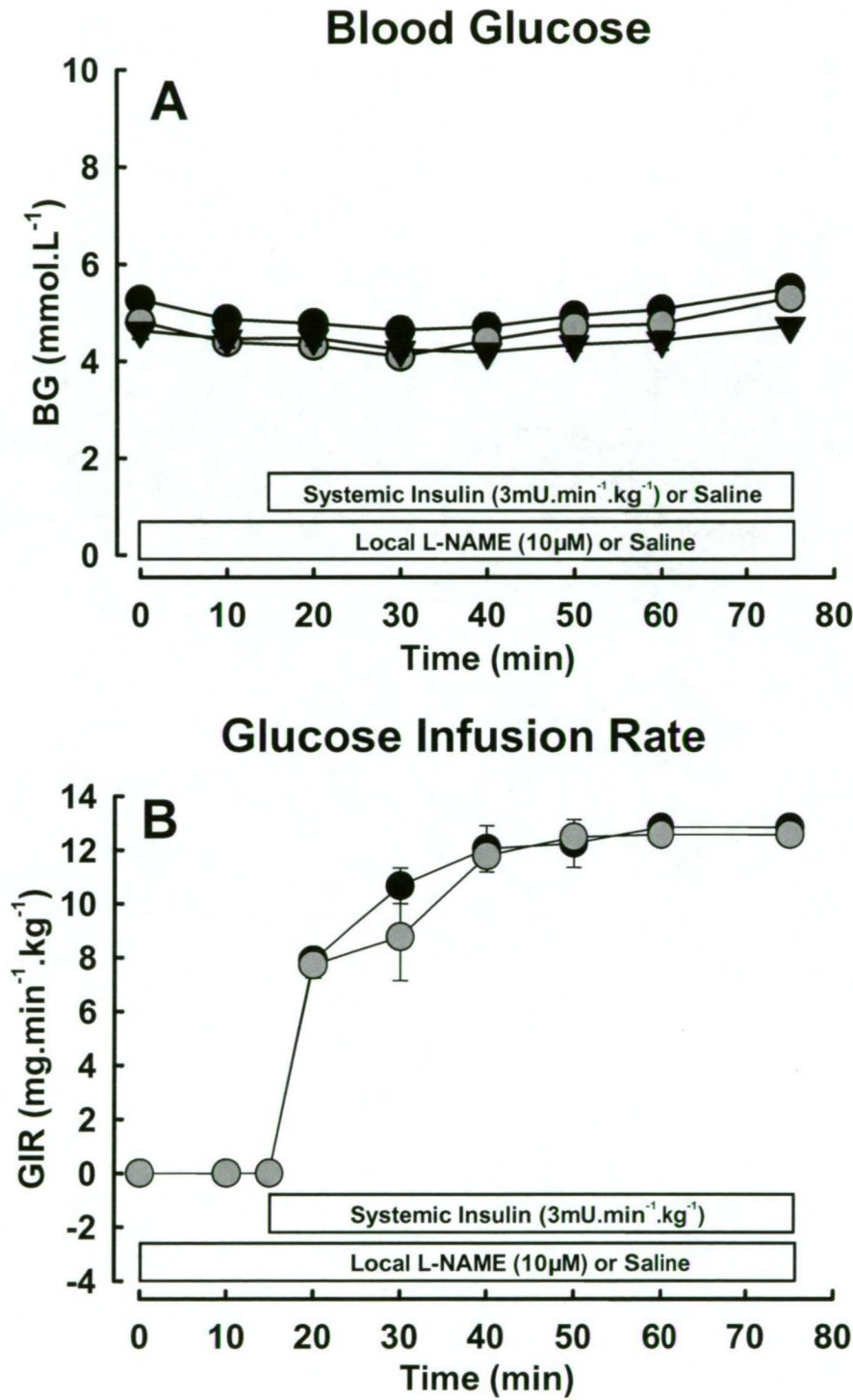


Figure 19: Time course for the effect of local L-NAME (●) or local saline (○) during systemic insulin and effect of local L-NAME (▼) during systemic saline treatment on blood glucose (BG, **A**) and glucose infusion rate (GIR, **B**). Local L-NAME or saline infusion was commenced at 0 minutes and systemic insulin or systemic saline was commenced at 15 minutes. Details are given in Figure 18. Values are given as means \pm SE. ($n = 6$ per group).

Hindleg 2-Deoxy glucose Uptake

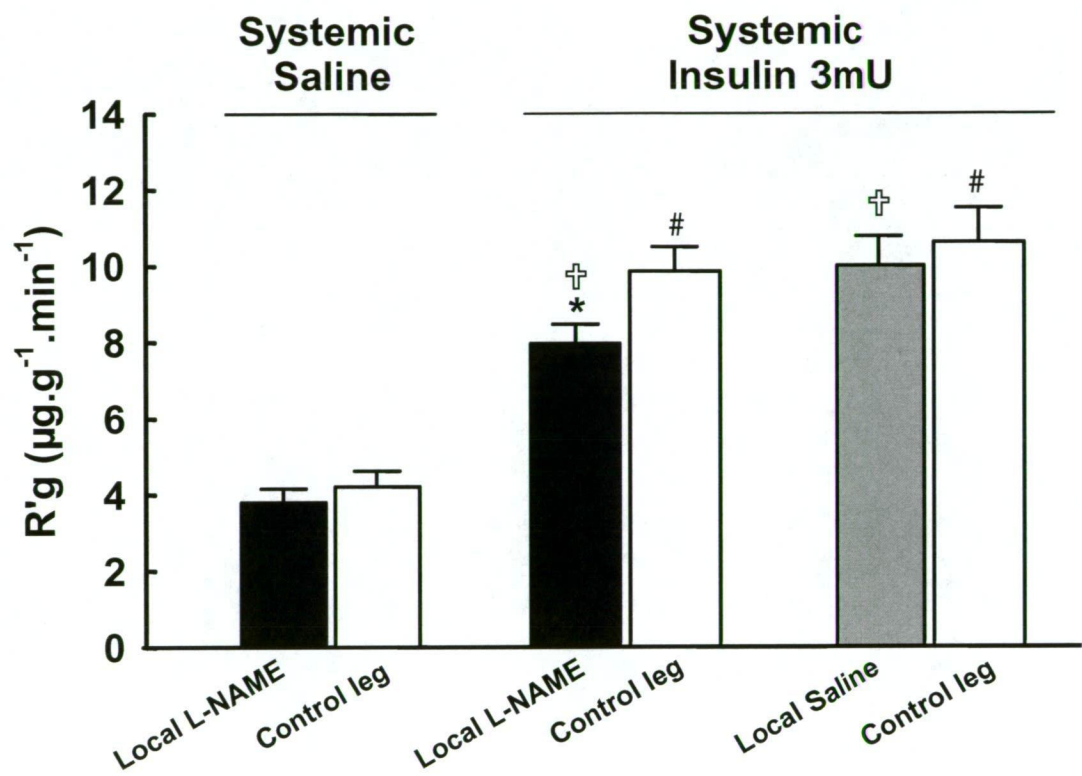


Figure 20: Effect of local L-NAME (filled bars) on systemic saline and systemic insulin and effect of local saline (grey bar) on systemic insulin treated animals on 2-deoxyglucose uptake (R'g) of the lower leg muscles. Details are given in Figure 18. Values were determined at the end of the experiment (t = 75 minutes) and are means \pm SE. * significantly different (P < 0.05) from the contra-lateral leg. # significantly different (P < 0.001) from the corresponding control leg in the systemic saline group. † significantly different (P < 0.001) from the corresponding treated leg in the systemic saline group (n = 6 per group).

4.3.2 Haemodynamic Effects

The dose of L-NAME infused was determined in preliminary experiments (data not shown) aimed at maintaining the dose in the test leg to $10\mu\text{M}$ without changes in FBF in the contra-lateral control leg, heart rate (HR) or mean arterial pressure (MAP).

Figure 21 shows time courses for mean arterial pressure (MAP) and heart rate. There were no significant differences between MAP or heart rate values for the three treatment groups throughout the time course. The values for MAP before the commencement of L-NAME infusion were 110 ± 2.3 (saline) and 115 ± 2.5 (insulin). After 75 minutes of L-NAME infusion there was no significant change in MAP and the values were 112 ± 3.4 (saline) and 112 ± 4.1 (insulin).

Figure 22 shows the change in FBF (ΔFBF) for the treatment leg and contra-lateral control leg for all three treatment groups. Figure 22A shows that the FBF in the contra-lateral control leg in the systemic saline group remained stable and constant over the experimental time course. The FBF in the L-NAME test leg within the systemic saline group was significantly decreased compared with the contra-lateral control leg, commencing at $t = 50$ minutes and continuing until the end of the experiment. Figure 22B shows that the FBF in the contra-lateral control leg increased by approximately $0.6 \text{ mL}\cdot\text{min}^{-1}$ after 50 minutes of systemic insulin infusion. FBF in the L-NAME test leg within the systemic insulin group did not change from basal and was significantly decreased compared with the contra-lateral control leg, commencing at $t = 40$ minutes and continuing until the end of the experiment. The slight decrease in the FBF observed at $t = 75$ minutes is likely to be due to blood sampling for 1-MX and [^3H] 2-DG assays. Figure 22C shows that in the systemic insulin group the FBF in the saline test leg and contra-lateral control leg increased by approximately $0.4 \text{ mL}\cdot\text{min}^{-1}$ after 60 minutes of systemic insulin infusion. FBF in the saline test leg was not significantly different compared with the contra-lateral control leg. The slight decrease in the FBF at $t = 75$ minutes may be attributed to blood withdrawal for 1-MX and [^3H] 2-DG assays.

Figure 23 shows the change in vascular resistance (ΔVR) for the test leg and contra-lateral control legs for the three treatment groups. Figure 23A shows that the VR in the L-NAME test leg within the systemic saline group was significantly increased compared with the contra-lateral control leg, commencing at $t = 50$ minutes and continuing until the end of the experiment. Figure 23B shows that the VR in the L-NAME test leg within the systemic insulin group decreased slightly by the end of the experiment but remained higher than the contra-lateral control leg, this was significant from $t = 40$ minutes until the end of the experiment. Figure 23C shows the VR of the local saline test leg within the systemic insulin group was not significantly different from the contra-lateral control leg. Both the control and test legs displayed a similar trend to decrease VR over the time course of the experiment.

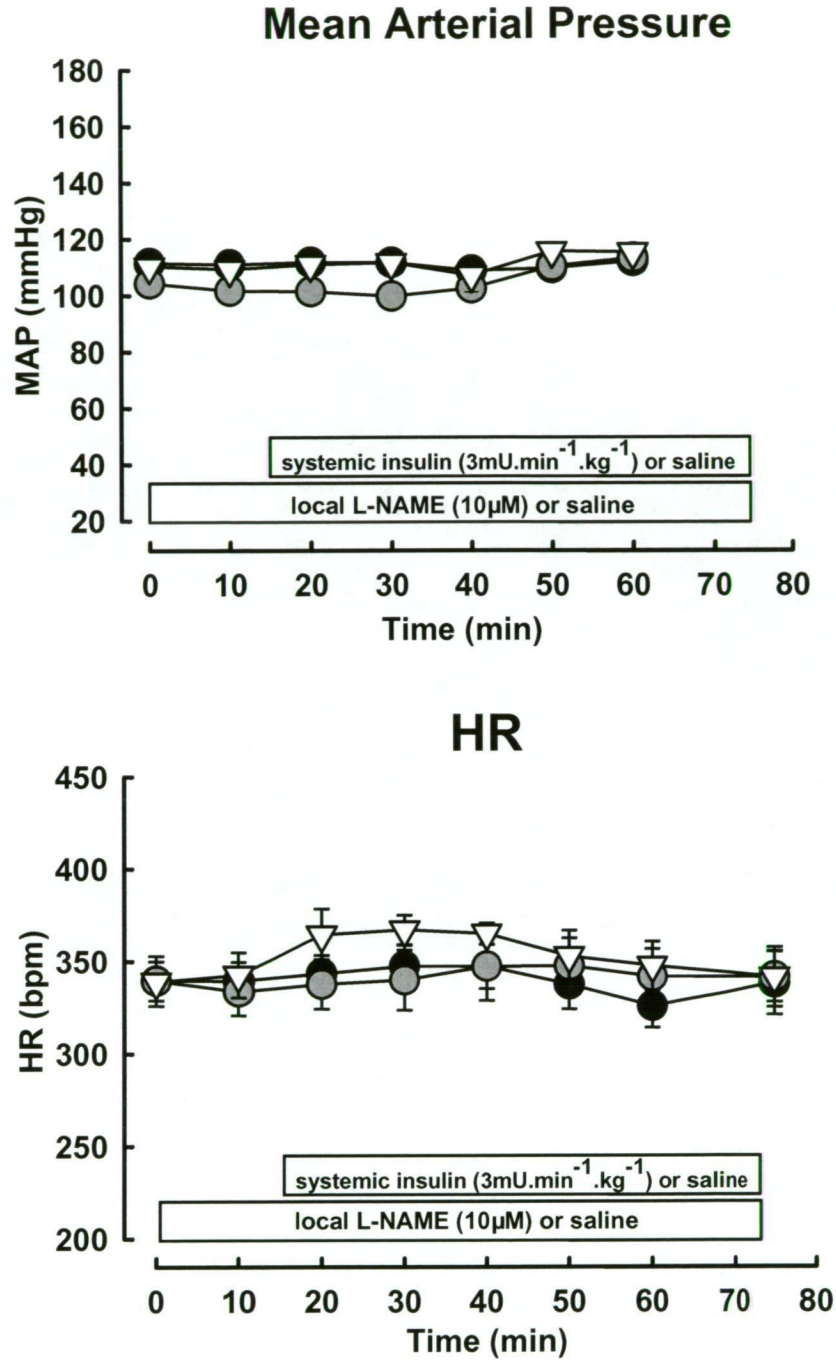


Figure 21: Time course for the effect of local L-NAME (●) or local saline (○) during systemic insulin and effect of local L-NAME (▽) during systemic saline treatment on mean arterial pressure (MAP) and heart rate (HR). Local L-NAME or saline infusion was commenced at 0 minutes and systemic insulin or systemic saline was commenced at 15 minutes. Details are given in Figure 18. Values are given as means \pm SE ($n = 6$ per group).

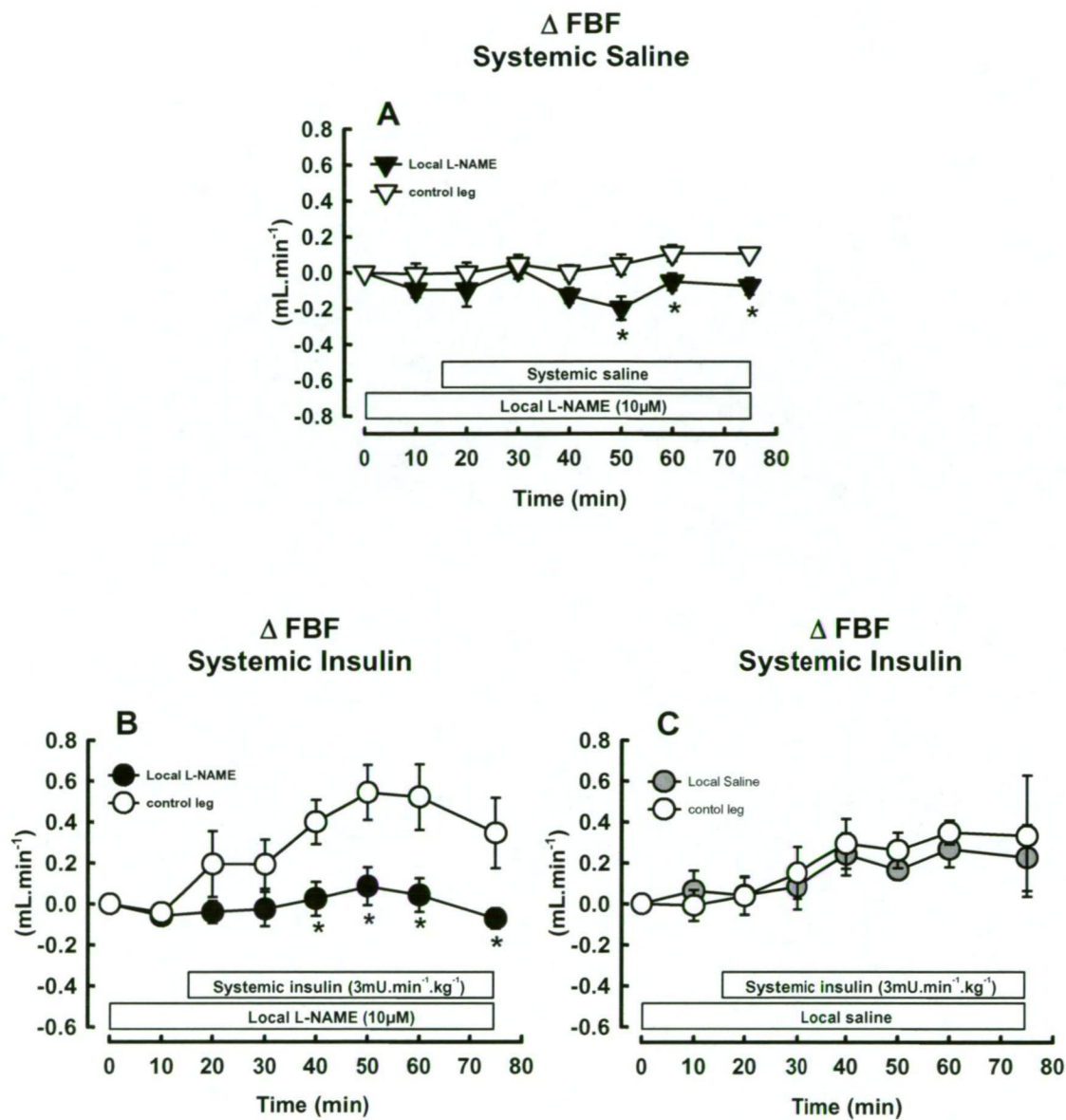


Figure 22: Time course for the effect of local L-NAME (▼) during systemic saline (▽) and the effect of local L-NAME (●) or local saline (○) during systemic insulin (○) treatment for change in femoral blood flow (ΔFBF). Local L-NAME or saline infusion was commenced at 0 minutes and systemic insulin or systemic saline was commenced at 15 minutes. Details are given in Figure 18. Values are expressed as means ± SE. * significantly different ($P < 0.05$) from the contra-lateral leg, ($n = 6$ per group).

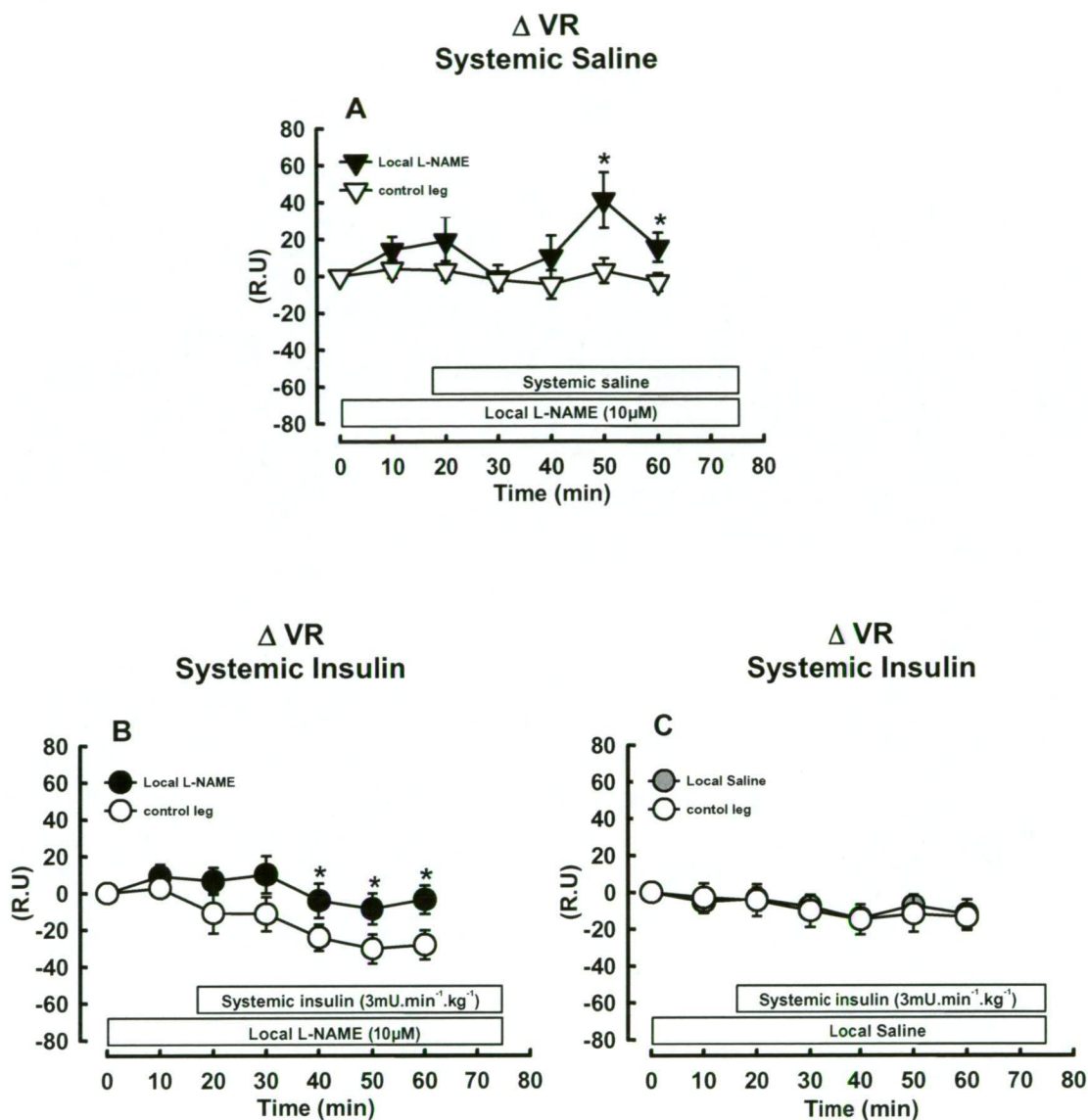


Figure 23: Time course for the effect of local L-NAME (\blacktriangledown) during systemic saline (\triangledown) and the effect of local L-NAME (\bullet) or local saline (\circ) during systemic insulin (\circ) treatment on change in vascular resistance (ΔVR). Local L-NAME or saline infusion was commenced at 0 minutes and systemic insulin or systemic saline was commenced at 10 minutes. Details are given in Figure 18. Values are expressed as means \pm SE. * significantly different ($P < 0.05$) from the contra-lateral leg, ($n = 6$ per group).

4.3.3 Microvascular Perfusion

Figure 24 shows the 1-MX disappearance (MXD) (measure of microvascular perfusion) for the test and control legs taken at the conclusion of the experiment ($t = 75$ minutes) in each experimental group. There were no significant differences in arterial 1-MX and oxypurinol concentrations (data not shown) between all three groups in the study. The mean arterial 1-MX concentration and mean oxypurinol concentration was $18.85 \pm 0.71 \mu\text{mol.L}^{-1}$ and $5.26 \pm 0.36 \mu\text{mol.L}^{-1}$ respectively.

The microvascular perfusion in the L-NAME test leg within the systemic saline group was not significantly different from the contra-lateral control leg. Microvascular perfusion in the L-NAME test leg within the systemic insulin group was significantly ($P < 0.05$) decreased by approximately 25% compared with the contra-lateral control leg. The microvascular perfusion in the saline test leg within the systemic insulin group was not significantly different from the contra-lateral control leg. Microvascular perfusion in the control leg in both systemic insulin groups was significantly ($P < 0.05$) increased compared with the control leg in the systemic saline group. Microvascular perfusion in the local saline test leg in the systemic insulin group significantly increased compared with the L-NAME test leg in the systemic saline group (Figure 24).

Microvascular Perfusion

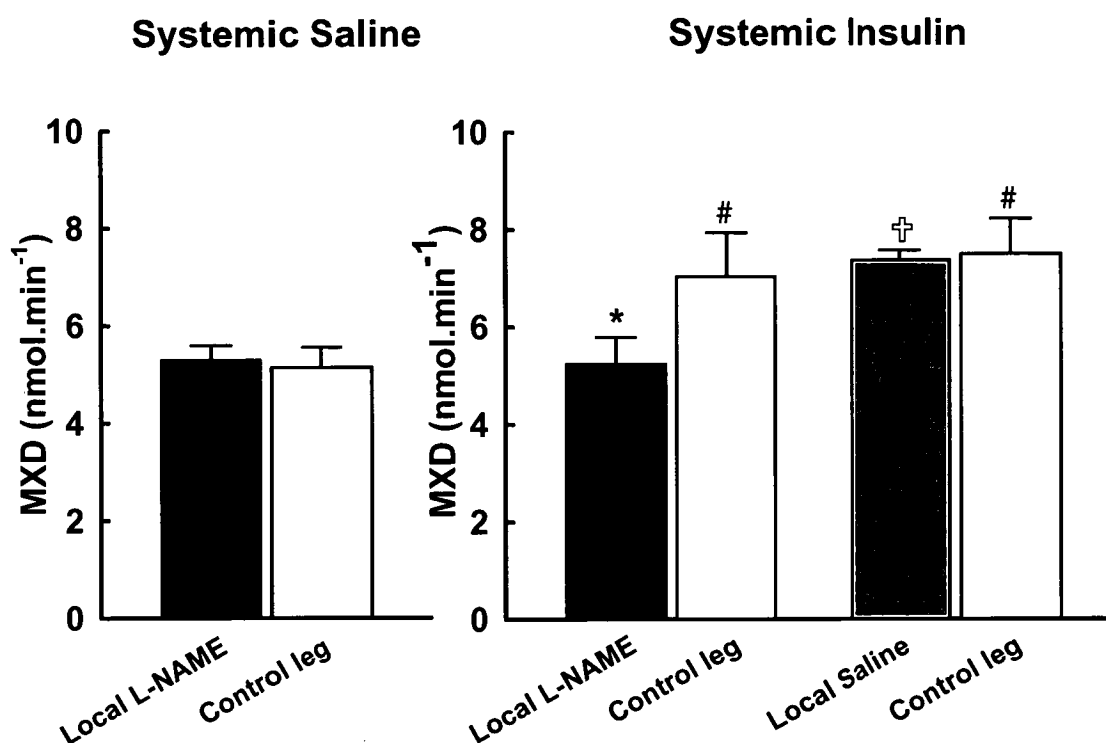


Figure 24: Effect of local L-NAME (filled bars) during systemic saline and systemic insulin and effect of local saline (grey bars) during systemic insulin treated animals on measurement of microvascular perfusion (MXD). Details are given Figure 18. Values were determined at the end of the experiment ($t = 75$ minutes) and are means \pm SE. * significantly different ($P < 0.05$) from the contra lateral leg. # significantly different from the corresponding control leg in the systemic saline group. † significantly different ($P < 0.05$) from the corresponding treated leg in the systemic saline group ($n = 6$ per group).

4.4 DISCUSSION

The main findings of this study are that local NOS inhibition attenuated increases in total blood flow, skeletal muscle glucose uptake and microvascular perfusion in the test leg during physiological insulin ($3\text{mU}\cdot\text{min}^{-1}\cdot\text{kg}^{-1}$) infusion in rats *in vivo*. These results suggest that microvascular blood flow effects are coupled with metabolic effects in the presence of insulin and that a nitric oxide (NO) producing mechanism is activated in muscle by insulin. Local NOS inhibition had no effect on blood pressure or heart rate which indicates that the observed effects on blood flow, glucose uptake and microvascular perfusion were due to local and not systemic action of the NOS inhibitor.

When given locally (via the epigastric artery of the systemically treated rat) the unwanted systemic side effects associated with systemic L-NAME infusion were eliminated. This novel technique facilitated the observation of the direct local NOS inhibitory effect of L-NAME on insulin action. The current study provides evidence that local L-NAME infusion, at the dose used, caused negligible systemic effects. The vasoconstrictor effects were limited to the test leg and effects on blood pressure, heart rate and FBF in the contra-lateral leg were absent. Previous studies by others have shown that systemic NOS inhibitors cause a marked rise in blood pressure which in turn triggers compensatory responses [88, 406] which may be due to central and sympathetic mechanisms [407]. It is possible that, when systemically infused, substances such as L-NAME may cross the blood brain barrier and thus trigger whole body responses. It has been reported that when administered systemically L-NAME can cross the blood brain barrier within 2 hours in rats resulting in reduction of NOS brain activity [408]. Studies by Shankar *et al.* [90] and Bradley *et al.* [91] revealed that ICV NOS inhibitor administration resulted in development of peripheral insulin resistance. An advantage of locally infused L-NAME is that the contra-lateral leg can be used as a control and that the effects of local NOS inhibition can be studied in isolation *in vivo*.

Studies by Vincent *et al.* [27, 88] are the only studies where the effect of NOS inhibition on insulin action in muscle microvasculature has been observed. In one

particular study [88], rats were infused for 2 hours with either saline, insulin ($10\text{mU}\cdot\text{min}^{-1}\cdot\text{kg}^{-1}$), L-NAME ($3\text{mg}\cdot\text{kg}^{-1}$ bolus followed by a continuous infusion of $50\mu\text{g}\cdot\text{min}^{-1}\cdot\text{kg}^{-1}$) or insulin plus L-NAME. The L-NAME was administered systemically by an initial bolus and then a continuous infusion which resulted in an increase in mean arterial pressure. Despite the differences in local versus systemic administration of L-NAME the results from the Vincent *et al.* [88] study and the present study are very similar. The combination of systemic L-NAME and insulin in the Vincent *et al.* [88] study blocked the effect of insulin on total limb flow and microvascular perfusion and blunted glucose uptake.

One of the key focuses of the current work was to explore the relationship between microvascular perfusion and NOS inhibition and determine whether this pathway is involved in the physiological processes leading to microvascular perfusion. It has been previously reported that insulin acts on the muscle vasculature causing microvascular perfusion which increases the delivery of nutrients and itself to the muscle myocytes [2, 49]. In the current study, it was observed that insulin at physiological doses increased microvascular perfusion as determined by 1-MX metabolism. Local infusion of L-NAME inhibited microvascular perfusion in the presence of physiological insulin; which indicates that insulin-mediated microvascular perfusion is NO dependant. This is in agreement with Vincent *et al.* [88] who reported that systemic L-NAME infusion completely abolished insulin mediated ($10\text{mU}\cdot\text{min}^{-1}\cdot\text{kg}^{-1}$) microvascular perfusion. The finding that insulin-mediated microvascular perfusion was blocked by L-NAME contrasts with a study by Ross *et al.* [409] who showed that contraction mediated microvascular perfusion was not blocked by local L-NAME, indicating that different mechanisms are involved in insulin and exercise mediated microvascular perfusion.

Studies by Baron and his colleagues showed that insulin increased total muscle blood flow and that this effect was impaired in states of insulin resistance [410, 411]. A number of studies have also demonstrated that insulin increases total flow and provided evidence that NO-dependant mechanisms are associated with this effect [41, 88, 89, 404]. In the present study, local L-NAME infusion significantly decreased the FBF response to a physiological dose of systemic insulin. This vasoconstrictor effect of L-NAME was also seen in the presence of saline where

local L-NAME decreased the FBF in the test leg compared with the contra lateral leg. This data is in agreement with Vincent *et al.* who demonstrated that systemic L-NAME significantly decreased FBF in the presence of $10\text{mU}\cdot\text{min}^{-1}\cdot\text{kg}^{-1}$ insulin as well as in the presence of saline [88].

As previously discussed, insulin has been shown to increase total flow and microvascular flow which is associated with a NO-dependant mechanism. Insulin receptors have been demonstrated on endothelial cells of both large and small blood vessels [412]. Studies by Chen and Messina have demonstrated that dilation of skeletal muscle arterioles by insulin is endothelium dependant and nitric oxide mediated [397]. It was demonstrated that insulin can induce vasodilation of first order arterioles in the perfused rat cremaster muscle and that this dilation can be blocked with the NOS inhibitor N^{ω} -nitro-L-arginine (L-NNA). In addition, removal of the arteriole endothelium prevented insulin mediated dilation. This effect was also demonstrated by Eringa *et al.* [388] who confirmed that insulin induces nitric oxide activity in rat cremaster first-order arterioles. Work done using vascular endothelial cell cultures has revealed that insulin stimulates a rapid dose-dependant increase in NO [413]. Studies using human subjects have shown that systemic hyperinsulinemia in skin augments nitric oxide mediated vasodilation and induces recruitment of capillaries [414]. It has also been demonstrated that endothelial NOS knockout mice are hypertensive and are not capable of increasing muscle blood flow [403] or glucose uptake [402, 403] in response to insulin to the same extent as wild type mice. In summary, work using endothelial cell cultures, isolated vessels and *in vivo* studies reporting a direct vasodilatory effect of locally administered insulin point to an endothelium insulin receptor mechanism being responsible for the vascular responses to insulin. In contrast, the observation that vascular endothelial cell insulin receptor knock-out (VENIRKO) mice had normal fasting glucose and insulin levels and were not insulin resistant challenges the role for endothelial insulin receptors in insulin action.

In the present study local L-NAME infusion partially blocked (30%) insulin-mediated glucose uptake. Vincent *et al.* have previously reported that systemic

L-NAME reduced insulin-mediated glucose uptake measured from FBF and arterio-venous difference [88]. Another study by Roy *et al.* [404] found that systemic L-NAME infusion during an insulin clamp in rats significantly blunted the whole body glucose disposal (16%) and muscle 2-DG (30%). The present study builds on the previous study by Vincent *et al.* since we have also provided a measure of muscle glucose uptake by the 2-DG method. The present study measured glucose uptake by the radioactive 2-Deoxyglucose uptake method which includes a direct measurement from the rat calf muscles.

This *in vivo* study demonstrates that NO is required for insulin-mediated microvascular perfusion to occur and is partly involved in glucose uptake during physiological insulin. An *in vitro* study by Balon *et al.* revealed that NOS inhibition (by L-NMMA) had no effect on insulin-stimulated 2-deoxy glucose uptake in isolated extensor digitorum longus muscles [415]. This finding indicates that the *in vivo* effect of NOS inhibition in the present study to blunt muscle glucose uptake may be attributed to the inhibition of the vascular effects of insulin. It cannot be ruled out however that L-NAME may have secondary effects which inhibit glucose disposal.

In conclusion, this study demonstrates that local L-NAME infusion blocks insulin mediated increases in total blood flow and microvascular perfusion as well as partially attenuating skeletal muscle glucose uptake. These findings suggest that nitric oxide is critical for microvascular perfusion and is involved in the normal increases in skeletal muscle glucose uptake during physiological insulin. Thus this study demonstrates that an impaired vascular responsiveness to insulin, due to NO inhibition, may contribute to insulin resistance.

CHAPTER 5

Acute Effects of AMPK Activation by AICAR on Muscle Microvascular Perfusion *In Vivo* & Isolated Muscle Resistance Arteries *In Vitro*

5.1 INTRODUCTION

Skeletal muscle AMP-kinase (AMPK) activity increases in response to muscle contraction which has been demonstrated *in vivo* [416] and *in vitro* [177]. Activation of AMPK can lead to muscle glucose uptake and this process can occur independently of insulin [286, 416, 417]. AMPK can be pharmacologically activated by 5-aminoimidazole-4-carboxamide-1- β -D-ribofuranoside (AICAR) in resting muscle [418]. Experiments using muscle treated with AICAR *in vitro* have established that AMPK-mediated glucose uptake involves GLUT4 translocation to the cell surface [314, 419-421].

AMPK is expressed in vascular endothelial cells [308] and smooth muscle cells [422]. A number of studies have shown that AMPK phosphorylates and activates endothelial nitric oxide synthase (eNOS) on its serine residue (Ser¹¹⁷⁷) [265, 307, 308, 423]. There is evidence that AMPK may mediate its effects of increasing glucose transport in part through an interaction with the vasoactive substance nitric oxide (NO) [424]. AMPK has been shown to regulate endothelial function. In conduit arteries, AMPK activation enhances endothelium-dependant vasodilation [235]. In addition, AMPK associates with eNOS in the microcirculation of the heart [307], suggesting a role for AMPK in the regulation of NO activity in the microvasculature.

Activation of AMPK by AICAR has been found to enhance insulin-mediated glucose uptake in muscle and ameliorate insulin resistance [339]. Insulin mediated glucose uptake involves enhancement of nutritive muscle blood flow in normal individuals [2]. It is possible that the effects of AICAR to increase muscle glucose uptake in insulin resistance *in vivo* may also be mediated to some extent by the muscle microcirculation. Additionally AMPK α 2 knockout mice display insulin resistance *in vivo* but not in isolated muscles obtained from these animals where - nutrients are accessed by diffusion independently of the vasculature [286, 425]. Despite these findings the direct effects of AMPK on the muscle microcirculation *in vivo* have not been demonstrated. Activation of the AMPK pathway is an attractive therapeutic target for type 2 diabetes and its role in vascular perfusion requires further investigation.

5.1.1 Aim of the Study

The aim of this study was to investigate whether a low dose AICAR infusion, below the threshold for effects on glucose uptake, acutely causes microvascular perfusion *in vivo*. The vasodilatory effects of AICAR on muscle resistance arteries *in vitro* and activation of AMPK in human microvascular endothelial cells were also studied.

5.2 RESEARCH AND DESIGN METHODS

5.2.1 Animals

For the *in vitro* experiments; in Amsterdam, male Harlan Wistar rats weighing 324 ± 9 g were kept at a constant temperature of $21 \pm 0.6^{\circ}\text{C}$, on a 12h light/dark cycle and allowed free access to standard laboratory rat chow and water. These experiments were performed in accordance with the guidelines of the Institutional Animal Care and Use Committee of the Vrije University Medical Center.

For the *in vivo* experiments; in Hobart, male Hooded Wistar rats weighing 245 ± 13 g were raised in the University of Tasmania Animal House as described in section 2.1.1. These experiments were performed in accordance with the guidelines of the University of Tasmania Ethics Committee.

5.2.2 *In vitro* Experiments

5.2.2.1 Preparation of Isolated Resistance Arteries

Vasoreactivity studies were performed on muscle resistance arteries. First order arterioles (passive inner diameter 176 ± 6 microns) were isolated from the cremaster muscle of male Wistar (Harlan) rats. A 1-2mm long segment was transferred to a pressure myograph and the pressure inside the vessel was set to

65mmHg and the surrounding temperature set to 34°C. Experiments were performed under low flow conditions and the vessels were exposed to vasoactive substances by adding them to the vessel chamber. Details are given in 2.2.2.

Effects of direct AMPK activation on vascular function were studied by exposing the cremaster resistance arteries to the AMPK agonist AICAR (2mmol.L⁻¹). AMPK phosphorylation at Thr¹⁷², a necessary step in its activation, was determined by Western blot. The acute effects of AMPK activation using the muscle resistance arteries were monitored for 30 minutes after the addition of AICAR (2mmol.L⁻¹). Effects of AMPK activation on endothelium dependant and independent vasodilation were studied by testing responses to acetylcholine and sodium nitroprusside (SNP) before and after pre-treatment with AICAR (data not shown). To confirm that the effects of AICAR on vascular diameter were mediated by AMPK, vasoreactivity to AICAR was studied in the presence of the selective inhibitor for AMPK [426], 6-[4-(2-Piperidin-1-ylethoxy)phenyl]-3-pyridin-4-ylpyrazolo[1,5-a] pyrimidine (compound C, 40µmol.L⁻¹). To examine the role of NO in AICAR-induced vasodilation, arteries were exposed to AICAR in the presence of the NO synthase inhibitor N-Nitro-L-Arginine (L-NA, 0.1mmol.L⁻¹ Sigma-Aldrich, St. Louis, MO). When more than 1 artery segment was isolated from the same muscle, they were assigned to different groups.

5.2.2.2 Preparation of Isolated Endothelial Cells

Human microvascular endothelial cells were isolated from the human foreskin (section 2.2.3, page:65). MVECs were treated with AICAR (2mM) for 0 (controls), 15 and 30 minutes or AICAR (2mM) and compound C for 30 minutes.

5.2.2.3 Enzyme Activation and Phosphorylation

For the determination of AICAR-mediated activation of AMPK in human microvascular endothelial cells equal amounts of protein (10µg/lane) were separated by sodium dodecyl sulfate-polyacrylamide gel electrophoresis on 5% to 8% gels, transferred to a nitrocellulose membrane and incubated with the primary antibody overnight (1:1000). After washing and addition of the secondary antibody, protein

bands were visualized with ECL reagent (Amersham Biosciences). Blots were stained with antibodies directed at Thr¹⁷² phospho-AMPK α and Ser⁷⁹ phospho-acetyl CoA Carboxylase (pACC) (Cell signalling technology). Densitometry of immunoblots was performed using AIDA software (Raytest, Straubenhardt, Germany) and untreated vessel samples (control) set at 1 and compared to treated vessels from the same animals.

5.2.3 *In vivo* Experiments

In vivo experiments were performed on non-fasted anaesthetised rats as described in section 2.1.2. Once the surgery was completed, a period of equilibration of approximately 60 minutes was allowed so that leg blood flow and pressure could become stable and constant.

5.2.3.1 Experimental Protocols

The experimental protocols are shown in Figure 25. There were two formats of this protocol, *a* and *b*. Protocols *a* and *b* shared the following details: Rats were allocated into two experimental groups ($n = 6$ per group).

1. Saline
2. AICAR ($3.75 \text{ mg} \cdot \text{min}^{-1} \cdot \text{kg}^{-1}$)

Rats were infused with saline or AICAR (Sigma Chemical Co., St. Louis, MO, USA). AICAR infusions were initiated by a bolus injection of $20 \text{ mg} \cdot \text{kg}^{-1}$ in 0.20 mL saline at $t = 0$ minutes followed by a constant infusion (jugular vein) for 1 hour at $3.75 \text{ mg} \cdot \text{min}^{-1} \cdot \text{kg}^{-1}$. Infusions are indicated by the bars in Figure 25.

In protocol *a*, arterial and venous blood and plasma samples were collected at $t = 60$ minutes and glucose and lactate concentrations were determined. Femoral blood flow (FBF) was recorded throughout the protocol. Blood plasma samples were taken at $t = 60$ minutes and stored at -20°C for subsequent determination of AICAR

concentration. The gastrocnemius group of muscles was removed at $t = 60$ minutes and stored at -80°C for later determination of AICAR and ZMP content.

Femoral blood flow measurements could not be made in protocol **b** due to microbubble infusion interfering with the signal of the transonic flow probe. In protocol **b**, contrast enhanced ultrasound (CEU) measurements of microvascular perfusion were made by microbubble (MB) infusion at three different time periods; immediately before AICAR infusion (basal, $t = 0$ minutes), after 1 hour of AICAR infusion ($t = 60$ minutes) and during muscle contraction ($t = 70$ minutes). Microbubble infusion periods are indicated in Figure 25. The microbubble infusion period consisted of a 10 minute infusion equilibration followed by 10 minutes of CEU measurements (pulsing interval curves). Muscle contraction (2Hz, 0.1ms and 30-35 volts) was performed in protocol **b** and commenced at $t = 60$ minutes for a duration of 10 minutes.

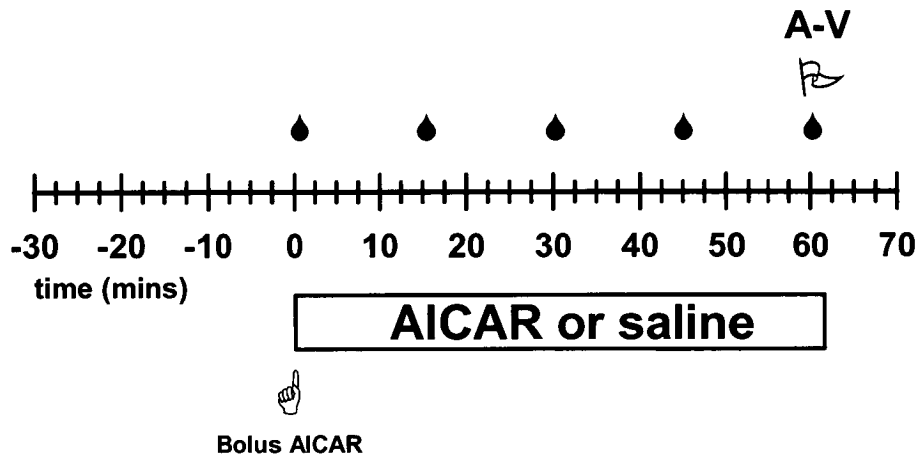
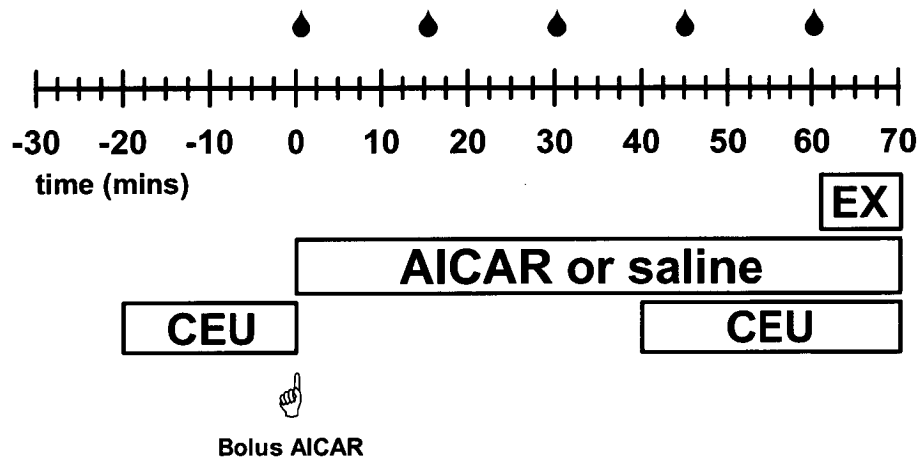
Protocol a**Protocol b**

Figure 25. Arterial blood samples (●) were taken for glucose analysis. A bolus injection (intra venous) of AICAR (20 mg.kg^{-1}) is indicated by ☞ and preceded AICAR infusion ($3.75 \text{ mg.min}^{-1}.\text{kg}^{-1}$) as indicated by the bar. In protocol *a* at $t = 60$ minutes; arterial and venous blood samples were taken (indicated by A-V) for plasma glucose determination, arterial plasma was sampled for AICAR concentration (indicated by \mathcal{R}) and the gastrocnemius group of muscles was freeze clamped for the determination of AICAR and ZMP content. In protocol *b* microbubble infusion ($40 \mu\text{L.min}^{-1}$) and periods where ultrasound measurement of microvascular volume and flow rate were made are shown by CEU. Muscle contraction (field stimulation: 2Hz, 0.1msec, 30-50V) is indicated by EX.

5.2.3.2 Plasma AICAR Assay

Arterial blood samples were taken at the end of the experiment (Figure 25, protocol *a*). Plasma AICAR was determined using HPLC analysis as described previously (section 2.1.9).

5.2.3.3 Skeletal Muscle AICAR and ZMP Assay

The gastrocnemius group of skeletal muscles was removed (taken *in situ*) at the end of the experiment ($t = 60$ minutes) and freeze clamped with aluminium tongs pre-cooled in liquid nitrogen (protocol *a*, Figure 25) and stored at -80°C until subsequent determination of AICAR and ZMP concentration using HPLC (section 2.1.9).

5.2.3.4 Microvascular Perfusion *In Vivo*

The thigh muscle of the left hindlimb was imaged in short axis with a linear array transducer which was secured for the duration of the experiment and connected to an ultrasound system (L7-4 transducer, HDI-5000, ATL Ultrasound). The muscles in the region of interest were essentially the adductor magnus and semimembranosus muscles. Intermittent imaging was performed using pulsing intervals (PI) ranging from 0.5 to 15 seconds to allow incremental microvascular replenishment with microbubbles between each pulse until the volume within the beam was completely refilled. Several frames were obtained at each PI. Data was analysed as described using QLAB™ Software (Version 2.0, Phillips Ultrasound, Bothwell, section 2.1.8.2).

5.2.3.4.1 Microbubbles

Albumin microbubbles (Optison™, GE Healthcare) were diluted 1:5 with perfluoropropane gassed saline and infused at $40\ \mu\text{L}\cdot\text{min}^{-1}$ via the left jugular vein using a polyethylene cannula (PE 20, Intramedic®) for the duration of the data acquisition.

5.2.4 Data Analysis

For the *in vitro* studies; steady-state responses are reported as mean changes in diameter from baseline (in percent) \pm standard error (SE). The baseline diameter was defined as the arterial diameter just before the addition of AICAR. For the *in vivo* studies; all data are expressed as means \pm SE. Data analysis was done as described in section 2.3.

5.2.5 Statistics for *In Vitro* Studies

In order to determine statistical differences between treatment groups during time course experiments, a two way repeated measures analysis of variance (ANOVA) was used. Differences between SNP responses in the absence and presence of AICAR at each concentration *in vitro* were assessed by a two-way ANOVA and Student-Newman-Keuls *post hoc* tests. Percent diameter change responses to AICAR and differences in pACC staining were tested with one-way ANOVA. Differences were considered statistically significant when $P < 0.05$.

5.2.6 Statistics for *In Vivo* Studies

A repeated measures two way analysis of variance was used to ascertain the differences between treatment groups for multiple data points during the experiment. When a significant difference ($P < 0.05$) was found between treatments the Student-Newman-Keuls *post hoc* test was used to determine which time and treatments were significantly different. (for mean arterial pressure, femoral blood flow and change in heart rate).

In order to ascertain the difference between the treatment groups at the end of the experiment (120 minutes) a two way analysis of variance was used. When a significant difference ($P < 0.05$) was found the Student-Newman-Keuls *post hoc* test was used to determine which treatments were significantly different (for microvascular volume and microvascular flow rate).

An unpaired student's t-test was used to determine whether there was a significant difference ($P < 0.05$) between the blood glucose and hindleg glucose uptake values for saline and AICAR treatments. All tests were performed using Sigma Stat™ statistical program (Jandel Software Corp.).

5.3 RESULTS

5.3.1 *In Vitro* Effects of AICAR

5.3.1.1 Effects of AICAR on Isolated Resistance Arteries

During the equilibration period all vessel segments developed spontaneous tone, reducing the diameter by $94 \pm 7 \mu\text{m}$ ($54 \pm 3\%$) to $82 \pm 7 \mu\text{m}$. Vessels were responsive to the endothelium-dependant vasodilator acetylcholine (ACh, $0.1 \mu\text{M}$) which caused a $43 \pm 11 \%$ dilation (data not shown).

Figure 26 shows the change in diameter of muscle resistance arteries treated with AICAR. The percent diameter change in the AICAR alone group showed a marked vasodilation ($18 \pm 5\%$) from the initial basal value, indicating that AICAR was acting as a dilator. The percent diameter change in the L-NA group showed a 5% percent decrease (vasoconstriction) which was significant ($P < 0.01$) when compared to the AICAR group. The vasoconstriction in the L-NA alone group due to inhibition of NO synthesis indicates the presence of basal NO synthesis. The vasodilation observed with AICAR treatment was abrogated by inhibition of NOS (with L-NA; $P < 0.001$) or AMPK (with compound C, $P < 0.05$). AICAR induced a small vasodilation during AMPK inhibition with compound C ($6 \pm 3 \%$), however this was not significantly different compared with the initial basal value ($P = 0.12$).

Figure 27 shows the effect of treatment of muscle resistance arteries with SNP in the presence or absence of AICAR. In paired experiments, pre-treatment of resistance artery segments with AICAR for 30 minutes was significantly ($P < 0.01$) greater compared to the untreated group at each concentration of SNP. The data indicates that AICAR had a secondary effect to sensitize the resistance arteries to the vasodilatory action of sodium nitroprusside (Figure 27).

5.3.1.2 Effects of AICAR on Endothelial Cells

In microvascular endothelial cells AICAR induced a time-dependant phosphorylation of AMPK α at Thr¹⁷² and a four fold increase of AMPK activity, measured by phosphorylation of the AMPK substrate ACC at Ser⁷⁹ (Figure 28). This increase was abolished by the AMPK inhibitor compound C (Figure 28).

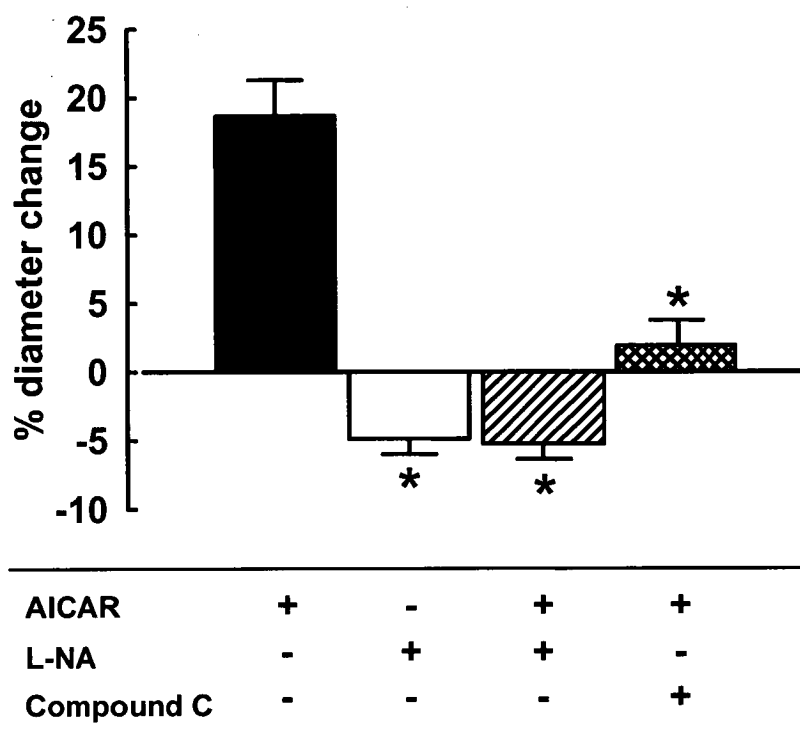


Figure 26: Effect of AICAR (2 mmol.L^{-1}) alone or in combination with the NOS inhibitor L-NA (0.1 mmol.L^{-1}) or the AMPK inhibitor compound C ($40 \text{ }\mu\text{mol.L}^{-1}$) on muscle resistance arteries. Responses were studied for 30 minutes after addition of AICAR and steady-state responses are given. Values are means \pm SE ($n = 4 - 6$ per group). * Significantly different ($P < 0.01$) from AICAR alone treatment.

(Data provided by **Dr. Etto C. Eringa**, Laboratory for Physiology, Institute for Cardiovascular Research (ICaR-VU), VU University Medical Center, Amsterdam, The Netherlands.)

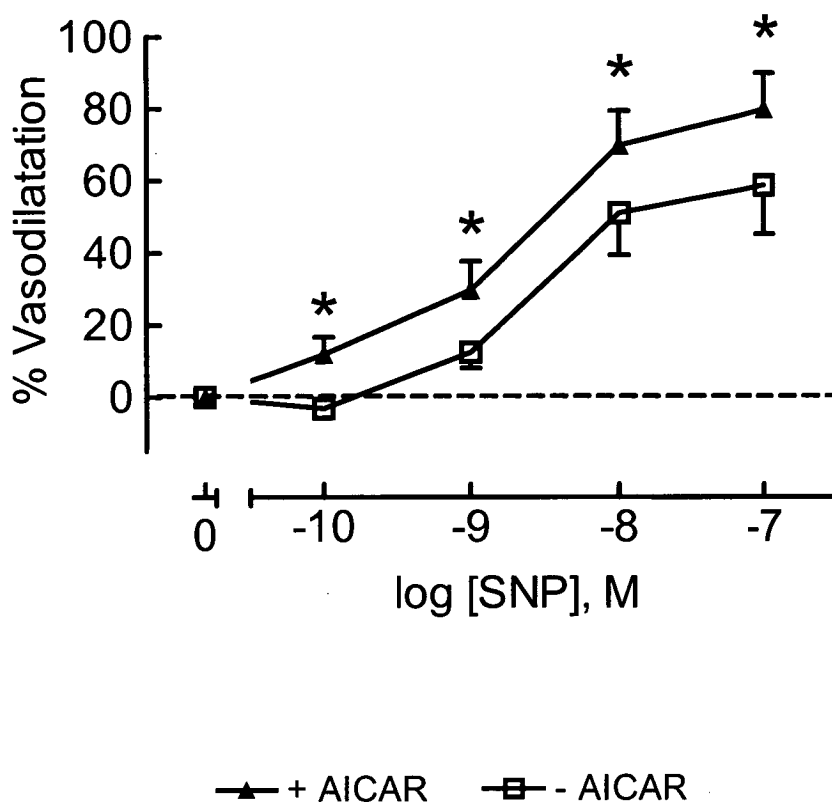


Figure 27: Effect of treatment of muscle resistance arteries with the presence or absence of AICAR and the NO donor sodium nitroprusside (SNP). Responses were studied for 30 minutes after addition of AICAR or vehicle and SNP. Steady state responses are given. Values are means \pm SE ($n = 4 - 6$ per group). * AICAR treated significantly different ($P < 0.01$) from untreated.

(Data provided by **Dr. Etto C. Eringa**, Laboratory for Physiology, Institute for Cardiovascular Research (ICaR-VU), VU University Medical Center, Amsterdam, The Netherlands.)

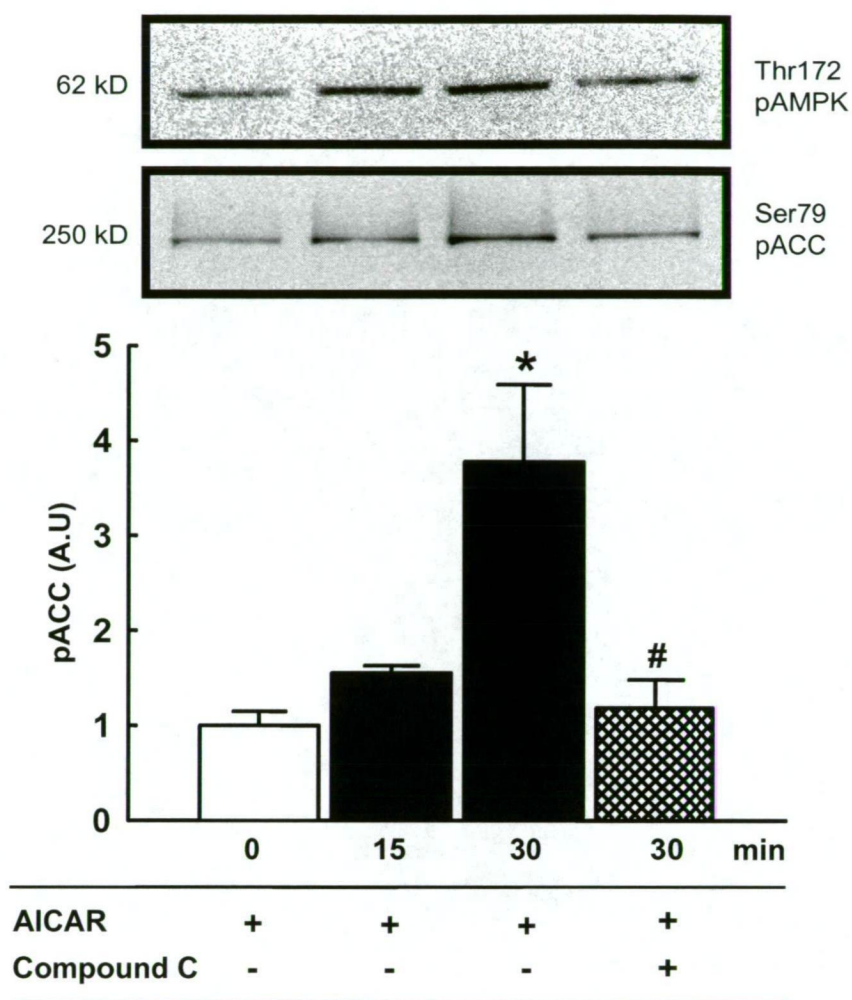


Figure 28: A time course for the effect of AICAR treatment (2mM) for 0 to 30 minutes on Thr¹⁷² phosphorylation of AMPKα and Ser⁷⁹ phosphorylation of ACC in human microvascular endothelial cells and the effect of pre-treatment with the AMPK inhibitor compound C. One representative Thr¹⁷² pAMPKα and Ser⁷⁹ pACC Western blot is displayed. Values are means ± SE (n = 3). * AICAR 30 minutes treated significantly different (P < 0.01) from AICAR 0 minutes treated. # Compound C treated is significantly different (P < 0.01) from AICAR 30 minutes treated.

(Data provided by **Dr. Etto C. Eringa**, Laboratory for Physiology, Institute for Cardiovascular Research (ICaR-VU), VU University Medical Center, Amsterdam, The Netherlands.)

5.3.2 *In Vivo* Effects of AICAR

5.3.2.1 Plasma and Muscle AICAR and Muscle ZMP Content

Table 4 shows plasma AICAR and muscle AICAR and ZMP values measured at $t = 60$ minutes for experiments with AICAR treatment ($3.75\text{mg}\cdot\text{min}^{-1}\cdot\text{kg}^{-1}$). AICAR content in both the muscle and plasma samples have shown an increase from a basal value of zero (data not shown). The ZMP levels in the muscle have also shown a corresponding increase due to AICAR treatment (Table 4).

Table 4: Plasma and muscle AICAR and muscle ZMP contents from AICAR treated animals taken at the end of the experiments.

	AICAR (nmol.g wet wt ⁻¹)	ZMP (nmol.g wet wt ⁻¹)	AICAR (μmol.L ⁻¹)
Gastrocnemius group	98 ± 9	207 ± 27	Plasma 266 ± 12

Details of sampling are given in Figure 25. Values are means ± SE ($n = 4$ muscle, $n = 10$ plasma).

5.3.2.2 Glucose Metabolism

Figure 29 shows the effect of AICAR on arterial blood glucose concentration at the end of the experiment ($t = 60$ minutes). The blood glucose concentration in the AICAR group was not significantly different compared with the saline alone group.

Figure 30 shows the effect of AICAR on hind leg glucose uptake taken at the end of the experiment ($t = 60$ minutes) for the saline and AICAR ($3.75\text{mg}\cdot\text{min}^{-1}\cdot\text{kg}^{-1}$) groups. There was no significant difference between the hind leg glucose uptake values for the two groups.

In summary no glucose infusion was required to maintain blood glucose levels during AICAR infusion alone and there was no stimulation of hind leg glucose uptake.

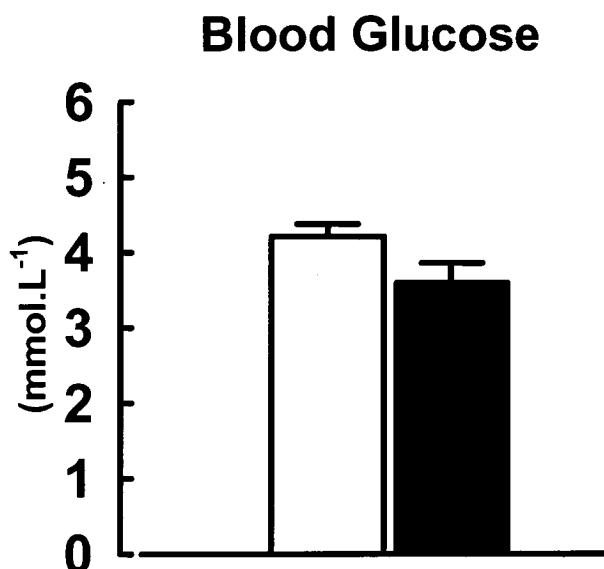


Figure 29: Blood glucose values for saline (open bar) and AICAR (filled bar) treatments. Values are determined at the end of the experiment ($t = 60$ minutes). Details are given in Figure 25. Values are means \pm SE ($n = 6-10$).



Figure 30: Hindleg glucose uptake values for saline (open bar) and AICAR (filled bar) treatments. Values are determined at the end of the experiment ($t = 60$ minutes). Details are given in Figure 25. Values are means \pm SE ($n = 6-10$).

5.3.2.3 Haemodynamic Changes

Figure 31 shows the time courses for mean arterial blood pressure, femoral blood flow and changes in heart rate over the 60 minute experimental period during saline (control) or AICAR infusion.

Figure 31A-B shows that there was no effect of AICAR on mean arterial pressure and femoral blood flow. Figure 31C shows that after 60 minutes of infusion AICAR caused a decrease in heart rate by approximately 40 bpm from a basal value of 312 ± 9 bpm. The decrease in heart rate caused by AICAR was significant ($P < 0.05$) 15 minutes after the commencement of AICAR infusion and continued to decrease until the end of the experiment.

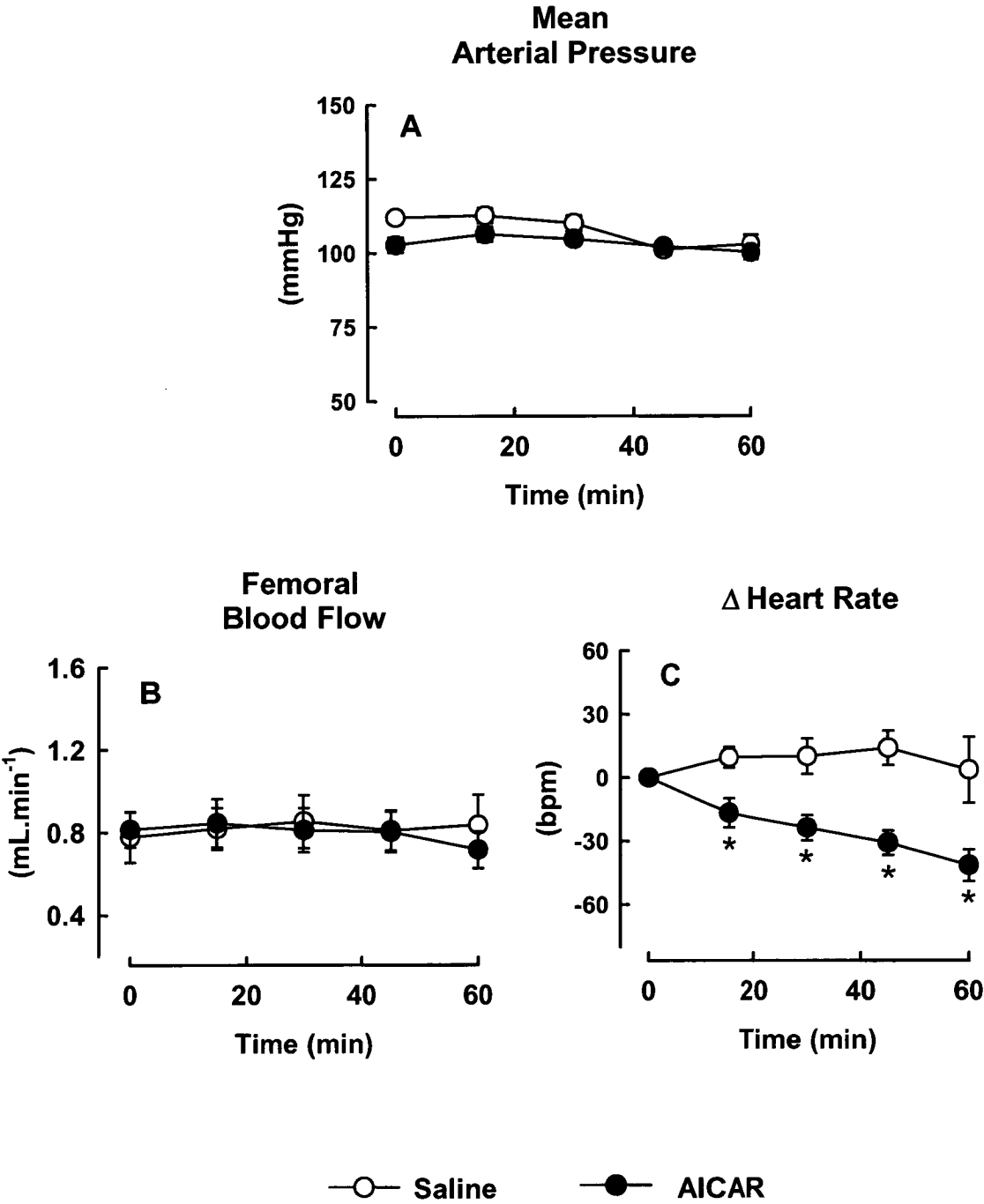


Figure 31: Effect of AICAR on mean arterial blood pressure (BP, **A**), femoral arterial blood flow (FBF, **B**) and change in heart rate (Δ HR, **C**). Mean values are shown for saline (n = 14) and AICAR (n = 10) treated rats. * Significantly different (p< 0.05) from saline values.

5.3.2.4 Microvascular Perfusion

Figure 32 and Figure 33 show changes in microvascular perfusion (reflected by an increase in the microvascular volume filled by microbubbles) in a representative experiment for the three treatments: saline, AICAR and contraction. Figure 32 shows a representative image taken at a 15 second pulsing interval showing changes in signal intensity indicated by colour saturation ranging from blue (the least intense) to red (the most intense). The colour saturation increased with AICAR treatment, compared with saline and further increased with muscle contraction. Figure 33 shows a representative pulsing interval curve showing that AICAR increased microvascular perfusion (*A-value*) by approx 17 AI, compared with basal and this was further increased with contraction treatment which increased by approx 28 AI, compared with basal. Figure 33 also shows that contraction treatment resulted in a 2 fold increase in microvascular flow rate (MFR) (*β-value*) compared with saline and AICAR treatments.

Figure 34 shows the effect of saline, AICAR and muscle contraction on microvascular volume (MV) and microvascular flow rate (MFR) taken at the commencement ($t = 0$ minutes) and completion of the experiment ($t = 60-70$ minutes). Figure 34A shows that saline infusion had no effect on the MV whereas contraction increased the MV compared with basal. Figure 34B shows that AICAR increased the MV compared with basal which was significant ($P < 0.05$) and this was further increased by contraction which was also significant ($P < 0.05$). Figure 34C shows that saline infusion had no effect on the MFR whereas contraction increased MFR which was significant ($P < 0.05$) compared with basal treatments. Figure 34D shows that AICAR treatment had no effect on the MFR compared with saline. In contrast contraction increased the MFR which was significant ($P < 0.05$) compared to the saline and AICAR treatments (Figure 34D).

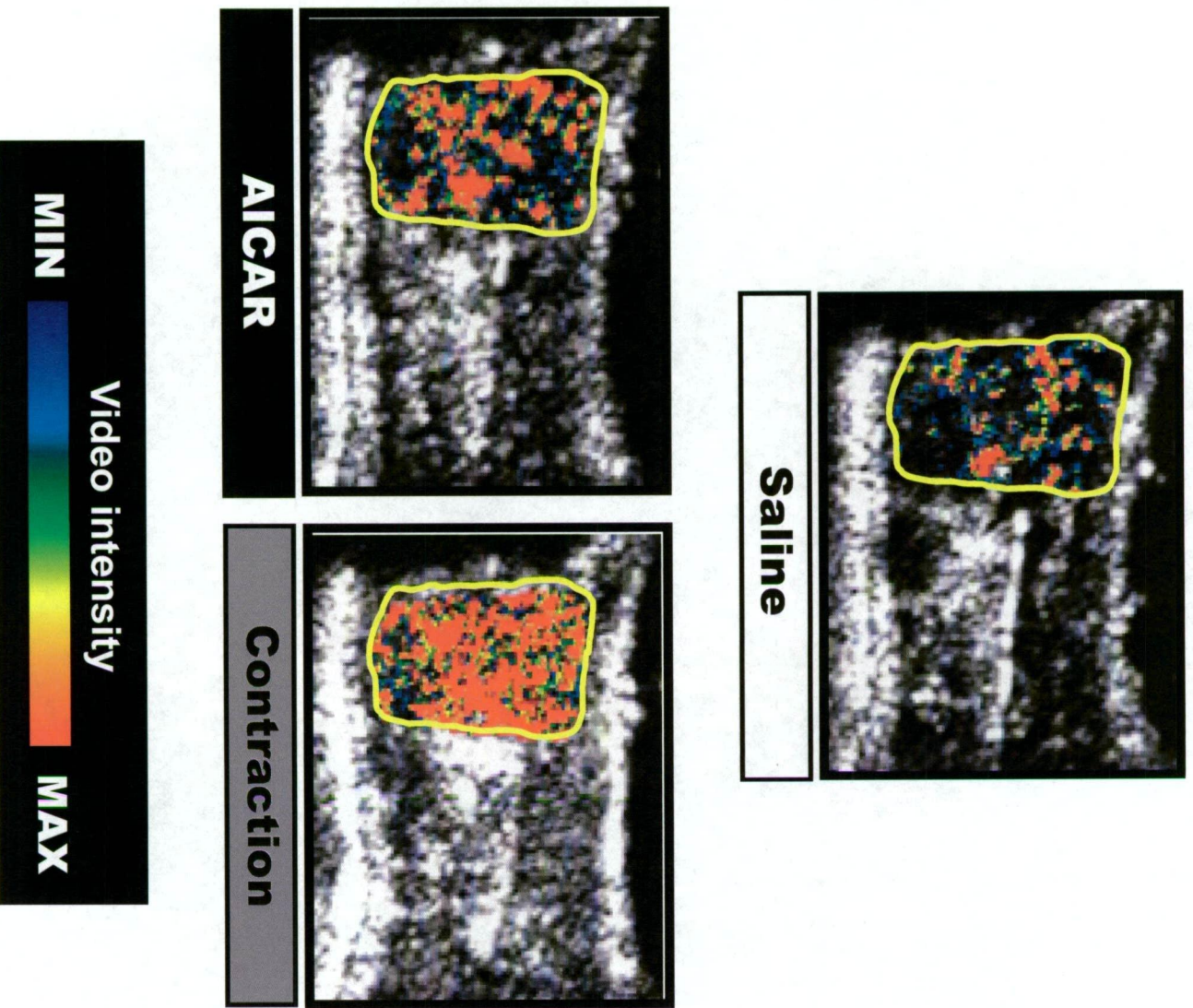


Figure 32: Representative images for the effects of saline, AICAR and muscle contraction on change in video intensity. The region of interest (defined by the yellow line) is colour-coded in proportion to the intensity of the signal (red being the most intense and blue the least). Images shown were captured at a pulsing interval of 15 seconds (Figure 33) and are representative of $n = 6$ for each group.

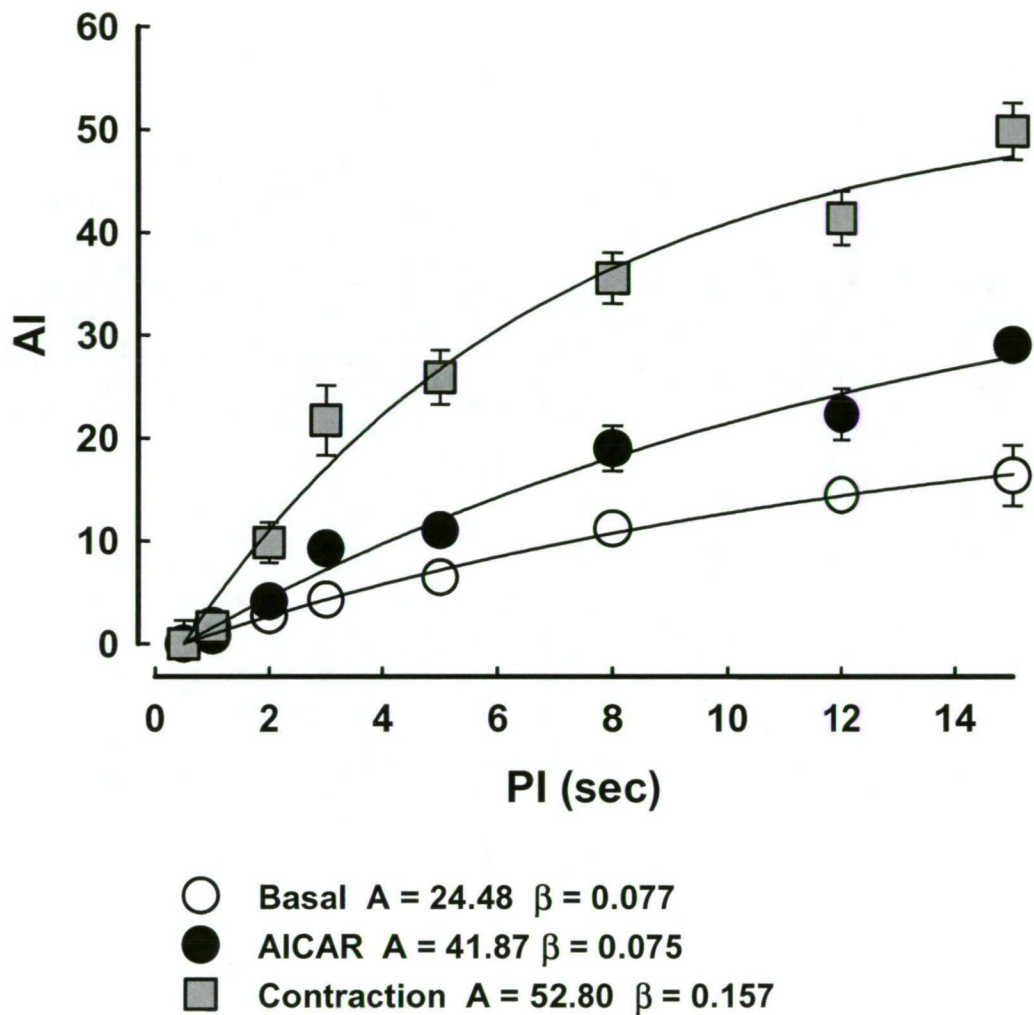


Figure 33: Representative pulsing interval curves for contrast enhanced ultrasound measurement of microvascular volume and flow velocity. Acoustic index (AI) of the region of interest (Figure 32) is plotted as a function of pulsing interval (PI) as described in the text. Values are means \pm SE for saline, AICAR and contraction. SE are indicated by the bars; when not visible these are within the symbols. The asymptote of each graph is the *A-value* and is a determination of the microvascular blood volume. The tangent at $PI = 0$ is the *β -value* and is a determination of the microvascular blood velocity (see text for equation describing the relationship between VI and PI in section 2.1.8.2).

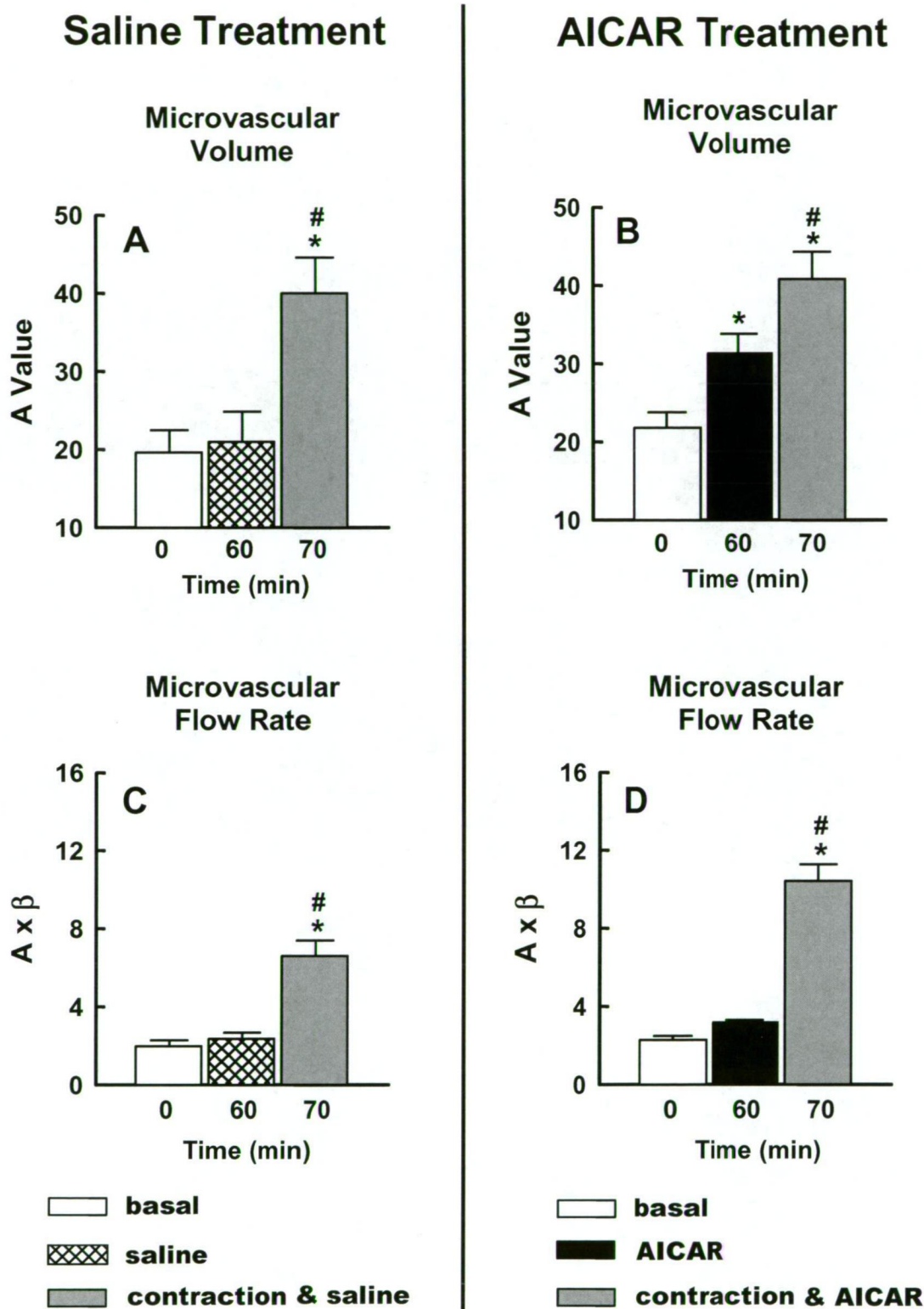


Figure 34: Measurements of the microvascular volume (MV) (*A*-value) for saline (A) and AICAR (B) groups and microvascular flow rate (MFR) ($A \times \beta$ -value) for saline (C) and AICAR (D) groups. Values are means \pm SE ($n = 6$ in each group). * significantly different ($P < 0.05$) from basal or saline values; # contraction treated significantly different ($P < 0.05$) from untreated.

5.4 DISCUSSION

One of the key findings in this study is that the acute administration of AICAR *in vivo*, at a dose below the threshold for causing muscle glucose uptake, stimulates microvascular perfusion in muscle. This study also demonstrated that muscle contraction and AICAR increase microvascular perfusion (microvascular blood volume) *in vivo* however unlike contraction low dose AICAR did not increase the microvascular flow rate or total flow. This study also attempts to determine the mechanisms by which AICAR causes microvascular perfusion and this was performed using *in vitro* resistance arteries and endothelial cell culture preparations. A second key finding of this study was that AICAR sensitized resistance arteries to the NO donor sodium nitroprusside and that vasodilator effects of AICAR were also blocked by L-NA treatment. Together these findings provide evidence for involvement of NO in AMPK mediated vascular relaxation, suggesting that microvascular perfusion *in vivo* also occurs via nitric oxide release.

The *in vitro* findings of this study provide evidence that AICAR and subsequent AMPK phosphorylation is associated with vascular function involving NO. In muscle resistance arteries AICAR was shown to increase NO activity by increasing smooth muscle sensitivity to NO as well as causing vasodilation which was inhibited with L-NA. There is also evidence to suggest that AMPK stimulates NO activity in endothelial cells. A study by Morrow *et al.* using human aortic endothelial cells found that AMPK activation by AICAR resulted in an increase in eNOS Ser¹¹⁷⁷ phosphorylation and subsequent NO production [308]. This group also demonstrated that the stimulation of NOS production is inhibited by infection of human aortic endothelial cells with an adenovirus expressing a dominant negative AMPK mutant [308]. In another study using cardiac endothelial cells Chen *et al.* showed that AMPK phosphorylated eNOS at Ser¹¹⁷⁷ [307]. Together results observed by others and results of the present study indicate that AMPK activation in the endothelium may contribute to the vasodilatory actions of AICAR by causing NO release from the endothelium and inducing the smooth muscle to become more sensitive to NO. The AMPK phosphorylation in endothelial cells and vasodilation caused by AICAR in resistance arteries was blocked by compound C, suggesting a link between AMPK activation and vascular NO activity.

In contrast, other research workers have provided evidence against a role for AMPK to phosphorylate eNOS. Mount *et al.* showed that activation of AMPK in the ischemic rat kidney was not associated with any change in phosphorylation of eNOS at Ser¹¹⁷⁷ or Thr⁴⁹⁵ [427]. A study by Goirand *et al.* [428] also provided evidence that AICAR is involved in vascular functioning when they demonstrated that AICAR (0.1-3mM) induced vasodilation in mouse aortic rings. In the same study AICAR induced vasorelaxation was not affected by treatment with a known NOS inhibitor L-NMMA (30μM) or by endothelium removal. This finding suggests that AICAR induced vasorelaxation is eNOS and endothelium independent, despite a clear demonstration that AMPK was phosphorylated. From their results, the authors concluded that AMPK can induce vasorelaxation in an endothelium and NOS independent manner by a direct action on the smooth muscle cells.

The role of AMPK in relation to phosphorylation of eNOS in the vascular endothelium appears to be inconsistent. These differences may also reflect differences in metabolism of AICAR and accumulation of ZMP between endothelial and smooth muscle cells from different vascular sources. The role of AMPK induced eNOS phosphorylation may vary between macrovascular (aorta) versus microvascular endothelial cells. Species differences also exist between these experiments and could have implications on the results. Caution should also be taken when extrapolating results from *in vitro* studies to the *in vivo* situation.

Phosphorylation of eNOS in microvascular cells can also be activated by other physiological stimuli such as shear-stress [387, 429] however the mechanisms by which eNOS is activated by sheer stress are yet to be resolved. A study by Zhang *et al.* demonstrated that changes in shear-stress activate AMPK in bovine aortic endothelial cells (BAECs) which leads to eNOS phosphorylation and NO production [430]. The increase in microvascular perfusion *in vivo* in the present study occurred in the absence of any increase in total blood flow measured in the femoral artery; hence it is unlikely that in this case microvascular perfusion was induced by shear-stress.

The mechanism by which AMPK activation causes vasodilation in the microcirculation has not been fully determined. Our data lacks *in vivo* evidence for the effects of NOS inhibition on the vasculature during AICAR treatment. One way to determine whether the effects of AICAR to increase microvascular perfusion *in vivo* are NO dependant would be to infuse L-NAME locally into one leg via the epigastric artery. The contra lateral leg could be used as the control. If microvascular perfusion in the L-NAME leg is inhibited then this would provide *in vivo* evidence to support our findings in isolated muscle resistance arteries.

A side effect of AICAR treatment was the profound decrease in heart rate which was demonstrated in the *in vivo* studies. To our knowledge this *in vivo* effect has not been previously reported. This effect on heart rate is probably a direct action of AICAR on the heart as it was not observed with isolated perfused hearts in a study by Longus *et al.* [328]. In addition, AICAR is a analogue of adenosine and in some studies has been reported to have physiological actions in the heart via adenosine receptor stimulation [431].

The *in vivo* protocol for AICAR treatment comprised of a 20mg.kg⁻¹ bolus of AICAR followed by constant infusion of 3.75mg.min⁻¹.kg⁻¹. The *in vivo* plasma concentrations of AICAR reached approximately 250μM. The study demonstrates that low dose AICAR infusion increases microvascular perfusion without increasing glucose uptake. A study by Bergeron *et al.* has reported on the use of AICAR *in vivo* at approximately double the dose (40mg.kg⁻¹ initial bolus followed by 7.5mg.min⁻¹.kg⁻¹ constant infusion) than used in the present study [313]. The AICAR dose used in the Bergeron *et al.* study resulted in a 2 fold increase in glucose uptake. It is likely that the low dose of AICAR used in our study, over the duration of the experiments, was below the threshold for translocation of GLUT4transporters to the plasma membrane. Preliminary studies (data not shown) also revealed that a higher dose (approximately 7.5mg.min⁻¹.kg⁻¹) of AICAR than used in the current study resulted in an increase in glucose uptake and total blood flow. In addition, infusion of AICAR (3.75mg.min⁻¹.kg⁻¹) for 3 hours resulted in development of glucose uptake which commenced after 120 minutes (data not shown). Since there was no increase in glucose uptake from the present study this indicates that microvascular perfusion is more sensitive than glucose uptake to AICAR. A study

by Vincent *et al.* [27] demonstrated that microvascular perfusion is more sensitive to insulin than glucose uptake when it was shown that microvascular perfusion occurs before increases in glucose uptake. Similarly Zhang *et al.* [63] have demonstrated that during low dose insulin infusion microvascular perfusion may occur independently of glucose uptake. Time course experiments would further define the relationship between AICAR induced microvascular perfusion and the subsequent development of glucose uptake.

In the present study AICAR increased microvascular perfusion *in vivo* and this has occurred without a corresponding increase in the total flow rate. One possible explanation for this would be that AICAR causes a redistribution of blood flow from the non-nutritive route to the nutritive route. As part of this action AICAR may have been involved in both vasodilation and vasoconstriction of vascular beds which determine microvascular perfusion and thereby re-directing blood to the nutritive route. AMPK may play a complex role in vascular function and vascular perfusion however the possible involvement of AMPK in a dual role of vasodilation and vasoconstriction remains to be tested.

In conclusion low dose AICAR stimulates microvascular perfusion in skeletal muscle *in vivo* at a dose below that known to increase muscle glucose uptake. The increase in microvascular perfusion potentially enhances hormone and nutrient delivery to muscle myocytes. Evidence from the high dose studies *in vitro* suggests that AICAR-mediated vasodilation results from AMPK-mediated activation of eNOS (but not production) and sensitization of vascular smooth muscle to NO. A vascular action may be an important factor for AICAR's potential as a therapeutic agent for treating muscle insulin resistance.

CHAPTER 6

Acute Effects of AICAR on Haemodynamic and Metabolic Actions of Insulin *In Vivo*

6.1 INTRODUCTION

Exercise has beneficial effects in insulin resistant subjects by increasing insulin sensitivity [194]. Insulin resistant subjects have normal levels of the glucose transporter GLUT4 in skeletal muscle but attenuated GLUT4 translocation to the plasma membrane in response to insulin [432]. However, skeletal muscle GLUT4 translocation and glucose uptake during exercise are normal in insulin resistant subjects. Exercise induced glucose uptake, unlike insulin, is not inhibited by the PI3K inhibitor wortmannin [2] indicating exercise and insulin have different pathways for glucose uptake. Numerous studies have demonstrated that exercise increases glucose transport [172, 433] which may involve AMP kinase [177]. Direct activation of AMPK by AICAR mimics some of the beneficial effects of exercise by enhancing insulin-mediated glucose uptake in muscle and ameliorating insulin resistance [339, 434, 435].

Because of the beneficial nature of exercise in increasing insulin sensitivity, some research groups have explored the use of AICAR as a potential anti diabetic agent [419] and AMPK as a target enzyme for treating type 2 diabetes [318]. Cuthbertson *et al.* [436] have examined the effects of AICAR administration ($10\text{mg}\cdot\text{kg}^{-1}\cdot\text{h}^{-1}$) in healthy male humans. There was a 2.1 fold increase in 2-DG uptake after 3hrs of AICAR infusion. Iglesias *et al.* [318] have examined the effect of subcutaneous injection of AICAR ($250\text{mg}\cdot\text{kg}^{-1}$) one day before conducting a hyperinsulinemic euglycemic clamp on insulin resistant high-fat fed rats. Whole body glucose infusion rate was found to be enhanced during the clamp by 50% in the AICAR treated HFF rats compared with the controls.

Evidence provided in the previous chapter on the effects of AICAR treatment *in vivo* and the NO dependant effects of AICAR to cause vasorelaxation show that the muscle microcirculation can be enhanced by AICAR. It was also shown that AICAR, at the dose used, caused microvascular perfusion in the absence of glucose uptake. The AMPK activator AICAR, at maximal doses acutely activates glucose transport in resting rat muscle *in vitro* and *in vivo* however it is not known if lower doses can sensitize physiologic insulin. There have been few studies examining the effect of AMPK activation combined with insulin action. Moreover, there have been

no studies examining whether AMPK activation by AICAR improves the ability of insulin to increase microvascular perfusion. Since insulin depends upon microvascular perfusion and bulk blood flow for optimal insulin mediated glucose uptake [437] it was hypothesised that AICAR treatment should enhance insulin action.

6.1.1 Aim of the Study

The aim of this study was to investigate whether the effects of a low dose AICAR infusion, below the dose to cause glucose uptake alone, contributes to enhanced insulin mediated glucose uptake *in vivo* during physiological insulin infusion.

6.2 RESEARCH AND DESIGN METHODS

6.2.1 Animals

Male Hooded Wistar rats weighing 245 ± 1 g were raised in the University of Tasmania Animal House as described in section 2.1.1. These experiments were performed in accordance with the guidelines of the University of Tasmania Animal Ethics Committee.

6.2.2 *In Vivo* Experiments

In vivo experiments were carried out using overnight fasted anaesthetized rats (16 hour fast from the time the food is removed at 5 p.m. on the day prior to the commencement of the experiment) as described in section 2.1.2. Once the surgery was completed a period of equilibration of approximately 60 minutes was allowed so that blood flow and pressure could become stable and constant.

6.2.2.1 Experimental Protocols

The experimental protocols are shown in Figure 35, page 147. There were two formats of this protocol, protocol *a* and protocol *b*. Both protocols *a* and *b* shared the following details: rats were randomly assigned into four experimental groups as shown in Table 5:

Table 5: Number (n) of experiments per experimental treatment group for protocol *a* and protocol *b*. Details are given in Figure 35.

Experimental Treatment Groups	Protocol <i>a</i>	Protocol <i>b</i>
	(n)	(n)
Saline (control)	6	6
Insulin ($3\text{mU}\cdot\text{min}^{-1}\cdot\text{kg}^{-1}$)	10	6
AICAR ($3.75\text{mg}\cdot\text{min}^{-1}\cdot\text{kg}^{-1}$) + saline	10	6
AICAR ($3.75\text{mg}\cdot\text{min}^{-1}\cdot\text{kg}^{-1}$) + insulin ($3\text{mU}\cdot\text{min}^{-1}\cdot\text{kg}^{-1}$)	12	6

Rats were infused with saline, AICAR ($3.75\text{mg}\cdot\text{min}^{-1}\cdot\text{kg}^{-1}$, Sigma Chemical Co., St. Louis, MO, USA), insulin ($3\text{mU}\cdot\text{min}^{-1}\cdot\text{kg}^{-1}$, Human R Eli Lilly, Indianapolis, IN, USA) or insulin + AICAR ($3\text{mU}\cdot\text{min}^{-1}\cdot\text{kg}^{-1}$ and $3.75\text{mg}\cdot\text{min}^{-1}\cdot\text{kg}^{-1}$ respectively).

AICAR infusions were initiated by a bolus injection ($20\text{mg}\cdot\text{kg}^{-1}$ in 0.20mL saline) at $t = 60$ minutes followed by a constant infusion ($3.75\text{mg}\cdot\text{min}^{-1}\cdot\text{kg}^{-1}$, via the jugular vein) for 1 hour commencing at $t = 60$ minutes and concluding at $t = 120$ minutes for protocol *a* and $t = 145$ minutes for protocol *b*. Infusions for protocols *a* and *b* are indicated by the bars in Figure 35.

6.2.2.1.1 Euglycaemic Hyperinsulinemic Clamp

Hyperinsulinemic euglycaemic clamps ($3\text{mU}\cdot\text{min}^{-1}\cdot\text{kg}^{-1}$, as described in section 2.1.2) were performed in the insulin and insulin + AICAR groups to assess insulin sensitivity [341]. Insulin infusions commenced at $t = 0$ minutes and concluded at $t = 120$ minutes for protocol *a* and $t = 145$ minutes for protocol *b*. In the experiments where rats received insulin, blood glucose was maintained at the initial blood value (euglycaemia) by co-infusion of variable rates of glucose (30% w/v solution) which began at $t = 2$ minutes and continued until the end of the experiment. Infusions are indicated by the bars in Figure 35.

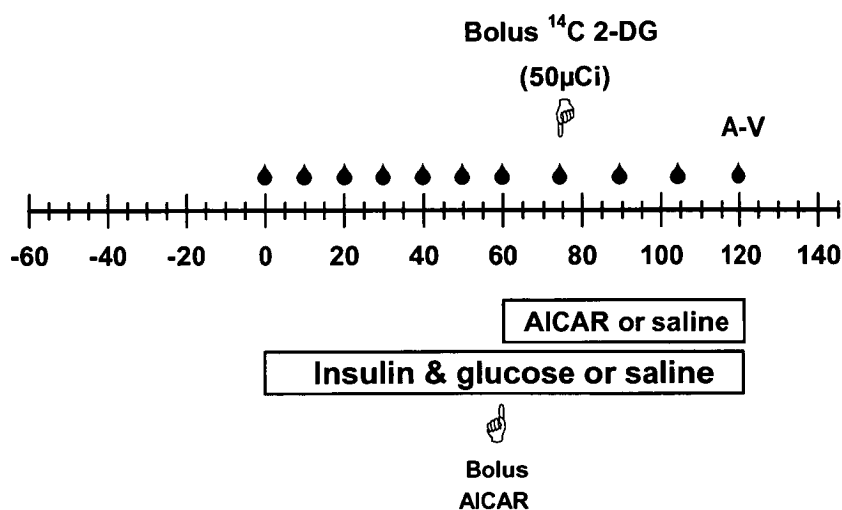
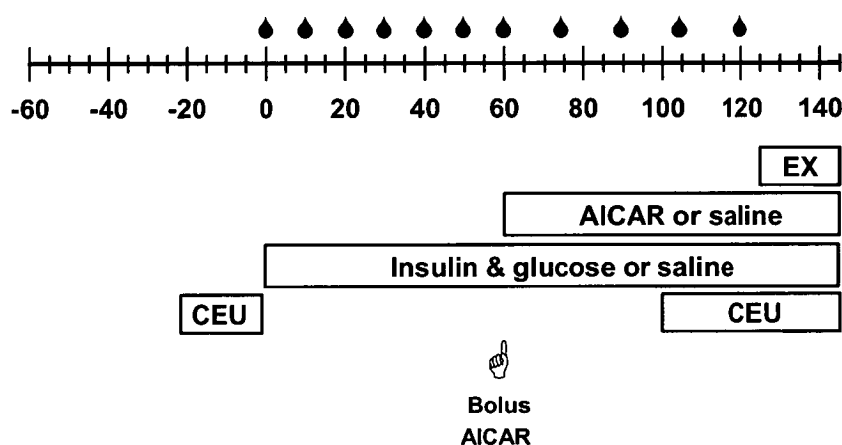


Protocol a**Protocol b**

Figure 35: Animals were subject to a 2 hour euglycaemic clamp of $3\text{mU}\cdot\text{kg}^{-1}\cdot\text{min}^{-1}$ insulin or saline infusion with or without AICAR. Arterial blood samples (◆) were taken for glucose and lactate analysis. A bolus injection (i.v.) of AICAR ($20\text{mg}\cdot\text{kg}^{-1}$) is indicated by  and preceded AICAR infusion ($3.75\text{mg}\cdot\text{min}^{-1}\cdot\text{kg}^{-1}$) as indicated by the bar. Other bolus infusions are indicated by . In protocol **a**, arterial and venous blood samples were taken (indicated as A-V) for plasma glucose determination as well as arterial insulin and AICAR determination. The gastrocnemius group of muscles was freeze clamped at 120 minutes for the determination of AICAR and ZMP content as well as R'g determination. In protocol **b**, microbubble infusion ($40\mu\text{L}\cdot\text{min}^{-1}$) and periods where ultrasound measurement of microvascular volume and flow rate were made are shown by **CEU**. Muscle contraction (field stimulation, 2Hz, 0.1msec, 30-50V) is indicated by **EX**.

Protocol a:

In protocol *a*, in order to measure the glucose uptake into individual muscles at 45 minutes prior to the completion of the experiment, a bolus dose (50 μ Ci) of [14 C] 2-DG was administered via the venous cannula in 0.20 mL saline. The clearance of 2-DG from the blood was determined from plasma samples (25 μ L) collected at 5, 10, 15, 30 and 45 minutes after administration of the 2-DG bolus. At the conclusion of the experiment individual muscles of the lower left leg were removed, freeze clamped in liquid nitrogen and stored at -80°C until assayed for 2-DG radioactivity as described in section 2.1.5.2.

Femoral blood flow (FBF) was continuously measured and recorded using a Transonic[®] flow probe positioned around the femoral artery. At the end of the experiment, arterial (A) and femoral vein (V) blood and plasma samples were collected at $t = 120$ minutes from the carotid artery and femoral vein. A portion of the blood plasma was stored at -20°C for subsequent determination of AICAR concentration as described in section 2.1.9. The remaining blood plasma was used for plasma glucose and lactate analysis (described in section 2.1.3.1.1) and the hindleg glucose uptake was calculated from the arterio venous difference (A-V) multiplied by the femoral blood flow. The gastrocnemius group of muscles was removed from the right leg and freeze clamped *in situ* at $t = 120$ minutes and stored at -80°C for later determination of AICAR and ZMP content.

Protocol b:

Femoral blood flow measurements could not be made in protocol *b* due to microbubble infusion interfering with the signal of the transonic flow probe. Femoral blood flow measurements obtained in protocol *b* were used to confirm the presence of microbubbles in the circulation. In protocol *b*, contrast enhanced ultrasound (CEU) measurements of microvascular perfusion were made by microbubble (MB) infusion at three different time periods; firstly, immediately before the commencement of the insulin clamp or saline infusion (basal, $t = -20$ to 0

minutes), secondly, during the saline (saline or AICAR + saline) or insulin (insulin or insulin + AICAR) clamp ($t = 100$ to 120 minutes) and thirdly, immediately before commencement of electrical stimulation and during electrical stimulation and saline (saline or AICAR + saline) or electrical stimulation and insulin (insulin or insulin + AICAR, $t = 120$ to 145 minutes). Microbubble infusion periods are indicated in Figure 35. The microbubble infusion period (Optison™ microbubbles diluted 1:5 with perfluoropropane gassed saline and infused at $40\mu\text{L}\cdot\text{min}^{-1}$) consisted of a 10 minute equilibration followed by 10 minutes of CEU measurements (continuous images and pulsing interval curves).

6.2.2.2 Plasma Insulin Assay

Arterial plasma samples were taken at the beginning ($t = -2$ minutes) and at the conclusion ($t = 120$ minutes) of the experimental protocol for insulin determination (Figure 35, protocol *a*). Samples were kept frozen at -20°C until subsequent insulin determination using a commercial rat insulin enzyme immunoassay kit (ELISA, Mercodia AB, Sweden). A correction factor calculation was performed to account for the cross reactivity between rat insulin and the exogenously infused human insulin.

6.2.2.3 Plasma AICAR Assay

Arterial samples were taken at the end of the experiment (Figure 35, protocol *a*). Plasma AICAR was determined using HPLC analysis as described previously (section 2.1.9).

6.2.2.4 Skeletal Muscle AICAR and ZMP Assay

In protocol *a*, the gastrocnemius group of skeletal muscles (taken *in situ*) were removed and freeze clamped with aluminium tongs pre-cooled in liquid nitrogen at the end of each experiment and stored at -80°C for subsequent determination of AICAR and ZMP. HPLC analysis was used for determination of AICAR and ZMP content as described in section 2.1.9.

6.2.2.5 Microvascular Perfusion Measurement *In Vivo*

In protocol *b*, the thigh muscle of the left hind limb was imaged in short axis with a linear array transducer which was secured in position for the duration of the experiment and connected to an ultrasound system (L7-4 transducer, HDI-5000, ATL Ultrasound). A schematic drawing showing the positioning of cannulae, flow probe and ultrasound inducer is shown in chapter 2: Figure 5, p42. The muscles in the region of interest were essentially the adductor magnus and semimembranosus muscles. Intermittent imaging was performed using pulsing intervals (PIs) ranging from 0.5 to 15 seconds to allow incremental microvascular replenishment with microbubbles between each pulse until the volume within the beam was completely refilled. Continuous imaging was also performed (0.05s) and used for background subtraction calculations. Details are given in section 2.1.8.2. Several frames were obtained at each PI. Data was analysed using QLAB™ Software (Version 2.0, Phillips Ultrasound, Bothwell).

6.2.2.5.1 Microbubbles

Albumin microbubbles (Optison™, GE Healthcare) were diluted 1:5 with perfluoropropane gassed saline and infused at $40\mu\text{L}\cdot\text{min}^{-1}$ via the left jugular vein using a polyethylene cannula (PE 20, Intramedic® infusion line connected to a PE 50, Intramedic® infusion line) for the duration of the data acquisition. The infusion pump containing the microbubbles was mounted in a hand driven mixing apparatus and the microbubbles were mixed continuously for the duration of the microbubble infusion period. The infusion tubing between the rat and the microbubble mixing apparatus was continuously mixed using a vortex mixer (John Morris Scientific). The mixing process was conducted to ensure that the microbubble suspension remained homogeneous.

6.2.3 Data Analysis

All data are expressed as means \pm SE. Data-analysis was conducted as described in section 2.3.

6.2.4 Statistical Analysis

Repeated two-way analysis of variance (ANOVA) was used to test the hypothesis that there was no difference among treatment groups for blood glucose, glucose infusion rate, blood lactate, blood pressure, femoral blood flow, femoral vascular resistance and heart rate throughout the time course. One-way ANOVA was used to test the hypothesis that there was no difference among treatment groups for plasma insulin values, muscle AICAR and ZMP levels, hindleg and 2-deoxy glucose uptake (combined muscles and individual muscles) and microvascular perfusion measurements at the end point of the experiments. When a significant difference ($P < 0.05$) was found between the treatment groups, pair wise comparisons by the Student-Newman-Keuls *post hoc* test was used to determine at which individual time points the differences were significant. Statistical difference among treatments for plasma AICAR values was determined by an unpaired t-test. All tests were performed using the SigmaStat™ statistical program (Jandel Software, version 2.03).

6.3 RESULTS

6.3.1 Plasma Insulin and AICAR Content

Table 6 shows plasma insulin values measured at the end of the experiment ($t = 120$ minutes) for the four protocols: saline, insulin ($3\text{mU}\cdot\text{min}^{-1}\cdot\text{kg}^{-1}$), AICAR ($3.75\text{mg}\cdot\text{min}^{-1}\cdot\text{kg}^{-1}$) and AICAR + insulin (AICAR: $3.75\text{mg}\cdot\text{min}^{-1}\cdot\text{kg}^{-1}$ and insulin: $3\text{mU}\cdot\text{min}^{-1}\cdot\text{kg}^{-1}$). The plasma insulin values were significantly increased (approximately 2 fold) when insulin was infused. An insulin infusion of $3\text{mU}\cdot\text{min}^{-1}\cdot\text{kg}^{-1}$ increased the basal value of $204 \pm 13\text{pM}$ to $395 \pm 17\text{pM}$ and $425 \pm 12\text{pM}$ (in the presence of AICAR). AICAR treatment alone or in combination with insulin had no significant effect on plasma insulin levels (Table 6).

AICAR content in the plasma samples increased from a basal value of zero (Table 6) when AICAR was infused. Plasma AICAR levels were slightly (22%) but significantly ($P < 0.05$) lower with insulin treatment than with saline treatment (Table 6), suggesting a stimulating effect of insulin on whole body AICAR clearance.

Table 6: Plasma values at the end of the experiment ($t = 120$ minutes). Details are given Figure 35 (protocol a).

Treatment	Saline	Insulin	Saline + AICAR	Insulin + AICAR
Plasma Insulin (pM)	204 ± 13	$395 \pm 17\#$	161 ± 43	$425 \pm 12\#$
Plasma AICAR (μM)	0	0	266 ± 12	$208 \pm 12\#$

Values are means \pm SE from saline ($n = 6$), insulin ($n = 10$), saline + AICAR ($n = 10$) and insulin + AICAR ($n = 12$) determined at $t = 120$ minutes. # insulin treated significantly different ($p < 0.05$) from corresponding untreated animals.

6.3.2 Muscle AICAR and ZMP Content

Table 7 shows AICAR and ZMP values measured at $t = 120$ minutes (Figure 35, protocol *a*) for experiments with AICAR ($3.75\text{mg}\cdot\text{min}^{-1}\cdot\text{kg}^{-1}$) and AICAR + insulin (AICAR: $3.75\text{mg}\cdot\text{min}^{-1}\cdot\text{kg}^{-1}$ and insulin: $3\text{mU}\cdot\text{min}^{-1}\cdot\text{kg}^{-1}$) treatments. AICAR and ZMP content in the soleus, plantaris, gastrocnemius red (GR) and gastrocnemius white (GW) increased from a basal value of zero (data not shown). The muscle content of AICAR and ZMP were not significantly different between insulin and saline treated animals. The muscle content of AICAR and ZMP in the GR and GW was significantly less than in the soleus muscle in the saline + AICAR group. The muscle content of AICAR in the plantaris was significantly less than in the soleus in the saline + AICAR group. There was a similar trend in the insulin + AICAR group for increased AICAR and ZMP levels in the soleus muscle but statistical significance was not reached with the number of experiments used for muscle analysis ($n = 4$).

Table 7: Muscle content of AICAR and ZMP from AICAR and insulin + AICAR treated animals determined at $t = 120$ minutes. Details are given in Figure 35, protocol *a*.

Treatment	Saline + AICAR		Insulin + AICAR	
	AICAR	ZMP	AICAR	ZMP
	(mmol.g ⁻¹ wet wt)			
Soleus	161 ± 9	325 ± 31	152 ± 22	237 ± 33
Plantaris	116 ± 11 *	252 ± 29	116 ± 17	207 ± 43
Gastrocnemius (White)	98 ± 16 *	170 ± 27 *	86 ± 12	145 ± 25
Gastrocnemius (Red)	86 ± 7 *	174 ± 30 *	110 ± 13	188 ± 23

Values are means ± SE. * AICAR and ZMP values significantly different ($P < 0.05$) from soleus values ($n = 7$ for saline + AICAR and $n = 4$ for insulin + AICAR).

6.3.3 Glucose Metabolism

Figure 36 shows time courses for blood glucose (BG) and glucose infusion rate (GIR) for experiments with or without insulin or AICAR treatment. There were no significant differences between blood glucose values for the four treatment groups. During experiments which underwent insulin infusions, blood glucose was maintained at a constant level (euglycaemia) by variable infusions of glucose (30% w/v solution) (Figure 36A).

The GIR from $t = 0$ to 120 minutes is shown in Figure 36B. During the $3\text{mU}\cdot\text{min}^{-1}\cdot\text{kg}^{-1}$ insulin clamp, glucose infusion was required in order to maintain basal blood glucose levels. The GIR increased during the first hour until a plateau was reached at $t = 60$ minutes.

The GIR in the insulin + AICAR experiments was significantly lower than for insulin alone from $t = 90$ to 120 minutes (Figure 36B). Values for the GIR at the end of the experiment showed that the GIR required to maintain euglycaemia decreased by approximately 30 percent from $9.7 \pm 0.5\text{mg}\cdot\text{min}^{-1}\cdot\text{kg}^{-1}$ at 60 minutes to $7.0 \pm 0.3\text{mg}\cdot\text{min}^{-1}\cdot\text{kg}^{-1}$ at 120 minutes, which was significantly ($P < 0.01$) lower than that required by insulin alone (Figure 36B).

Glucose infusion was not required in order to maintain the basal blood glucose levels during AICAR infusion alone.

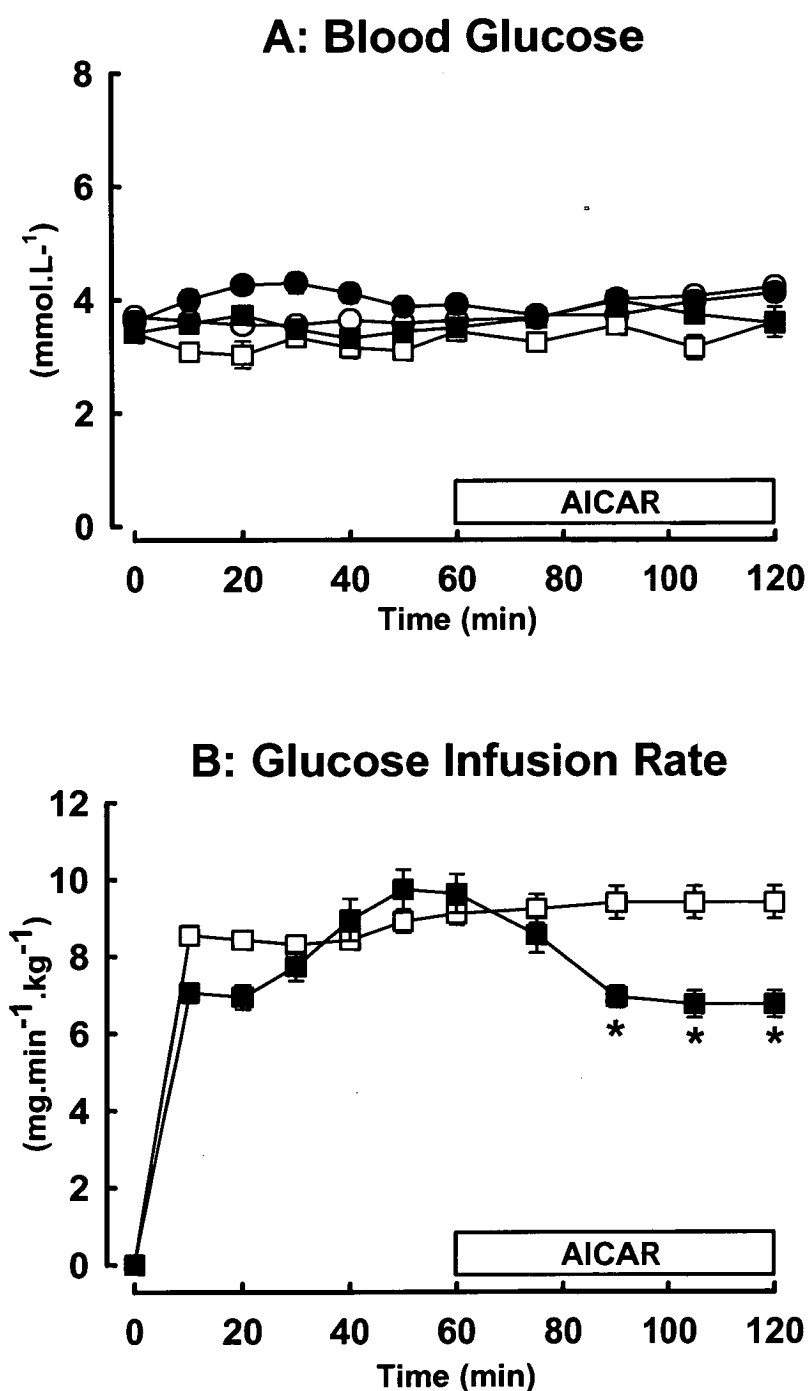


Figure 36: Time course for the effect of saline (O), insulin (□), AICAR (●) and AICAR + insulin (■) treatment on blood glucose (BG, A) and glucose infusion rate (GIR, B). AICAR infusion commenced at 60 minutes. Details are given in Figure 35. Values are given as means \pm SE. * AICAR treated significantly different ($P < 0.05$) from corresponding untreated animals ($n = 6 - 12$ per group). If error bars are not visible they fall within the symbol.

Figure 37 shows the effects of AICAR and insulin on hindleg glucose uptake and hindleg 2-deoxy glucose uptake (R'g) of the combined muscles of the lower leg. Glucose uptake measured by hindleg glucose uptake and lower leg R'g in combined muscles was significantly increased during insulin treatment compared with the saline control (Figure 37A-B). Glucose uptake (hindleg glucose uptake and lower leg R'g combined muscles) was not significantly different during AICAR treatment alone compared with the saline control treatment. When combined with insulin, AICAR infusion during the last 60 minutes of infusion resulted in a significantly greater ($P < 0.05$) uptake of hindleg glucose (2 fold) and R'g in combined lower leg muscles compared with insulin alone treatment (Figure 37A and Figure 37B respectively).

Figure 38 shows the effects of AICAR and insulin on the individual muscles of the lower leg. The glucose uptake (R'g) in the insulin alone group was significantly increased compared to the saline control group in all muscles of the lower leg except the white gastrocnemius. The glucose uptake (R'g) in the AICAR alone group was not significantly different to the control group in any of the lower leg muscles. The glucose uptake (R'g) in the AICAR + insulin group for the soleus, which consists of type I fiber type muscle [438], was significantly ($P < 0.05$) lower compared with the insulin alone group. The glucose uptake (R'g) in the AICAR + insulin group for gastrocnemius red was not significantly different from the insulin alone group which consists of a mixture of type I and type IIA fibers [438]. The glucose uptake (R'g) in the AICAR + insulin group was significantly increased compared with insulin alone group in the plantaris, tibialis, EDL and white gastrocnemius muscles which are a mixture of type IIA and IIB fibers [438]. Since the white fiber type muscles or the IIA and IIB fiber type muscles make up the bulk of the muscles in the lower leg, the overall effect of AICAR on muscle glucose uptake (R'g) was a significant increase in insulin mediated glucose uptake (Figure 37B).

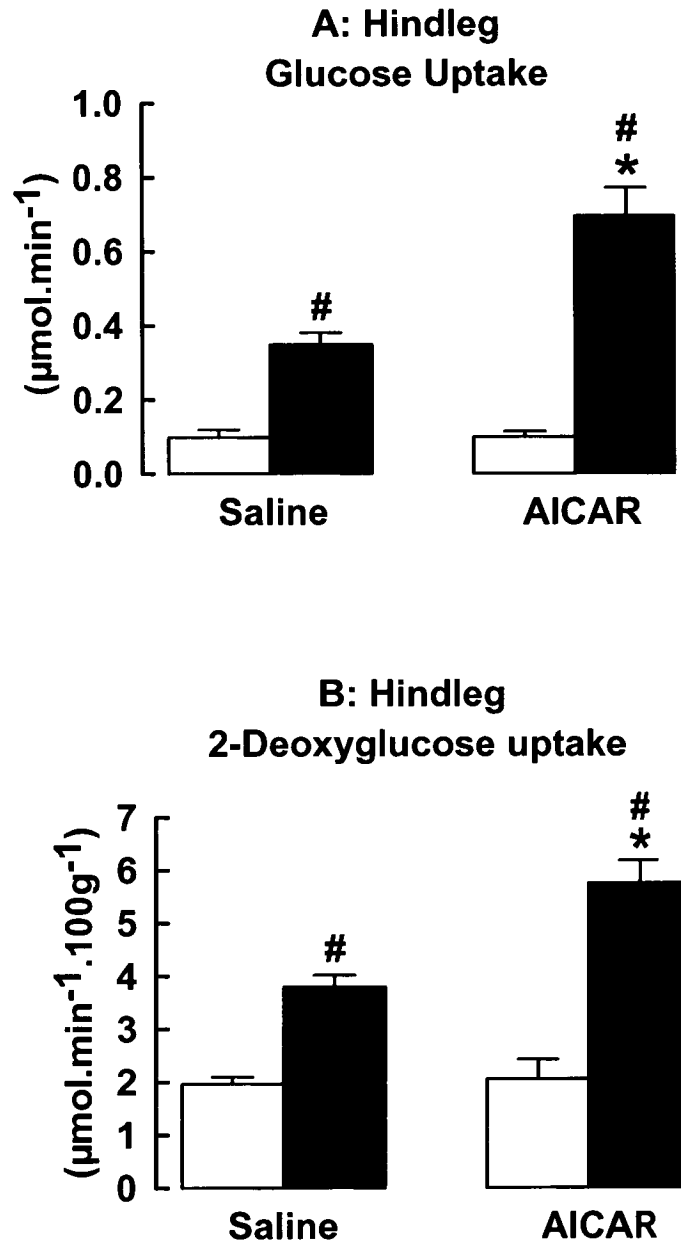


Figure 37: Effect of saline, insulin, AICAR and AICAR + insulin treatments on hind leg glucose uptake (HLGU, **A**) and 2-deoxyglucose uptake (R'g, **B**) of lower leg muscles. Saline or AICAR treatment (open bars) as indicated and insulin treatment (filled bars) as indicated. Details are given in Figure 35. Values were determined at the end of the experiment ($t = 120\text{min}$) and are means \pm SE. # insulin treated significantly different ($P < 0.05$) from untreated animals. * AICAR treated significantly different ($P < 0.05$) from untreated animals ($n = 6 - 12$ per group).

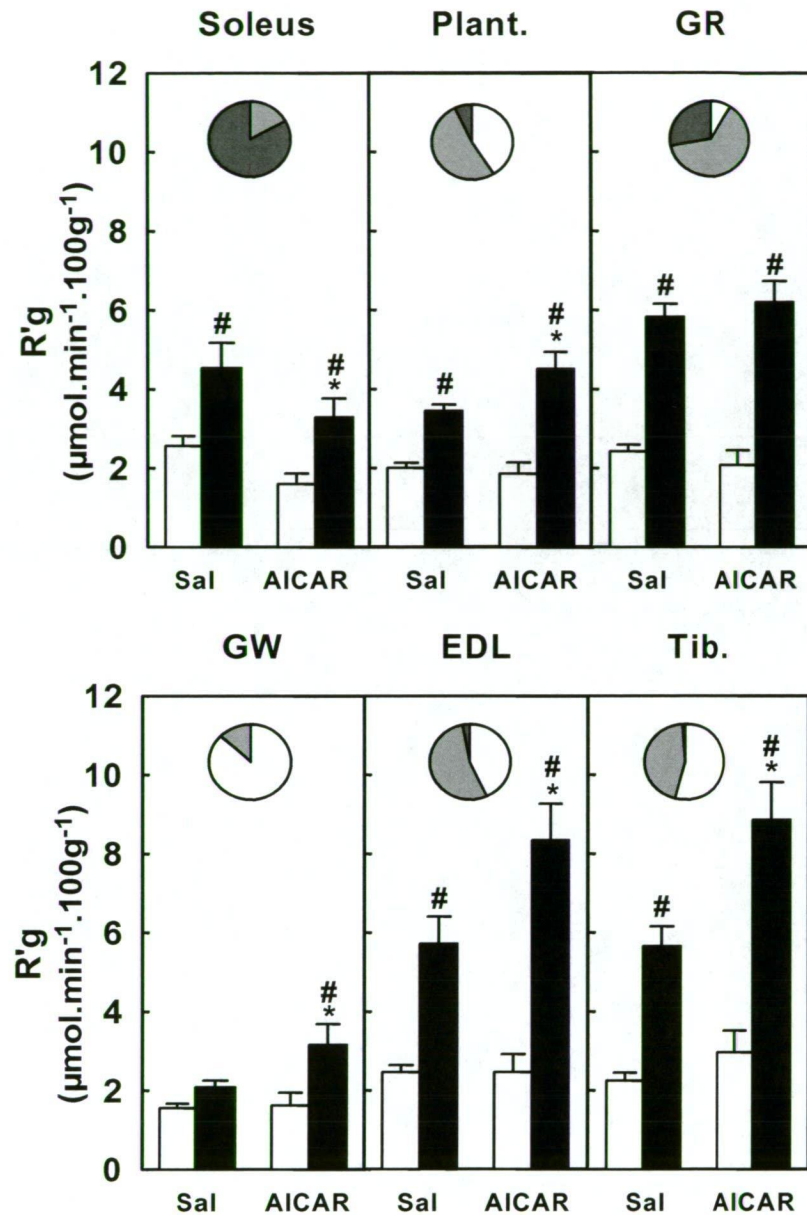


Figure 38: Effect of saline, insulin, AICAR and AICAR + insulin treatments on 2-deoxyglucose uptake ($R'g$) of soleus, plantaris (plant.), gastrocnemius red (GR), gastrocnemius white (GW), extensor digitorum longus (EDL) and tibialis (Tib.) lower leg muscles. Saline or AICAR treatment (open bars) as indicated and insulin treatment (filled bars) as indicated. Details are given in Figure 35. Percent (%) fiber type is indicated by pie charts; dark grey – slow oxidative; light grey – fast oxidative glycolytic; white – fast glycolytic. Values were determined at the end of the experiment ($t = 120\text{min}$) and are means \pm SE. # insulin treated significantly different ($P < 0.05$) from untreated animals. * AICAR treated significantly different ($P < 0.05$) from untreated animals ($n = 6 - 12$ per group).

6.3.4 Lactate Metabolism

Figure 39 shows the time courses for changes in arterial blood lactate concentration during saline, insulin, saline + AICAR and insulin + AICAR treatments. The arterial blood lactate concentration in the saline and insulin groups remained constant throughout the experiment. The arterial lactate concentration in the insulin group increased compared with the saline group but this difference was not significant. The arterial blood lactate concentration in the AICAR alone group was significantly ($P < 0.05$) greater 30 minutes after the commencement of AICAR infusion compared with the saline group and remained significant until the end of the experiment. The arterial blood lactate concentration in the AICAR + insulin group was significantly ($P < 0.05$) greater 45 minutes after the commencement of AICAR infusion compared to the insulin group and remained significant until the end of the experiment (Figure 39).

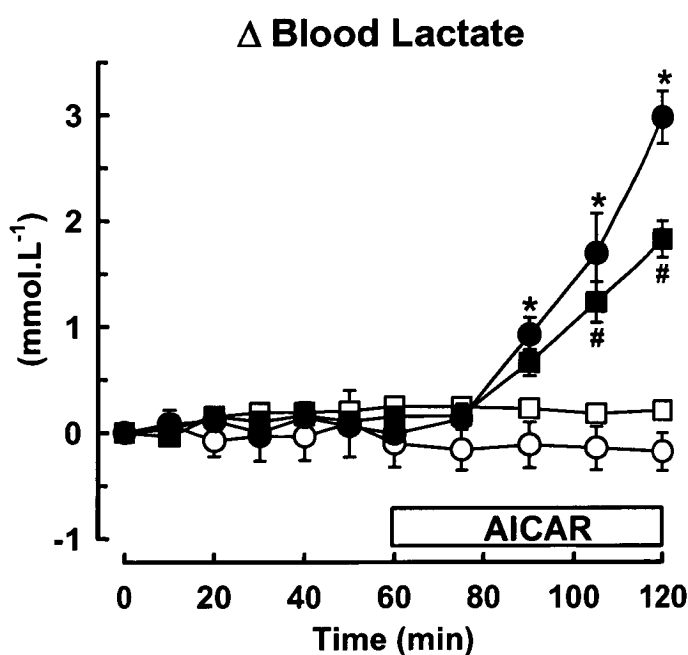


Figure 39: Time course for the effect of saline (O), insulin (□), AICAR (●) and AICAR + insulin (■) treatments on change in blood lactate. AICAR infusion commenced at 60 minutes. Details are given in Figure 35. Values are given as means \pm SE. * AICAR treated significantly different ($P < 0.05$) from corresponding untreated animals. # Insulin + AICAR treated significantly different ($P < 0.05$) from insulin treated animals ($n = 6 - 12$ per group).

6.3.5 Haemodynamic Measurements

Figure 40 shows the mean arterial blood pressure (MAP) time course for saline, insulin, saline + AICAR and insulin + AICAR treatments. The basal MAP remained constant throughout the experiment for all treatment groups.

Figure 41 shows the time course for change in femoral blood flow and change in femoral vascular resistance. The FBF in the insulin alone group tended to increase over the duration of the experimental time course compared to the saline control group and AICAR alone group. This increase became significant at $t = 75$ minutes and continued until the end of the experiment. The FBF in the insulin + AICAR group showed a similar trend to the insulin alone group but this was only statistically significant compared to the saline control and AICAR alone group at $t = 105$ minutes (Figure 41A). The FBF in the AICAR alone group showed no significant difference from the saline control. There was a trend for the insulin and the insulin + AICAR groups to decrease FVR compared to the saline and AICAR alone control groups (Figure 41B), however this was not statistically significant.

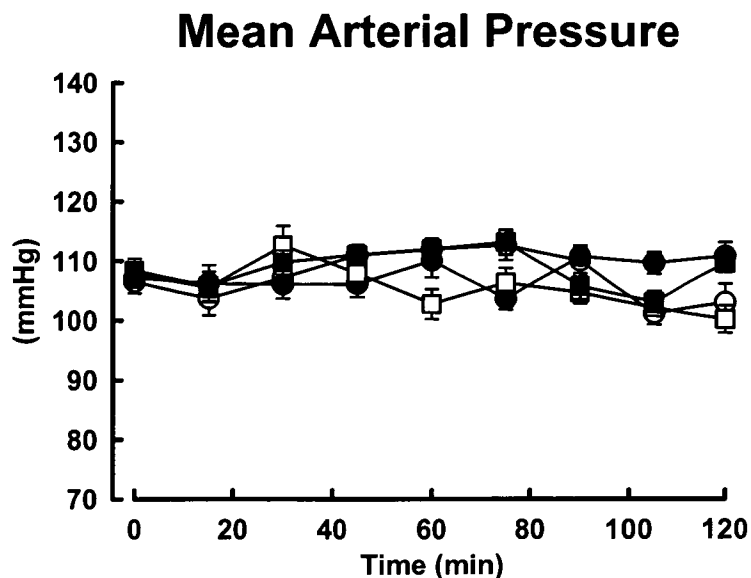


Figure 40: Time course for the effect of saline (O), insulin (□), AICAR (●) and AICAR + insulin (■) treatments on mean arterial pressure (MAP). AICAR infusion was commenced at $t = 60$ minutes. Details are given in Figure 35. Values are given as means \pm SE ($n = 6 - 12$ per group).

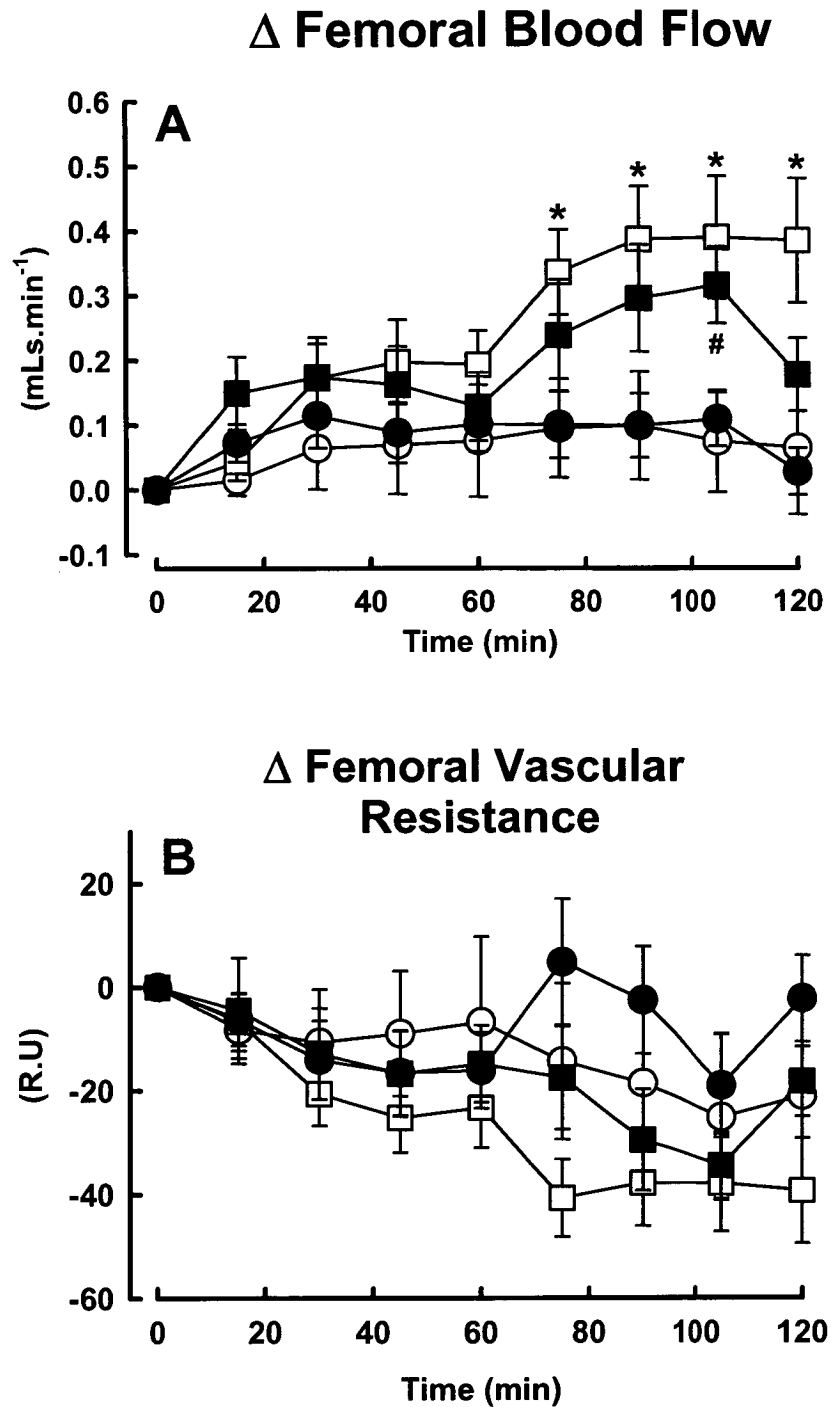


Figure 41: Time course for the effect of saline (○), insulin (□), AICAR (●) and AICAR + insulin (■) treated animals on change femoral blood flow (Δ FBF, A) and change in femoral vascular resistance (Δ FVR, B). AICAR was commenced at $t = 60$ minutes. Details are given in Figure 35. Values are given as means \pm SE. * Insulin treated significantly different ($P < 0.05$) from saline treated and AICAR alone treated animals. # Insulin + AICAR treated significantly different ($P < 0.05$) from saline treated and AICAR alone treated animals ($n = 6 - 12$ per group).

Figure 42 shows the time course for the change in heart rate during saline, insulin, saline + AICAR and insulin + AICAR treatments. The HR in the insulin group was not significantly different to the saline control group. The HR in the AICAR alone and the AICAR + insulin group was significantly ($P < 0.05$) less after the first 15 minutes of AICAR infusion compared with the corresponding control group and this decrease continued until the conclusion of the experiment.

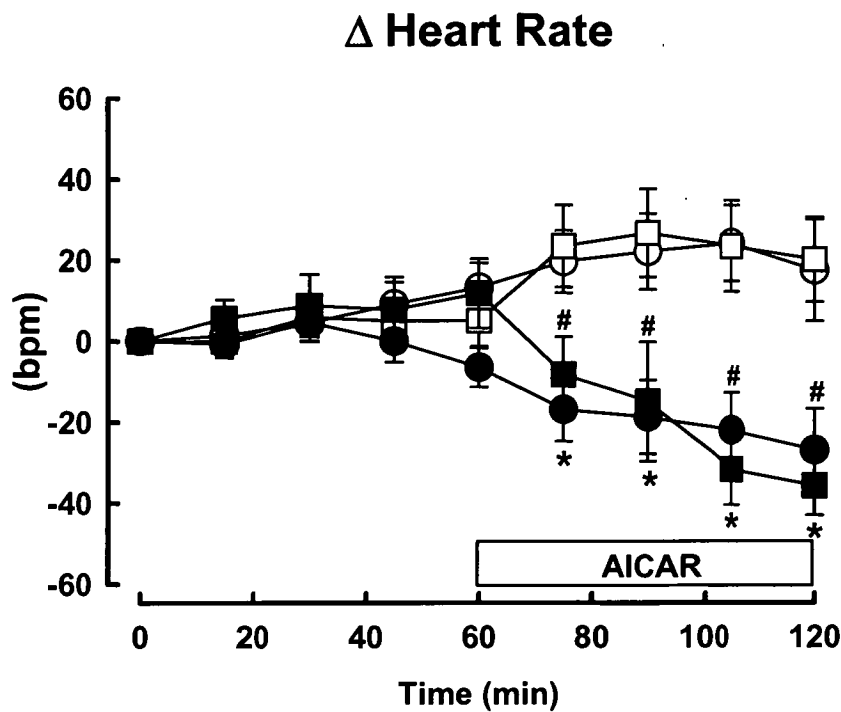


Figure 42: Effect of saline (O), insulin (□), AICAR (●) and AICAR + insulin (■) treatment on the time course for change in heart rate (Δ HR). AICAR infusion commenced at 60 minutes. Details are given in Figure 35. Values are given as means \pm SE. * AICAR treated significantly different ($P < 0.05$) from corresponding untreated animals. # AICAR + insulin treated significantly different ($P < 0.05$) from corresponding untreated animals ($n = 6 - 12$ per group).

6.3.6 Microvascular Perfusion

Figure 43 shows the effect of insulin and insulin + AICAR on microvascular volume (MV) and microvascular flow rate (MFR) taken at the commencement ($t = 0$ minutes) and prior to the commencement of contraction stimulation ($t = 120$ minutes). The effect of contraction for each group is shown at $t = 145$ minutes. Figure 43A shows that insulin significantly increased the MV compared with basal which was further significantly increased by contraction. Figure 43B shows that insulin + AICAR treatment significantly increased MV compared to basal and this was not further significantly increased with contraction treatment. Figure 43C shows that insulin infusion had no effect on the MFR compared to basal however MFR significantly increased after contraction. Figure 43D shows that insulin + AICAR treatment significantly increased MFR compared to basal which was further significantly increased with contraction stimulation.

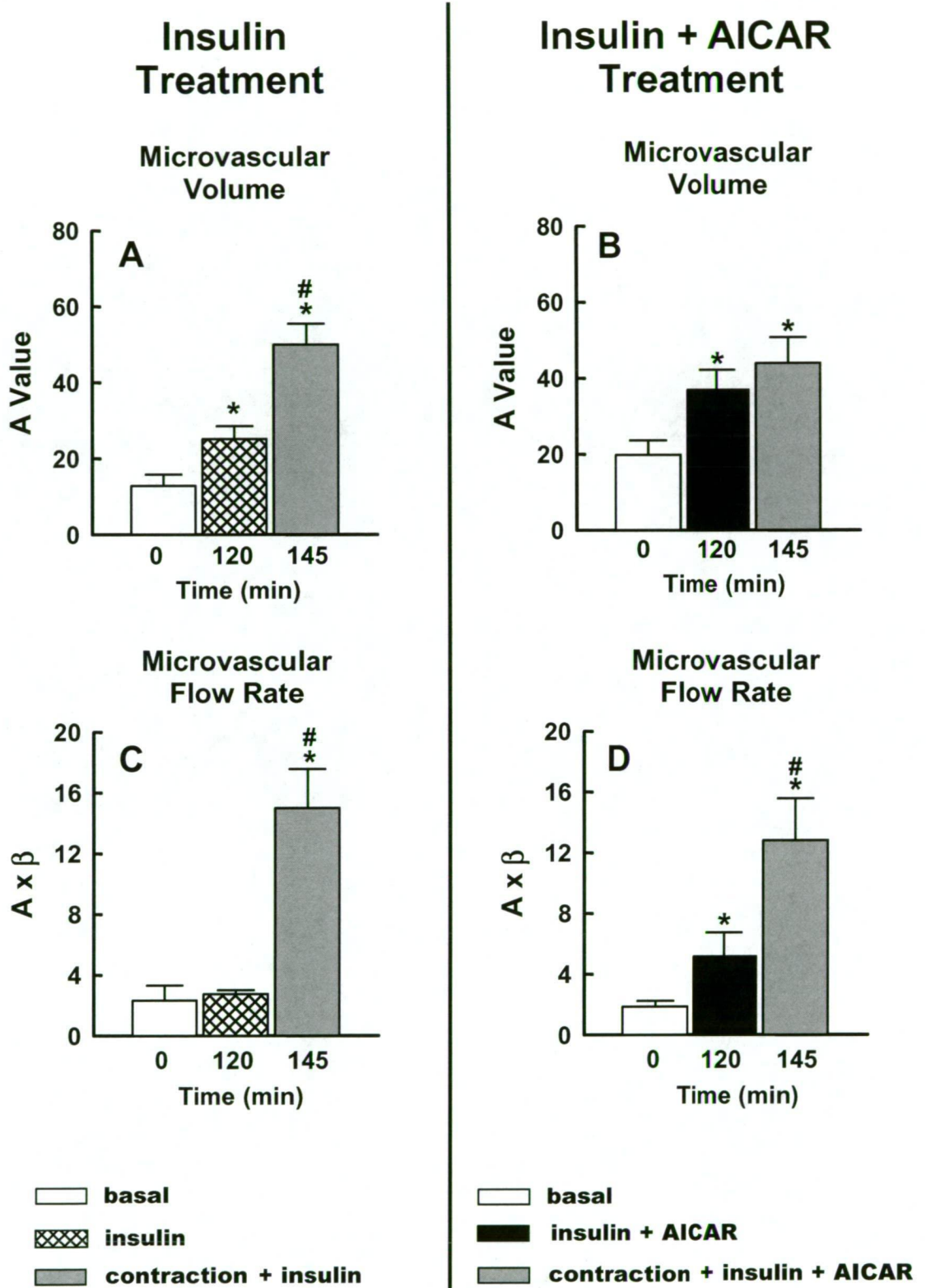


Figure 43: Measurements of the microvascular volume (MV) (*A*-value) for insulin (A) and insulin + AICAR (B) groups and microvascular flow rate (MFR) ($A \times \beta$ -value) for insulin (C) and insulin + AICAR (D) groups. Values are means \pm SE (n = 6 in each group). * Significantly different ($P < 0.05$) from basal values; # contraction treated significantly different from untreated.

Figure 44 shows the changes in microvascular volume (A-value) for saline, insulin, saline + AICAR and insulin + AICAR treatments. The MV measurement was taken prior to the commencement of contraction stimulation ($t = 120$ minutes) for the four experimental groups and compared with basal values (ΔMV). The ΔMV in the insulin and the AICAR alone group was significantly increased compared to the saline control. The ΔMV in the AICAR + insulin group was significantly increased compared to the insulin alone group, indicating that the effect of AICAR alone and insulin alone to increase microvascular perfusion is additive.

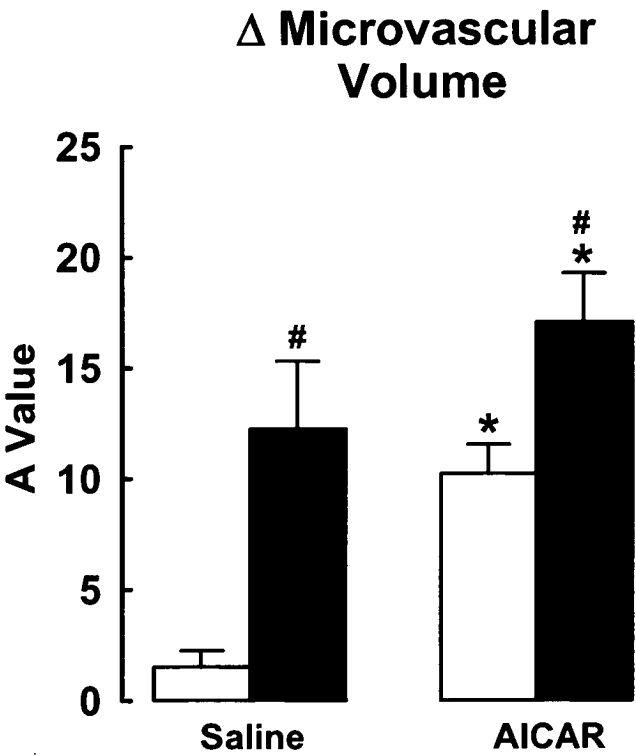


Figure 44: Changes in the microvascular volume (*A-value*) for saline, AICAR, insulin and insulin + AICAR groups. Saline or AICAR treatment (open bars) and insulin treatment (filled bars). Details are given in Figure 35. Values were determined at the end of the experiment ($t = 130$ minutes). Values are means \pm SE ($n = 6$). # Insulin treated significantly different ($p < 0.05$) from untreated. * AICAR treated significantly different ($p < 0.05$) from untreated.

6.3.7 Additional Experiments: Glycogen Depleted

A sub-set of insulin + AICAR experiments were performed using protocol *a*, and A-V sampling was omitted. The *in vivo* experiments were carried out using rats which were fasted for 40 hours in order to deplete liver glycogen content (food removed at 5pm 40 hours prior to the commencement of the experiment).

6.3.7.1 Glucose Metabolism

Figure 45 shows the effects of insulin and AICAR + insulin on glucose infusion rate (GIR) and hindleg 2-deoxyglucose uptake ($R'g$) of the combined muscles of the lower leg for 16 hour and 40 hour fasted groups. During the insulin infusions blood glucose was maintained at the initial value (euglycaemia) by a variable infusion of glucose (30% w/v solution). There were no significant differences between blood glucose values for the three treatment groups at the end of the experiment (data not shown).

The GIR at the end of the experiment ($t = 120$ minutes) is shown in Figure 45A. The GIR in the 16 hour fasted insulin + AICAR group was significantly lower (30% less) compared with the insulin alone group (time course values shown in Figure 36B). The GIR in the 40 hour fasted insulin + AICAR group was significantly higher compared with the 16 hour fasted insulin and insulin + AICAR groups. Figure 45B shows that there was no significant difference between the $R'g$ of the 40 hour fasted insulin + AICAR group compared with the equivalent 16 hour fasted group.

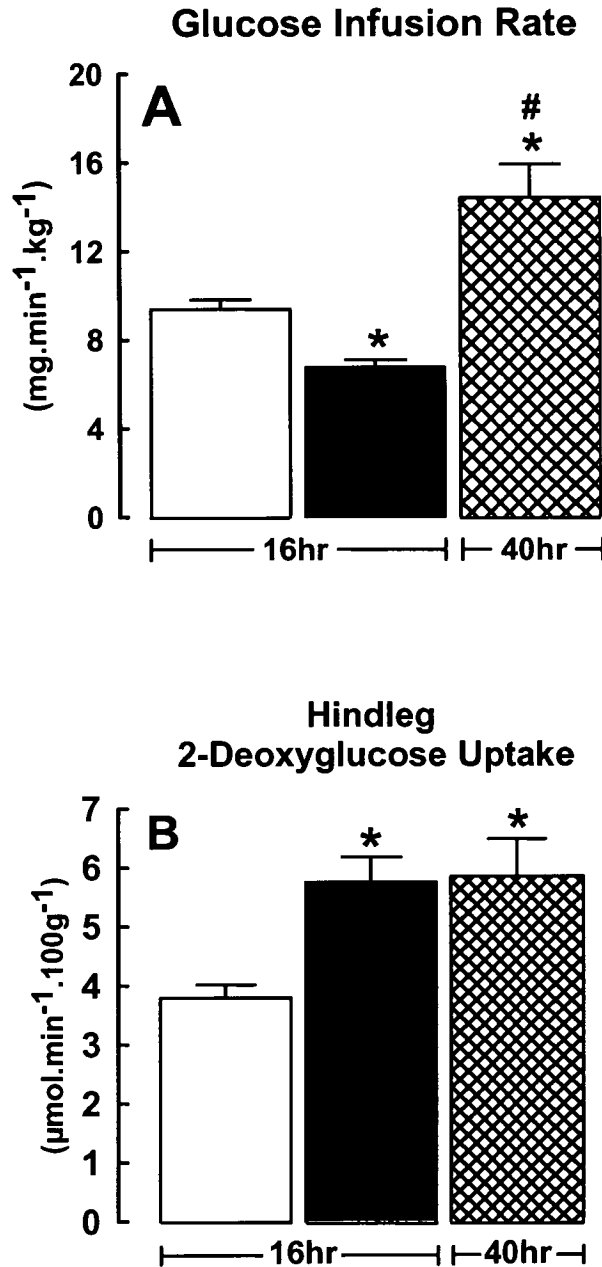


Figure 45: Effect of insulin (□) and insulin + AICAR (■) [16 hour fasted animals] and insulin + AICAR (⊠) [40 hour fasted animals] treatment on glucose infusion rate (GIR, A) and hindleg 2-deoxyglucose uptake (R'g, B). Details are given in Figure 35. Values were determined at the end of the experiment ($t = 120$) and are means \pm SE. * AICAR treated significantly different ($P < 0.05$) from corresponding untreated animals; # 40 hour fast treated significantly different ($P < 0.05$) from corresponding 16 hour fasted group ($n = 12$ per group [16 hour fast], $n = 6$ per group [40 hour fast]).

6.4 DISCUSSION

This study was undertaken to investigate the effects of the AMPK activator AICAR on insulin-mediated microvascular perfusion and skeletal muscle glucose uptake. The main finding of this study was that acute administration of AICAR *in vivo*, at a dose which does not stimulate glucose uptake by itself, improves insulin mediated glucose uptake. A second major finding of this study was that AICAR increased microvascular perfusion (microvascular blood volume) *in vivo* and this was further increased with the addition of insulin. This study also demonstrated that AICAR induced increases in insulin mediated muscle glucose uptake were greater in the white fiber type muscles.

The effects of insulin to increase total blood flow and microvascular perfusion [49] have been established by others and were also observed in the present study. As discussed in the previous chapter, at the dose used, AICAR was found to increase microvascular perfusion and microvascular flow without a corresponding increase in total flow or glucose uptake. Plasma concentrations of AICAR reached approximately 0.24mM and although these treatments alone were without effect on muscle glucose uptake they were found to markedly potentiate physiological insulin mediated glucose uptake. Bergeron *et al.* [313], demonstrated that the effects of AICAR on glucose transport activity are additive with insulin. The results from the present study differ from Bergeron as a lower dose of AICAR was used which was below the threshold to stimulate glucose uptake however insulin mediated glucose uptake was markedly increased. It likely that increased insulin mediated glucose uptake in the presence of low dose AICAR is due to increased availability of glucose and insulin to muscle through enhancement of nutritive blood flow. It has been shown that there is a strong correlation between nutritive blood flow and glucose uptake in the presence of insulin [2].

In this study AICAR enhanced insulin-mediated increases in skeletal muscle glucose uptake which were found to be dependant upon the fiber type composition of the muscles. Type I (red) muscles showed a decrease in insulin mediated glucose uptake while the type IIA and IIB (white) muscles showed a marked increase in insulin-mediated glucose uptake. The fiber type specific effects of AICAR have also

been reported by other workers at higher doses than used in the current study. Bergeron *et al.* [313] reported AICAR (0.58 mM, *in vivo*) to directly stimulate 2-DG uptake, in the absence of insulin, in the lateral and medial gastrocnemius and the soleus muscle. Iglesias *et al.* [318], reported that subcutaneous injection of 250 mg.kg⁻¹ AICAR to insulin resistant high fat fed rats one day before conducting a hyperinsulinemic euglycaemic clamp markedly improved insulin-stimulated glucose uptake (2-DG) in white but not red quadriceps muscles. In this study enhancement of insulin mediated glucose uptake occurred after the expected time of AMPK activation had passed. Follow up studies by Iglesias *et al.* [318] also revealed that significant enhancement of insulin stimulated glucose uptake in white muscle also occurred in normal rats. Ai *et al.* also reported that 0.5 - 4 mM AICAR stimulated 2-DG uptake occurred in incubated epitrochlearis, less in flexor digitorum brevis (FDB) and not at all in soleus muscle [323]. Of these muscles, the epitrochlearis is richest in type IIB, the soleus in type I and the FDB in type IIA fibers [323]. Ai *et al.* also reported AMPK α 1 expression to be highest in the epitrochlearis and lowest in the soleus; FDB muscles had the lowest expression of AMPK α 2 [323]. In contrast, Putman *et al.* [439] also demonstrated that the α 1 and α 2 isoforms of AMPK are consistently expressed in a fiber type specific manner. They showed that both the α 1 and α 2 protein levels were greatest in the slow-twitch oxidative soleus, slightly less with in the mixed fast-twitch red gastrocnemius and lowest within the fast-twitch white gastrocnemius.

The *in vivo* findings of this study provide evidence that AICAR increases insulin-mediated hindleg glucose uptake and 2-deoxy-glucose uptake. Despite this finding there was no increase in whole body glucose infusion rate (GIR). The GIR during the insulin + AICAR infusion was significantly reduced, such that by the end of the experiment the rate was approximately 30% less than during infusion of insulin alone. This implies that AICAR inhibits the ability of insulin to suppress hepatic glucose output (HGO). A number of studies have provided *in vivo* evidence in support of AICAR having the ability to inhibit insulin induced suppression of HGO. A study by Peneck *et al.* [440], using conscious dogs, showed that intra-portal AICAR infusion of 1 mg.min⁻¹.kg⁻¹ abolished net hepatic glucose uptake (NHGU) and infusion of 2 mg.min⁻¹.kg⁻¹ stimulated net hepatic glucose out-put (NHGO). In another *in vivo* study by Camacho *et al.* [441], 1 mg.min⁻¹.kg⁻¹ AICAR was infused

into dogs for 90 minutes during a $2 \text{ mU} \cdot \text{min}^{-1} \cdot \text{kg}^{-1}$ hyperinsulinemic insulin clamp. AICAR caused a stimulation of both hepatic glucose output and hepatic glycogenolysis even in the presence of physiological insulin. Another similar study by Camacho *et al.* [442] revealed that AICAR is effective in countering the suppressive effect of pharmacological insulin on NHGO which occurred even though AICAR-stimulated ACC phosphorylation was completely blocked. These findings indicate that, when activated, AMPK increases the availability of blood glucose to skeletal muscle by countering insulin induced inhibition of hepatic glucose production. Thus AICAR induced HGO provides a reasonable explanation for the observed decrease in GIR during AICAR + insulin treatment in this study in the presence of a net increase in skeletal muscle glucose uptake.

An additional set of experiments were performed with animals fasted for 40 hours. It was assumed that liver glycogen content would be markedly depleted in 40 hour fasted animals compared with the over night fasted animals. A significantly increased GIR was required to maintain euglycemia in the 40 hour fasted AICAR + insulin treatment compared with the corresponding overnight fasted treatment while R'g was unchanged. This finding supports the idea that in over night fasted animals AICAR inhibited insulin's suppression of HGO. Similarly, Camacho *et al.* [441], noted that the stimulation of NHGO during AICAR treatment was lost in animals subject to a 42 hour fast where liver glycogen was markedly reduced (unpublished observation). The use of radio-labelled tracers in the current study for an accurate determination of the rates of hepatic glucose appearance and disappearance from the liver in the presence of AICAR would clarify this issue.

An additional finding of this study was that AICAR treatment increased lactate production in resting muscle. This finding is in agreement with other reports which have also observed an increase in lactate concentration with AICAR treatment *in vitro* [269, 314] and *in vivo* [313, 336, 441, 443]. Merrill *et al.*, using the perfused rat hindlimb, demonstrated that AICAR treatment (2mM) increased lactate production by approximately 2 fold over 45 minutes compared with the control group [269]. Bergeron *et al.* [313], using conscious rats, also reported a marked increase in plasma lactate to about 13 mM at 90 minutes when the plasma levels of AICAR had reached 2.5 mM. Chamacho *et al.* [441] also reported that AICAR

significantly increased net hepatic lactate output in the presence of hypoglycemia. The increased blood lactate concentration in AICAR treated animals was also noted by W. Winder in a review article [444] who suggested that increased intra-muscular glucose concentration in response to AICAR is not all oxidised in resting muscle and may be shunted towards lactate production. A number of studies have also demonstrated that AMPK phosphorylates phosphofructokinase and thereby stimulates glycolysis [445-447] and this action is likely to account for the observed increase in net hepatic lactate production.

The genetically obese Zucker rat (OZR) displays impaired insulin mediated glucose transport in skeletal muscle [448] and insulin mediated microvascular perfusion is absent [338]. In contrast, contraction-mediated glucose uptake by muscles of the obese Zucker rat appears to be essentially normal as does the increase in microvascular perfusion in response to exercise [338]. This suggests that, in the OZR, the defects particular to insulin signalling may explain the insulin resistance. It has been demonstrated by Bergeron *et al.* [317] that acute infusion of AICAR in the OZR increases glucose transport during a physiological insulin clamp. The mechanism for enhanced insulin sensitivity in the Bergeron study may be partly due to increased microvascular perfusion allowing greater access of insulin and glucose to the myocyte. It is yet to be determined whether AICAR enhances insulin mediated microvascular perfusion and thus glucose uptake in models of insulin resistance, such as the OZR and this area needs further investigation.

In conclusion low dose AICAR stimulates microvascular perfusion in skeletal muscle *in vivo* at a dose which does not stimulate glucose uptake by itself and enhances insulin stimulated glucose uptake and microvascular perfusion. The increase in microvascular perfusion caused by AICAR is likely to enhance hormone and nutrient delivery to the muscle myocytes which in turn increases glucose uptake in skeletal muscle when insulin is present. The AICAR enhanced insulin-stimulated glucose uptake occurred predominantly in the white fiber type muscles. AICAR inhibited insulin's ability to increase whole body glucose uptake which is likely to be due to inhibition of insulin's suppression of hepatic glucose output. The stimulation of lactate accumulation and the suppression of heart rate detract from the use of AICAR for the treatment of insulin resistance.

CHAPTER 7

General Discussion

7.1 Major Findings

The work presented in this thesis explores the links between insulin and AMPK activated microvascular perfusion and glucose uptake in muscle *in vivo*. The mechanisms relating to insulin were examined by infusing the PI3K inhibitor wortmannin systemically and the NOS inhibitor L-NAME locally during a hyperinsulinemic euglycaemic clamp in anaesthetised rats. The mechanisms relating to AMPK activation were examined using muscle resistance arteries *in vitro* and with AICAR infusion alone or combined with a euglycaemic hyperinsulinemic clamp *in vivo*.

The experiments resulted in new previously unpublished findings that; (i) inhibiting the insulin signalling step at PI3K, using the PI3K inhibitor wortmannin, blocked insulin-mediated glucose uptake and microvascular perfusion, (ii) local infusion of L-NAME blocked insulin-mediated microvascular perfusion and blunted glucose uptake in the treated leg, (iii) in isolated resistance arteries, AICAR induced vasodilation, which was abolished by NOS or AMPK inhibition and sensitised resistance arteries to sodium nitroprusside (SNP), (iv) *in vivo*, infusion of low dose AICAR increased microvascular perfusion in the absence of increased glucose uptake. When combined with insulin, low dose AICAR enhanced insulin-mediated glucose uptake, possibly by allowing greater access of insulin and glucose via increased microvascular perfusion.

Collectively these findings suggest that insulin activation of NOS via PI3K and AMPK activation can enhance glucose uptake through increased microvascular perfusion. These results further strengthen the previous reports regarding the important contribution of microvascular blood flow to glucose uptake.

7.2 Insulin Mediated Microvascular Perfusion and its Effects on Glucose Uptake

Previous studies in our laboratory have provided considerable evidence for the existence of two vascular routes in skeletal muscle which have been termed nutritive and non-nutritive vascular flow routes (reviewed in [2]). Experiments using the vasodilator ephedrine demonstrated that total blood flow can be increased without affecting microvascular perfusion or glucose uptake [49]. The exact anatomical arrangement of the nutritive and non-nutritive vascular routes is unknown; however it is thought that the nutritive route consists of long tortuous capillaries which allow extensive microvascular perfusion of the muscle. The non-nutritive route is thought to be made up of shorter slightly larger and wider vessels [449]. The 1-MX and more recently CEU techniques were developed for specifically measuring skeletal muscle microvascular perfusion *in vivo*. Using these techniques it was possible to clearly demonstrate the ability of insulin to increase microvascular perfusion [49, 57, 58] either with or without a corresponding increase in total blood flow. Insulin may act via the insulin receptors on the endothelium at key flow controlling points in the muscle microvasculature relaxing the arterioles supplying the nutritive flow route. This action of insulin thus facilitates the delivery of glucose and itself to the muscle and contributes to the action of insulin to increase glucose uptake [5].

In individuals who have a normal response to insulin, a significant and positive correlation can be observed between microvascular perfusion and glucose uptake in skeletal muscle. This relationship can be observed using a number of interventions in rats demonstrating that impairment of microvascular perfusion can cause impairment in muscle glucose uptake. For example; α -methyl serotonin, TNF- α or intralipid + heparin infusions acutely block the ability of insulin to induce microvascular perfusion and impair insulin-mediated glucose disposal. The same correlation was observed in chapter 4 of this thesis with local L-NAME infusion. Also, AICAR caused an increase in microvascular perfusion, which when combined with insulin, potentiated insulin-mediated microvascular perfusion and glucose uptake (see chapter 6).

Evidence for a role for the endothelium involvement in the vasoactive action of insulin is supported by results from the eNOS knockout mouse which are hypertensive and display a 40% reduction in muscle blood flow and glucose uptake compared with wild type (WT) mice [403]. Similarly Shankar *et al.* [402] demonstrated, using euglycaemic hyperinsulinemic clamps in eNOS^{-/-} mice, that glucose infusion and glucose turnover rates were decreased. In addition the endothelial-specific IRS-2 knockout mouse displayed insulin resistance and impaired glucose tolerance compared with the wild type mouse as assessed by the hyperinsulinemic-euglycaemic clamp [450]. Together these studies strongly support an important role for a vascular component in maintaining normal responses to glucose disposal.

In contrast, some studies using gene knockout and transgenic mouse models present evidence against a role for the endothelium in microvascular perfusion for regulation of glucose disposal. The vascular endothelial cell insulin receptor knock-out (VENIRKO) mouse displays no major abnormality in vascular development or glucose homeostasis [451]. However, VENIRKO mice placed on a low salt diet display altered eNOS expression and insulin resistance, suggesting that eNOS is required to maintain insulin sensitivity.

The transgenic mouse with an endothelium specific mutant insulin receptor over expression (ESMIRO) retains intact insulin receptor binding but signal transduction is absent [452]. This transgenic model displays normal glucose homeostasis despite significant endothelial dysfunction evidenced by blunted aortic vasorelaxation responses to acetylcholine and calcium ionophore. Glucose and insulin tolerance testing demonstrated that there was no attenuation of insulin sensitivity in the ESMIRO mouse compared with the WT mouse. This result is despite a loss of insulin stimulated vascular function and blunted insulin induced eNOS phosphorylation.

Evidence from the ESMIRO and VENIRKO mice seem to indicate that endothelial dependant vascular actions of insulin lack importance however an

assessment of insulin-mediated microvascular perfusion has not been made in these models. Results from the VENIRKO and ESMIRO studies should be interpreted with caution as compensatory changes may occur in knockout or transgenic models. One possible explanation may be that the loss of endothelial insulin receptors may be compensated by signalling via the IGF-1 pathway. There are substantially more IGF-1 receptors on endothelial cells than insulin receptors and insulin is able to bind and activate IGF-1 receptors [453]. IGF-1 signalling shares the same downstream pathway so when this pathway is impaired such as in the eNOS knockout or IRS-2 knockout, the vascular contribution to insulin resistance becomes evident.

The hyperinsulemic euglycaemic clamp would also provide a more accurate measure of insulin sensitivity compared with tolerance tests performed in the ESMIRO mouse studies [452]. A significant and positive correlation exists between microvascular perfusion and glucose uptake so that in normal individuals microvascular perfusion can account for up to 50% of glucose uptake [2]. If insulin interacts with insulin receptors on the endothelium to enhance perfusion and therefore glucose uptake then it would be expected that the VENIRKO and ESMIRO mouse models would display some degree of insulin resistance. The development of the VENIRKO and ESMIRO has opened up some new and interesting areas for research. A detailed examination of insulin-mediated microvascular perfusion and glucose metabolism in these models has not been assessed and needs to be determined to resolve this issue.

Alternatively, it is possible that insulin can act directly on the VSMC leading to vasodilation in an endothelium independent mechanism. Studies using VSMC have demonstrated that insulin can directly activate a constitutive Ca^{2+} dependant NOS (cNOS) and increase cGMP and cAMP levels thereby causing vasorelaxation [72, 73]. This finding suggests that insulin-induced vasodilation is not entirely endothelium-mediated but does not exclude an insulin-induced endothelium mediated process *in vivo*.

7.3 Involvement of NO in Insulin Action

There is substantial evidence suggesting that NO is involved in the action of insulin to increase limb blood flow [41, 89, 397, 399, 454]. Within muscle, NO is produced by NOS located in the vascular endothelium [400] and myocytes [401]. It has been demonstrated that endothelial and vascular smooth muscle cells have insulin receptors and that insulin stimulates phosphorylation and activation of Akt, which can in turn phosphorylate and activate eNOS [37, 38, 455].

Previous studies provided evidence that insulin interacts with the vasculature when it was demonstrated that inhibition of NO production can fully abolish the effect of insulin to increase total flow [5, 41, 89, 399] and glucose uptake [399]. Insulin induced vasodilation in the rat cremaster muscle has been abolished with the addition of a NOS inhibitor or endothelium removal [397]. It has also been reported by Vincent *et al.* that systemic NO inhibition abolishes insulin-stimulated microvascular perfusion and inhibits glucose uptake by approximately 50% [88]. The results presented in chapter 4 are in agreement with these findings.

7.4 Microvascular Perfusion: Dependant on PI3K

Results from chapter 3 demonstrated that the PI3K inhibitor wortmannin abolished insulin mediated increases in total flow and microvascular perfusion. The main finding of this chapter indicates that the PI3K pathway is involved in downstream signalling resulting in modulation of vascular function *in vivo*. This finding is in agreement with previous studies (section 7.3) that insulin mediated increases in blood flow are nitric oxide dependant [41, 89] and that insulin mediated NO production involves Akt mediated activation of eNOS [84].

Wortmannin treatment completely abolished microvascular perfusion and attenuated insulin-mediated glucose uptake by approximately 50%. Inhibition of PI3K by wortmannin would be expected to completely block muscle glucose uptake. Although wortmannin administration caused unexpected increases in plasma insulin,

Akt phosphorylation in the liver and aorta was completely blocked whereas there was no significant inhibition in skeletal muscle. It is likely that wortmannin did not reach the myocyte due to its insolubility and thus passage across the microvascular endothelial barrier may have been restricted. The 50% inhibition of insulin mediated glucose uptake may be the result of reduced delivery of insulin and glucose because of the total inhibition of microvascular perfusion.

7.5 Local NOS Inhibition: Blocks Insulin Action

Impairment of vascular endothelial function is a feature of type 2 diabetes [456] and this feature may contribute to reduced substrate delivery for insulin-stimulated glucose uptake. Results from chapter 4 indicate that local NOS inhibition blocks insulin mediated increases in total blood flow and microvascular perfusion and well as partially inhibiting skeletal muscle glucose uptake. This finding suggests that NOS activation in the vasculature plays an important role in insulin action.

It has been shown that ICV administration of NOS inhibitors during systemic insulin infusion caused a reduction in insulin mediated glucose disposal [90, 91] and microvascular perfusion [91]. Due to these reported effects, a key question is whether the effects of systemically administered NOS inhibitors to block insulin-mediated increases in microvascular perfusion [88] are due to the NOS inhibitor accessing central sites. In the present study L-NAME was administered locally thus eliminating systemic and central effects.

7.6 AMPK Activation Stimulates Microvascular Perfusion by Association with NO

Studies which involved AICAR activation of AMPK were made for two main reasons. AMPK is known to increase NO and is involved in exercise effects. The hypothesis to be tested is whether AMPK activation to increase NO effects microcirculation and enhances the action of insulin.

Previously AMPK has been shown to regulate endothelial function. In conduit arteries AMPK enhances endothelium-dependant vasodilation [235] and increases eNOS phosphorylation at Ser¹¹⁷⁷ [308]. In addition to previous studies, the findings in chapter 5 demonstrate an important role for the vascular smooth muscle sensitisation to NO. AMPK activation by AICAR directly caused vasodilation of skeletal muscle resistance arteries by enhancing NO activity and enhanced microvascular perfusion in skeletal muscle *in vivo*. These findings indicate a link between AMPK activation and vascular NO activity. These findings also highlight an important link between vascular function and metabolism as greater microvascular perfusion, to increase capillary surface area, potentially enhances hormone and nutrient delivery to skeletal muscle.

In summary, AICAR administration *in vivo*, at a dose that did not stimulate glucose uptake by itself, significantly enhanced insulin-stimulated glucose uptake. Low dose AICAR infusion increased microvascular perfusion and further increased insulin-mediated microvascular perfusion. It is likely that increased microvascular perfusion is responsible for the observed potentiation of insulin mediated glucose uptake through increased access of insulin and glucose to myocytes. The ability AICAR to potentiate insulin mediated glucose uptake was greater in white rather than red fiber type skeletal muscle. The present study suggests that AMPK activators such as AICAR may have potential for the treatment of insulin resistance and type 2 diabetes. However the effect of AICAR to stimulate lactate accumulation and the effects on heart rate pose challenges to be overcome before AMPK activators such as AICAR are used as therapeutic agents.

7.7 Other Future Directions

The results outlined in the present thesis confirm microvascular involvement in skeletal muscle glucose metabolism. The stimulation of NO production leading to increases in microvascular perfusion is common to both insulin and AMPK mediated pathways for increased glucose uptake. Previously it has been

demonstrated that insulin-mediated glucose uptake and microvascular perfusions is impaired in insulin resistance, obesity, hypertension and diabetes. Exercise enhances insulin action and part of this mechanism involves AMPK activation. A major finding of this study is that phosphorylation and activation of AMPK enhances microvascular perfusion. A key question which needs to be addressed is can increasing microvascular perfusion reverse impairments in insulin resistance?

The effect of AMPK activation by acute AICAR administration in models of insulin resistance have been investigated using lean and *ob/ob* mice [457] and in *db/db* diabetic mice [458] which resulted in increased glucose disposal. It has also been demonstrated that a single dose of AICAR leads to an improvement in whole body, muscle and liver insulin action in high fat fed rats [318]. In the latter study, it is possible that part of the action of AICAR to improve the insulin response was through increased microvascular perfusion which would be otherwise unresponsive to insulin. The effects of AICAR and insulin on microvascular perfusion and glucose uptake in an insulin resistant model such as the high fat red rat or the obese Zucker rat should be further investigated. Also the effect of chronic AICAR treatment in relation to improved microvascular perfusion and insulin stimulated glucose uptake could be examined.

A recent study demonstrated that NOS inhibition attenuated increases in skeletal muscle glucose uptake during contraction without affecting microvascular perfusion, suggesting that NO is critical for part of the normal increase in skeletal muscle glucose uptake during contraction [409] however AMPK is not the only signalling process involved during exercise. The effects of local NOS inhibition during AICAR infusion *in vivo* should be investigated which may further consolidate the results reported in chapter 5.

7.8 Conclusions

In conclusion, the work presented in this thesis explored a number of possible mechanisms of insulin and AMPK activation extending previous findings of our laboratory. Insulin mediated increases in total flow, microvascular perfusion and glucose uptake were attenuated with both PI3K and NOS inhibition. These results highlight the importance of the haemodynamic effect of insulin for enhancing glucose uptake. The AMPK activator AICAR enhanced NO activity in muscle resistance arteries and markedly increased microvascular perfusion which could enhance hormone and nutrient delivery to the myocyte. AICAR treatment combined with insulin had an additive effect on microvascular perfusion. Insulin-mediated glucose uptake, which predominantly occurred in the white fiber types muscles, was markedly enhanced with AICAR treatment. These results identify AMPK as a potential target for pharmacological interventions for the treatment of impaired vascular function in insulin resistance. Collectively these findings demonstrate an important relationship between microvascular perfusion and glucose uptake.

REFERENCES

1. Saltiel, A.R. and C.R. Kahn, *Insulin signalling and the regulation of glucose and lipid metabolism*. Nature, 2001. **414**(6865): p. 799-806.
2. Clark, M.G., M.G. Wallis, E.J. Barrett, M.A. Vincent, S.M. Richards, L.H. Clerk, and S. Rattigan, *Blood flow and muscle metabolism: a focus on insulin action*. Am J Physiol Endocrinol Metab, 2003. **284**(2): p. E241-58.
3. Klip, A. and M.R. Paquet, *Glucose transport and glucose transporters in muscle and their metabolic regulation*. Diabetes Care, 1990. **13**(3): p. 228-43.
4. Laakso, M., S.V. Edelman, G. Brechtel, and A.D. Baron, *Decreased effect of insulin to stimulate skeletal muscle blood flow in obese man. A novel mechanism for insulin resistance*. J Clin Invest, 1990. **85**(6): p. 1844-52.
5. Baron, A.D. and M.G. Clark, *Role of blood flow in the regulation of muscle glucose uptake*. Annu Rev Nutr, 1997. **17**: p. 487-99.
6. Dela, F., J.J. Larssen, K.J. Mikines, and H. Galbo, *Normal effect of insulin to stimulate leg blood flow in NIDDM*. Diabetes, 1995. **44**: p. 221-226.
7. Anderson, E.A., R.P. Hoffman, T.W. Balon, C.A. Sinkey, and A.L. Mark, *Hyperinsulinemia produces both sympathetic neural activation and vasodilation in normal humans*. Journal of Clinical Investigation, 1991. **87**: p. 2246-2252.
8. Liang, C., J.U. Doherty, R. Faillace, K. Maekawa, S. Arnold, H. Gavras, and W.B. Hood, Jr., *Insulin infusion in conscious dogs. Effects on systemic and coronary hemodynamics, regional blood flows, and plasma catecholamines*. Journal of Clinical Investigation, 1982. **69**(6): p. 1321-1336.
9. DeFronzo, R.A., E. Jacot, E. Jequier, E. Maeder, J. Wahren, and J.P. Felber, *The effect of insulin on the disposal of intravenous glucose. Results from indirect calorimetry and hepatic and femoral venous catheterization*. Diabetes, 1981. **30**(12): p. 1000-7.

-
10. Yki-Jarvinen, H., A.A. Young, C. Lamkin, and J.E. Foley, *Kinetics of glucose disposal in whole body and across the forearm in man*. Journal of Clinical Investigation, 1987. **79**(6): p. 1713-1719.
 11. Jackson, R.A., J.B. Hamling, P.M. Blix, B.M. Sim, M.I. Hawa, J.B. Jaspan, J. Belin, and J.D. abarro, *The influence of graded hyperglycemia with and without physiological hyperinsulinemia on forearm glucose uptake and other metabolic responses in man*. Journal of Clinical Endocrinology and Metabolism, 1986. **63**(3): p. 594-604.
 12. Kelley, D.E., J.P. Reilly, T. Veneman, and L.J. Mandarino, *Effects of insulin on skeletal muscle glucose storage, oxidation, and glycolysis in humans*. American Journal of Physiology, 1990. **258**: p. E923-E929.
 13. Sakai, K., T. Imaizumi, H. Masaki, and A. Takeshita, *Intra-arterial infusion of insulin attenuates vasoreactivity in human forearm*. Hypertension, 1993. **22**: p. 67-73.
 14. Sjostrand, M., A. Holmang, L. Strindberg, and P. Lonnroth, *Estimations of muscle interstitial insulin, glucose, and lactate in type 2 diabetic subjects*. Am J Physiol Endocrinol Metab, 2000. **279**(5): p. E1097-103.
 15. Nuutila, P., M. Raitakari, H. Laine, O. Kirvela, T. Takala, T. Utriainen, S. Makimattila, O.P. Pitkanen, U. Ruotsalainen, H. Iida, J. Knuuti, and H. Yki-Jarvinen, *Role of blood flow in regulating insulin-stimulated glucose uptake in humans. Studies using bradykinin, [15O]water, and [18F]fluoro-deoxy-glucose and positron emission tomography*. Journal of Clinical Investigation, 1996. **97**(7): p. 1741-1747.
 16. Muller, M., A. Holmang, O.K. Andersson, H.G. Eichler, and P. Lonnroth, *Measurement of interstitial muscle glucose and lactate concentrations during an oral glucose tolerance test*. American Journal of Physiology, 1996. **271**: p. E1003-E1007.
 17. Holmang, A., C. Nilsson, M. Niklasson, B.M. Larsson, and P. Lonroth, *Induction of insulin resistance by glucosamine reduces blood flow but not*
-

- interstitial levels of either glucose or insulin*. Diabetes, 1999. **48**(1): p. 106-111.
18. Natali, A., G. Buzzigoli, S. Taddei, D. Santoro, M. Cerri, R. Pedrinelli, and E. Ferrannini, *Effects of insulin on hemodynamics and metabolism in human forearm*. Diabetes, 1990. **39**: p. 490-500.
 19. Natali, A., D. Santoro, C. Palombo, M. Cerri, S. Ghione, and E. Ferrannini, *Impaired insulin action on skeletal muscle metabolism in essential hypertension*. Hypertension, 1991. **17**: p. 170-178.
 20. Neahring, J.M., K. Stepniakowski, A.S. Greene, and B.M. Egan, *Insulin does not reduce forearm alpha-vasoreactivity in obese hypertensive or lean normotensive men*. Hypertension, 1993. **22**: p. 584-590.
 21. Tack, C.J.J., A.E.P. Schefman, J.L. Willems, T. Thien, J.A. Lutterman, and P. Smits, *Direct vasodilator effects of physiological hyperinsulinaemia in human skeletal muscle*. European Journal of Clinical Investigation, 1996. **26**(9): p. 772-778.
 22. Cardillo, C., C.M. Kilcoyne, S.S. Nambi, R.O. Cannon, 3rd, M.J. Quon, and J.A. Panza, *Vasodilator response to systemic but not to local hyperinsulinemia in the human forearm*. Hypertension, 1998. **32**(4): p. 740-5.
 23. Hermann, T.S., N. Ihlemann, H. Dominguez, C. Rask-Madsen, L. Kober, and C. Torp-Pedersen, *Prolonged local forearm hyperinsulinemia induces sustained enhancement of nitric oxide-dependent vasodilation in healthy subjects*. Endothelium, 2004. **11**(5-6): p. 231-9.
 24. Yki-Jarvinen, H. and T. Utriainen, *Insulin-induced vasodilatation: physiology or pharmacology?* Diabetologia, 1998. **41**(4): p. 369-379.
 25. Baron, A.D. and G. Brechtel, *Insulin differentially regulates systemic and skeletal muscle vascular resistance*. Am J Physiol, 1993. **265**(1 Pt 1): p. E61-7.

-
26. Laakso, M., S.V. Edelman, G. Brechtel, and A.D. Baron, *Impaired insulin-mediated skeletal muscle blood flow in patients with NIDDM*. Diabetes, 1992. **41**(9): p. 1076-83.
 27. Vincent, M.A., L.H. Clerk, J.R. Lindner, A.L. Klibanov, M.G. Clark, S. Rattigan, and E.J. Barrett, *Microvascular recruitment is an early insulin effect that regulates skeletal muscle glucose uptake in vivo*. Diabetes, 2004. **53**(6): p. 1418-23.
 28. Sweeney, T.E. and I.H. Sarelius, *Arteriolar control of capillary cell flow in striated muscle*. Circ Res, 1989. **64**(1): p. 112-20.
 29. Sweeney, T.E. and I.H. Sarelius, *Arteriolar control of capillary cell flow in striated muscle*. Circulation Research, 1989. **64**: p. 112-120.
 30. Murrant, C.L. and I.H. Sarelius, *Coupling of muscle metabolism and muscle blood flow in capillary units during contraction*. Acta Physiologica Scandinavica, 2000. **168**(4): p. 531-541.
 31. Borgstrom, P., L. Lindbom, K.E. Arfors, and M. Intaglietta, *Beta-adrenergic control of resistance in individual vessels in rabbit tenuissimus muscle*. American Journal of Physiology, 1988. **254**(4 Pt 2): p. H631-H635.
 32. Krogh, A., *The supply of oxygen to the tissues and the regulation of the capillary circulation*. Journal of Physiology, 1919. **52**(6): p. 457-474.
 33. Honig, C.R., C.L. Odoroff, and J.L. Frierson, *Active and passive capillary control in red muscle at rest and in exercise*. American Journal of Physiology, 1982. **243**: p. H196-H206.
 34. Intaglietta, M. and J.F. Gross, *Vasomotion, tissue fluid flow and the formation of lymph*. International Journal of Microcirculation: Clinical and Experimental, 1982. **1**(1): p. 55-65.
 35. Baron, A.D., G. Brechtel-Hook, A. Johnson, J. Cronin, R. Leaming, and H.O. Steinberg, *Effect of perfusion rate on the time course of insulin-*
-

- mediated skeletal muscle glucose uptake*. American Journal of Physiology, 1996. **271**: p. E1067-E1072.
36. Segal, S.S., *Regulation of blood flow in the microcirculation*. Microcirculation, 2005. **12**(1): p. 33-45.
37. Zeng, G.Y. and M.J. Quon, *Insulin-stimulated production of nitric oxide is inhibited by wortmannin - Direct measurement in vascular endothelial cells*. Journal of Clinical Investigation, 1996. **98**(4): p. 894-898.
38. Zeng, G., F.H. Nystrom, L.V. Ravichandran, L.N. Cong, M. Kirby, H. Mostowski, and M.J. Quon, *Roles for insulin receptor, PI3-kinase, and Akt in insulin-signaling pathways related to production of nitric oxide in human vascular endothelial cells*. Circulation, 2000. **101**(13): p. 1539-1545.
39. Vita, J., J. Keaney, and J. Loscalzo, *Endothelial dysfunction in vascular disease*. Vascular Medicine. A Textbook of Vascular Biology and Disease, 1996. **New York: Little Brown**: p. 245-265.
40. Quyyumi, A.A., *Endothelial function in health and disease: new insights into the genesis of cardiovascular disease*. Am J Med, 1998. **105**(1A): p. 32S-39S.
41. Steinberg, H.O., G. Brechtel, A. Johnson, N. Fineberg, and A.D. Baron, *Insulin-mediated skeletal muscle vasodilation is nitric oxide dependent. A novel action of insulin to increase nitric oxide release*. J Clin Invest, 1994. **94**(3): p. 1172-9.
42. Newman, J.M., J.T. Steen, and M.G. Clark, *Vessels supplying septa and tendons as functional shunts in perfused rat hindlimb*. Microvascular Research, 1997. **54**(1): p. 49-57.
43. Clerk, L.H., M.E. Smith, S. Rattigan, and M.G. Clark, *Increased chylomicron triglyceride hydrolysis by connective tissue flow in perfused rat hindlimb. Implications for lipid storage*. Journal of Lipid Research, 2000. **41**(3): p. 329-335.

-
44. Clark, M.G., S. Rattigan, J.M. Newman, and T.P. Eldershaw, *Vascular control of nutrient delivery by flow redistribution within muscle: implications for exercise and post-exercise muscle metabolism*. International Journal of Sports Medicine, 1998. **19**(6): p. 391-400.
 45. Clark, M.G., E.Q. Colquhoun, S. Rattigan, K.A. Dora, T.P. Eldershaw, J.L. Hall, and J. Ye, *Vascular and endocrine control of muscle metabolism*. American Journal of Physiology, 1995. **268**(5 Pt 1): p. E797-E812.
 46. Clark, M.G., E.Q. Colquhoun, S. Rattigan, K.A. Dora, T.P. Eldershaw, J.L. Hall, and J. Ye, *Vascular and endocrine control of muscle metabolism*. Am J Physiol, 1995. **268**(5 Pt 1): p. E797-812.
 47. Newman, J.M., K.A. Dora, S. Rattigan, S.J. Edwards, E.Q. Colquhoun, and M.G. Clark, *Norepinephrine and serotonin vasoconstriction in rat hindlimb control different vascular flow routes*. American Journal of Physiology, 1996. **270**(4 Pt 1): p. E689-E699.
 48. Natali, A., R. Bonadonna, D. Santoro, A.Q. Galvan, S. Baldi, S. Frascerra, C. Palombo, S. Ghione, and E. Ferrannini, *Insulin resistance and vasodilation in essential hypertension. Studies with adenosine*. Journal of Clinical Investigation, 1994. **94**(4): p. 1570-1576.
 49. Rattigan, S., M.G. Clark, and E.J. Barrett, *Hemodynamic actions of insulin in rat skeletal muscle: evidence for capillary recruitment*. Diabetes, 1997. **46**(9): p. 1381-8.
 50. Jarasch, E.D., G. Bruder, and H.W. Heid, *Significance of xanthine oxidase in capillary endothelial cells*. Acta Physiol Scand Suppl, 1986. **548**: p. 39-46.
 51. Parks, D.A. and D.N. Granger, *Xanthine oxidase: biochemistry, distribution and physiology*. Acta Physiol Scand Suppl, 1986. **548**: p. 87-99.
 52. Rattigan, S., G.J. Appleby, K.A. Miller, J.T. Steen, K.A. Dora, E.Q. Colquhoun, and M.G. Clark, *Serotonin inhibition of 1-methylxanthine metabolism parallels its vasoconstrictor activity and inhibition of oxygen uptake in perfused rat hindlimb*. Acta Physiol Scand, 1997. **161**(2): p. 161-9.
-

-
53. Clark, M.G., S. Rattigan, L.H. Clerk, M.A. Vincent, A.D. Clark, J.M. Youd, and J.M. Newman, *Nutritive and non-nutritive blood flow: rest and exercise*. Acta Physiol Scand, 2000. **168**(4): p. 519-30.
54. Youd, J.M., J.M. Newman, M.G. Clark, G.J. Appleby, S. Rattigan, A.C. Tong, and M.A. Vincent, *Increased metabolism of infused 1-methylxanthine by working muscle*. Acta Physiologica Scandinavica, 1999. **166**(4): p. 301-308.
55. Rattigan, S., M.G. Clark, and E.J. Barrett, *Acute vasoconstriction-induced insulin resistance in rat muscle in vivo*. Diabetes, 1999. **48**(3): p. 564-9.
56. Vincent, M.A., L.H. Clerk, J.R. Lindner, W.J. Price, L.A. Jahn, H. Leong-Poi, and E.J. Barrett, *Mixed meal and light exercise each recruit muscle capillaries in healthy humans*. Am J Physiol Endocrinol Metab, 2006. **290**(6): p. E1191-7.
57. Coggins, M., J. Lindner, S. Rattigan, L. Jahn, E. Fasy, S. Kaul, and E. Barrett, *Physiologic hyperinsulinemia enhances human skeletal muscle perfusion by capillary recruitment*. Diabetes, 2001. **50**(12): p. 2682-90.
58. Dawson, D., M.A. Vincent, E.J. Barrett, S. Kaul, A. Clark, H. Leong-Poi, and J.R. Lindner, *Vascular recruitment in skeletal muscle during exercise and hyperinsulinemia assessed by contrast ultrasound*. Am J Physiol Endocrinol Metab, 2002. **282**(3): p. E714-20.
59. Wei, K., E. Le, J.P. Bin, M. Coggins, J. Thorpe, and S. Kaul, *Quantification of renal blood flow with contrast-enhanced ultrasound*. J Am Coll Cardiol, 2001. **37**(4): p. 1135-40.
60. Vincent, M.A., D. Dawson, A.D. Clark, J.R. Lindner, S. Rattigan, M.G. Clark, and E.J. Barrett, *Skeletal muscle microvascular recruitment by physiological hyperinsulinemia precedes increases in total blood flow*. Diabetes, 2002. **51**(1): p. 42-8.
61. Vincent, M.A., Dawson, D., Clark, A. D., Lindner, J. and Barrett, E. J., *Physiologic hyperinsulinemia recruits capillaries in skeletal muscle in vivo*
-

- independent of changes in total muscle blood flow*. Diabetes, 2001. **50**(Suppl 2): p. A334.
62. Clark, M.G., E.J. Barrett, M.G. Wallis, M.A. Vincent, and S. Rattigan, *The microvasculature in insulin resistance and type 2 diabetes*. Semin Vasc Med, 2002. **2**(1): p. 21-31.
63. Zhang, L., M.A. Vincent, S.M. Richards, L.H. Clerk, S. Rattigan, M.G. Clark, and E.J. Barrett, *Insulin sensitivity of muscle capillary recruitment in vivo*. Diabetes, 2004. **53**(2): p. 447-53.
64. Fugmann, A., L. Lind, P.E. Andersson, J. Millgard, A. Hanni, C. Berne, and H. Lithell, *The effect of euglucaemic hyperinsulinaemia on forearm blood flow and glucose uptake in the human forearm*. Acta Diabetol, 1998. **35**(4): p. 203-6.
65. Tack, C.J., A.E. Schefman, J.L. Willems, T. Thien, J.A. Lutterman, and P. Smits, *Direct vasodilator effects of physiological hyperinsulin-aemia in human skeletal muscle*. Eur J Clin Invest, 1996. **26**(9): p. 772-8.
66. Hill, D.J. and R.D. Milner, *Insulin as a growth factor*. Pediatr Res, 1985. **19**(9): p. 879-86.
67. Chen, Y.L. and E.J. Messina, *Dilation of isolated skeletal muscle arterioles by insulin is endothelium dependent and nitric oxide mediated*. American Journal of Physiology, 1996. **270**(6 Pt 2): p. H2120-H2124.
68. Schroeder, C.A., Jr., Y.L. Chen, and E.J. Messina, *Inhibition of NO synthesis or endothelium removal reveals a vasoconstrictor effect of insulin on isolated arterioles*. American Journal of Physiology, 1999. **276**(3 Pt 2): p. H815-H820.
69. Segal, S.S., D.R. Lamb, and C.V. Gisolfi, *Convection, diffusion and mitochondrial utilization of oxygen during exercise*, in *Perspectives in Exercise Science and Sports Medicine Vol. 5: Energy Metabolism in Exercise and Sport*. 1992, Brown & Benchmark. p. 269-344.

-
70. Chen, Y.L., M.S. Wolin, and E.J. Messina, *Evidence for cGMP mediation of skeletal muscle arteriolar dilation to lactate*. J Appl Physiol, 1996. **81**(1): p. 349-54.
71. McKay, M.K. and R.L. Hester, *Role of nitric oxide, adenosine, and ATP-sensitive potassium channels in insulin-induced vasodilation*. Hypertension, 1996. **28**(2): p. 202-208.
72. Trovati, M., P. Massucco, L. Mattiello, C. Costamagna, E. Aldieri, F. Cavalot, G. Anfossi, A. Bosia, and D. Ghigo, *Human vascular smooth muscle cells express a constitutive nitric oxide synthase that insulin rapidly activates, thus increasing guanosine 3':5'-cyclic monophosphate and adenosine 3':5'-cyclic monophosphate concentrations*. Diabetologia, 1999. **42**(7): p. 831-839.
73. Trovati, M., P. Massucco, L. Mattiello, F. Cavalot, E. Mularoni, A. Hahn, and G. Anfossi, *Insulin increases cyclic nucleotide content in human vascular smooth muscle cells: a mechanism potentially involved in insulin-induced modulation of vascular tone*. Diabetologia, 1995. **38**(8): p. 936-41.
74. Kahn, A.M. and T. Song, *Insulin inhibits dog vascular smooth muscle contraction and lowers Ca^{2+} by inhibiting Ca^{2+} influx*. Journal of Nutrition, 1995. **125**: p. 1732S-1737S.
75. Griffith, T.M., D.H. Edwards, M.J. Lewis, A.C. Newby, and A.H. Henderson, *The nature of endothelium-derived vascular relaxant factor*. Nature, 1984. **308**: p. 645-647.
76. Palmer, R.M., D.S. Ashton, and S. Moncada, *Vascular endothelial cells synthesize nitric oxide from L-arginine*. Nature, 1988. **333**: p. 664-665.
77. Stuehr, D.J., *Mammalian nitric oxide synthases*. Biochim Biophys Acta, 1999. **1411**(2-3): p. 217-30.
78. Stuehr, D.J., J. Santolini, Z.Q. Wang, C.C. Wei, and S. Adak, *Update on mechanism and catalytic regulation in the NO synthases*. Journal of Biological Chemistry, 2004. **279**(35): p. 36167-36170.
-

-
79. Brophy, C.M., L. Knoepp, J. Xin, and J.S. Pollock, *Functional expression of NOS 1 in vascular smooth muscle*. Am J Physiol Heart Circ Physiol, 2000. **278**(3): p. H991-7.
 80. Ignarro, L.J., *Endothelium-derived nitric oxide: actions and properties*. FASEB Journal, 1989. **3**(1): p. 31-36.
 81. Palmer, R.M., A.G. Ferrige, and S. Moncada, *Nitric oxide release accounts for the biological activity of endothelium-derived relaxing factor*. Nature, 1987. **327**(6122): p. 524-6.
 82. McDaniel, N.L., X.L. Chen, H.A. Singer, R.A. Murphy, and C.M. Rembold, *Nitrovasodilators relax arterial smooth muscle by decreasing $[Ca^{2+}]_i$ and uncoupling stress from myosin phosphorylation*. American Journal of Physiology, 1992. **263**: p. C461-C467.
 83. Furchgott, R.F., *The role of endothelium in the responses of vascular smooth muscle to drugs*. Annual Review of Pharmacology and Toxicology, 1984. **24**: p. 175-197.
 84. Montagnani, M., H. Chen, V.A. Barr, and M.J. Quon, *Insulin-stimulated activation of eNOS is independent of Ca^{2+} but requires phosphorylation by Akt at Ser(1179)*. J Biol Chem, 2001. **276**(32): p. 30392-8.
 85. Kim, F., B. Gallis, and M.A. Corson, *TNF- α inhibits flow and insulin signaling leading to NO production in aortic endothelial cells*. American Journal of Physiology Cell Physiology, 2001. **280**(5): p. C1057-C1065.
 86. Baron, A.D., J.S. Zhu, S. Marshall, O. Irsula, G. Brechtel, and C. Keech, *Insulin resistance after hypertension induced by the nitric oxide synthesis inhibitor L-NMMA in rats*. Am J Physiol, 1995. **269**(4 Pt 1): p. E709-15.
 87. Roy, D., M. Perreault, and A. Marette, *Insulin stimulation of glucose uptake in skeletal muscles and adipose tissues in vivo is NO dependent*. American Journal of Physiology, 1998. **274**(4 Pt 1): p. E692-E699.
-

-
88. Vincent, M.A., E.J. Barrett, J.R. Lindner, M.G. Clark, and S. Rattigan, *Inhibiting NOS blocks microvascular recruitment and blunts muscle glucose uptake in response to insulin*. Am J Physiol Endocrinol Metab, 2003. **285**(1): p. E123-9.
89. Scherrer, U., D. Randin, P. Vollenweider, L. Vollenweider, and P. Nicod, *Nitric oxide release accounts for insulin's vascular effects in humans*. J Clin Invest, 1994. **94**(6): p. 2511-5.
90. Shankar, R., J.S. Zhu, B. Ladd, D. Henry, H.Q. Shen, and A.D. Baron, *Central nervous system nitric oxide synthase activity regulates insulin secretion and insulin action*. J Clin Invest, 1998. **102**(7): p. 1403-12.
91. Bradley, E.A., K. Willson, D. Choi-Lundberg, M.G. Clark, and S. Ratigan, *Insulin-mediated capillary recruitment in muscle is sensitive to intra-cerebroventricular NOS inhibitor*. Diabetologia, 2008. **51**([Suppl1] S1-S588): p. 627.
92. Iwashita, S., K. Yanagi, N. Ohshima, and M. Suzuki, *Insulin increases blood flow rate in the microvasculature of cremaster muscle of the anesthetized rats*. In Vivo, 2001. **15**(1): p. 11-15.
93. Mahajan, H., C.M. Kolka, J.M. Newman, S. Rattigan, S.M. Richards, and M.G. Clark, *Vascular and metabolic effects of methacholine in relation to insulin action in muscle*. Diabetologia, 2006. **49**(4): p. 713-23.
94. Kahn, C.R., *The molecular mechanism of insulin action*. Annu Rev Med, 1985. **36**: p. 429-51.
95. White, M.F., R. Maron, and C.R. Kahn, *Insulin rapidly stimulates tyrosine phosphorylation of a Mr-185,000 protein in intact cells*. Nature, 1985. **318**: p. 183-186.
96. Nystrom, F.H. and M.J. Quon, *Insulin signalling: metabolic pathways and mechanisms for specificity*. Cell Signal, 1999. **11**(8): p. 563-74.
-

-
97. Kasuga, M., J.A. Hedo, K.M. Yamada, and C.R. Kahn, *The structure of insulin receptor and its subunits. Evidence for multiple nonreduced forms and a 210,000 possible proreceptor*. J Biol Chem, 1982. **257**(17): p. 10392-9.
 98. Patti, M.E. and C.R. Kahn, *The insulin receptor--a critical link in glucose homeostasis and insulin action*. J Basic Clin Physiol Pharmacol, 1998. **9**(2-4): p. 89-109.
 99. Hedo, J.A. and I.A. Simpson, *Internalization of insulin receptors in the isolated rat adipose cell. Demonstration of the vectorial disposition of receptor subunits*. J Biol Chem, 1984. **259**(17): p. 11083-9.
 100. White, M.F., R. Maron, and C.R. Kahn, *Insulin rapidly stimulates tyrosine phosphorylation of a Mr-185,000 protein in intact cells*. Nature, 1985. **318**(6042): p. 183-6.
 101. Kasuga, M., F.A. Karlsson, and C.R. Kahn, *Insulin stimulates the phosphorylation of the 95,000-dalton subunit of its own receptor*. Science, 1982. **215**(4529): p. 185-7.
 102. White, M.F., *IRS proteins and the common path to diabetes*. American Journal of Physiology Endocrinology and Metabolism, 2002. **283**(3): p. E413-E422.
 103. Hayashi, H., Y. Nishioka, S. Kamohara, F. Kanai, K. Ishii, Y. Fukui, F. Shibasaki, T. Takenawa, H. Kido, N. Katsunuma, and et al., *The alpha-type 85-kDa subunit of phosphatidylinositol 3-kinase is phosphorylated at tyrosines 368, 580, and 607 by the insulin receptor*. J Biol Chem, 1993. **268**(10): p. 7107-17.
 104. Shepherd, P.R., B.T. Nave, and K. Siddle, *Insulin stimulation of glycogen synthesis and glycogen synthase activity is blocked by wortmannin and rapamycin in 3T3-L1 adipocytes: evidence for the involvement of phosphoinositide 3-kinase and p70 ribosomal protein-S6 kinase*. Biochem J, 1995. **305** (Pt 1): p. 25-8.
-

-
105. Cheatham, B., C.J. Vlahos, L. Cheatham, L. Wang, J. Blenis, and C.R. Kahn, *Phosphatidylinositol 3-kinase activation is required for insulin stimulation of pp70 S6 kinase, DNA synthesis, and glucose transporter translocation*. Mol Cell Biol, 1994. **14**(7): p. 4902-11.
 106. Stephens, L.R., T.R. Jackson, and P.T. Hawkins, *Agonist-stimulated synthesis of phosphatidylinositol(3,4,5)-trisphosphate: a new intracellular signalling system?* Biochim Biophys Acta, 1993. **1179**(1): p. 27-75.
 107. Fry, M.J., *Structure, regulation and function of phosphoinositide 3-kinases*. Biochim Biophys Acta, 1994. **1226**(3): p. 237-68.
 108. Shibasaki, F., Y. Homma, and T. Takenawa, *Two types of phosphatidylinositol 3-kinase from bovine thymus. Monomer and heterodimer form*. J Biol Chem, 1991. **266**(13): p. 8108-14.
 109. Backer, J.M., M.G. Myers, Jr., S.E. Shoelson, D.J. Chin, X.J. Sun, M. Miralpeix, P. Hu, B. Margolis, E.Y. Skolnik, J. Schlessinger, and et al., *Phosphatidylinositol 3'-kinase is activated by association with IRS-1 during insulin stimulation*. Embo J, 1992. **11**(9): p. 3469-79.
 110. Cantley, L.C., *The phosphoinositide 3-kinase pathway*. Science, 2002. **296**(5573): p. 1655-7.
 111. Pessin, J.E. and A.R. Saltiel, *Signaling pathways in insulin action: molecular targets of insulin resistance*. J Clin Invest, 2000. **106**(2): p. 165-9.
 112. Alessi, D.R., S.R. James, C.P. Downes, A.B. Holmes, P.R. Gaffney, C.B. Reese, and P. Cohen, *Characterization of a 3-phosphoinositide-dependent protein kinase which phosphorylates and activates protein kinase Balpha*. Curr Biol, 1997. **7**(4): p. 261-9.
 113. Vanhaesebroeck, B. and D.R. Alessi, *The PI3K-PDK1 connection: more than just a road to PKB*. Biochem J, 2000. **346 Pt 3**: p. 561-76.
-

-
114. Kahn, B.B. and S.W. Cushman, *Subcellular translocation of glucose transporters: role in insulin action and its perturbation in altered metabolic states*. Diabetes, 1985. **1**: p. 203-227.
115. James, D.E., M. Strube, and M. Mueckler, *Molecular cloning and characterization of an insulin-regulatable glucose transporter*. Nature, 1989. **338**(6210): p. 83-7.
116. Czech, M.P. and S. Corvera, *Signaling mechanisms that regulate glucose transport*. J Biol Chem, 1999. **274**(4): p. 1865-8.
117. Whiteman, E.L., H. Cho, and M.J. Birnbaum, *Role of Akt/protein kinase B in metabolism*. Trends Endocrinol Metab, 2002. **13**(10): p. 444-51.
118. Brancho, D., N. Tanaka, A. Jaeschke, J.J. Ventura, N. Kelkar, Y. Tanaka, M. Kyuuma, T. Takeshita, R.A. Flavell, and R.J. Davis, *Mechanism of p38 MAP kinase activation in vivo*. Genes Dev, 2003. **17**(16): p. 1969-78.
119. Han, J., J.D. Lee, L. Bibbs, and R.J. Ulevitch, *A MAP kinase targeted by endotoxin and hyperosmolarity in mammalian cells*. Science, 1994. **265**(5173): p. 808-11.
120. Ono, K. and J. Han, *The p38 signal transduction pathway: activation and function*. Cell Signal, 2000. **12**(1): p. 1-13.
121. Kyriakis, J.M. and J. Avruch, *Mammalian mitogen-activated protein kinase signal transduction pathways activated by stress and inflammation*. Physiol Rev, 2001. **81**(2): p. 807-69.
122. Zarubin, T. and J. Han, *Activation and signaling of the p38 MAP kinase pathway*. Cell Res, 2005. **15**(1): p. 11-8.
123. Kramer, H.F. and L.J. Goodyear, *Exercise, MAPK, and NF-kappaB signaling in skeletal muscle*. J Appl Physiol, 2007. **103**(1): p. 388-95.
124. Morrison, D.K. and R.J. Davis, *Regulation of MAP kinase signaling modules by scaffold proteins in mammals*. Annu Rev Cell Dev Biol, 2003. **19**: p. 91-118.
-

-
125. Ho, R.C., O. Alcazar, N. Fujii, M.F. Hirshman, and L.J. Goodyear, *p38gamma MAPK regulation of glucose transporter expression and glucose uptake in L6 myotubes and mouse skeletal muscle*. Am J Physiol Regul Integr Comp Physiol, 2004. **286**(2): p. R342-9.
126. Ryder, J.W., R. Fahlman, H. Wallberg-Henriksson, D.R. Alessi, A. Krook, and J.R. Zierath, *Effect of contraction on mitogen-activated protein kinase signal transduction in skeletal muscle. Involvement Of the mitogen- and stress-activated protein kinase 1*. J Biol Chem, 2000. **275**(2): p. 1457-62.
127. Tong, H., W. Chen, R.E. London, E. Murphy, and C. Steenbergen, *Preconditioning enhanced glucose uptake is mediated by p38 MAP kinase not by phosphatidylinositol 3-kinase*. J Biol Chem, 2000. **275**(16): p. 11981-6.
128. Conrad, P.W., R.T. Rust, J. Han, D.E. Millhorn, and D. Beitner-Johnson, *Selective activation of p38alpha and p38gamma by hypoxia. Role in regulation of cyclin D1 by hypoxia in PC12 cells*. J Biol Chem, 1999. **274**(33): p. 23570-6.
129. Lemieux, K., D. Konrad, A. Klip, and A. Marette, *The AMP-activated protein kinase activator AICAR does not induce GLUT4 translocation to transverse tubules but stimulates glucose uptake and p38 mitogen-activated protein kinases alpha and beta in skeletal muscle*. Faseb J, 2003. **17**(12): p. 1658-65.
130. Xi, X., J. Han, and J.Z. Zhang, *Stimulation of glucose transport by AMP-activated protein kinase via activation of p38 mitogen-activated protein kinase*. 2001. **276**(44): p. 41029-41034.
131. Brian, P., P. Curtis, H. Hemming, and G. Norris, *Wortmannin, an antibiotic produced by Penicillium wortmanni*. Trans. Brit. Mycol. Soc., 1957. **40**: p. 365-368.
132. Powis, G., R. Bonjouklian, M.M. Berggren, A. Gallegos, R. Abraham, C. Ashendel, L. Zalkow, W.F. Matter, J. Dodge, G. Grindey, and et al.,
-

-
- Wortmannin, a potent and selective inhibitor of phosphatidylinositol-3-kinase*. Cancer Res, 1994. **54**(9): p. 2419-23.
133. Ui, M., T. Okada, K. Hazeki, and O. Hazeki, *Wortmannin as a unique probe for an intracellular signalling protein, phosphoinositide 3-kinase*. Trends Biochem Sci, 1995. **20**(8): p. 303-7.
134. Stein, R.C., *Prospects for phosphoinositide 3-kinase inhibition as a cancer treatment*. Endocr Relat Cancer, 2001. **8**(3): p. 237-48.
135. Okada, T., Y. Kawano, T. Sakakibara, O. Hazeki, and M. Ui, *Essential role of phosphatidylinositol 3-kinase in insulin-induced glucose transport and antilipolysis in rat adipocytes. Studies with a selective inhibitor wortmannin*. J Biol Chem, 1994. **269**(5): p. 3568-73.
136. Lee, A.D., P.A. Hansen, and J.O. Holloszy, *Wortmannin inhibits insulin-stimulated but not contraction-stimulated glucose transport activity in skeletal muscle*. FEBS Lett, 1995. **361**(1): p. 51-4.
137. Gerich, J.E., *The genetic basis of type 2 diabetes mellitus: impaired insulin secretion versus impaired insulin sensitivity*. Endocr Rev, 1998. **19**(4): p. 491-503.
138. Ferrannini, E., *Insulin resistance versus insulin deficiency in non-insulin-dependent diabetes mellitus: problems and prospects*. Endocr Rev, 1998. **19**(4): p. 477-90.
139. Zimmet, P., K.G. Alberti, and J. Shaw, *Global and societal implications of the diabetes epidemic*. Nature, 2001. **414**(6865): p. 782-7.
140. Ginsberg, H., G. Kimmerling, J.M. Olefsky, and G.M. Reaven, *Demonstration of insulin resistance in untreated adult onset diabetic subjects with fasting hyperglycemia*. J Clin Invest, 1975. **55**(3): p. 454-61.
141. Shaw, J.E. and D.J. Chisholm, *1: Epidemiology and prevention of type 2 diabetes and the metabolic syndrome*. Med J Aust, 2003. **179**(7): p. 379-83.
-

-
142. Wild, S., G. Roglic, A. Green, R. Sicree, and H. King, *Global prevalence of diabetes: estimates for the year 2000 and projections for 2030*. Diabetes Care, 2004. **27**(5): p. 1047-53.
143. Zimmet, P., *Globalization, coca-colonization and the chronic disease epidemic: can the Doomsday scenario be averted?* J Intern Med, 2000. **247**(3): p. 301-10.
144. Dunstan, D.W., P.Z. Zimmet, T.A. Welborn, A.J. Cameron, J. Shaw, M. de Courten, D. Jolley, and D.J. McCarty, *The Australian Diabetes, Obesity and Lifestyle Study (AusDiab)--methods and response rates*. Diabetes Res Clin Pract, 2002. **57**(2): p. 119-29.
145. Caro, J.F., M.K. Sinha, S.M. Raju, O. Ittoop, W.J. Pories, E.G. Flickinger, D. Meelheim, and G.L. Dohm, *Insulin receptor kinase in human skeletal muscle from obese subjects with and without noninsulin dependent diabetes*. J Clin Invest, 1987. **79**(5): p. 1330-7.
146. Dohm, G.L., E.B. Tapscott, W.J. Pories, D.J. Dabbs, E.G. Flickinger, D. Meelheim, T. Fushiki, S.M. Atkinson, C.W. Elton, and J.F. Caro, *An in vitro human muscle preparation suitable for metabolic studies: Decreased insulin stimulation of glucose transport in muscle from morbidly obese and diabetic subjects*. Journal of Clinical Investigation, 1988. **82**: p. 486-494.
147. Shulman, G.I., D.L. Rothman, T. Jue, P. Stein, R.A. DeFronzo, and R.G. Shulman, *Quantitation of muscle glycogen synthesis in normal subjects and subjects with non-insulin-dependent diabetes by ^{13}C nuclear magnetic resonance spectroscopy*. N Engl J Med, 1990. **322**(4): p. 223-8.
148. Crettaz, M., M. Prentki, D. Zaninetti, and B. Jeanrenaud, *Insulin resistance in soleus muscle from obese Zucker rats*. Biochemical Journal, 1980. **186**: p. 525-534.
149. Bjornholm, M., Y. Kawano, M. Lehtihet, and J.R. Zierath, *Insulin receptor substrate-1 phosphorylation and phosphatidylinositol 3-kinase activity in*
-

- skeletal muscle from NIDDM subjects after in vivo insulin stimulation.* Diabetes, 1997. **46**(3): p. 524-7..
150. Marshall, S.M. and A. Flyvbjerg, *Prevention and early detection of vascular complications of diabetes.* Bmj, 2006. **333**(7566): p. 475-80.
 151. Vincent, M.A., M. Montagnani, and M.J. Quon, *Molecular and physiologic actions of insulin related to production of nitric oxide in vascular endothelium.* Current Diabetes Reports, 2003. **3**(4): p. 279-288.
 152. Schalkwijk, C.G. and C.D. Stehouwer, *Vascular complications in diabetes mellitus: the role of endothelial dysfunction.* Clinical Science, 2005. **109**(2): p. 143-159.
 153. Baron, A.D., M. Laakso, G. Brechtel, and S.V. Edelman, *Mechanism of insulin resistance in insulin-dependent diabetes mellitus: a major role for reduced skeletal muscle blood flow.* Journal of Clinical Endocrinology and Metabolism, 1991. **73**: p. 637-643.
 154. Baron, A.D., H. Steinberg, G. Brechtel, and A. Johnson, *Skeletal muscle blood flow independently modulates insulin-mediated glucose uptake.* American Journal of Physiology, 1994. **266**(2 Pt 1): p. E248-E253.
 155. James, D.E., K.M. Burleigh, L.H. Storlien, S.P. Bennett, and E.W. Kraegen, *Heterogeneity of insulin action in muscle: influence of blood flow.* American Journal of Physiology, 1986. **251**: p. E422-E430.
 156. Laakso, M., S.V. Edelman, G. Brechtel, and A.D. Baron, *Impaired insulin-mediated skeletal muscle blood flow in patients with NIDDM.* Diabetes, 1992. **41**: p. 1076-1083.
 157. McAuley, D.F., A.G. Nugent, C. McGurk, S. Maguire, J.R. Hayes, and G.D. Johnston, *Vasoconstriction to endogenous endothelin-1 is impaired in patients with Type II diabetes mellitus.* Clinical Science, 2000. **99**(3): p. 175-179.

-
158. Dela, F., J.J. Larsen, K.J. Mikines, and H. Galbo, *Normal effect of insulin to stimulate leg blood flow in NIDDM*. Diabetes, 1995. **44**(2): p. 221-6.
159. Francesconi, M., C. Koizar, and T.C. Wascher, *Postprandial impairment of resistance vessel function in insulin treated patients with diabetes mellitus type-2*. Clinical Physiology, 2001. **21**(3): p. 300-307.
160. Tack, C.J.J., P. Smits, J.J. Willemsen, J.W.M. Lenders, T. Thien, and J.A. Lutterman, *Effects of insulin on vascular tone and sympathetic nervous system in NIDDM*. Diabetes, 1996. **45**: p. 15-22.
161. Utriainen, T., P. Nuutila, T. Takala, P. Vicini, U. Ruotsalainen, T. Ronnema, T. Tolvanen, M. Raitakari, M. Haaparanta, O. Kirvela, C. Cobelli, and H. Yki-Jarvinen, *Intact insulin stimulation of skeletal muscle blood flow, its heterogeneity and redistribution, but not of glucose uptake in non-insulin-dependent diabetes mellitus*. Journal of Clinical Investigation, 1997. **100**(4): p. 777-785.
162. Williams, S.B., J.A. Cusco, M.A. Roddy, M.T. Johnstone, and M.A. Creager, *Impaired nitric oxide-mediated vasodilation in patients with non-insulin-dependent diabetes mellitus*. Journal of the American College of Cardiology, 1996. **27**(3): p. 567-574.
163. Clark, M.G., M.G. Wallis, E.J. Barrett, M.A. Vincent, S.M. Richards, L.H. Clerk, and S. Rattigan, *Blood flow and muscle metabolism: a focus on insulin action*. American Journal of Physiology Endocrinology and Metabolism, 2003. **284**(2): p. E241-E258.
164. Wallis, M.G., C.M. Wheatley, S. Rattigan, E.J. Barrett, A.D. Clark, and M.G. Clark, *Insulin-mediated hemodynamic changes are impaired in muscle of Zucker obese rats*. Diabetes, 2002. **51**(12): p. 3492-3498.
165. Clerk, L.H., M.A. Vincent, L.A. Jahn, Z. Liu, J.R. Lindner, and E.J. Barrett, *Obesity blunts insulin-mediated microvascular recruitment in human forearm muscle*. Diabetes, 2006. **55**(5): p. 1436-42.
-

-
166. Rattigan, S., K.A. Dora, E.Q. Colquhoun, and M.G. Clark, *Serotonin-mediated acute insulin resistance in the perfused rat hindlimb but not in incubated muscle: a role for the vascular system*. Life Sciences, 1993. **53**(20): p. 1545-1555.
167. Youd, J.M., S. Rattigan, and M.G. Clark, *Acute impairment of insulin-mediated capillary recruitment and glucose uptake in rat skeletal muscle in vivo by TNF α* . Diabetes, 2000. **49**(11): p. 1904-1909.
168. Clerk, L.H., S. Rattigan, and M.G. Clark, *Lipid infusion impairs physiologic insulin-mediated capillary recruitment and muscle glucose uptake in vivo*. Diabetes, 2002. **51**(4): p. 1138-1145.
169. Ploug, T., H. Galbo, and E.A. Richter, *Increased muscle glucose uptake during contractions: no need for insulin*. Am J Physiol, 1984. **247**(6 Pt 1): p. E726-31.
170. Wallberg-Henriksson, H. and J.O. Holloszy, *Contractile activity increases glucose uptake by muscle in severely diabetic rats*. J Appl Physiol, 1984. **57**(4): p. 1045-9.
171. Douen, A.G., T. Ramlal, A. Klip, D.A. Young, G.D. Cartee, and J.O. Holloszy, *Exercise-induced increase in glucose transporters in plasma membranes of rat skeletal muscle*. Endocrinology, 1989. **124**: p. 449-454.
172. Goodyear, L.J. and B.B. Kahn, *Exercise, glucose transport, and insulin sensitivity*. Annu Rev Med, 1998. **49**: p. 235-61.
173. Richter, E.A., W. Derave, and J.F. Wojtaszewski, *Glucose, exercise and insulin: emerging concepts*. Journal of Physiology, 2001. **535**(Pt 2): p. 313-322.
174. Holloszy, J.O., *Exercise-induced increase in muscle insulin sensitivity*. J Appl Physiol, 2005. **99**(1): p. 338-43.
-

-
175. DeFronzo, R.A., E. Ferrannini, Y. Sato, P. Felig, and J. Wahren, *Synergistic interaction between exercise and insulin on peripheral glucose uptake*. J Clin Invest, 1981. **68**(6): p. 1468-74.
176. Sakamoto, K. and L.J. Goodyear, *Invited review: intracellular signaling in contracting skeletal muscle*. J Appl Physiol, 2002. **93**(1): p. 369-83.
177. Hayashi, T., M.F. Hirshman, E.J. Kurth, W.W. Winder, and L.J. Goodyear, *Evidence for 5' AMP-activated protein kinase mediation of the effect of muscle contraction on glucose transport*. Diabetes, 1998. **47**(8): p. 1369-73.
178. Goodyear, L.J. and B.B. Kahn, *Exercise, glucose transport, and insulin sensitivity*. Annual Review of Medicine, 1998. **49**: p. 235-261.
179. Kelley, D.E. and B.H. Goodpaster, *Effects of exercise on glucose homeostasis in Type 2 diabetes mellitus*. Med Sci Sports Exerc, 2001. **33**(6 Suppl): p. S495-501; discussion S528-9.
180. Pan, X.R., G.W. Li, Y.H. Hu, J.X. Wang, W.Y. Yang, Z.X. An, Z.X. Hu, J. Lin, J.Z. Xiao, H.B. Cao, P.A. Liu, X.G. Jiang, Y.Y. Jiang, J.P. Wang, H. Zheng, H. Zhang, P.H. Bennett, and B.V. Howard, *Effects of diet and exercise in preventing NIDDM in people with impaired glucose tolerance. The Da Qing IGT and Diabetes Study*. Diabetes Care, 1997. **20**(4): p. 537-44.
181. Devlin, J.T. and E.S. Horton, *Effects of prior high-intensity exercise on glucose metabolism in normal and insulin-resistant men*. Diabetes, 1985. **34**(10): p. 973-9.
182. Oakes, N.D., K.S. Bell, S.M. Furler, S. Camilleri, A.K. Saha, N.B. Ruderman, D.J. Chisholm, and E.W. Kraegen, *Diet-induced muscle insulin resistance in rats is ameliorated by acute dietary lipid withdrawal or a single bout of exercise: parallel relationship between insulin stimulation of glucose uptake and suppression of long-chain fatty acyl-CoA*. Diabetes, 1997. **46**(12): p. 2022-8.
-

-
183. Padwal, R., S.R. Majumdar, J.A. Johnson, J. Varney, and F.A. McAlister, *A systematic review of drug therapy to delay or prevent type 2 diabetes*. Diabetes Care, 2005. **28**(3): p. 736-44.
184. Kennedy, J.W., M.F. Hirshman, E.V. Gervino, J.V. Ocel, R.A. Forse, S.J. Hoenig, D. Aronson, L.J. Goodyear, and E.S. Horton, *Acute exercise induces GLUT4 translocation in skeletal muscle of normal human subjects and subjects with type 2 diabetes*. Diabetes, 1999. **48**(5): p. 1192-1197.
185. Devlin, J.T., M. Hirshman, E.D. Horton, and E.S. Horton, *Enhanced peripheral and splanchnic insulin sensitivity in NIDDM men after single bout of exercise*. Diabetes, 1987. **36**(4): p. 434-9.
186. Mikines, K.J., B. Sonne, P.A. Farrell, B. Tronier, and H. Galbo, *Effect of physical exercise on sensitivity and responsiveness to insulin in humans*. Am J Physiol, 1988. **254**(3 Pt 1): p. E248-59.
187. Perseghin, G., T.B. Price, K.F. Petersen, M. Roden, G.W. Cline, K. Gerow, D.L. Rothman, and G.I. Shulman, *Increased glucose transport-phosphorylation and muscle glycogen synthesis after exercise training in insulin-resistant subjects*. N Engl J Med, 1996. **335**(18): p. 1357-62.
188. Wojtaszewski, J.F., J.N. Nielsen, and E.A. Richter, *Invited review: effect of acute exercise on insulin signaling and action in humans*. J Appl Physiol, 2002. **93**(1): p. 384-92.
189. Cartee, G.D., D.A. Young, M.D. Sleeper, J. Zierath, H. Wallberg-Henriksson, and J.O. Holloszy, *Prolonged increase in insulin-stimulated glucose transport in muscle after exercise*. American Journal of Physiology, 1989. **256**(4 Pt 1): p. E494-E499.
190. Borghouts, L.B. and H.A. Keizer, *Exercise and insulin sensitivity: a review*. International Journal of Sports Medicine, 2000. **21**(1): p. 1-12.
191. Richter, E.A., L.P. Garetto, M.N. Goodman, and N.B. Ruderman, *Enhanced muscle glucose metabolism after exercise: Modulation by local factors*. American Journal of Physiology, 1984. **246**: p. E476-E482.
-

-
192. Richter, E.A., K.J. Mikines, H. Galbo, and B. Kiens, *Effect of exercise on insulin action in human skeletal muscle*. Journal of Applied Physiology, 1989. **66**: p. 876-885.
 193. Zierath, J.R., *Invited review: Exercise training-induced changes in insulin signaling in skeletal muscle*. Journal of Applied Physiology, 2002. **93**(2): p. 773-781.
 194. Borghouts, L.B. and H.A. Keizer, *Exercise and insulin sensitivity: a review*. Int J Sports Med, 2000. **21**(1): p. 1-12.
 195. Colberg, S.R., J.M. Hagberg, S.D. McCole, J.M. Zmuda, P.D. Thompson, and D.E. Kelley, *Utilization of glycogen but not plasma glucose is reduced in individuals with NIDDM during mild-intensity exercise*. Journal of Applied Physiology, 1996. **81**: p. 2027-2033.
 196. Giacca, A., Y. Groenewoud, E. Tsui, P. McClean, and B. Zinman, *Glucose production, utilization, and cycling in response to moderate exercise in obese subjects with type 2 diabetes and mild hyperglycemia*. Diabetes, 1998. **47**(11): p. 1763-70.
 197. Dela, F., J.J. Larsen, K.J. Mikines, T. Ploug, L.N. Petersen, and H. Galbo, *Insulin-stimulated muscle glucose clearance in patients with NIDDM - Effects of one-legged physical training*. Diabetes, 1995. **44**: p. 1010-1020.
 198. Soman, V.R., V.A. Koivisto, D. Deibert, P. Felig, and R.A. DeFronzo, *Increased insulin sensitivity and insulin binding to monocytes after physical training*. N Engl J Med, 1979. **301**(22): p. 1200-4.
 199. Hudlicka, O., *Regulation of muscle blood flow*. Clinical Physiology, 1985. **5**(3): p. 201-229.
 200. Honig, C.R., C.L. Odoroff, and J.L. Frierson, *Active and passive capillary control in red muscle at rest and in exercise*. Am J Physiol, 1982. **243**(2): p. H196-206.
-

-
201. Ivy, J.L., *Role of exercise training in the prevention and treatment of insulin resistance and non-insulin-dependent diabetes mellitus*. Sports Medicine, 1997. **24**(5): p. 321-336.
202. Andersen, P. and J. Henriksson, *Capillary supply of the quadriceps femoris muscle of man: adaptive response to exercise*. Journal of Physiology, 1977. **270**(3): p. 677-690.
203. Hepple, R.T., S.L. Mackinnon, J.M. Goodman, S.G. Thomas, and M.J. Plyley, *Resistance and aerobic training in older men: effects on VO_{2peak} and the capillary supply to skeletal muscle*. Journal of Applied Physiology, 1997. **82**(4): p. 1305-1310.
204. Gute, D., C. Fraga, M.H. Laughlin, and J.F. Amann, *Regional changes in capillary supply in skeletal muscle of high-intensity endurance-trained rats*. Journal of Applied Physiology, 1996. **81**: p. 619-626.
205. Rattigan, S., M.G. Wallis, J.M. Youd, and M.G. Clark, *Exercise training improves insulin-mediated capillary recruitment in association with glucose uptake in rat hindlimb*. Diabetes, 2001. **50**(12): p. 2659-65.
206. Carlson, C.A. and K.H. Kim, *Regulation of hepatic acetyl coenzyme A carboxylase by phosphorylation and dephosphorylation*. J Biol Chem, 1973. **248**(1): p. 378-80.
207. Beg, Z.H., D.W. Allmann, and D.M. Gibson, *Modulation of 3-hydroxy-3-methylglutaryl coenzyme A reductase activity with cAMP and with protein fractions of rat liver cytosol*. Biochem Biophys Res Commun, 1973. **54**(4): p. 1362-9.
208. Yeh, L.A., K.H. Lee, and K.H. Kim, *Regulation of rat liver acetyl-CoA carboxylase. Regulation of phosphorylation and inactivation of acetyl-CoA carboxylase by the adenylate energy charge*. J Biol Chem, 1980. **255**(6): p. 2308-14.
209. Ferrer, A., C. Caelles, N. Massot, and F.G. Hegardt, *Activation of rat liver cytosolic 3-hydroxy-3-methylglutaryl coenzyme A reductase kinase by*
-

- adenosine 5'-monophosphate*. Biochem Biophys Res Commun, 1985. **132**(2): p. 497-504.
210. Carling, D., V.A. Zammit, and D.G. Hardie, *A common bicyclic protein kinase cascade inactivates the regulatory enzymes of fatty acid and cholesterol biosynthesis*. FEBS Lett, 1987. **223**(2): p. 217-22.
211. Sim, A.T. and D.G. Hardie, *The low activity of acetyl-CoA carboxylase in basal and glucagon-stimulated hepatocytes is due to phosphorylation by the AMP-activated protein kinase and not cyclic AMP-dependent protein kinase*. FEBS Lett, 1988. **233**(2): p. 294-8.
212. Mitchelhill, K.I., D. Stapleton, G. Gao, C. House, B. Michell, F. Katsis, L.A. Witters, and B.E. Kemp, *Mammalian AMP-activated protein kinase shares structural and functional homology with the catalytic domain of yeast Snf1 protein kinase*. J Biol Chem, 1994. **269**(4): p. 2361-4.
213. Stapleton, D., G. Gao, B.J. Michell, J. Widmer, K. Mitchelhill, T. Teh, C.M. House, L.A. Witters, and B.E. Kemp, *Mammalian 5'-AMP-activated protein kinase non-catalytic subunits are homologs of proteins that interact with yeast Snf1 protein kinase*. J Biol Chem, 1994. **269**(47): p. 29343-6.
214. Carling, D., K. Aguan, A. Woods, A.J. Verhoeven, R.K. Beri, C.H. Brennan, C. Sidebottom, M.D. Davison, and J. Scott, *Mammalian AMP-activated protein kinase is homologous to yeast and plant protein kinases involved in the regulation of carbon metabolism*. J Biol Chem, 1994. **269**(15): p. 11442-8.
215. Gao, G., J. Widmer, D. Stapleton, T. Teh, T. Cox, B.E. Kemp, and L.A. Witters, *Catalytic subunits of the porcine and rat 5'-AMP-activated protein kinase are members of the SNF1 protein kinase family*. Biochim Biophys Acta, 1995. **1266**(1): p. 73-82.
216. Hanks, S.K. and T. Hunter, *Protein kinases 6. The eukaryotic protein kinase superfamily: kinase (catalytic) domain structure and classification*. Faseb J, 1995. **9**(8): p. 576-96.

-
217. Hardie, D.G., D. Carling, and M. Carlson, *The AMP-activated/SNF1 protein kinase subfamily: metabolic sensors of the eukaryotic cell?* Annu Rev Biochem, 1998. **67**: p. 821-55.
218. Rutter, G.A., G. Da Silva Xavier, and I. Leclerc, *Roles of 5'-AMP-activated protein kinase (AMPK) in mammalian glucose homoeostasis.* Biochem J, 2003. **375**(Pt 1): p. 1-16.
219. Winder, W.W. and D.G. Hardie, *AMP-activated protein kinase, a metabolic master switch: possible roles in type 2 diabetes.* 1999. **277**(1 Pt 1): p. E1-10.
220. Hardie, D.G., J.W. Scott, D.A. Pan, and E.R. Hudson, *Management of cellular energy by the AMP-activated protein kinase system.* FEBS Lett, 2003. **546**(1): p. 113-20.
221. Carling, D., *The AMP-activated protein kinase cascade--a unifying system for energy control.* Trends Biochem Sci, 2004. **29**(1): p. 18-24.
222. Kemp, B.E., K.I. Mitchelhill, D. Stapleton, B.J. Michell, Z.P. Chen, and L.A. Witters, *Dealing with energy demand: the AMP-activated protein kinase.* Trends Biochem Sci, 1999. **24**(1): p. 22-5.
223. Woods, A., P.C. Cheung, F.C. Smith, M.D. Davison, J. Scott, R.K. Beri, and D. Carling, *Characterization of AMP-activated protein kinase beta and gamma subunits. Assembly of the heterotrimeric complex in vitro.* J Biol Chem, 1996. **271**(17): p. 10282-90.
224. Davies, S.P., S.A. Hawley, A. Woods, D. Carling, T.A. Haystead, and D.G. Hardie, *Purification of the AMP-activated protein kinase on ATP-gamma-sepharose and analysis of its subunit structure.* Eur J Biochem, 1994. **223**(2): p. 351-7.
225. Dyck, J.R., G. Gao, J. Widmer, D. Stapleton, C.S. Fernandez, B.E. Kemp, and L.A. Witters, *Regulation of 5'-AMP-activated protein kinase activity by the noncatalytic beta and gamma subunits.* J Biol Chem, 1996. **271**(30): p. 17798-803.
-

-
226. Hardie, D.G., *Minireview: the AMP-activated protein kinase cascade: the key sensor of cellular energy status*. *Endocrinology*, 2003. **144**(12): p. 5179-83.
227. Woods, A., I. Salt, J. Scott, D.G. Hardie, and D. Carling, *The alpha1 and alpha2 isoforms of the AMP-activated protein kinase have similar activities in rat liver but exhibit differences in substrate specificity in vitro*. *FEBS Lett*, 1996. **397**(2-3): p. 347-51.
228. Cheung, P.C., I.P. Salt, S.P. Davies, D.G. Hardie, and D. Carling, *Characterization of AMP-activated protein kinase gamma-subunit isoforms and their role in AMP binding*. *Biochem J*, 2000. **346 Pt 3**: p. 659-69.
229. Thornton, C., M.A. Snowden, and D. Carling, *Identification of a novel AMP-activated protein kinase beta subunit isoform that is highly expressed in skeletal muscle*. *J Biol Chem*, 1998. **273**(20): p. 12443-50.
230. Hardie, D.G. and D. Carling, *The AMP-activated protein kinase--fuel gauge of the mammalian cell?* *Eur J Biochem*, 1997. **246**(2): p. 259-73.
231. Stapleton, D., K.I. Mitchelhill, G. Gao, J. Widmer, B.J. Michell, T. Teh, C.M. House, C.S. Fernandez, T. Cox, L.A. Witters, and B.E. Kemp, *Mammalian AMP-activated protein kinase subfamily*. *J Biol Chem*, 1996. **271**(2): p. 611-4.
232. Daval, M., F. Diot-Dupuy, R. Bazin, I. Hainault, B. Viollet, S. Vaulont, E. Hajdouch, P. Ferre, and F. Foufelle, *Anti-lipolytic action of AMP-activated protein kinase in rodent adipocytes*. *J Biol Chem*, 2005. **280**(26): p. 25250-7.
233. Woods, A., D. Azzout-Marniche, M. Foretz, S.C. Stein, P. Lemarchand, P. Ferre, F. Foufelle, and D. Carling, *Characterization of the role of AMP-activated protein kinase in the regulation of glucose-activated gene expression using constitutively active and dominant negative forms of the kinase*. *Mol Cell Biol*, 2000. **20**(18): p. 6704-11.
234. Evans, A.M., D.G. Hardie, A. Galione, C. Peers, P. Kumar, and C.N. Wyatt, *AMP-activated protein kinase couples mitochondrial inhibition by hypoxia to*
-

- cell-specific Ca²⁺ signalling mechanisms in oxygen-sensing cells*. Novartis Found Symp, 2006. **272**: p. 234-52; discussion 252-8, 274-9.
235. Davis, B.J., Z. Xie, B. Viollet, and M.H. Zou, *Activation of the AMP-activated kinase by antidiabetes drug metformin stimulates nitric oxide synthesis in vivo by promoting the association of heat shock protein 90 and endothelial nitric oxide synthase*. Diabetes, 2006. **55**(2): p. 496-505.
236. Zou, M.H., S.S. Kirkpatrick, B.J. Davis, J.S. Nelson, W.G.t. Wiles, U. Schlattner, D. Neumann, M. Brownlee, M.B. Freeman, and M.H. Goldman, *Activation of the AMP-activated protein kinase by the anti-diabetic drug metformin in vivo. Role of mitochondrial reactive nitrogen species*. J Biol Chem, 2004. **279**(42): p. 43940-51.
237. Crute, B.E., K. Seefeld, J. Gamble, B.E. Kemp, and L.A. Witters, *Functional domains of the alpha catalytic subunit of the AMP-activated protein kinase*. J Biol Chem, 1998. **273**(52): p. 35347-54.
238. Carling, D. and D.G. Hardie, *The substrate and sequence specificity of the AMP-activated protein kinase. Phosphorylation of glycogen synthase and phosphorylase kinase*. Biochim Biophys Acta, 1989. **1012**(1): p. 81-6.
239. Wojtaszewski, J.F., S.B. Jorgensen, Y. Hellsten, D.G. Hardie, and E.A. Richter, *Glycogen-dependent effects of 5-aminoimidazole-4-carboxamide (AICA)-riboside on AMP-activated protein kinase and glycogen synthase activities in rat skeletal muscle*. Diabetes, 2002. **51**(2): p. 284-92.
240. Hudson, E.R., D.A. Pan, J. James, J.M. Lucocq, S.A. Hawley, K.A. Green, O. Baba, T. Terashima, and D.G. Hardie, *A novel domain in AMP-activated protein kinase causes glycogen storage bodies similar to those seen in hereditary cardiac arrhythmias*. Curr Biol, 2003. **13**(10): p. 861-6.
241. Polekhina, G., A. Gupta, B.J. Michell, B. van Denderen, S. Murthy, S.C. Feil, I.G. Jennings, D.J. Campbell, L.A. Witters, M.W. Parker, B.E. Kemp, and D. Stapleton, *AMPK beta subunit targets metabolic stress sensing to glycogen*. Curr Biol, 2003. **13**(10): p. 867-71.

-
242. Chen, Z., J. Heierhorst, R.J. Mann, K.I. Mitchelhill, B.J. Michell, L.A. Witters, G.S. Lynch, B.E. Kemp, and D. Stapleton, *Expression of the AMP-activated protein kinase beta1 and beta2 subunits in skeletal muscle*. FEBS Lett, 1999. **460**(2): p. 343-8.
243. Gao, G., C.S. Fernandez, D. Stapleton, A.S. Auster, J. Widmer, J.R. Dyck, B.E. Kemp, and L.A. Witters, *Non-catalytic beta- and gamma-subunit isoforms of the 5'-AMP-activated protein kinase*. J Biol Chem, 1996. **271**(15): p. 8675-81.
244. Mahlapuu, M., C. Johansson, K. Lindgren, G. Hjalml, B.R. Barnes, A. Krook, J.R. Zierath, L. Andersson, and S. Marklund, *Expression profiling of the gamma-subunit isoforms of AMP-activated protein kinase suggests a major role for gamma3 in white skeletal muscle*. Am J Physiol Endocrinol Metab, 2004. **286**(2): p. E194-200.
245. Kahn, B.B., T. Alquier, D. Carling, and D.G. Hardie, *AMP-activated protein kinase: ancient energy gauge provides clues to modern understanding of metabolism*. Cell Metab, 2005. **1**(1): p. 15-25.
246. Hardie, D.G., I.P. Salt, S.A. Hawley, and S.P. Davies, *AMP-activated protein kinase: an ultrasensitive system for monitoring cellular energy charge*. Biochem J, 1999. **338** (Pt 3): p. 717-22.
247. Woods, A., S.R. Johnstone, K. Dickerson, F.C. Leiper, L.G. Fryer, D. Neumann, U. Schlattner, T. Wallimann, M. Carlson, and D. Carling, *LKB1 is the upstream kinase in the AMP-activated protein kinase cascade*. Curr Biol, 2003. **13**(22): p. 2004-8.
248. Hawley, S.A., J. Boudeau, J.L. Reid, K.J. Mustard, L. Udd, T.P. Makela, D.R. Alessi, and D.G. Hardie, *Complexes between the LKB1 tumor suppressor, STRAD alpha/beta and MO25 alpha/beta are upstream kinases in the AMP-activated protein kinase cascade*. J Biol, 2003. **2**(4): p. 28.
249. Hurley, R.L., K.A. Anderson, J.M. Franzone, B.E. Kemp, A.R. Means, and L.A. Witters, *The Ca²⁺/calmodulin-dependent protein kinase kinases are*
-

- AMP-activated protein kinase kinases*. J Biol Chem, 2005. **280**(32): p. 29060-6.
250. Soltoff, S.P., *Evidence that tyrphostins AG10 and AG18 are mitochondrial uncouplers that alter phosphorylation-dependent cell signaling*. J Biol Chem, 2004. **279**(12): p. 10910-8.
251. Uotani, S., T. Abe, and Y. Yamaguchi, *Leptin activates AMP-activated protein kinase in hepatic cells via a JAK2-dependent pathway*. Biochem Biophys Res Commun, 2006. **351**(1): p. 171-5.
252. Kubota, N., W. Yano, T. Kubota, T. Yamauchi, S. Itoh, H. Kumagai, H. Kozono, I. Takamoto, S. Okamoto, T. Shiuchi, R. Suzuki, H. Satoh, A. Tsuchida, M. Moroi, K. Sugi, T. Noda, H. Ebinuma, Y. Ueta, T. Kondo, E. Araki, O. Ezaki, R. Nagai, K. Tobe, Y. Terauchi, K. Ueki, Y. Minokoshi, and T. Kadowaki, *Adiponectin stimulates AMP-activated protein kinase in the hypothalamus and increases food intake*. Cell Metab, 2007. **6**(1): p. 55-68.
253. Cammisotto, P.G. and M. Bendayan, *Adiponectin stimulates phosphorylation of AMP-activated protein kinase alpha in renal glomeruli*. J Mol Histol, 2008. **39**(6): p. 579-84.
254. Hutchinson, D.S., E. Chernogubova, O.S. Dallner, B. Cannon, and T. Bengtsson, *Beta-adrenoceptors, but not alpha-adrenoceptors, stimulate AMP-activated protein kinase in brown adipocytes independently of uncoupling protein-1*. Diabetologia, 2005. **48**(11): p. 2386-95.
255. Winder, W.W., *Energy-sensing and signaling by AMP-activated protein kinase in skeletal muscle*. J Appl Physiol, 2001. **91**(3): p. 1017-28.
256. Winder, W.W. and D.G. Hardie, *Inactivation of acetyl-CoA carboxylase and activation of AMP-activated protein kinase in muscle during exercise*. Am J Physiol, 1996. **270**(2 Pt 1): p. E299-304.
257. Hutber, C.A., D.G. Hardie, and W.W. Winder, *Electrical stimulation inactivates muscle acetyl-CoA carboxylase and increases AMP-activated protein kinase*. Am J Physiol, 1997. **272**(2 Pt 1): p. E262-6.

-
258. Vavvas, D., A. Apazidis, A.K. Saha, J. Gamble, A. Patel, B.E. Kemp, L.A. Witters, and N.B. Ruderman, *Contraction-induced changes in acetyl-CoA carboxylase and 5'-AMP-activated kinase in skeletal muscle*. J Biol Chem, 1997. **272**(20): p. 13255-61.
259. Ihlemann, J., T. Ploug, Y. Hellsten, and H. Galbo, *Effect of tension on contraction-induced glucose transport in rat skeletal muscle*. American Journal of Physiology, 1999. **277**(2 Pt 1): p. E208-E214.
260. Musi, N., T. Hayashi, N. Fujii, M.F. Hirshman, L.A. Witters, and L.J. Goodyear, *AMP-activated protein kinase activity and glucose uptake in rat skeletal muscle*. Am J Physiol Endocrinol Metab, 2001. **280**(5): p. E677-84.
261. Derave, W., H. Ai, J. Ihlemann, L.A. Witters, S. Kristiansen, E.A. Richter, and T. Ploug, *Dissociation of AMP-activated protein kinase activation and glucose transport in contracting slow-twitch muscle*. Diabetes, 2000. **49**(8): p. 1281-7.
262. Rasmussen, B.B. and W.W. Winder, *Effect of exercise intensity on skeletal muscle malonyl-CoA and acetyl-CoA carboxylase*. J Appl Physiol, 1997. **83**(4): p. 1104-9.
263. Fujii, N., T. Hayashi, M.F. Hirshman, J.T. Smith, S.A. Habinowski, L. Kaijser, J. Mu, O. Ljungqvist, M.J. Birnbaum, L.A. Witters, A. Thorell, and L.J. Goodyear, *Exercise induces isoform-specific increase in 5'AMP-activated protein kinase activity in human skeletal muscle*. Biochem Biophys Res Commun, 2000. **273**(3): p. 1150-5.
264. Wojtaszewski, J.F., P. Nielsen, B.F. Hansen, E.A. Richter, and B. Kiens, *Isoform-specific and exercise intensity-dependent activation of 5'-AMP-activated protein kinase in human skeletal muscle*. J Physiol, 2000. **528 Pt 1**: p. 221-6.
265. Chen, Z.P., G.K. McConell, B.J. Michell, R.J. Snow, B.J. Canny, and B.E. Kemp, *AMPK signaling in contracting human skeletal muscle: acetyl-CoA*
-

- carboxylase and NO synthase phosphorylation*. Am J Physiol Endocrinol Metab, 2000. **279**(5): p. E1202-6.
266. Musi, N., N. Fujii, M.F. Hirshman, I. Ekberg, S. Froberg, O. Ljungqvist, A. Thorell, and L.J. Goodyear, *AMP-activated protein kinase (AMPK) is activated in muscle of subjects with type 2 diabetes during exercise*. 2001. **50**(5): p. 921-927.
267. Corton, J.M., J.G. Gillespie, S.A. Hawley, and D.G. Hardie, *5-aminoimidazole-4-carboxamide ribonucleoside. A specific method for activating AMP-activated protein kinase in intact cells?* Eur J Biochem, 1995. **229**(2): p. 558-65.
268. Henin, N., M.F. Vincent, and G. Van den Berghe, *Stimulation of rat liver AMP-activated protein kinase by AMP analogues*. Biochim Biophys Acta, 1996. **1290**(2): p. 197-203.
269. Merrill, G.F., E.J. Kurth, D.G. Hardie, and W.W. Winder, *AICA riboside increases AMP-activated protein kinase, fatty acid oxidation, and glucose uptake in rat muscle*. 1997. **273**(6 Pt 1): p. E1107-E1112.
270. Sabina, R.L., D. Patterson, and E.W. Holmes, *5-Amino-4-imidazolecarboxamide riboside (Z-riboside) metabolism in eukaryotic cells*. J Biol Chem, 1985. **260**(10): p. 6107-14.
271. Sullivan, J.E., K.J. Brocklehurst, A.E. Marley, F. Carey, D. Carling, and R.K. Beri, *Inhibition of lipolysis and lipogenesis in isolated rat adipocytes with AICAR, a cell-permeable activator of AMP-activated protein kinase*. FEBS Lett, 1994. **353**(1): p. 33-6.
272. Henin, N., M.F. Vincent, H.E. Gruber, and G. Van den Berghe, *Inhibition of fatty acid and cholesterol synthesis by stimulation of AMP-activated protein kinase*. Faseb J, 1995. **9**(7): p. 541-6.
273. Bontemps, F., G. Van den Berghe, and H.G. Hers, *Pathways of adenine nucleotide catabolism in erythrocytes*. J Clin Invest, 1986. **77**(3): p. 824-30.

-
274. Carling, D., P.R. Clarke, V.A. Zammit, and D.G. Hardie, *Purification and characterization of the AMP-activated protein kinase. Copurification of acetyl-CoA carboxylase kinase and 3-hydroxy-3-methylglutaryl-CoA reductase kinase activities*. Eur J Biochem, 1989. **186**(1-2): p. 129-36.
275. Bailey, C.J. and C. Day, *Traditional plant medicines as treatments for diabetes*. Diabetes Care, 1989. **12**(8): p. 553-64.
276. Witters, L.A., *The blooming of the French lilac*. 2001. **108**(8): p. 1105-1107.
277. Bailey, C.J. and R.C. Turner, *Metformin*. N Engl J Med, 1996. **334**(9): p. 574-9.
278. Zhou, G., R. Myers, Y. Li, Y. Chen, X. Shen, J. Fenyk-Melody, M. Wu, J. Ventre, T. Doebber, N. Fujii, N. Musi, M.F. Hirshman, L.J. Goodyear, and D.E. Moller, *Role of AMP-activated protein kinase in mechanism of metformin action*. 2001. **108**(8): p. 1167-1174.
279. Cusi, K., A. Consoli, and R.A. DeFronzo, *Metabolic effects of metformin on glucose and lactate metabolism in noninsulin-dependent diabetes mellitus*. J Clin Endocrinol Metab, 1996. **81**(11): p. 4059-67.
280. Wiernsperger, N.F. and C.J. Bailey, *The antihyperglycaemic effect of metformin: therapeutic and cellular mechanisms*. Drugs, 1999. **58 Suppl 1**: p. 31-9; discussion 75-82.
281. Musi, N., M.F. Hirshman, J. Nygren, M. Svanfeldt, P. Bavenholm, O. Rooyackers, G. Zhou, J.M. Williamson, O. Ljunqvist, S. Efendic, D.E. Moller, A. Thorell, and L.J. Goodyear, *Metformin increases AMP-activated protein kinase activity in skeletal muscle of subjects with type 2 diabetes*. Diabetes, 2002. **51**(7): p. 2074-81.
282. Fryer, L.G., A. Parbu-Patel, and D. Carling, *The Anti-diabetic drugs rosiglitazone and metformin stimulate AMP-activated protein kinase through distinct signaling pathways*. J Biol Chem, 2002. **277**(28): p. 25226-32.
-

-
283. Saha, A.K., P.R. Avilucea, J.M. Ye, M.M. Assifi, E.W. Kraegen, and N.B. Ruderman, *Pioglitazone treatment activates AMP-activated protein kinase in rat liver and adipose tissue in vivo*. *Biochem Biophys Res Commun*, 2004. **314**(2): p. 580-5.
284. LeBrasseur, N.K., M. Kelly, T.S. Tsao, S.R. Farmer, A.K. Saha, N.B. Ruderman, and E. Tomas, *Thiazolidinediones can rapidly activate AMP-activated protein kinase in mammalian tissues*. *Am J Physiol Endocrinol Metab*, 2006. **291**(1): p. E175-81.
285. Cartee, G.D., A.G. Douen, T. Ramlal, A. Klip, and J.O. Holloszy, *Stimulation of glucose transport in skeletal muscle by hypoxia*. *J Appl Physiol*, 1991. **70**(4): p. 1593-600.
286. Mu, J., J.T. Brozinick, Jr., O. Valladares, M. Bucan, and M.J. Birnbaum, *A role for AMP-activated protein kinase in contraction- and hypoxia-regulated glucose transport in skeletal muscle*. *Mol Cell*, 2001. **7**(5): p. 1085-94.
287. Marsin, A.S., C. Bouzin, L. Bertrand, and L. Hue, *The stimulation of glycolysis by hypoxia in activated monocytes is mediated by AMP-activated protein kinase and inducible 6-phosphofructo-2-kinase*. *J Biol Chem*, 2002. **277**(34): p. 30778-83.
288. Kudo, N., A.J. Barr, R.L. Barr, S. Desai, and G.D. Lopaschuk, *High rates of fatty acid oxidation during reperfusion of ischemic hearts are associated with a decrease in malonyl-CoA levels due to an increase in 5'-AMP-activated protein kinase inhibition of acetyl-CoA carboxylase*. *J Biol Chem*, 1995. **270**(29): p. 17513-20.
289. Russell, R.R., 3rd, J. Li, D.L. Coven, M. Pypaert, C. Zechner, M. Palmeri, F.J. Giordano, J. Mu, M.J. Birnbaum, and L.H. Young, *AMP-activated protein kinase mediates ischemic glucose uptake and prevents postischemic cardiac dysfunction, apoptosis, and injury*. *J Clin Invest*, 2004. **114**(4): p. 495-503.
-

-
290. Minokoshi, Y., Y.B. Kim, O.D. Peroni, L.G. Fryer, C. Muller, D. Carling, and B.B. Kahn, *Leptin stimulates fatty-acid oxidation by activating AMP-activated protein kinase*. Nature, 2002. **415**(6869): p. 339-343.
291. Tomas, E., T.S. Tsao, A.K. Saha, H.E. Murrey, C.C. Zhang, S.I. Itani, H.F. Lodish, and N.B. Ruderman, *Enhanced muscle fat oxidation and glucose transport by ACRP30 globular domain: acetyl-CoA carboxylase inhibition and AMP-activated protein kinase activation*. Proceedings of the National Academy of Sciences of the United States of America, 2002. **99**(25): p. 16309-16313.
292. Yamauchi, T., J. Kamon, Y. Minokoshi, Y. Ito, H. Waki, S. Uchida, S. Yamashita, M. Noda, S. Kita, K. Ueki, K. Eto, Y. Akanuma, P. Froguel, F. Foufelle, P. Ferre, D. Carling, S. Kimura, R. Nagai, B.B. Kahn, and T. Kadowaki, *Adiponectin stimulates glucose utilization and fatty-acid oxidation by activating AMP-activated protein kinase*. Nat Med, 2002. **8**(11): p. 1288-95.
293. Zang, M., S. Xu, K.A. Maitland-Toolan, A. Zuccollo, X. Hou, B. Jiang, M. Wierzbicki, T.J. Verbeuren, and R.A. Cohen, *Polyphenols stimulate AMP-activated protein kinase, lower lipids, and inhibit accelerated atherosclerosis in diabetic LDL receptor-deficient mice*. Diabetes, 2006. **55**(8): p. 2180-91.
294. Wolfram, S., D. Raederstorff, M. Preller, Y. Wang, S.R. Teixeira, C. Riegger, and P. Weber, *Epigallocatechin gallate supplementation alleviates diabetes in rodents*. J Nutr, 2006. **136**(10): p. 2512-8.
295. Collins, Q.F., H.Y. Liu, J. Pi, Z. Liu, M.J. Quon, and W. Cao, *Epigallocatechin-3-gallate (EGCG), a green tea polyphenol, suppresses hepatic gluconeogenesis through 5'-AMP-activated protein kinase*. J Biol Chem, 2007. **282**(41): p. 30143-9.
296. Moon, H.S., H.G. Lee, Y.J. Choi, T.G. Kim, and C.S. Cho, *Proposed mechanisms of (-)-epigallocatechin-3-gallate for anti-obesity*. Chem Biol Interact, 2007. **167**(2): p. 85-98.
-

-
297. Hwang, J.T., J. Ha, I.J. Park, S.K. Lee, H.W. Baik, Y.M. Kim, and O.J. Park, *Apoptotic effect of EGCG in HT-29 colon cancer cells via AMPK signal pathway*. *Cancer Lett*, 2007. **247**(1): p. 115-21.
298. Potenza, M.A., F.L. Marasciulo, M. Tarquinio, E. Tiravanti, G. Colantuono, A. Federici, J.A. Kim, M.J. Quon, and M. Montagnani, *EGCG, a green tea polyphenol, improves endothelial function and insulin sensitivity, reduces blood pressure, and protects against myocardial I/R injury in SHR*. *Am J Physiol Endocrinol Metab*, 2007. **292**(5): p. E1378-87.
299. Watt, M.J., N. Dzamko, W.G. Thomas, S. Rose-John, M. Ernst, D. Carling, B.E. Kemp, M.A. Febbraio, and G.R. Steinberg, *CNTF reverses obesity-induced insulin resistance by activating skeletal muscle AMPK*. *Nat Med*, 2006. **12**(5): p. 541-8.
300. McInnes, K.J., A. Corbould, E.R. Simpson, and M.E. Jones, *Regulation of adenosine 5',monophosphate-activated protein kinase and lipogenesis by androgens contributes to visceral obesity in an estrogen-deficient state*. *Endocrinology*, 2006. **147**(12): p. 5907-13.
301. Cool, B., B. Zinker, W. Chiou, L. Kifle, N. Cao, M. Perham, R. Dickinson, A. Adler, G. Gagne, R. Iyengar, G. Zhao, K. Marsh, P. Kym, P. Jung, H.S. Camp, and E. Frevert, *Identification and characterization of a small molecule AMPK activator that treats key components of type 2 diabetes and the metabolic syndrome*. *Cell Metab*, 2006. **3**(6): p. 403-16.
302. Goransson, O., A. McBride, S.A. Hawley, F.A. Ross, N. Shpiro, M. Foretz, B. Viollet, D.G. Hardie, and K. Sakamoto, *Mechanism of action of A-769662, a valuable tool for activation of AMP-activated protein kinase*. *J Biol Chem*, 2007. **282**(45): p. 32549-60.
303. Sanders, M.J., Z.S. Ali, B.D. Hegarty, R. Heath, M.A. Snowden, and D. Carling, *Defining the mechanism of activation of AMP-activated protein kinase by the small molecule A-769662, a member of the thienopyridone family*. *J Biol Chem*, 2007. **282**(45): p. 32539-48.
-

-
304. Scott, J.W., B.J. van Denderen, S.B. Jorgensen, J.E. Honeyman, G.R. Steinberg, J.S. Oakhill, T.J. Iseli, A. Koay, P.R. Gooley, D. Stapleton, and B.E. Kemp, *Thienopyridone drugs are selective activators of AMP-activated protein kinase beta1-containing complexes*. Chem Biol, 2008. **15**(11): p. 1220-30.
305. Yin, J., Z. Gao, D. Liu, Z. Liu, and J. Ye, *Berberine improves glucose metabolism through induction of glycolysis*. Am J Physiol Endocrinol Metab, 2008. **294**(1): p. E148-56.
306. Turner, N., J.Y. Li, A. Gosby, S.W. To, Z. Cheng, H. Miyoshi, M.M. Taketo, G.J. Cooney, E.W. Kraegen, D.E. James, L.H. Hu, J. Li, and J.M. Ye, *Berberine and its more biologically available derivative, dihydroberberine, inhibit mitochondrial respiratory complex I: a mechanism for the action of berberine to activate AMP-activated protein kinase and improve insulin action*. Diabetes, 2008. **57**(5): p. 1414-8.
307. Chen, Z.P., K.I. Mitchelhill, B.J. Michell, D. Stapleton, I. Rodriguez-Crespo, L.A. Witters, D.A. Power, P.R. Ortiz de Montellano, and B.E. Kemp, *AMP-activated protein kinase phosphorylation of endothelial NO synthase*. 1999. **443**(3): p. 285-289.
308. Morrow, V.A., F. Foufelle, J.M. Connell, J.R. Petrie, G.W. Gould, and I.P. Salt, *Direct activation of AMP-activated protein kinase stimulates nitric-oxide synthesis in human aortic endothelial cells*. J Biol Chem, 2003. **278**(34): p. 31629-39.
309. Schulz, E., E. Anter, M.H. Zou, and J.F. Keaney, Jr., *Estradiol-mediated endothelial nitric oxide synthase association with heat shock protein 90 requires adenosine monophosphate-dependent protein kinase*. Circulation, 2005. **111**(25): p. 3473-80.
310. Nagata, D., M. Mogi, and K. Walsh, *AMP-activated protein kinase (AMPK) signaling in endothelial cells is essential for angiogenesis in response to hypoxic stress*. J Biol Chem, 2003. **278**(33): p. 31000-6.
-

-
311. Murakami, H., R. Murakami, F. Kambe, X. Cao, R. Takahashi, T. Asai, T. Hirai, Y. Numaguchi, K. Okumura, H. Seo, and T. Murohara, *Fenofibrate activates AMPK and increases eNOS phosphorylation in HUVEC*. *Biochem Biophys Res Commun*, 2006. **341**(4): p. 973-8.
312. Chen, H., M. Montagnani, T. Funahashi, I. Shimomura, and M.J. Quon, *Adiponectin stimulates production of nitric oxide in vascular endothelial cells*. *J Biol Chem*, 2003. **278**(45): p. 45021-6.
313. Bergeron, R., R.R. Russell, III, L.H. Young, J.M. Ren, M. Marcucci, A. Lee, and G.I. Shulman, *Effect of AMPK activation on muscle glucose metabolism in conscious rats*. 1999. **276**(5 Pt 1): p. E938-E944.
314. Kurth-Kraczek, E.J., M.F. Hirshman, L.J. Goodyear, and W.W. Winder, *5' AMP-activated protein kinase activation causes GLUT4 translocation in skeletal muscle*. 1999. **48**(8): p. 1667-1671.
315. Fryer, L.G., F. Foufelle, K. Barnes, S.A. Baldwin, A. Woods, and D. Carling, *Characterization of the role of the AMP-activated protein kinase in the stimulation of glucose transport in skeletal muscle cells*. *Biochem J*, 2002. **363**(Pt 1): p. 167-74.
316. Sakoda, H., T. Ogihara, M. Anai, M. Fujishiro, H. Ono, Y. Onishi, H. Katagiri, M. Abe, Y. Fukushima, N. Shojima, K. Inukai, M. Kikuchi, Y. Oka, and T. Asano, *Activation of AMPK is essential for AICAR-induced glucose uptake by skeletal muscle but not adipocytes*. 2002. **282**(6): p. E1239-E1244.
317. Bergeron, R., S.F. Previs, G.W. Cline, P. Perret, R.R. Russell, 3rd, L.H. Young, and G.I. Shulman, *Effect of 5-aminoimidazole-4-carboxamide-1-beta-D-ribofuranoside infusion on in vivo glucose and lipid metabolism in lean and obese Zucker rats*. *Diabetes*, 2001. **50**(5): p. 1076-82.
318. Iglesias, M.A., J.M. Ye, G. Frangioudakis, A.K. Saha, E. Tomas, N.B. Ruderman, G.J. Cooney, and E.W. Kraegen, *AICAR administration causes*
-

- an apparent enhancement of muscle and liver insulin action in insulin-resistant high-fat-fed rats.* Diabetes, 2002. **51**(10): p. 2886-94.
319. Cuthbertson, D.J., J.A. Babraj, K.J. Mustard, M.C. Towler, K.A. Green, H. Wackerhage, G.P. Leese, K. Baar, M. Thomason-Hughes, C. Sutherland, D.G. Hardie, and M.J. Rennie, *AICAR acutely stimulates skeletal muscle 2-deoxyglucose uptake in healthy men.* Diabetes, 2007. **19**: p. 19.
320. Boon, H., M. Bosselaar, S.F. Praet, E.E. Blaak, W.H. Saris, A.J. Wagenmakers, S.L. McGee, C.J. Tack, P. Smits, M. Hargreaves, and L.J. van Loon, *Intravenous AICAR administration reduces hepatic glucose output and inhibits whole body lipolysis in type 2 diabetic patients.* Diabetologia, 2008. **16**: p. 16.
321. Winder, W.W., B.F. Holmes, D.S. Rubink, E.B. Jensen, M. Chen, and J.O. Holloszy, *Activation of AMP-activated protein kinase increases mitochondrial enzymes in skeletal muscle.* 2000. **88**(6): p. 2219-2226.
322. Ihlemann, J., T. Ploug, and H. Galbo, *Effect of force development on contraction induced glucose transport in fast twitch rat muscle.* Acta Physiologica Scandinavica, 2001. **171**(4): p. 439-444.
323. Ai, H., J. Ihlemann, Y. Hellsten, H.P. Lauritzen, D.G. Hardie, H. Galbo, and T. Ploug, *Effect of fiber type and nutritional state on AICAR- and contraction-stimulated glucose transport in rat muscle.* 2002. **282**(6): p. E1291-E1300.
324. Fryer, L.G., A. Parbu-Patel, and D. Carling, *Protein kinase inhibitors block the stimulation of the AMP-activated protein kinase by 5-amino-4-imidazolecarboxamide riboside.* FEBS Lett, 2002. **531**(2): p. 189-92.
325. Fujii, N., N. Jessen, and L.J. Goodyear, *AMP-activated protein kinase and the regulation of glucose transport.* Am J Physiol Endocrinol Metab, 2006. **291**(5): p. E867-77.
326. Long, Y.C. and J.R. Zierath, *AMP-activated protein kinase signaling in metabolic regulation.* J Clin Invest, 2006. **116**(7): p. 1776-83.

-
327. Danchin, A. and H. Buc, *Proton magnetic resonance studies on 5'-AMP site in glycogen phosphorylase b*. FEBS Lett, 1972. **22**(3): p. 289-293.
328. Longnus, S.L., R.B. Wambolt, H.L. Parsons, R.W. Brownsey, and M.F. Allard, *5-Aminoimidazole-4-carboxamide 1-beta-D-ribofuranoside (AICAR) stimulates myocardial glycogenolysis by allosteric mechanisms*. Am J Physiol Regul Integr Comp Physiol, 2003. **284**(4): p. R936-44.
329. Chen, H.C., G. Bandyopadhyay, M.P. Sajan, Y. Kanoh, M. Standaert, R.V. Farese, Jr., and R.V. Farese, *Activation of the ERK pathway and atypical protein kinase C isoforms in exercise- and aminoimidazole-4-carboxamide-1-beta-D-ribose (AICAR)-stimulated glucose transport*. 2002. **277**(26): p. 23554-23562.
330. Vincent, M.F., P.J. Marangos, H.E. Gruber, and G. Van den Berghe, *Inhibition by AICA riboside of gluconeogenesis in isolated rat hepatocytes*. Diabetes, 1991. **40**(10): p. 1259-66.
331. Thong, F.S. and T.E. Graham, *The putative roles of adenosine in insulin- and exercise-mediated regulation of glucose transport and glycogen metabolism in skeletal muscle*. Can J Appl Physiol, 2002. **27**(2): p. 152-78.
332. Gadalla, A.E., T. Pearson, A.J. Currie, N. Dale, S.A. Hawley, M. Sheehan, W. Hirst, A.D. Michel, A. Randall, D.G. Hardie, and B.G. Frenguelli, *AICA riboside both activates AMP-activated protein kinase and competes with adenosine for the nucleoside transporter in the CA1 region of the rat hippocampus*. J Neurochem, 2004. **88**(5): p. 1272-82.
333. Han, D.H., P.A. Hansen, L.A. Nolte, and J.O. Holloszy, *Removal of adenosine decreases the responsiveness of muscle glucose transport to insulin and contractions*. Diabetes, 1998. **47**(11): p. 1671-1675.
334. Gruber, H.E., M.E. Hoffer, D.R. McAllister, P.K. Laikind, T.A. Lane, G.W. Schmid-Schoenbein, and R.L. Engler, *Increased adenosine concentration in blood from ischemic myocardium by AICA riboside. Effects on flow, granulocytes, and injury*. Circulation, 1989. **80**(5): p. 1400-11.
-

-
335. Winder, W.W., B.F. Holmes, D.S. Rubink, E.B. Jensen, M. Chen, and J.O. Holloszy, *Activation of AMP-activated protein kinase increases mitochondrial enzymes in skeletal muscle*. *Journal of Applied Physiology*, 2000. **88**(6): p. 2219-2226.
336. Holmes, B.F., E.J. Kurth-Kraczek, and W.W. Winder, *Chronic activation of 5'-AMP-activated protein kinase increases GLUT-4, hexokinase, and glycogen in muscle*. 1999. **87**(5): p. 1990-1995.
337. Douen, A.G., T. Ramlal, G.D. Cartee, and A. Klip, *Exercise modulates the insulin-induced translocation of glucose transporters in rat skeletal muscle*. *FEBS Letters*, 1990. **261**: p. 256-260.
338. Wallis, M.G., C.M. Wheatley, S. Rattigan, E.J. Barrett, A.D. Clark, and M.G. Clark, *Insulin-mediated hemodynamic changes are impaired in muscle of Zucker obese rats*. *Diabetes*, 2002. **51**(12): p. 3492-8.
339. Buhl, E.S., N. Jessen, R. Pold, T. Ledet, A. Flyvbjerg, S.B. Pedersen, O. Pedersen, O. Schmitz, and S. Lund, *Long-term AICAR administration reduces metabolic disturbances and lowers blood pressure in rats displaying features of the insulin resistance syndrome*. 2002. **51**(7): p. 2199-2206.
340. DeFronzo, R.A., J.D. Tobin, and R. Andres, *Glucose clamp technique: a method for quantifying insulin secretion and resistance*. *Am J Physiol*, 1979. **237**(3): p. E214-23.
341. Kraegen, E.W., D.E. James, S.P. Bennett, and D.J. Chisholm, *In vivo insulin sensitivity in the rat determined by euglycemic clamp*. *Am J Physiol*, 1983. **245**(1): p. E1-7.
342. Burnol, A.F., A. Leturque, P. Ferre, and J. Girard, *A method for quantifying insulin sensitivity in vivo in the anesthetized rat: the euglycemic insulin clamp technique coupled with isotopic measurement of glucose turnover*. *Reprod Nutr Dev*, 1983. **23**(2 B): p. 429-35.
-

-
343. Terrettaz, J. and B. Jeanrenaud, *In vivo hepatic and peripheral insulin resistance in genetically obese (fa/fa) rats*. *Endocrinology*, 1983. **112**(4): p. 1346-51.
344. Scheen, A.J., N. Paquot, M.J. Castillo, and P.J. Lefebvre, *How to measure insulin action in vivo*. *Diabetes/Metabolism Reviews*, 1994. **10**: p. 151-188.
345. Kraegen, E.W., D.E. James, A.B. Jenkins, and D.J. Chisholm, *Dose-response curves for in vivo insulin sensitivity in individual tissues in rats*. *Am J Physiol*, 1985. **248**(3 Pt 1): p. E353-62.
346. James, D.E., A.B. Jenkins, and E.W. Kraegen, *Heterogeneity of insulin action in individual muscles in vivo: euglycemic clamp studies in rats*. *Am J Physiol*, 1985. **248**(5 Pt 1): p. E567-74.
347. James, D.E., K.M. Burleigh, and E.W. Kraegen, *In vivo glucose metabolism in individual tissues of the rat. Interaction between epinephrine and insulin*. *J Biol Chem*, 1986. **261**(14): p. 6366-74.
348. Hom, F.G., C.J. Goodner, and M.A. Berrie, *A [³H]2-deoxyglucose method for comparing rates of glucose metabolism and insulin responses among rat tissues in vivo. Validation of the model and the absence of an insulin effect on brain*. *Diabetes*, 1984. **33**(2): p. 141-52.
349. Day, R.O., J. Miners, D.J. Birkett, G.G. Graham, and A. Whitehead, *Relationship between plasma oxipurinol concentrations and xanthine oxidase activity in volunteers dosed with allopurinol*. *Br J Clin Pharmacol*, 1988. **26**(4): p. 429-34.
350. Hellsten, Y., U. Frandsen, N. Orthenblad, B. Sjodin, and E.A. Richter, *Xanthine oxidase in human skeletal muscle following eccentric exercise: a role in inflammation*. *J Physiol*, 1997. **498** (Pt 1): p. 239-48.
351. Emmerson, B.T., R.B. Gordon, M. Cross, and D.B. Thomson, *Plasma oxipurinol concentrations during allopurinol therapy*. *Br J Rheumatol*, 1987. **26**(6): p. 445-9.
-

-
352. Jayaweera, A.R., N. Edwards, W.P. Glasheen, F.S. Villanueva, R.D. Abbott, and S. Kaul, *In vivo myocardial kinetics of air-filled albumin microbubbles during myocardial contrast echocardiography. Comparison with radiolabeled red blood cells*. Circ Res, 1994. **74**(6): p. 1157-65.
353. Wei, K., A.R. Jayaweera, S. Firoozan, A. Linka, D.M. Skyba, and S. Kaul, *Quantification of myocardial blood flow with ultrasound-induced destruction of microbubbles administered as a constant venous infusion*. Circulation, 1998. **97**(5): p. 473-83.
354. Hester, R.L. and B.R. Duling, *Red cell velocity during functional hyperemia: implications for rheology and oxygen transport*. Am J Physiol, 1988. **255**(2 Pt 2): p. H236-44.
355. Kassab, G.S., D.H. Lin, and Y.C. Fung, *Morphometry of pig coronary venous system*. Am J Physiol, 1994. **267**(6 Pt 2): p. H2100-13.
356. Wynants, J., B. Petrov, J. Nijhof, and H. Van Belle, *Optimization of a high-performance liquid chromatographic method for the determination of nucleosides and their catabolites. Application to cat and rabbit heart perfusates*. J Chromatogr, 1987. **386**: p. 297-308.
357. Meininger, G.A., K.L. Fehr, and M.B. Yates, *Anatomic and hemodynamic characteristics of the blood vessels feeding the cremaster skeletal muscle in the rat*. Microvasc Res, 1987. **33**(1): p. 81-97.
358. Karasek, M.A., *Microvascular endothelial cell culture*. J Invest Dermatol, 1989. **93**(2 Suppl): p. 33S-38S.
359. van Nieuw Amerongen, G.P., P. Koolwijk, A. Versteilen, and V.W. van Hinsbergh, *Involvement of RhoA/Rho kinase signaling in VEGF-induced endothelial cell migration and angiogenesis in vitro*. Arterioscler Thromb Vasc Biol, 2003. **23**(2): p. 211-7.
360. Baggiolini, M., B. Dewald, J. Schnyder, W. Ruch, P.H. Cooper, and T.G. Payne, *Inhibition of the phagocytosis-induced respiratory burst by the fungal*
-

- metabolite wortmannin and some analogues. Exp Cell Res*, 1987. **169**(2): p. 408-18.
361. Dewald, B., M. Thelen, and M. Baggiolini, *Two transduction sequences are necessary for neutrophil activation by receptor agonists. J Biol Chem*, 1988. **263**(31): p. 16179-84.
362. Yatomi, Y., O. Hazeki, S. Kume, and M. Ui, *Suppression by wortmannin of platelet responses to stimuli due to inhibition of pleckstrin phosphorylation. Biochem J*, 1992. **285 (Pt 3)**(Pt 3): p. 745-51.
363. Arcaro, A. and M.P. Wymann, *Wortmannin is a potent phosphatidylinositol 3-kinase inhibitor: the role of phosphatidylinositol 3,4,5-trisphosphate in neutrophil responses. Biochem J*, 1993. **296 (Pt 2)**: p. 297-301.
364. Okada, T., L. Sakuma, Y. Fukui, O. Hazeki, and M. Ui, *Blockage of chemotactic peptide-induced stimulation of neutrophils by wortmannin as a result of selective inhibition of phosphatidylinositol 3-kinase. J Biol Chem*, 1994. **269**(5): p. 3563-7.
365. Rahn, T., M. Ridderstrale, H. Tornqvist, V. Manganiello, G. Fredrikson, P. Belfrage, and E. Degerman, *Essential role of phosphatidylinositol 3-kinase in insulin-induced activation and phosphorylation of the cGMP-inhibited cAMP phosphodiesterase in rat adipocytes. Studies using the selective inhibitor wortmannin. FEBS Lett*, 1994. **350**(2-3): p. 314-8.
366. Kanai, F., K. Ito, M. Todaka, H. Hayashi, S. Kamohara, K. Ishii, T. Okada, O. Hazeki, M. Ui, and Y. Ebina, *Insulin-stimulated GLUT4 translocation is relevant to the phosphorylation of IRS-1 and the activity of PI3-kinase. Biochem Biophys Res Commun*, 1993. **195**(2): p. 762-8.
367. Yano, H., S. Nakanishi, K. Kimura, N. Hanai, Y. Saitoh, Y. Fukui, Y. Nonomura, and Y. Matsuda, *Inhibition of histamine secretion by wortmannin through the blockade of phosphatidylinositol 3-kinase in RBL-2H3 cells. J Biol Chem*, 1993. **268**(34): p. 25846-56.

-
368. Wymann, M. and A. Arcaro, *Platelet-derived growth factor-induced phosphatidylinositol 3-kinase activation mediates actin rearrangements in fibroblasts*. Biochem J, 1994. **298 Pt 3**: p. 517-20.
369. Thelen, M., M.P. Wymann, and H. Langen, *Wortmannin binds specifically to 1-phosphatidylinositol 3-kinase while inhibiting guanine nucleotide-binding protein-coupled receptor signaling in neutrophil leukocytes*. Proc Natl Acad Sci U S A, 1994. **91**(11): p. 4960-4.
370. Wymann, M.P., G. Bulgarelli-Leva, M.J. Zvelebil, L. Pirola, B. Vanhaesebroeck, M.D. Waterfield, and G. Panayotou, *Wortmannin inactivates phosphoinositide 3-kinase by covalent modification of Lys-802, a residue involved in the phosphate transfer reaction*. Mol Cell Biol, 1996. **16**(4): p. 1722-33.
371. Nakanishi, S., K.J. Catt, and T. Balla, *A wortmannin-sensitive phosphatidylinositol 4-kinase that regulates hormone-sensitive pools of inositolphospholipids*. Proc Natl Acad Sci U S A, 1995. **92**(12): p. 5317-21.
372. Chung, J., T.C. Grammer, K.P. Lemon, A. Kazlauskas, and J. Blenis, *PDGF- and insulin-dependent pp70S6k activation mediated by phosphatidylinositol-3-OH kinase*. Nature, 1994. **370**(6484): p. 71-5.
373. Cross, D.A., D.R. Alessi, J.R. Vandenheede, H.E. McDowell, H.S. Hundal, and P. Cohen, *The inhibition of glycogen synthase kinase-3 by insulin or insulin-like growth factor I in the rat skeletal muscle cell line L6 is blocked by wortmannin, but not by rapamycin: evidence that wortmannin blocks activation of the mitogen-activated protein kinase pathway in L6 cells between Ras and Raf*. Biochem J, 1994. **303 (Pt 1)**: p. 21-6.
374. Yeh, J.I., E.A. Gulve, L. Rameh, and M.J. Birnbaum, *The effects of wortmannin on rat skeletal muscle. Dissociation of signaling pathways for insulin- and contraction-activated hexose transport*. J Biol Chem, 1995. **270**(5): p. 2107-11.
-

-
375. Cross, M.J., A. Stewart, M.N. Hodgkin, D.J. Kerr, and M.J. Wakelam, *Wortmannin and its structural analogue demethoxyviridin inhibit stimulated phospholipase A2 activity in Swiss 3T3 cells. Wortmannin is not a specific inhibitor of phosphatidylinositol 3-kinase*. J Biol Chem, 1995. **270**(43): p. 25352-5.
376. Gunther, R., P.N. Kishore, H.K. Abbas, and C.J. Mirocha, *Immunosuppressive effects of dietary wortmannin on rats and mice*. Immunopharmacol Immunotoxicol, 1989. **11**(4): p. 559-70.
377. Gunther, R., H.K. Abbas, and C.J. Mirocha, *Acute pathological effects on rats of orally administered wortmannin-containing preparations and purified wortmannin from Fusarium oxysporum*. Food Chem Toxicol, 1989. **27**(3): p. 173-9.
378. Boehle, A.S., R. Kurdow, L. Boenicke, B. Schniewind, F. Faendrich, P. Dohrmann, and H. Kalthoff, *Wortmannin inhibits growth of human non-small-cell lung cancer in vitro and in vivo*. Langenbecks Arch Surg, 2002. **387**(5-6): p. 234-9.
379. Davol, P.A., A. Bizuneh, and A.R. Frackelton, Jr., *Wortmannin, a phosphoinositide 3-kinase inhibitor, selectively enhances cytotoxicity of receptor-directed-toxin chimeras in vitro and in vivo*. Anticancer Res, 1999. **19**(3A): p. 1705-13.
380. Schultz, R.M., R.L. Merriman, S.L. Andis, R. Bonjouklian, G.B. Grindey, P.G. Rutherford, A. Gallegos, K. Massey, and G. Powis, *In vitro and in vivo antitumor activity of the phosphatidylinositol-3-kinase inhibitor, wortmannin*. Anticancer Res, 1995. **15**(4): p. 1135-9.
381. Sato, M., H.U. Bryant, J.A. Dodge, H. Davis, W.F. Matter, and C.J. Vlahos, *Effects of wortmannin analogs on bone in vitro and in vivo*. J Pharmacol Exp Ther, 1996. **277**(1): p. 543-50.
-

-
382. Borelli, M.I., F. Francini, and J.J. Gagliardino, *Autocrine regulation of glucose metabolism in pancreatic islets*. Am J Physiol Endocrinol Metab, 2004. **286**(1): p. E111-5.
383. Nunoi, K., K. Yasuda, H. Tanaka, A. Kubota, Y. Okamoto, T. Adachi, N. Shihara, M. Uno, L.M. Xu, S. Kagimoto, Y. Seino, Y. Yamada, and K. Tsuda, *Wortmannin, a PI3-kinase inhibitor: promoting effect on insulin secretion from pancreatic beta cells through a cAMP-dependent pathway*. Biochem Biophys Res Commun, 2000. **270**(3): p. 798-805.
384. Zawalich, W.S., G.J. Tesz, and K.C. Zawalich, *Inhibitors of phosphatidylinositol 3-kinase amplify insulin release from islets of lean but not obese mice*. J Endocrinol, 2002. **174**(2): p. 247-58.
385. Zawalich, W.S. and K.C. Zawalich, *A link between insulin resistance and hyperinsulinemia: inhibitors of phosphatidylinositol 3-kinase augment glucose-induced insulin secretion from islets of lean, but not obese, rats*. Endocrinology, 2000. **141**(9): p. 3287-95.
386. Kulkarni, R.N., J.C. Bruning, J.N. Winnay, C. Postic, M.A. Magnuson, and C.R. Kahn, *Tissue-specific knockout of the insulin receptor in pancreatic beta cells creates an insulin secretory defect similar to that in type 2 diabetes*. Cell, 1999. **96**(3): p. 329-39.
387. Dimmeler, S., I. Fleming, B. Fisslthaler, C. Hermann, R. Busse, and A.M. Zeiher, *Activation of nitric oxide synthase in endothelial cells by Akt-dependent phosphorylation*. Nature, 1999. **399**(6736): p. 601-5.
388. Eringa, E.C., C.D. Stehouwer, T. Merlijn, N. Westerhof, and P. Sipkema, *Physiological concentrations of insulin induce endothelin-mediated vasoconstriction during inhibition of NOS or PI3-kinase in skeletal muscle arterioles*. Cardiovasc Res, 2002. **56**(3): p. 464-71.
389. Potenza, M.A., F.L. Marasciulo, D.M. Chieppa, G.S. Brigiani, G. Formoso, M.J. Quon, and M. Montagnani, *Insulin resistance in spontaneously hypertensive rats is associated with endothelial dysfunction characterized by*
-

- imbalance between NO and ET-1 production. Am J Physiol Heart Circ Physiol*, 2005. **289**(2): p. H813-22.
390. Youd, J.M., S. Rattigan, and M.G. Clark, *Acute impairment of insulin-mediated capillary recruitment and glucose uptake in rat skeletal muscle in vivo by TNF-alpha*. *Diabetes*, 2000. **49**(11): p. 1904-9.
391. Clerk, L.H., S. Rattigan, and M.G. Clark, *Lipid infusion impairs physiologic insulin-mediated capillary recruitment and muscle glucose uptake in vivo*. *Diabetes*, 2002. **51**(4): p. 1138-45.
392. Wallis, M.G., M.E. Smith, C.M. Kolka, L. Zhang, S.M. Richards, S. Rattigan, and M.G. Clark, *Acute glucosamine-induced insulin resistance in muscle in vivo is associated with impaired capillary recruitment*. *Diabetologia*, 2005. **48**(10): p. 2131-9.
393. Wojtaszewski, J.F., B.F. Hansen, B. Urso, and E.A. Richter, *Wortmannin inhibits both insulin- and contraction-stimulated glucose uptake and transport in rat skeletal muscle*. *J Appl Physiol*, 1996. **81**(4): p. 1501-9.
394. Wang, Y., K. Yoshioka, M.A. Azam, N. Takuwa, S. Sakurada, Y. Kayaba, N. Sugimoto, I. Inoki, T. Kimura, T. Kuwaki, and Y. Takuwa, *Class II phosphoinositide 3-kinase alpha-isoform regulates Rho, myosin phosphatase and contraction in vascular smooth muscle*. *Biochem J*, 2006. **394**(Pt 3): p. 581-92.
395. Baron, A.D., *Hemodynamic actions of insulin*. *Am J Physiol*, 1994. **267**(2 Pt 1): p. E187-202.
396. Pitre, M., A. Nadeau, and H. Bachelard, *Insulin sensitivity and hemodynamic responses to insulin in Wistar-Kyoto and spontaneously hypertensive rats*. *Am J Physiol*, 1996. **271**(4 Pt 1): p. E658-68.
397. Chen, Y.L. and E.J. Messina, *Dilation of isolated skeletal muscle arterioles by insulin is endothelium dependent and nitric oxide mediated*. *Am J Physiol*, 1996. **270**(6 Pt 2): p. H2120-4.

-
398. Kahn, N.N., K. Acharya, S. Bhattacharya, R. Acharya, S. Mazumder, W.A. Bauman, and A.K. Sinha, *Nitric oxide: the "second messenger" of insulin*. IUBMB Life, 2000. **49**(5): p. 441-50.
399. Baron, A.D., M. Tarshoby, G. Hook, E.N. Lazaridis, J. Cronin, A. Johnson, and H.O. Steinberg, *Interaction between insulin sensitivity and muscle perfusion on glucose uptake in human skeletal muscle: evidence for capillary recruitment*. Diabetes, 2000. **49**(5): p. 768-74.
400. Singh, S. and T.W. Evans, *Nitric oxide, the biological mediator of the decade: fact or fiction?* Eur Respir J, 1997. **10**(3): p. 699-707.
401. Knowles, R.G. and S. Moncada, *Nitric oxide as a signal in blood vessels*. Trends Biochem Sci, 1992. **17**(10): p. 399-402.
402. Shankar, R.R., Y. Wu, H.Q. Shen, J.S. Zhu, and A.D. Baron, *Mice with gene disruption of both endothelial and neuronal nitric oxide synthase exhibit insulin resistance*. Diabetes, 2000. **49**(5): p. 684-7.
403. Duplain, H., R. Burcelin, C. Sartori, S. Cook, M. Egli, M. Lepori, P. Vollenweider, T. Pedrazzini, P. Nicod, B. Thorens, and U. Scherrer, *Insulin resistance, hyperlipidemia, and hypertension in mice lacking endothelial nitric oxide synthase*. Circulation, 2001. **104**(3): p. 342-5.
404. Roy, D., M. Perreault, and A. Marette, *Insulin stimulation of glucose uptake in skeletal muscles and adipose tissues in vivo is NO dependent*. 1998. **274**(4 Pt 1): p. E692-E699.
405. Baron, A.D., H.O. Steinberg, H. Chaker, R. Leaming, A. Johnson, and G. Brechtel, *Insulin-mediated skeletal muscle vasodilation contributes to both insulin sensitivity and responsiveness in lean humans*. J Clin Invest, 1995. **96**(2): p. 786-92.
406. Frandsen, U., J. Bangsbo, H. Langberg, B. Saltin, and Y. Hellsten, *Inhibition of nitric oxide synthesis by systemic N(G)-monomethyl-L-arginine administration in humans: effects on interstitial adenosine, prostacyclin and*
-

- potassium concentrations in resting and contracting skeletal muscle. J Vasc Res*, 2000. **37**(4): p. 297-302.
407. Huang, F., S. Villafana, and E. Hong, *Role of central and sympathetic nervous systems in pressor effect of L-NAME. J Cardiovasc Pharmacol*, 2003. **41**(1): p. 68-72.
408. Traystman, R.J., L.E. Moore, M.A. Helfaer, S. Davis, K. Banasiak, M. Williams, and P.D. Hurn, *Nitro-L-arginine analogues. Dose- and time-related nitric oxide synthase inhibition in brain. Stroke*, 1995. **26**(5): p. 864-9.
409. Ross, R.M., G.D. Wadley, M.G. Clark, S. Rattigan, and G.K. McConell, *Local NOS inhibition reduces skeletal muscle glucose uptake but not capillary blood flow during in situ muscle contraction in rats. Diabetes*, 2007.
410. Baron, A.D., M. Laakso, G. Brechtel, and S.V. Edelman, *Mechanism of insulin resistance in insulin-dependent diabetes mellitus: a major role for reduced skeletal muscle blood flow. J Clin Endocrinol Metab*, 1991. **73**(3): p. 637-43.
411. Baron, A.D., H. Steinberg, G. Brechtel, and A. Johnson, *Skeletal muscle blood flow independently modulates insulin-mediated glucose uptake. Am J Physiol*, 1994. **266**(2 Pt 1): p. E248-53.
412. Jialal, I., M. Crettaz, H.L. Hachiya, C.R. Kahn, A.C. Moses, S.M. Buzney, and G.L. King, *Characterization of the receptors for insulin and the insulin-like growth factors on micro- and macrovascular tissues. Endocrinology*, 1985. **117**(3): p. 1222-9.
413. Montagnani, M., L.V. Ravichandran, H. Chen, D.L. Esposito, and M.J. Quon, *Insulin receptor substrate-1 and phosphoinositide-dependent kinase-1 are required for insulin-stimulated production of nitric oxide in endothelial cells. Mol Endocrinol*, 2002. **16**(8): p. 1931-42.

-
414. Serne, E.H., I.J. RG, R.O. Gans, R. Nijveldt, G. De Vries, R. Evertz, A.J. Donker, and C.D. Stehouwer, *Direct evidence for insulin-induced capillary recruitment in skin of healthy subjects during physiological hyperinsulinemia*. Diabetes, 2002. **51**(5): p. 1515-22.
415. Balon, T.W. and J.L. Nadler, *Evidence that nitric oxide increases glucose transport in skeletal muscle*. J Appl Physiol, 1997. **82**(1): p. 359-63.
416. Richter, E.A., J.N. Nielsen, S.B. Jorgensen, C. Frosig, J.B. Birk, and J.F. Wojtaszewski, *Exercise signalling to glucose transport in skeletal muscle*. Proc Nutr Soc, 2004. **63**(2): p. 211-6.
417. Musi, N. and L.J. Goodyear, *AMP-activated protein kinase and muscle glucose uptake*. Acta Physiol Scand, 2003. **178**(4): p. 337-45.
418. Balon, T.W. and A.P. Jasman, *Acute exposure to AICAR increases glucose transport in mouse EDL and soleus muscle*. 2001. **282**(4): p. 1008-1011.
419. Hayashi, T., M.F. Hirshman, N. Fujii, S.A. Habinowski, L.A. Witters, and L.J. Goodyear, *Metabolic stress and altered glucose transport: activation of AMP-activated protein kinase as a unifying coupling mechanism*. 2000. **49**(4): p. 527-531.
420. Russell, R.R., 3rd, R. Bergeron, G.I. Shulman, and L.H. Young, *Translocation of myocardial GLUT-4 and increased glucose uptake through activation of AMPK by AICAR*. Am J Physiol, 1999. **277**(2 Pt 2): p. H643-9.
421. Ojuka, E.O., L.A. Nolte, and J.O. Holloszy, *Increased expression of GLUT-4 and hexokinase in rat epitrochlearis muscles exposed to AICAR in vitro*. 2000. **88**(3): p. 1072-1075.
422. Rubin, L.J., L. Magliola, X. Feng, A.W. Jones, and C.C. Hale, *Metabolic Activation of AMP-kinase in Vascular Smooth Muscle*. J Appl Physiol, 2004.
423. Thors, B., H. Halldorsson, and G. Thorgeirsson, *Thrombin and histamine stimulate endothelial nitric-oxide synthase phosphorylation at Ser1177 via*
-

- an AMPK mediated pathway independent of PI3K-Akt*. FEBS Lett, 2004. **573**(1-3): p. 175-80.
424. Li, J., X. Hu, P. Selvakumar, R.R. Russell, 3rd, S.W. Cushman, G.D. Holman, and L.H. Young, *Role of the nitric oxide pathway in AMPK-mediated glucose uptake and GLUT4 translocation in heart muscle*. Am J Physiol Endocrinol Metab, 2004. **287**(5): p. E834-41.
425. Viollet, B., F. Andreelli, S.B. Jorgensen, C. Perrin, A. Geloën, D. Flamez, J. Mu, C. Lenzner, O. Baud, M. Bennoun, E. Gomas, G. Nicolas, J.F. Wojtaszewski, A. Kahn, D. Carling, F.C. Schuit, M.J. Birnbaum, E.A. Richter, R. Burcelin, and S. Vaulont, *The AMP-activated protein kinase alpha2 catalytic subunit controls whole-body insulin sensitivity*. J Clin Invest, 2003. **111**(1): p. 91-8.
426. Zhou, G., R. Myers, Y. Li, Y. Chen, X. Shen, J. Fenyk-Melody, M. Wu, J. Ventre, T. Doebber, N. Fujii, N. Musi, M.F. Hirshman, L.J. Goodyear, and D.E. Moller, *Role of AMP-activated protein kinase in mechanism of metformin action*. Journal of Clinical Investigation, 2001. **108**(8): p. 1167-1174.
427. Mount, P.F., R.E. Hill, S.A. Fraser, V. Levidiotis, F. Katsis, B.E. Kemp, and D.A. Power, *Acute renal ischemia rapidly activates the energy sensor AMPK but does not increase phosphorylation of eNOS-Ser1177*. Am J Physiol Renal Physiol, 2005. **289**(5): p. F1103-15.
428. Goirand, F., M. Solar, Y. Athea, B. Viollet, P. Mateo, D. Fortin, J. Leclerc, J. Hoerter, R. Ventura-Clapier, and A. Garnier, *Activation of AMP kinase alpha1 subunit induces aortic vasorelaxation in mice*. J Physiol, 2007. **581**(Pt 3): p. 1163-71.
429. Gallis, B., G.L. Corthals, D.R. Goodlett, H. Ueba, F. Kim, S.R. Presnell, D. Figeys, D.G. Harrison, B.C. Berk, R. Aebersold, and M.A. Corson, *Identification of flow-dependent endothelial nitric-oxide synthase phosphorylation sites by mass spectrometry and regulation of*

- phosphorylation and nitric oxide production by the phosphatidylinositol 3-kinase inhibitor LY294002*. J Biol Chem, 1999. **274**(42): p. 30101-8.
430. Zhang, Y., T.S. Lee, E.M. Kolb, K. Sun, X. Lu, F.M. Sladek, G.S. Kassab, T. Garland, Jr., and J.Y. Shyy, *AMP-activated protein kinase is involved in endothelial NO synthase activation in response to shear stress*. Arterioscler Thromb Vasc Biol, 2006. **26**(6): p. 1281-7.
431. Zhao, Z.Q., M.W. Williams, H. Sato, D.A. Hudspeth, D.S. McGee, J. Vinten-Johansen, and D.G. Van Wylen, *Acadesine reduces myocardial infarct size by an adenosine mediated mechanism*. Cardiovasc Res, 1995. **29**(4): p. 495-505.
432. Richter, E.A., W. Derave, and J.F. Wojtaszewski, *Glucose, exercise and insulin: emerging concepts*. J Physiol, 2001. **535**(Pt 2): p. 313-22.
433. Hayashi, T., J.F. Wojtaszewski, and L.J. Goodyear, *Exercise regulation of glucose transport in skeletal muscle*. Am J Physiol, 1997. **273**(6 Pt 1): p. E1039-51.
434. Fisher, J.S., J. Gao, D.H. Han, J.O. Holloszy, and L.A. Nolte, *Activation of AMP kinase enhances sensitivity of muscle glucose transport to insulin*. 2002. **282**(1): p. E18-E23.
435. Buhl, E.S., N. Jessen, O. Schmitz, S.B. Pedersen, O. Pedersen, G.D. Holman, and S. Lund, *Chronic treatment with 5-aminoimidazole-4-carboxamide-1-beta-D-ribofuranoside increases insulin-stimulated glucose uptake and GLUT4 translocation in rat skeletal muscles in a fiber type-specific manner*. 2001. **50**(1): p. 12-17.
436. Cuthbertson, D.J., J.A. Babraj, K.J. Mustard, M.C. Towler, K.A. Green, H. Wackerhage, G.P. Leese, K. Baar, M. Thomason-Hughes, C. Sutherland, D.G. Hardie, and M.J. Rennie, *5-aminoimidazole-4-carboxamide 1-beta-D-ribofuranoside acutely stimulates skeletal muscle 2-deoxyglucose uptake in healthy men*. Diabetes, 2007. **56**(8): p. 2078-84.

-
437. Rattigan, Z., Mahajan, Kolka, Richards, *Factors Influencing the Hemodynamic and Metabolic Effects of Insulin in Muscle*. Current Diabetes Reviews, 2006.
438. Laughlin, M.H. and R.B. Armstrong, *Rat muscle blood flows as a function of time during prolonged slow treadmill exercise*. Am J Physiol, 1983. **244**(6): p. H814-24.
439. Putman, C.T., K.J. Martins, M.E. Gallo, G.D. Lopaschuk, J.A. Pearcey, I.M. MacLean, R.J. Saranchuk, and D. Pette, *Alpha-catalytic subunits of 5'AMP-activated protein kinase display fiber-specific expression and are upregulated by chronic low-frequency stimulation in rat muscle*. Am J Physiol Regul Integr Comp Physiol, 2007. **293**(3): p. R1325-34.
440. Pencek, R.R., J. Shearer, R.C. Camacho, F.D. James, D.B. Lacy, P.T. Fueger, E.P. Donahue, W. Snead, and D.H. Wasserman, *5-Aminoimidazole-4-carboxamide-1-beta-D-ribofuranoside causes acute hepatic insulin resistance in vivo*. Diabetes, 2005. **54**(2): p. 355-60.
441. Camacho, R.C., R.R. Pencek, D.B. Lacy, F.D. James, E.P. Donahue, and D.H. Wasserman, *Portal venous 5-aminoimidazole-4-carboxamide-1-beta-D-ribofuranoside infusion overcomes hyperinsulinemic suppression of endogenous glucose output*. Diabetes, 2005. **54**(2): p. 373-82.
442. Camacho, R.C., D.B. Lacy, F.D. James, E.P. Donahue, and D.H. Wasserman, *5-Aminoimidazole-4-carboxamide-1-beta-D-ribofuranoside renders glucose output by the liver of the dog insensitive to a pharmacological increment in insulin*. Am J Physiol Endocrinol Metab, 2005. **289**(6): p. E1039-43.
443. Rantzau, C., M.J. Christopher, and F.P. Alford, *Contrasting Effects of Exercise, AICAR and Increased Fatty Acid Supply on In Vivo and Skeletal Muscle Glucose Metabolism*. J Appl Physiol, 2007.
444. Winder, W.W., *AMP-activated protein kinase: possible target for treatment of type 2 diabetes*. 2000. **2**(3): p. 441-448.
-

-
445. Halse, R., L.G. Fryer, J.G. McCormack, D. Carling, and S.J. Yeaman, *Regulation of glycogen synthase by glucose and glycogen: a possible role for AMP-activated protein kinase*. *Diabetes*, 2003. **52**(1): p. 9-15.
446. Atkinson, L.L., R. Kozak, S.E. Kelly, A. Onay Besikci, J.C. Russell, and G.D. Lopaschuk, *Potential mechanisms and consequences of cardiac triacylglycerol accumulation in insulin-resistant rats*. *Am J Physiol Endocrinol Metab*, 2003. **284**(5): p. E923-30.
447. Hue, L., C. Beauloye, A.S. Marsin, L. Bertrand, S. Horman, and M.H. Rider, *Insulin and ischemia stimulate glycolysis by acting on the same targets through different and opposing signaling pathways*. *J Mol Cell Cardiol*, 2002. **34**(9): p. 1091-7.
448. Wheatley, C.M., S. Rattigan, S.M. Richards, E.J. Barrett, and M.G. Clark, *Skeletal muscle contraction stimulates capillary recruitment and glucose uptake in insulin-resistant obese Zucker rats*. *Am J Physiol Endocrinol Metab*, 2004. **287**(4): p. E804-9.
449. Clark, M.G., A.D. Clark, and S. Rattigan, *Failure of laser Doppler signal to correlate with total flow in muscle: Is this a question of vessel architecture?* *Microvascular Research*, 2000. **60**: p. 294-301.
450. Kubota, T., N. Kubota, H. Kozono, S. Itoh, M. Moroi, K. Sugi, T. Yamauchi, K. Ueki, Y. Terauchi, K. Tobe, and T. Kadowaki, *Endothelial-cell Specific IRS-2 Deficient Mice Showed Endothelial Dysfunction And Muscle Insulin Resistance*. *Diabetes* 2007. **56**(Suppl 1): p. A347-A348.
451. Vicent, D., J. Ilany, T. Kondo, K. Naruse, S.J. Fisher, Y.Y. Kisanuki, S. Bursell, M. Yanagisawa, G.L. King, and C.R. Kahn, *The role of endothelial insulin signaling in the regulation of vascular tone and insulin resistance*. *J Clin Invest*, 2003. **111**(9): p. 1373-80.
452. Duncan, E., P. Crossey, S. Walker, N. Anilkumar, L. Poston, G. Douglas, V. Ezzat, S. Wheatcroft, A.M. Shah, and M. Kearney, *The effect of endothelium*
-

- specific insulin resistance on endothelial function in vivo*. Diabetes, 2008. **3**: p. 3.
453. Zeng, G. and M.J. Quon, *Insulin-stimulated production of nitric oxide is inhibited by wortmannin. Direct measurement in vascular endothelial cells*. J Clin Invest, 1996. **98**(4): p. 894-8.
454. Sartori, C., L. Trueb, P. Nicod, and U. Scherrer, *Effects of sympathectomy and nitric oxide synthase inhibition on vascular actions of insulin in humans*. Hypertension, 1999. **34**(4 Pt 1): p. 586-9.
455. Montagnani, M., H. Chen, V.A. Barr, and M.J. Quon, *Insulin-stimulated activation of eNOS is independent of Ca²⁺ but requires phosphorylation by Akt at Ser(1179)*. Journal of Biological Chemistry, 2001. **276**(32): p. 30392-30398.
456. Williams, S.B., J.A. Cusco, M.A. Roddy, M.T. Johnstone, and M.A. Creager, *Impaired nitric oxide-mediated vasodilation in patients with non-insulin-dependent diabetes mellitus*. J Am Coll Cardiol, 1996. **27**(3): p. 567-74.
457. Song, X.M., M. Fiedler, D. Galuska, J.W. Ryder, M. Fernstrom, A.V. Chibalin, H. Wallberg-Henriksson, and J.R. Zierath, *5-Aminoimidazole-4-carboxamide ribonucleoside treatment improves glucose homeostasis in insulin-resistant diabetic (ob/ob) mice*. 2002. **45**(1): p. 56-65.
458. Halseth, A.E., N.J. Ensor, T.A. White, S.A. Ross, and E.A. Gulve, *Acute and chronic treatment of ob/ob and db/db mice with AICAR decreases blood glucose concentrations*. 2002. **294**(4): p. 798-805.